STRUCTURALLY DIVERSE ARABINOXYLAN HYDROLYZATES: THEIR ACTIVITY AS IMMUNOMODULATORS AND THEIR EFFECT ON GROWTH OF BACTEROIDETES

A Dissertation
Submitted to the Graduate Faculty
of the
North Dakota State University
of Agriculture and Applied Science

By

Balapuwaduge Mihiri Marini Judith Mendis

In Partial Fulfillment of the Requirements
for the Degree of
DOCTOR OF PHILOSOPHY

Major Program:
Cereal Science

December 2014

Fargo, North Dakota

North Dakota State University
Graduate School

STRUCTURALLY DIVERSE ARABINOXYLAN HYDROLYZATES: THEIR ACTIVITY AS IMMUNOMODULATORS AND THEIR EFFECT ON GROWTH OF BACTEROIDETES

By

Balapuwaduge Mihiri Marini Judith Mendis

The Supervisory Committee certifies that this ***disquisition*** complies with North Dakota State University's regulations and meets the accepted standards for the degree of

DOCTOR OF PHILOSOPHY

SUPERVISORY COMMITTEE:

Dr. Senay Simsek
Chair

Dr. Estelle Leclerc

Dr. Jae B. Ohm

Dr. Paul Schwarz

Dr. Sheela Ramamoorthy

Approved:

14 April 2015
Date

Dr. Richard D. Horsley
Department Chair

ABSTRACT

Arabinoxylan (AX) is a plant polysaccharide which consists of a xylan backbone on which arabinose is substituted. Thirty structurally different wheat arabinoxylan hydrolyzates (AXH) were prepared by means of different combinations of xylanase (*Cellvibrio japonicas* xylanase (CJX) and *Aspergillus niger* xylanase (ANX)) and arabinofuranosidase (*Bifidobacterium adolescentis* arabinofuranosidase (BAF) and *Clostridium thermocellum* arabinofuranosidase (CAF)). The AXH were analyzed using GC-FID, GC-MS, ^{1}H-NMR and SEC-MALS techniques. In general, the AXH had high proportion of unsubstituted xylose and lesser amount of di- or mono-substituted xylose. The average molecular weights of the AXH varied between 0.78-5.64 million Da. Between the two xylanases, ANX might be an enzyme of choice for the production of arabinoxylan hydrolyzates with simple structural details while the enzyme CJX might be selected for the production of arabinoxylan hydrolyzates with more complex structural features. Addition of BAF followed by CAF was more effective in generating AXH with higher amount of unsubstituted xylose as well as lesser amount of disubstituted xylose. The structural contribution to the immunomodulatory properties of the AXH was also evaluated using LPS induced macrophage cell line. The AXH being tested exhibited both pro- and anti-inflammatory properties. Structure-function relationship of arabinoxylan hydrolyzates as immunomodulators was further assessed using LPS induced colon cancer cell lines: Caco-2 and HT-29. Fine structural details had a strong correlation with the immunological properties of the AXH. The influence of the fine structural details of AXH on the growth of human gut Bacteroides strains was also evaluated. In general, *B. cellulosilyticus* DSM 14830 had the highest growth while *B. eggerthii* DSM 20697 had the lowest growth on AXH. Interestingly, *B. cellulosilyticus* DSM 14830, *B. ovatus* 3_1_23, *B. ovatus* ATCC 8483 and *B. xylanisolvens*

XB1A displayed clearly distinguishable phase shifts along the growth curves indicating their ability to tune in their gene expressions to overcome the hindrances to growth exerted by structural details on the substrate polysaccharide. This research confirmed the ability of Bacteroides to utilize structurally diverse arrays of polysaccharides. Overall, the current study indicates that there might be a structure- function relationship between AXH and their immunomodulatory properties as well as prebiotic properties.

ACKNOWLEDGEMENTS

Thanks and praise to my God the Father, Son and the Holy Spirit for all His love and blessings He has bestowed upon my life.

My sincere appreciation and thanks to my major adviser, Dr. Senay Simsek, for her invaluable advice, assistance, guidance, and continuous encouragement during the course of my graduate studies. Her guidance has helped me immensely to develop my professional life.

My appreciation extends to all members of my graduate committee, Dr. Paul Schwarz, Dr. Sheela Ramamoorthy, Dr. Jae B. Ohm and Dr. Estelle Leclerc for their valuable inputs and support. It was a pleasure to have them in my committee.

My gratitude to Dr. Estelle Leclerc for welcoming me into her laboratory and giving me the opportunity to learn many new things.

My gratitude also extends to Dr. Eric Martens for his time and continuous support rendered to this research. His willingness to collaborate and sharing his knowledge and resource with us is highly regarded.

Special acknowledgement to Kristin Whitney, James Gillespie and Nicholas Pudlo for their excellent professional skills extended to this research.

My thanks extend to my lab-mates Hammed Ademola, Venkata Indurthi, Mohit Koladia and Varsha Meghnani for the many help.

My office mates Lingzhu Deng and Tsogtbayar Baasandorj are appreciated for their friendship.

North Dakota Wheat Commission and Agriculture Product Utilization Commission are acknowledged for funding this research.

I would also like to thank the faculty members, research and support staff, and the office staff of the Department of Plant Sciences and the Cereal Science Graduate Program for their assistance and cooperation throughout my graduate studies.

All the graduate students in the program and all my friends are sincerely acknowledged for their support and friendship throughout my graduate studies

A special gratitude and appreciation to my parents, Mr. Cycil Mendis and Mrs. Hilda Mendis and my brother, Mr. Praneeth Mendis for their love, support and continuous encouragement which has helped me immensely in all aspects of my life.

My heartfelt gratitude and appreciation extend to my husband, Mr. Dulan Samarappuli for his love, support and understanding that has made the fulfillment of this work possible.

TABLE OF CONTENTS

LIST OF TABLES

Table Page

LIST OF FIGURES

LIST OF ABBREVIATIONS

ANX…… *Aspergillus niger* xylanase

CJX……. *Cellvibrio japonicas* xylanase

CAF…… *Clostridium thermocellum* arabinofuranosidase

BAF……*Bifidobacterium adolescentis* arabinofuranosidase

AX……..Arabinoxylan

AXH……...Arabinoxylan hydrolyzates

WAX……..Wheat arabinoxylan

GENERAL INTRODUCTION

In wheat grain, the major polymer of the cell wall is arabinoxylan (AX) (Saulnier et al., 2007). AX consists of a backbone of β-(1,4)-linked xylose residues, which are substituted with arabinose residues on the C(O)-2 and/or C(O)-3 position (Dornez et al., 2009). Endo-xylanases are the major enzymes involved in AX degradation. They cleave AX by internally hydrolyzing the 1,4- β-D-xylosidic linkage between xylose residues in the xylan backbone in a random manner (Collins et al., 2005; Dornez et al., 2009). α-L-arabinofuranosidase is an exo-enzyme that hydrolyzes terminal nonreducing α-arabinofuranose from arabinoxylans (Saha, 2000). Xylan is the most abundant polysaccharide in cell walls of cereals, and cereals being a large proportion of the human diet, large quantities of xylan are introduced to the gastro intestinal tract. However, large proportion of these polysaccharides are indigestible by the human gut enzymes and their degradation relies on the gut microbiome. In the case of xylans, the genus *Bacteroides* are adept with a wide repertoire of genes that target xylan degradation (Zhang et al., 2014). A shift in the Bacteriodates population in the gut with respect to disease conditions has been reported (Ley et al., 2005; Ley et al., 2006) indicating an important contribution from these bacteria to maintenance of health. Previous work has demonstrated the influence of structural differences of cereal polysaccharides such as AX on their fermentation profiles by bacteria. Rose et al. (2010) indicated differences among the fermentation profiles for AX from different cereals (maize, rice and wheat), which consists of different structural features. Xu (2012) concluded that specific molecular regions of dietary fibers differentiate gut bacteria.

Apart from being fermented by the gut bacteria, the ingested polysaccharides interact directly with the intestinal tract. Thus, these polysaccharides, depending on their structure might exert stimulatory or inhibitory signals in the immune system of the gut acting as

immunomodulators. The immunomodulatory effects of AX have been demonstrated by several researchers in the recent years (Cao et al., 2011; Hromádková et al., 2013; Monobe et al., 2008; Zhou et al., 2010). Due to the structural heterogeneity of the enzymatic products (arabinoxylan hydrolyzates, AXH) obtained by hydrolysis of AX by enzymes, we hypothesized that the fine structural details affect the biological activity of these AXH as substrate for gut bacteria and as immunomodulators.

Overall Objectives

The current research was carried out with four specific objectives in mind.

i Production and characterization of structurally different arabinoxylan hydrolyzates (AXH) using xylanases and arabinofuranosidases with different substrate specificity

ii Evaluate the immunomodulatory properties of enzymatically derived AXH using cell culture models derived from the immune system cells

iii Evaluate the immunomodulatory properties of enzymatically derived AXH using cell culture models derived from the intestinal cells

iv Understand the effect of enzymatically derived AXH on human gut bacteria

CHAPTER 1. LITERATURE REVIEW

Wheat is one of the dominant grains produced in the world. It is a grass, which belongs to the family Poaceae (syn. Gramineae). It is considered a "cereal" as it is grown primarily for its grain (or caryopsis) (Gooding, 2009). Although the term 'wheat' describes a number of species and subspecies in the genus *Triticum,* the most important are the hexaploid common wheat (*T. aestivum* subsp. *aestivum*), also known as the bread wheat, which account for more than 90% of world wheat production. However, within this subspecies not all varieties are equally suitable for bread making. Some genotypes have been shown to possess more desirable qualities than others. Mostly, these qualities are inherited and have led to common wheat being generally classified on the basis of their seed coat color, endosperm texture, dough strength and sowing season. The longitudinal and cross sectional view of the wheat kernel is shown in Figure 1.1.

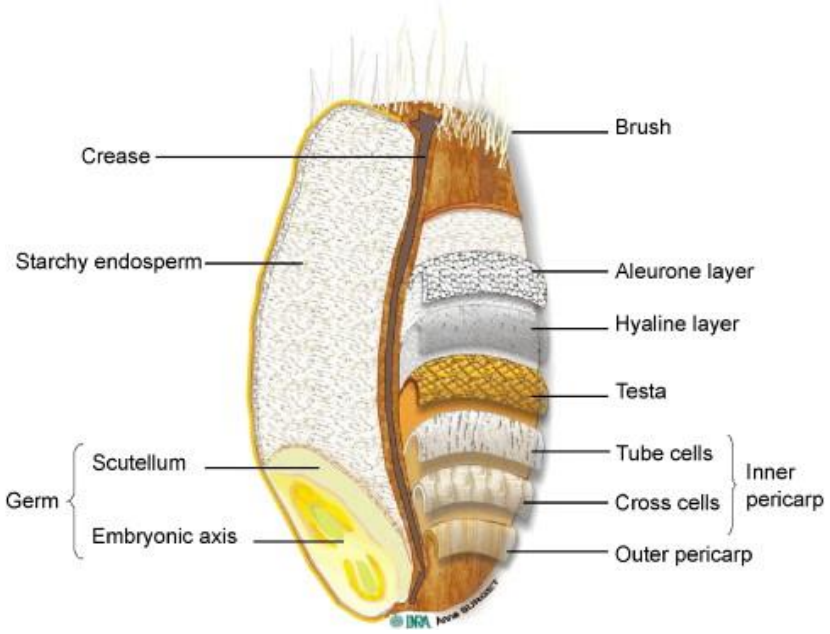

Figure 1.1. Wheat grain showing its component tissues. Reprinted from Saulnier et al (2007).

During cereal milling, the starchy endosperm is reduced in particle size to produce flour (Delcour and Hoseney, 2010a). The outer layers of the grain from the pericarp to aleurone layer

are removed to produce bran. The germ is also separated from the endosperm and usually collected in the bran fraction. The general composition of wheat bran can be summarized as in Table 1.1.

Table 1.1. General composition of wheat bran. Adapted from Apprich et. al (2014).

Compound	Amount (%)
Water	12.1
Protein	13.2-18.4
Fat	3.5-3.9
Total carbohydrates	56.8
Starch	13.8-24.9
Arabinoxylan	10.9-26.0
Cellulose	11.0
Beta-glucan	2.1-2.5
Phenolic acids	1.1
Ferulic acid	0.02-1.5
Phytic acid	4.2-5.4
Ash	3.4-8.1

The bran is the most important by-product of wheat flour milling and it accounts for about 25% of the grain weight (Neves et al., 2006). Many health benefits associated with whole grain foods are traced back to compounds in bran. The ability of bran or whole grain to modulate hunger and satiety moods, influence the glycemic, lipidic and inflammatory status of consumer, or the prebiotic activity has been under extensive research in the recent years. Wheat bran is rich in dietary fibers as well as many other compounds that are biologically active such as antioxidants and phytoestrogens or lignans (Pruckler et al., 2014). A concise summary of different components of the wheat bran and their beneficial health effects are given in Table 1.2.

1.1. Arabinoxylans

In wheat grain, the major polymer of the cell wall is arabinoxylan (Saulnier et al., 2007). Even though they occur as a minor constituent of the grain, their unique physico-chemical properties allow them to have a considerable effect on the cereals food industry, including bread making (Courtin and Delcour, 2002), gluten-starch separation (Frederix et al., 2004), refrigerated dough syruping (Courtin et al., 2005; Simsek and Ohm, 2009) and in animal feeds (Bedford and Schulze, 1998). Furthermore, AX has been associated with beneficial health effect in patients with impaired glucose tolerance (Garcia et al., 2006). AX consists of a backbone of β-(1,4)-linked xylose residues, which are substituted with arabinose residues on the C(O)-2 and/or C(O)-3 position (Dornez et al., 2009). Since AX is mainly composed of pentose sugars xylose and arabinose, they are commonly referred to as pentosans. Phenolic acids such as ferulic acid can be ester linked on the C(O)-5 position of arabinose. Under oxidative conditions, these ferulic acid residues undergo oxidative cross-linking forming inter/intra chain diferulic acid bridges (Geissman and Neukom, 1973). Ferulic acid can also function as a radical scavenger, thus it has a potential health benefit as an antioxidant (Mpofu et al., 2006). The structure of AX and enzymes involved in its degradation are shown in Figure 1.2.

Table 1.2. Components of wheat bran and their beneficial health effects. Adapted from Pruckler et al (2014).

Component	Beneficial action	Advantages/limitation	Mechanism
Soluble dietary fiber (SDF)	Improves gut health	Stimulating the growth of potentially beneficial bacteria/only partially elucidated mechanism depending on individual gut flora	Prebiotic action
	Control glycemic index	"Food, not drug" concept/investigated in whole wheat	Only partially elucidated
	Reduces plasma cholesterol level	"Food, not drug" concept/2-10 g/d are hard to reach with bran bread, triacylglycerols and HDL cholesterol were not significantly influenced, increasing soluble fiber contributes only to a small extend on dietary therapy	Only partially elucidated
Dietary fiber	Prolongs bowel transition time	Multiple gastrointestinal effects/investigated in rye	SCFA decrease the gastric tone
	Increases stool volume	Multiple gastrointestinal effects/investigated in rye	Increased mucin production
Alkylresorcinol	Reduces human colon cancer cell growth	Wheat bran oil has shown cancer reduction in mice/multifactorial impact of cereal bran	Only partially elucidated cytotoxic effects on cancer cells
Ferulic acid	Antioxidant, anti-microbial, anti-inflammatory, antithrombosis and anticarcinogenic activities	Fiber-antioxidant complex preserving antioxidants from gastric degradation/bound in cell wall matrix	Inhibits oxidation of LDL, does not initiate a chain reaction
Beta-glucan	Lower/reduce blood cholesterol	Lower cholesterol may reduce the risk of heart disease/health claim just given for oats and barley	Increases the synthesis of bile acids from cholesterol and the fecal excretion of neutral sterols
	Beneficial role in insulin resistance, dyslipidemia, hypertension, and obesity	No human adverse effects have been reported/extraction of pure b-glucan is relatively costly, in wheat just 2.5% in wheat bran, hard to provide 3 g/d beta-glucan	Only partially elucidated
Arabinoxylan	Reduction of postprandial glycemic response	Reduce the risk of developing type 2 diabetes/health claim just given for arabinoxylan from wheat endosperm	Cross-linked arabinoxylans maintain their viscosity within the gastrointestinal tract, blunting the postprandial glucose response
Lignans	Protection against hormone related breast and prostate cancer	Consumption of 30 g DF/d results in a significantly reduced odds ratio (0.57), matairesinol is a direct precursor to enterolactone/conversion occurs by gut microflora, oilseeds have 40 times higher amount per 100 g than cereal bran	Estrogenic effect after transformation into enterodiol and enterolactone
Sterols	Reduces total cholesterol	"Food, not drug" concept/use of wheat bran resulted in a non-significant 4% reduction in serum cholesterol, application of 3-9 g/d sitosterol can be achieved only with concentrates	Lowering of serum cholesterol level by inhibiting cholesterol absorption

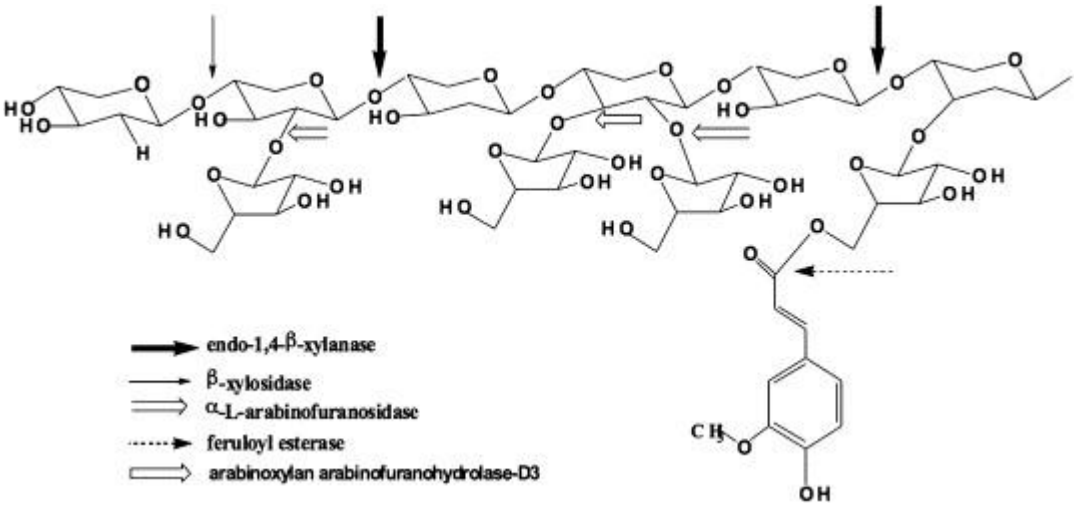

Figure 1.2. Structure of arabinoxylan (AX) and the sites of attack by xylanolytic enzymes involved in its degradation (adapted from Grootaert et al. (2007)). The backbone of AX is composed of β-(1,4)-linked xylose residues, which can be substituted with arabinose residues on the C(O)-2 and/or C(O)-3 position. Ferulic acid can be esterified on the C(O)-5 position of arabinose. Endo-β-(1,4)-d-xylanases (EC 3.2.1.8) cleave the xylan backbone internally, β-d-xylosidases (EC 3.2.1.37) remove xylose monomers from the non-reducing end of xylo-oligosaccharides, α-l-arabinofuranosidases (EC 3.2.1.55) remove arabinose substituents from the xylan backbone, and ferulic acid esterases (EC 3.1.1.73) remove ferulic acid groups from arabinose substituents (Dornez et al., 2009).

Even though AX can be described using a general structure, two different classes of AX exist in wheat. They are the water-extractable AX (WE-AX), which account for about 25-30% of AX in wheat flour and water-unextractable AX (WU-AX), which account for the remainder of AX in wheat flour (Meuser and Suckow, 1986). WE-AX are loosely bound to the cell wall surface (Mares and Stone, 1973). In contrast, WU-AX are retained in the cell wall by covalent and non-covalent interactions with AX and protein, lignin and cellulose (Iiyama et al., 1994).

1.2. Endo-β-(1,4)-d-xylanases (xylanases)

Xylanases were originally termed pentosanases (Collins et al., 2005) and were given the official name endo-β-(1,4)-D-xylanases with the enzyme code EC 3.2.1.8. However, commonly used synonyms include endoxylanase, 1,4-β-d-xylan-xylanohydrolase, endo-1,4-β-d-xylanase, β-

1,4-xylanase, β-xylanase and xylanase (here after referred to as xylanase). Xylanases are the major enzymes involved in AX degradation. They cleave AX by internally hydrolyzing the 1,4-β-D-xylosidic linkage between xylose residues in the xylan backbone (Figure 1.2) (Collins et al., 2005; Dornez et al., 2009). The complex and diverse nature of xylan has given rise to various xylanases. Thus, classification of xylanase is not simple and straight forward. Wong et al., (1988) classified xylanases based on their physicochemical properties. They classified xylanases into two groups: those with low molecular weights (<30 kDa) and basic p*I*, and those with higher molecular weight (>30 kDa) and acidic p*I*. However, this classification was having drawbacks as xylanases of properties opposing to this classification were discovered. Later a more complete classification system was introduced, which was based on primary structure comparisons of the catalytic domain of the enzymes (Henrissat et al., 1989; Henrissat and Coutinho, 2001). This classification not only covers xylanase but covers all glycosidase in general, and has come to wide spread use. Initially, cellulases and xylanases were classified into six families A to F (Henrissat et al., 1989). However, this was updated to 77 families in 1999 (1-77) (Henrissat and Coutinho, 2001). At the time of this writing, 133 Glycoside hydrolases (GH) (EC 3.2.1.x) families exist (Lombard et al., 2014).

Over 290 xylanases have been identified (Fierens, 2007), which have been grouped into different glycoside hydrolase (GH) families (5, 7, 8, 10, 11 and 43) (Collins et al., 2005; Dornez et al., 2009). Most of these xylanases are from fungal or bacterial origin. All plant xylanases identified so far belong to GH family 10, while most of the microbial xylanases are of GH family 10 or 11 (Simpson et al., 2003). Thus, within our research only xylanases of GH 10 and 11 are being discussed. Xylanases of family 10 are characterized by a (beta/alpha)-8 –fold conformation and molecular masses that exceed 30 kDa, while xylanases of family 11 contain a jelly roll

conformation and molecular masses of around 20 kDa (Biely et al., 1997; Kulkarni et al., 1999). The differences of xylanases of GH family 10 and 11 are shown in Table 1.3.

Table 1.3. Basic comparison between the xylanases of GH 10 and 11 with respect to their origin, molecular mass, conformation, and products. Adapted from Mendis (2012).

	Xylanase	
	GH family 10	GH family 11
Origin	All plant xylanase Microbial	Microbial
Molecular mass	Higher molecular mass (>30 kDa)	Lower molecular mass (~20 kDa)
Conformation	$(\beta/\alpha)_8$ barrel fold	β-jelly roll
Products	Smaller oligosaccharides	Larger oligosaccharides

The general retaining mechanism for glycoside hydrolase family 10 and 11 has been described by many authors (Collins et al., 2005; McCarter and Stephen Withers, 1994; Rye and Withers, 2000; Zechel and Withers, 1999). Xylanase of both family 10 and 11 catalyze the hydrolysis of the xylosidic linkage with retention of anomeric configuration (Rye and Withers, 2000).The general reaction mechanism for this reaction is given in Figure 1.3. The reaction proceeds through a double displacement mechanism (Collins et al., 2005; McCarter and Stephen Withers, 1994; Rye and Withers, 2000; Zechel and Withers, 1999). Two carboxylic acid residues in the active site are involved in formation of the enzyme-substrate intermediate; one acts as an acid by protonating the substrate, while other performs a nucleophilic attack. With the departure of the leaving group, a covalent glycosyl-enzyme intermediate is formed (inversion from β to α). In the second step, the first carboxylic acid acts as a base and abstracts a proton from a water molecule upon, which the nucleophilic water molecule attacks the anomeric carbon of the xylan. This leads to the formation of the second intermediate state in which the anomeric carbon

undergoes an oxocarbonium-ion-like transition state (inversion from α to β). This proceeds with the release of the substrate with retention of the original conformation at the anomeric center. Hydrolysis of AX by xylanase causes a decrease in the degree of polymerization in the AX and produce AX oligosaccharides, xylobiose and xylose with retention of their conformation (Dekker and Richards, 1976; Delcour and Hoseney, 2010b; Reilly, 1981).

1.2.1. GH10 xylanases

Most of the glycoside hydrolases that are classified in GH10 are endo-β-1,4-xylanases (e.g. endo-1,4-β-xylanase from *Cellvibrio japonicus*) while only a few are endo-β-1,3-xylanases (Pollet et al., 2010). GH10 xylanases have broad substrate specificity and attack both linear substrates as well as decorated heteroxylans. They attack the glycosidic linkage next to a single or double substituted xylose toward the non-reducing end and require two unsubstituted xylose residues between branched residues (Figure 1.4). As a result, GH10 xylanases can even degrade AX with high degree of substitution (DS) into smaller fragments. The catalytic domain of GH10 xylanases has a $(\beta/\alpha)_8$- barrel fold, called a triosephosphate isomerase (TIM)-barrel fold which consists of a shape of a salad bowl (Figure 1.5.)

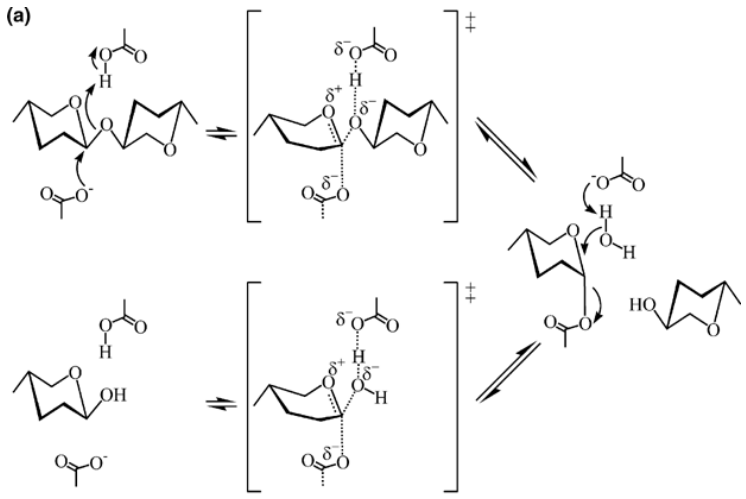

Figure 1.3. General mechanism for catalytic hydrolysis of xylan backbone by xylanases of GH 10 and 11 (cited from Rye and Withers (2000)).

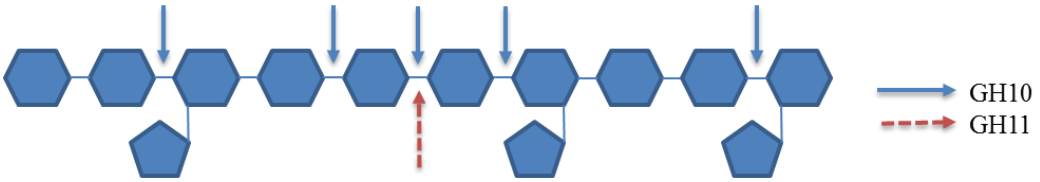

Figure 1.4. Hydrolytic activity of GH 10 and GH 11 xylanase on arabinoxylan (cited from Pollet et al (2010)).

1.2.2. GH11 xylanases

GH11 xylanases (e.g. endo-1,4-β-xylanase M4 from *Aspergillus niger*) exclusively consist of true endo-β-1,4-xylanases that cleave internal β-1,4-xylosidic bonds (Pollet et al., 2010). GH11 xylanase preferably cleaves unsubstiuted regions of the backbone. GH11 cannot attack the xylosidic linkage toward the non-reducing end next to a branched xylose and in contrast to GH10 xylanase, require three unsubstituted consecutive xylose residues for hydrolysis (Figure 1.4). Hence, GH11 xylanases have a low activity on heteroxylans with a high DS.

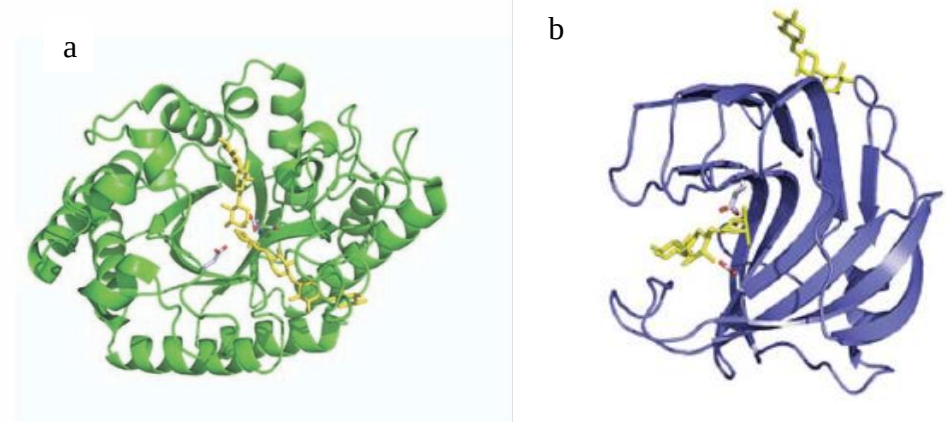

Figure 1.5. Overall structure of xylanase of two glycoside hydrolase families. (a) Structure of GH10 xylanase. The catalytic domain has a $(\beta/\alpha)_8$-barell fold. (b) Structure of GH11 xylanase. The catalytic domain has a β-jelly roll fold (cited from Pollet et al. (2010)).

The catalytic domain of GH11 xylanase consists of a β-jelly roll structure that resembles the shape of a partially closed right hand and consists of two twisted antiparallel β-sheets and a single α-helix (Figure 1.5). The two β-sheets constitute the fingers while the twisted part of β-sheet B and the α-helix form the palm of the hand. The active site is situated at the concave side of the palm.

1.3. Arabinofuranosidases

α-L-arabinofuranosidase (α-L-arabinofuranosidase arabinofuranohydrolase, EC 3.2.1.55, arabinofuranosidase) is an exo-enzyme that hydrolyzes terminal nonreducing α-arabinofuranose from arabinoxylans (Saha, 2000). Based on their amino acid sequence similarities α-L-arabinofuranosidases have been classified into seven glycoside hydrolase families (GH2, 3, 10, 43, 51, 54 and 62) (Lombard et al., 2014).

1.3.1. α-L-arabinofuranosidase from *Bifidobacterium adolescentis* (GH43)

Arabinoxylan arabinofuranohydrolase-D3 (AXHd3) from *Bifidobacterium adolescentis* releases only C3-linked arabinose residues from double-substituted xylose residues (Van den Broek et al., 2005). Laere et al. (1997) isolated two different arabinofuranosidases from *B. adolescentis* able to release arabinose residues from arabinoxylan. These enzymes were named arabinofurano-hydrolase-D3 (AXHd3; which hydrolyzed only C3-linked arabinose residues from double-substituted xylose residues)

1.3.2. α-L-arabinofuranosidase from *Clostridium thermocellum* (GH51)

This enzyme catalyses the hydrolysis of "α-1,5-linked arabino-oligosaccharides and the α-1,3 arabinosyl side chain decorations of xylan with equal efficiency" (Taylor et al., 2006). It was also highly active on small soluble oligosaccharides, notably α-1,5-linked arabinobiose/arabinotriose and the α-1,3-linked arabinoside of xylobiose which reflect the natural limit dextrin products of the action of arabinanases on arabinan and xylanases on wheat arabinoxylan. Indeed, it is also highly efficient in the removal of the α-1,3-linked arabinoside decorations of polymeric wheat arabinoxylan itself (Taylor et al., 2006). According to the existing literature, the substrate specificity of α-L-arabinofuranosidase from *Clostridium thermocellum* is specified with respect to arabinose substitutes to monosubstituted xylose (Taylor et al., 2006) and whether or not this specific enzyme acts on 1,3-linked arabinose when linked to disubstituted xylose is currently unknown. However, based on what was observed for other arabinofuranosidases belonging to GH51, since they hydrolyze the 1,3-linked arabinose from monosubstituted xylose and not disubstituted xylose (Sorensen et al., 2006), we speculate that this arabinofuranosidase also prefers monosubstituted xylose.

Based on the literature available on the two xylanases and arabinofuranosidases discussed above, the substrate specificity of these four enzymes could be illustrated as in Figure 1.6.

1.4. Human Gut Microbiota

The intestine is an important organ that consists of a huge surface area and permits vital interactions with the external world, including the gut microbiota (Cani et al., 2013). The microbiota refers to "*the microbial life forms within a given habitat or host"* while the microbiome refers to *"the microbial life forms inhabiting a living host, their combined genomes, and their interactions with the host"* (Walter and Ley, 2011). The gut microbiota exerts a significant impact on host physiology, impacting the control of energy homeostasis, the immune system, digestion and vitamin synthesis (Cani et al., 2013) and inhibition of pathogen colonization (Wardwell et al., 2011).

The human digestive tract is colonized by a large array of microbes. However, the digestive tract has evolved in such a way that the host has the first shot at dietary substances. Most of the host digestive enzymes act on the dietary substances along the way from mouth to the small intestine. It is then in the large intestine that the saccharolytic bacteria extract additional energy from the dietary substances that are resistant to digestion by the human enzymes (Walter and Ley, 2011). The distribution of microbial biomass along the human digestive track varies in an ascending order with the highest microbial load occurring in the large intestine (1011 cells/mL) (Walter and Ley, 2011). This distribution is well summarized in the review by Walter and Ley (2011).

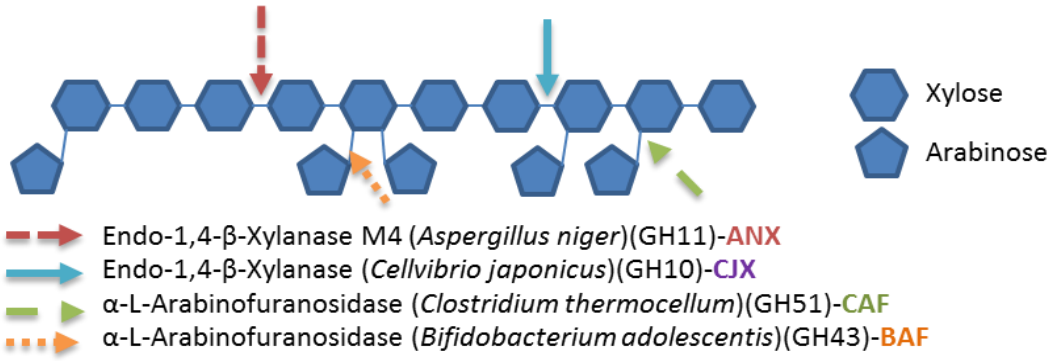

Figure 1.6. Simplified illustration of hydrolysis specificities of two different xylanases and two different abinofuranosidases along the arabinoxylan molecule. Endo-1,4-β-xylanases from *Cellvibrio japonicus* (GH10) attack the glycosidic linkage next to a single or double substituted xylose toward the non-reducing end and require two unsubstituted xylose residues between branched residues (Pollet et al., 2010). As a result, GH10 xylanases can even degrade AX with high degree of substitution into smaller fragments. GH11 xylanases (e.g. endo-1,4-β-xylanase M4 from *Aspergillus niger*) (GH11) exclusively consist of true endo-β-1,4-xylanases that cleave internal β-1,4-xylosidic bonds (Pollet et al., 2010) and preferably cleave unsubstituted regions of the backbone. It cannot attack the xylosidic linkage toward the non-reducing end next to a branched xylose and require three unsubstituted consecutive xylose residues for hydrolysis. Hence, GH11 xylanases have a low activity on heteroxylans with a high DS. α-L-arabinofuranosidase from *Bifidobacterium adolescentis* (GH43) releases only C3-linked arabinose residues from double-substituted xylose residues (Van den Broek et al., 2005). α-L-arabinofuranosidase from *Clostridium thermocellum* (GH51) catalyzes the hydrolysis of C3-linked arabinosyl side chain of xylan (Taylor et al., 2006).

The human diet is rich with plant and animal derived glycans. However, there is a large array of glycans that are resistant to digestion by human enzymes and rely on microbial enzymes for their digestion. The fermentation of these glycans by microbes yield energy for the microbial growth, and the end products such as short chain fatty acids (SCFA), mainly acetate, propionate and butyrate which have profound effects on the health of the host (Tremaroli and Backhed, 2012). Butyrate acts mainly as the energy substrate for the colonic epithelium because it is the preferred energy source of colonocytes (Hamer et al., 2008; Koropatkin et al., 2012). Acetate and propionate are absorbed into the blood stream and travel to the liver where they get incorporated into lipid and glucose metabolism, respectively (Rombeau and Kripke, 1990). Thus, acetate and propionate act as energy source to peripheral tissue cells. In addition to that, SCFA have an

important effect on the host immune system as well. Low levels of butyrate modify the cytokine production profile of T_H cells (Kau et al., 2011), promote intestinal epithelial barrier integrity and has also been associated with colonic tumor suppression (Hamer et al., 2008). In addition to being absorbed by the host, acetate is linked to maintaining the intestinal barrier function (Kau et al., 2011), and preventing colonization of some enteric pathogens (Fukuda et al., 2011). The functional association among the intestinal microbiota, intestinal epithelial cells and the host immune system helps maintain the balance between tolerance and immunity to a particular pathogenic or non pathogenic microbe or food ingredient. Figure 1.7 illustrates this fragile balance among intestinal epithelial cells, microbiota and immune cells.

Xylan is the most abundant polysaccharide in cell walls of cereals and cereals being a large proportion of the human diet, large quantities of xylan are introduced to the gastro intestinal tract (GIT). Healthy adult gut microbiota is composed primarily of members of two bacterial phyla, the Bacteroidetes and Firmicutes (McNulty et al., 2013). However, the most expanded glycolytic gene collection that target xylan degradation is possessed by genus Bacteroides (Zhang et al., 2014). The members of the genus *Bacteroides* are adept at utilizing plant and host derived polysaccharides (Koropatkin et al., 2012). These *Bacteroides* are rich in genes involved in the acquisition and metabolism of various glycosides including glycoside hydrolases and polysaccharide lyases which are organized into polysaccharide utilization loci (PULs) that are distributed throughout the genome (Koropatkin et al., 2012).

In the phylum Bacteroidetes, the metabolism of starch from the external environment is achieved via the starch utilization system (Sus) (Koropatkin et al., 2012). There have been similar systems unique to the phylum Bacteroidetes identified in the Bacteroidetes genome that

function by a similar mechanism as Sus but harbor enzymes that target glycans other than starch, thus these systems are termed Sus-like systems (Koropatkin et al., 2012).

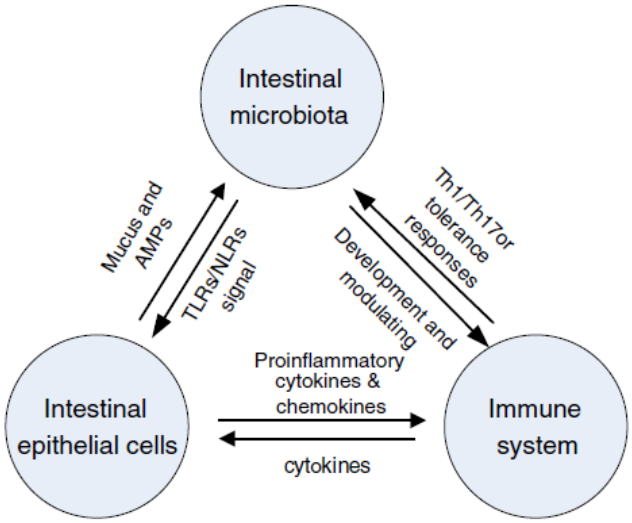

Figure 1.7. The association among intestinal microbiota, intestinal epithelial cells (IECs) and host immune system (Adapted from Xu et al (2013). Intestinal microbiota activates the Pattern Recognition Receptors (PRRs) and ER stress signals in IECs, resulting in IECs proliferation, integrity barrier function, production of anti-microbial peptides (AMPs) and mucus, and the secretion of cytokines such as IL-1β, IL-18, IL-25. The commensal bacteria, together with the signals from IECs activate the tolerance responses by the immune system. On the other hand, pathogenic bacteria triggers T_H1/T_H17 responses, which will drive the immune system to eliminate these pathogens. Thus the careful balance among the intestinal microbiota, IECs and immune system is vital for the health of the host and any disruption of this homeostasis may result in uncontrolled inflammation leading to tissue damage, inflammatory bowel disease (IBD), colonic cancer, and metabolic diseases. TLRs: Toll-like receptor; NLRs: Nod-like receptor.

These Sus-like systems are involved in metabolism of many other glylans by the Bacteroidetes. The molecular mechanisms used to utilize xylan have been suggested to be analogous to the Sus-like paradigm (Dodd et al., 2011; Martens et al., 2009). A gene cluster that was highly induced during growth of Bacteroidetes on wheat AX was identified and termed the xylan utilization system (Xus) (Dodd et al., 2011). A schematic model predicting the utilization of xylan by Xus is given in Figure 1.8. The system consists of a set of polysaccharide binding proteins, glycolytic enzymes that hydrolyze large polysaccharides into smaller oligosaccharides

and TonB-dependent transporters that transport these oligosaccharides into the periplasm (Zhang et al., 2014). These oligosaccharides are then converted to smaller monosaccharides by an array of glycolytic enzymes before being transported to the cytosol (Martens et al., 2009).

The biochemical pathway for xylose metabolism is the pentose phosphate pathway (PPP) (Jeffries, 2006). There are two main routes of how xylan enters the PPP; xylose isomerase pathway, which is common among bacteria, and the redox pathway, which is common among eukaryotes. In the bacterial pathway, xylose gets converted to xylulose by the action of xylose isomerase and then phosphorylated to xylulose-5-phosphate by xylulokinase and xylulose-5-phosphate may enter the PPP (Dodd et al., 2011; Jeffries, 2006).

1.5. Immunological Effects of Polysaccharides

1.5.1. Overview of the immune system

Immunity is the resistance to disease by the body (Abbas and Lichtman, 2011). The cells, tissues, organs and the molecules that collectively function to maintain immunity constitutes the immune system. The immune system consists of innate immunity (natural or native immunity) which mediates the initial resistance against infection and the adaptive immunity (specific or acquired immunity) which develops more slowly and comes into play later during infection and is more specific and effective defense. The principal components of the innate and adaptive immunity are illustrated in Figure 1.9.

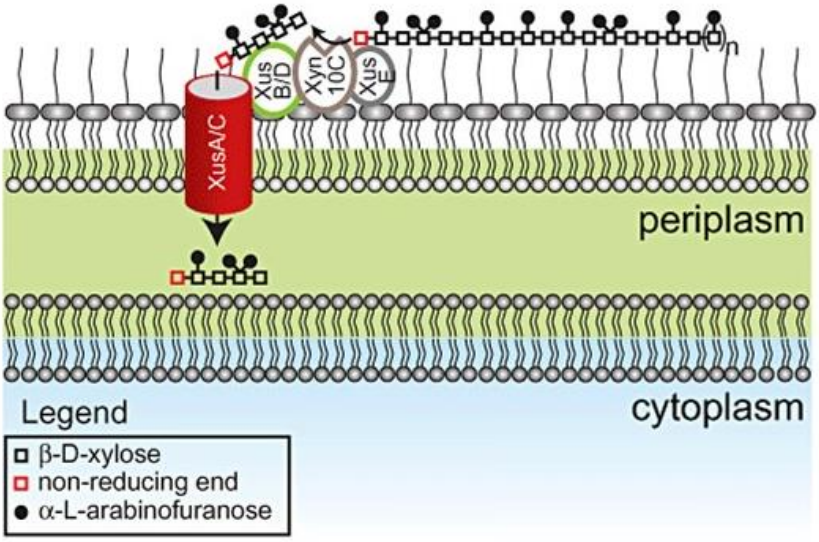

Figure 1.8. Predicted model for binding of xylan, cleavage and transport of xylan fragments across the outer membrane by components of the Xus cluster (adapted from Dodd et al., (2011). The proteins, XusA and XusC, are homologues of the SusC TonB-dependent receptor, which is involved in oligosaccharide transport across the outer membrane. XusB and XusD are homologues of SusD, which binds polysaccharides on the outer leaflet of the outer membrane. XusE has no homology to other characterized proteins.In the predicted model, XusE, Xyn10C and the XusB/D proteins bind to extracellular xylan polymers. Xyn10C then catalyses the endo-cleavage of these polymers and XusB/D facilitates transport of these fragments across the outer membrane and into the periplasm through the TonB-dependent receptors XusA and XusC.

1.5.1.1. Innate immunity

The cells of the innate immune system are first line of defense against microbes and infectious agents that are encountered by the body (Delcenserie et al., 2008). Since these initial defense mechanisms are always present in a healthy individual, this form of immunity is named innate immunity (Abbas and Lichtman, 2011). The components of the innate immune system consist of epithelial barriers, phagocytes (neutrophils, monocytes and macrophages), dendritic cells, natural killer (NK) cells, complement proteins, cytokines and other types of proteins. The two principle reactions of the innate immunity are inflammation and antiviral defense.

The cells of the innate immune system consist of receptors that recognize structures that are non-self and that are not present in the host cells (Abbas and Lichtman, 2011). Specific molecules present at the surface of microbes are targeted by the innate immune system and are termed microbe-associated molecular patterns (MAMPs) or pathogen associated molecular patterns (PAMPs). The receptors of the innate immune system that recognize these foreign components are called pattern recognition receptors and include receptors of the toll like receptor (TLR) family and mannose receptors. TLRs are involved in the recognition of many bacterial lipopolysaccharides. Recognition of PAMPs by receptors of the innate immune system results in a cascade of cellular events that bring about effector functions to eliminate the threat. For instance, activation of TLRs by PAMPs involves cellular processes such as recruitment and activation of protein kinases which leads to the activation of transcription factors such as nuclear factor κB (NF-κB) and interferon response factor-3 (IRF-3), which direct the gene transcription of inflammatory cytokines (e.g. interleukin (IL)-1, IL-8), enzymes and proteins involved in eliminating the microbial infection. Cytokines are secreted proteins that mediate inflammatory reactions. However, innate immunity is not restricted to the initial defense against infection. They play a vital role in instructing the adaptive immunity to activate its response.

1.5.1.2. Adaptive immunity

Adaptive immunity is the second line of defense in the body against infection. Although it comes into play much later that innate immunity, it is very efficient and specific, diverse and constitutes the ‘memory’ of the immune system (Abbas and Lichtman, 2011). It consists of two types of immunity: humoral immunity and cell-mediated immunity. Humoral immunity is specialized in defense against extracellular microbes while cell mediated immunity provides defense against intracellular microbes. Lymphocytes and their products such as antibodies

constitute the adaptive immune system. Lymphocytes are the only cells in the immune system that are capable of producing specific receptors for the specific antigen. Lymphocytes of the adaptive immunity are mainly B-lymphocytes and T-lymphocytes (although NK cells are lymphocytes they are involved in the innate immune response). Only B-lymphocytes are capable of producing antibodies and thus mediate the humoral immunity. The cell-mediated immunity is achieved via T-lymphocytes.

1.5.1.3. Gut associated lymphoid tissue (GALT)

The immune response of the intestinal mucosa is mediated by the specialized immune system features associated with the intestinal mucosa. It consists of the Peyer's patches, isolated lymphoid follicles (ILFs) and mesenteric lymph nodes (MLNs) (Maynard et al., 2012) (Figure 1.10). Peyer's patches are lymphoid follicle aggregates which contain T and B lymphocytes, plasma cells, macrophages and dendritic cells ((Langkamp-Henken et al., 1992). M-cells (microfold cells) are specialized epithelial cells that overlie the Peyers patches (Kagnoff, 1993; Schley and Field, 2002). M-cells are involved in endocytose and transport of antigens from the intestinal lumen to the Peyer's patches where they are presented to T- and B-lymphoctes which gets activated (Kagnoff, 1993; Langkamp-Henken et al., 1992). The activated B-lymphocytes lead to the production of antibodies. Also, the activated immune cells exit and Peyer's patches and enter the systemic circulation. Thus, Peyer's patches act as main sampling sights for ingested antigens (Schley and Field, 2002). T- and B-lymphocytes, plasma cells, mast cells and macrophages are distributed throughout the lamina propria (Langkamp-Henken et al., 1992). Interepithelial lymphocytes are spread on the interstitial spaces of the epithelial cells and are in direct contact with intestinal antigens suggesting that they might be the first cells of the immune system that interact with and respond to ingested antigens (Schley and Field, 2002). MLNs

comprise of the immune cells entering and leaving the gut (Schley and Field, 2002). ILFs are similar to Peyer's patches but they mainly consist of B-cells, dendritic cells and the overlying epithelium comprising of M cells. (Lamichhane et al., 2014; Tsuji et al., 2008). They are proposed to be involved in the production of T cell independent IgA production (Tsuji et al., 2008).

1.5.2. Plant polysaccharides as immunomodulators

A possible mode of action of dietary polysaccharides, apart from being fermented by intestinal microbiota, is associated with its immunological effects. Evidence suggests that addition of fiber to the diet alters the structure and function of the gut, and modifies the gut-derived hormones and production of cytokines (Mikkelsen et al., 2014; Schley and Field, 2002). Most of the research on this area has been performed with beta-glucans while other cereal polysaccharides such as arabinoxylans are starting to gain interest as possible immunomodulators. Immunomodulators or biologic response modifiers are compounds that interact with the host immune system and bring about upregulation or downregulation of specific immune responses (Tzianabos, 2000). Some of the immunomodulatory effects of different fibers are summarized in a review by Schley and Field (2002). Experimental work performed *in vitro* with monoculture cell lines have suggested that these polysaccharides are capable of directly stimulating the intestinal epithelial cells and monocytes, thereby bringing about immunological outcomes (Chan et al., 2009; Mikkelsen et al., 2014; Rieder and Samuelsen, 2012; Volman et al., 2008; Xu et al., 2013).

Inflammation is an adaptive response that is triggered by noxious stimuli and conditions, such as infection and tissue injury (Medzhitov, 2008). Under healthy physiological conditions inflammation is a defense response that serves a protective function in the body. Although the

exact mechanism of how the dietary fibers affect the immune response and inflammation is not well understood, several mechanisms have been studied to explain this effect (Schley and Field, 2002). Depending on their structure, dietary fibers can be uptaken by M-cells in the Peyer's patches and be transported to underlying immune cells and other cells which results in local cytokine production (Volman et al., 2008). This in turn will influence T-cells, B-cells, antigen presenting cells and other immune cells. Fibers may also be up taken by intestinal macrophages and dendritic cells and transported to lymph nodes, spleen and bone marrow. Moreover, direct interaction of fibers with colonic epithelial cells or leukocytes may induce changes in immune reactions related to inflammation and development of cancer (Samuelsen et al., 2011; Volman et al., 2008).

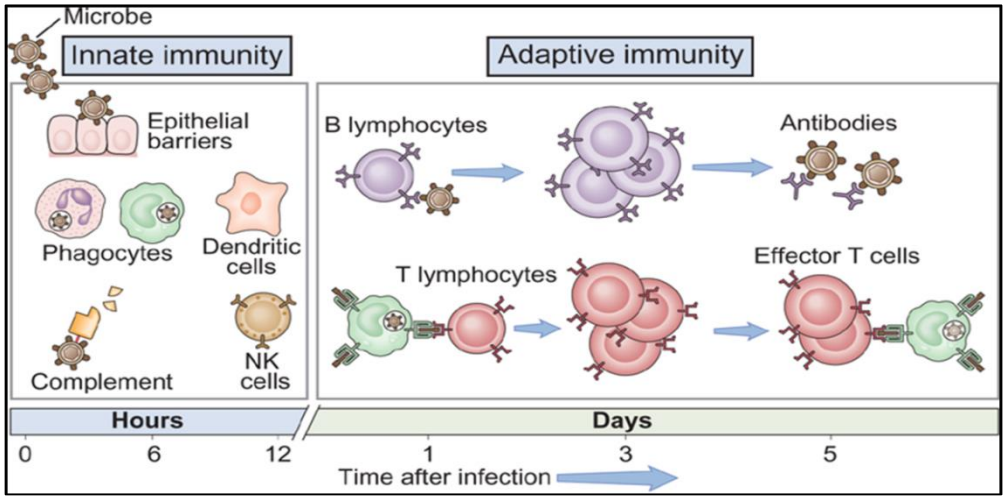

Figure 1.9. The principal components of the innate and adaptive immunity. The innate immunity is the first line of defense against infection. Epithelial barriers prevent entrance of microbes and infectious agents while their elimination is via cells such as phagocytes and natural killer (NK) cells and components such as complement proteins. The adaptive immunity develops much later and is mediated by lymphocytes (B/T). The B lymphocytes results in the production of antibodies against microbes and infectious agents. T lymphocytes mature into effector T cells which lead to the elimination of infected cells. Cited from Abbas and Lichtman (2011).

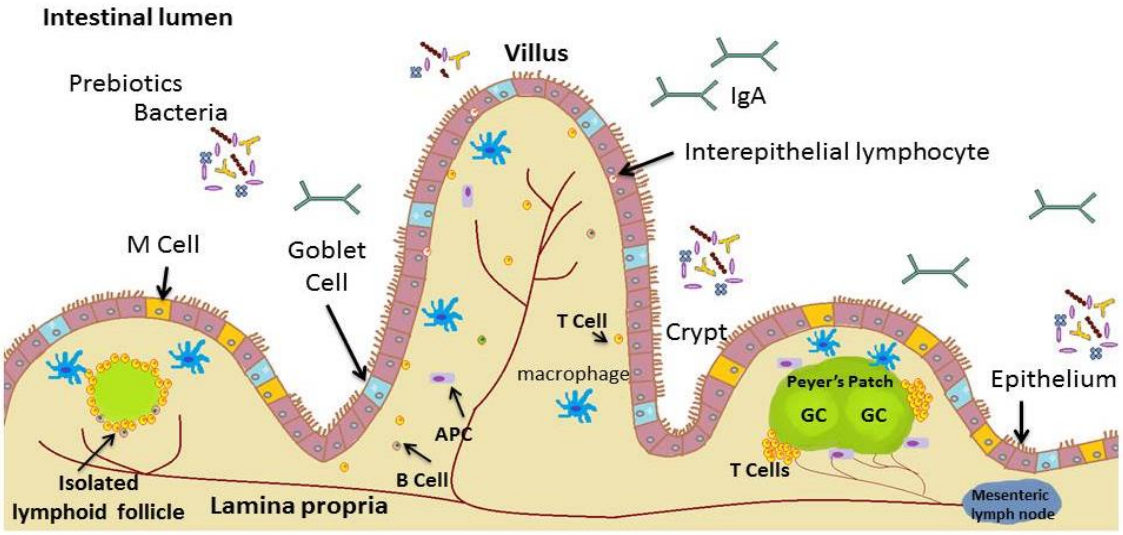

Figure 1.10. The gut associated lymphoid tissue (GALT). Intestinal epithelial cells maintain a barrier between the contents of the intestinal lumen and the underline immune cells. APC: antigen presenting cells; M-cells: microfold cells; IgA: immunoglobulin A. Cited from Aimutis (2011).

According to one reviewer (Mälkki, 2004) it is still too early to draw full conclusions on the effect of dietary fibers on the immune system. However, animal studies have clearly demonstrated that dietary fiber type and content can modulate measures of immune function. AX extracted from wheat bran has been shown to have potent effects on innate and acquired immune response in mice (Cao et al., 2011). Thus, it has been suggested that AX extracted from wheat bran by alkaline or enzymatic procedures could be a good source of natural immunomodulation. Studies have suggested that the antitumor activity of AX is mainly due to its immunostimulatory properties (Cao et al., 2011). AX significantly increases the activation potential of T and B cells and enhances the humoral and cell-mediated immunity in tumor bearing mice. Akhtar et al. (2012) demonstrated that wheat bran derived AXs have the potential to stimulate the antibody mediated immune response in chickens. Thus, AX has the potential as immuno-enhancing and antioxidant additives in functional foods (Hromádková et al., 2013).

AXs are ingested as part of cereal and non-cereal foods from our diet. AX is a complex plant polysaccharide that relays on many different enzymes for its hydrolysis into smaller oligosaccharides. Many gut microbes have evolved to contain enzymes, receptors and transporters that achieve efficient degradation and utilization of these complex AX molecules. The enrichment of different AX utilizing bacteria in the gut upon the consumption of AX rich diet could have beneficial health effects to the host. Furthermore, AXs and their hydrolyzates, as well as microbial fermentation by-products could contribute towards the immune stimulation of the consumer. Due to their variation in degree of polymerization, degree of arabinose substitution, and ferulic acid substitution AX hydrolyzates are considerably diverse and complex molecules compared to many other prebiotic compounds. Thus, AXs and their hydrolyzates should be closely evaluated for their structurally driven biological properties especially related to their effect on gut bacteria and immunomodulatory aspects.

1.6. References

Abbas, A. K., and Lichtman, A. H., eds. (2011). "Basic immunology: functions and disorders of the immune system." Saunders Elsevier, Philadelphia, PA, USA.

Aimutis, T. M. P. W. R. (2011). "Nondigestible Carbohydrates and Digestive Health," 1/Ed. Wiley-Blackwell, Ames, Iowa, USA.

Akhtar, M., Tariq, A. F., Awais, M. M., Iqbal, Z., Muhammad, F., Shahid, M., and Hiszczynska-Sawicka, E. (2012). Studies on wheat bran Arabinoxylan for its immunostimulatory and protective effects against avian coccidiosis. *Carbohydrate Polymers* **90**, 333-339.

Apprich, S., Tirpanalan, û., Hell, J., Reisinger, M., Bohmdorfer, S., Siebenhandl-Ehn, S., Novalin, S., and Kneifel, W. (2014). Wheat bran-based biorefinery 2: Valorization of products. *LWT - Food Science and Technology* **56**, 222-231.

Bedford, M. R., and Schulze, H. (1998). Exogenous enzymes for pigs and poultry. *Nutrition Research Reviews* **11**, 91-114.

Biely, P., Vrsanska, M., Tenkanen, M., and Kluepfel, D. (1997). Endo-beta-1,4-xylanase families: differences in catalytic properties. *Journal of Biotechnology* **57**, 151-166.

Cani, P. D., Everard, A., and Duparc, T. (2013). Gut microbiota, enteroendocrine functions and metabolism. *Current Opinion in Pharmacology Gastrointestinal Endocrine and metabolic diseases* **13**, 935-940.

Cao, L., Liu, X., Qian, T., Sun, G., Guo, Y., Chang, F., Zhou, S., and Sun, X. (2011). Antitumor and immunomodulatory activity of arabinoxylans: A major constituent of wheat bran. *International Journal of Biological Macromolecules* **48**, 160-164.

Chan, G. C., Chan, W. K., and Sze, D. M. (2009). The effects of beta-glucan on human immune and cancer cells. *J Hematol Oncol* **2**, 1-11.

Collins, T., Gerday, C., and Feller, G. (2005). Xylanases, xylanase families and extremophilic xylanases. *FEMS Microbiology Reviews* **29**, 3-23.

Courtin, C. M., and Delcour, J. A. (2002). Arabinoxylans and Endoxylanases in Wheat Flour Bread-making. *Journal of Cereal Science* **35**, 225-243.

Courtin, C. M., Gys, W., Gebruers, K., and Delcour, J. A. (2005). Evidence for the Involvement of Arabinoxylan and Xylanases in Refrigerated Dough Syruping. *Journal of Agricultural and Food Chemistry* **53**, 7623-7629.

Dekker, R. F., and Richards, G. N. (1976). Hemicellulose: their occurrence, purification properties and mode of action. *Adv.Carbohydr.Chem.Biochem.* **32**, 277-352.

Delcenserie, V., Martel, D., Lamoureux, M., Amiot, J., Boutin, Y., and Roy, D. (2008). Immunomodulatory effects of probiotics in the intestinal tract. *Curr Issues Mol Biol* **10**, 37-54.

Delcour, J. A., and Hoseney, R. C. (2010a). Dry Milling. *In* "Principles of Cereal Science and Technology" (J. A. Delcour and R. C. Hoseney, eds.), pp. 121-137. AACC International, Inc., MN.

Delcour, J. A., and Hoseney, R. C. (2010b). Minor constituents. *In* "Principles of Cereal Science and Technology" (J. A. Delcour and R. C. Hoseney, eds.), pp. 71-84. AACC International, Inc., MN.

Dodd, D., Mackie, R. I., and Cann, I. K. (2011). Xylan degradation, a metabolic property shared by rumen and human colonic Bacteroidetes. *Molecular microbiology* **79**, 292-304.

Dornez, E., Gebruers, K., Delcour, J., and Courtin, C. (2009). Grain-associated xylanases: occurrence, variability, and implications for cereal processing. *Trends in food science & technology.* **20**, 495-510.

Fierens, E. (2007). TLXI, athaumatin-like xylanase inhibitor: isolation, characterisation and comparision with other wheat (*Triticum aestivum* L.) xylanase inhibiting proteins. Dissertation, Katholieke Universiteit Leuven, Belgium.

Frederix, S. A., Van hoeymissen, K. E., Courtin, C. M., and Delcour, J. A. (2004). Water-Extractable and Water-Unextractable Arabinoxylans Affect Gluten Agglomeration Behavior during Wheat Flour Gluten-Starch Separation. *Journal of Agricultural and Food Chemistry* **52**, 7950-7956.

Fukuda, S., Toh, H., Hase, K., Oshima, K., Nakanishi, Y., Yoshimura, K., Tobe, T., Clarke, J. M., Topping, D. L., Suzuki, T., Taylor, T. D., Itoh, K., Kikuchi, J., Morita, H., Hattori,

M., and Ohno, H. (2011). Bifidobacteria can protect from enteropathogenic infection through production of acetate. *Nature* **469**, 543-547.

Garcia, A. L., Otto, B., Reich, S. C., Weickert, M. O., Steiniger, J., Machowetz, A., Rudovich, N. N., Mohlig, M., Katz, N., Speth, M., Meuser, F., Doerfer, J., Zunft, H. J. F., Pfeiffer, A. H. F., and Koebnick, C. (2006). Arabinoxylan consumption decreases postprandial serum glucose, serum insulin and plasma total ghrelin response in subjects with impaired glucose tolerance. *Eur J Clin Nutr* **61**, 334-341.

Geissman, T., and Neukom, H. (1973). A note on ferulic acid as a constituent of water insoluble pentosans of wheat flour. *Cereal Chemistry* **50**, 414-416.

Gooding, M. J. (2009). The wheat crop. *In* "Wheat Chemistry and Technology" (K. Khan and P. R. Shewry, eds.), pp. 19-49. AACC International, Minnesota.

Grootaert, C., Delcour, J. A., Courtin, C. M., Broekaert, W. F., Verstraete, W., and Van de Wiele, T. (2007). Microbial metabolism and prebiotic potency of arabinoxylan oligosaccharides in the human intestine. *Trends in Food Science & Technology* 18, 64-71.

Hamer, H. M., Jonkers, D. M. A. E., Venema, K., Vanhoutvin, S. A. L. W., Troost, F. J., and BRUMMER, R. (2008). Review article: the role of butyrate on colonic function. *Alimentary pharmacology & therapeutics* **27**, 104-119.

Henrissat, B., Claeyssens, M., Tomme, P., Lemesle, L., and Mornon, J. P. (1989). Cellulase families revealed by hydrophobic cluster analysis. *Gene* **81**, 83-95.

Henrissat, B., and Coutinho, P. M. (2001). Classification of glycoside hydrolases and glycosyltransferases from hyperthermophiles. *In* "Methods in Enzymology.

Hyperthermophilic Enzymes Part A" (W. W. A. Michael, ed.), pp. 183-201. Academic Press.

Hromádková, Z., Paulsen, B. S., Polovka, M., Košťálová, Z., and Ebringerová, A. (2013). Structural features of two heteroxylan polysaccharide fractions from wheat bran with anti-complementary and antioxidant activities. *Carbohydrate Polymers* **93**, 22-30.

Iiyama, K., Lam, T. B. T., and Stone, B. A. (1994). Covalent cross-links in the cell wall. *Plant physiology* **104**, 315-320.

Jeffries, T. W. (2006). Engineering yeasts for xylose metabolism. *Current Opinion in Biotechnology Environmental biotechnology/Energy biotechnology* **17**, 320-326

Kagnoff, M. F. (1993). Immunology of the intestinal tract. *Gastroenterology* **105**, 1275-80.

Kau, A. L., Ahern, P. P., Griffin, N. W., Goodman, A. L., and Gordon, J. I. (2011). Human nutrition, the gut microbiome and the immune system. *Nature* **474**, 327-336.

Koropatkin, N. M., Cameron, E. A., and Martens, E. C. (2012). How glycan metabolism shapes the human gut microbiota. *Nature Reviews Microbiology* **10**, 323-335.

Kulkarni, N., Shendye, A., and Rao, M. (1999). Molecular and biotechnological aspects of xylanase. *FEMS Microbiology Reviews* **23**, 411-456.

Laere, K. M. J. V., Beldman, G., and Voragen, A. G. J. (1997). A new arabinofuranohydrolase from Bifidobacterium adolescentis able to remove arabinosyl residues from double-substituted xylose units in arabinoxylan. *Applied Microbiology and Biotechnology* 47, 231-235.

Lamichhane, A., Azegami, T., and Kiyono, H. (2014). The mucosal immune system for vaccine development. *Vaccine* **32**, 6711-6723.

Langkamp-Henken, B., Glezer, J. A., and Kudsk, K. A. (1992). Immunologic structure and function of the gastrointestinal tract. *Nutrition in clinical practice : official publication of the American Society for Parenteral and Enteral Nutrition* **7**, 100-108.

Ley, R. E., Bäckhed, F., Turnbaugh, P., Lozupone, C. A., Knight, R. D., and Gordon, J. I. (2005). Obesity alters gut microbial ecology. *Proceedings of the National Academy of Sciences of the United States of America* **102**, 11070-11075.

Ley, R. E., Turnbaugh, P. J., Klein, S., and Gordon, J. I. (2006). Microbial ecology: Human gut microbes associated with obesity. *Nature* **444**, 1022-1023.

Lombard, V., Golaconda, R. H., Drula, E., Coutinho, P. M., and Henrissat, B. (2014). The carbohydrarte-active enzyme database (CAZy) in 2013. Vol. 2014.

Mälkki, Y. (2004). Trends in dietary fibre research and development. *Acta Alimentaria* **33**, 39-62.

Mares, D. J., and Stone, B. A. (1973). Studies on wheat endosperm. I Chemical composition and ultrastructure of the cell wall. *Australian journal of biological sciences* **26**, 793-812.

Martens, E. C., Koropatkin, N. M., Smith, T. J., and Gordon, J. I. (2009). Complex Glycan Catabolism by the Human Gut Microbiota: The Bacteroidetes Sus-like Paradigm. *Journal of Biological Chemistry* **284**, 24673-24677.

Maynard, C. L., Elson, C. O., Hatton, R. D., and Weaver, C. T. (2012). Reciprocal interactions of the intestinal microbiota and immune system. *Nature* **489**, 231-241.

McCarter, J. D., and Stephen Withers, G. (1994). Mechanisms of enzymatic glycoside hydrolysis. *Current Opinion in Structural Biology* **4**, 885-892.

McNulty, N. P., Wu, M., Erickson, A. R., Pan, C., Erickson, B. K., Martens, E. C., Pudlo, N. A., Muegge, B. D., Henrissat, B., and Hettich, R. L. (2013). Effects of diet on resource

utilization by a model human gut microbiota containing Bacteroides cellulosilyticus WH2, a symbiont with an extensive glycobiome. *PLoS biology* **11**, e1001637.

Medzhitov, R. (2008). Origin and physiological roles of inflammation. *Nature* **454**, 428-435.

Mendis, M. (2012). Variability in arabinoxylan, xylanase activity and xylanase inhibitor levels in hard spring wheat, Cereal Science Program, North Dakota State University.

Meuser, F., and Suckow, P. (1986). Nonstarch polysaccharides. *In* "Chemistry and Physics of Baking" (J. M. V. Blanshard, P. J. Frazier and T. Galliard, eds.), pp. 42-61. The Royal Society of Chemistry, London, UK.

Mikkelsen, M. S., Jespersen, B. M., Mehlsen, A., Engelsen, S. B., and Frokiaer, H. (2014). Cereal bets-glucan immune modulating activity depends on the polymer fine structure. *Food Research International* **62**, 829-836.

Monobe, M., Maeda-Yamamoto, M., Matsuoka, Y., Kaneko, A., and Hiramoto, S. (2008). Immunostimulating activity and molecular weight dependence of an arabinoxylan derived from wheat bran. *Journal of the Japanese Society for Food Science and Technology-Nippon Shokuhin Kagaku Kogaku Kaishi* **55**, 245-249.

Mpofu, A., Sapirstein, H. D., and Beta, T. (2006). Genotype and Environmental Variation in Phenolic Content, Phenolic Acid Composition, and Antioxidant Activity of Hard Spring Wheat. *Journal of Agricultural and Food Chemistry* **54**, 1265-1270.

Neves, M. A. d., Kimura, T., Shimizu, N., and Shiiba, K. (2006). Production of alcohol by simultaneous saccharification and fermentation of low-grade wheat flour. *Brazilian Archives of Biology and Technology* **49**, 481-490.

Pollet, A., Delcour, J. A., and Courtin, C. M. (2010). Structural determinants of the substrate specificities of xylanases from different glycoside hydrolase families. *Critical reviews in biotechnology* **30**, 176-191.

Pruckler, M., Siebenhandl-Ehn, S., Apprich, S., Holtinger, S., Haas, C., Schmid, E., and Kneifel, W. (2014). Wheat bran-based biorefinery 1: Composition of wheat bran and strategies of functionalization. *LWT-Food Science and Technology* **56**, 211-221.

Reilly, P. J. (1981). Xylanase: Structure and Function. *In* "Trends in the Biology of Fermentation for Fuels and Chemicals." (A. Hollaender, ed.), pp. 111-129. Basic Life Sciences, Plenum Press, New York.

Rieder, A., and Samuelsen, A. B. (2012). Do cereal mixed-linked beta-glucans possess immune-modulating activities? *Molecular nutrition & food research* **56**, 536-547.

Rombeau, J. L., and Kripke, S. A. (1990). Metabolic and Intestinal Effects of Short-Chain Fatty Acids. *Journal of Parenteral and Enteral Nutrition* **14**, 181S-185S.

Rose, D. J., Patterson, J. A., and Hamaker, B. R. (2010). Structural differences among alkali-soluble arabinoxylans from maize (Zea mays), rice (Oryza sativa), and wheat (Triticum aestivum) brans influence human fecal fermentation profiles. *Journal of Agricultural and Food Chemistry* **58**, 493-499.

Rye, C. S., and Withers, S. G. (2000). Glycosidase mechanisms. *Current Opinion in Chemical Biology* **4**, 573-580.

Saha, B. C. (2000). Alpha-L-arabinofuranosidases: biochemistry, molecular biology and application in biotechnology. *Biotechnol Adv* **18**, 403-23.

Samuelsen, A. B., Rieder, A., Grimmer, S., Michaelsen, T. E., and Knutsen, S. H. (2011). Immunomodulatory activity of dietary fiber: arabinoxylan and mixed-linked beta-glucan

isolated from barley show modest activities in vitro. *International journal of molecular sciences* **12**, 570-587.

Saulnier, L., Sado, P. E., Branlard, G., Charmet, G., and Guillon, F. (2007). Wheat arabinoxylans: Exploiting variation in amount and composition to develop enhanced varieties. *Journal of Cereal Science* **46**, 261-281.

Schley, P. D., and Field, C. J. (2002). The immune-enhancing effects of dietary fibres and prebiotics. *British Journal of Nutrition* **87**, S221-S230.

Simpson, D. J., Fincher, G. B., Huang, A. H. C., and Cameron-Mills, V. (2003). Structure and Function of Cereal and Related Higher Plant (1→4)-β-Xylan Endohydrolases. *Journal of Cereal Science* **37**, 111-127.

Simsek, S., and Ohm, J. B. (2009). Structural changes of arabinoxylans in refrigerated dough. *Carbohydrate Polymers* **77**, 87-94.

Sorensen, H. R., Jorgensen, C. T., Hansen, C. H., Jorgensen, C. I., Pedersen, S., and Meyer, A. S. (2006). A novel GH43 alpha-L-arabinofuranosidase from Humicola insolens: mode of action and synergy with GH51 alpha-L-arabinofuranosidases on wheat arabinoxylan. *Appl Microbiol Biotechnol* **73**, 850-61.

Taylor, E., Smith, N., Turkenburg, J., D'souza, S., Gilbert, H., and Davies, G. (2006). Structural insight into the ligand specificity of a thermostable family 51 arabinofuranosidase, Araf51, from Clostridium thermocellum. *Biochem.J* **395**, 31-37.

Tremaroli, V., and Backhed, F. (2012). Functional interactions between the gut microbiota and host metabolism. *Nature* **489**, 242-249.

Tsuji, M., Suzuki, K., Kitamura, H., Maruya, M., Kinoshita, K., Ivanov, I. I., Itoh, K., Littman, D. R., and Fagarasan, S. (2008). Requirement for Lymphoid Tissue-Inducer Cells in

Isolated Follicle Formation and T Cell-Independent Immunoglobulin A Generation in the Gut. *Immunity* **29**, 261-271.

Tzianabos, A. O. (2000). Polysaccharide immunomodulators as therapeutic agents: structural aspects and biologic function. *Clin Microbiol Rev* **13**, 523-33.

Van den Broek, L., Lloyd, R., Beldman, G., Verdoes, J., McCleary, B., and Voragen, A. (2005). Cloning and characterization of arabinoxylan arabinofuranohydrolase-D3 (AXHd3) from Bifidobacterium adolescentis DSM20083. *Applied Microbiology and Biotechnology* **67**, 641-647.

Volman, J. J., Ramakers, J. D., and Plat, J. (2008). Dietary modulation of immune function by beta-glucans. *Physiology & behavior* **94**, 276-284.

Walter, J., and Ley, R. (2011). The Human Gut Microbiome: Ecology and Recent Evolutionary Changes. *Annual Review of Microbiology* **65**, 411-429.

Wardwell, L. H., Huttenhower, C., and Garrett, W. S. (2011). Current concepts of the intestinal microbiota and the pathogenesis of infection. *Current infectious disease reports* **13**, 28-34.

Wong, K. K. Y., Tan, L. U. L., and Saddler, J. N. (1988). Multiplicity of beta-1,4-xylanase in microorganisms: functions and applications. *Microbiol.Rev.* **52**, 305-317.

Xu, H. (2012). Influence of the structural complexicity of cereal arabinoxylans on human fecal fermentation and their degradation mechanism by gut bacteria. Dissertation, Purdue University, Indiana.

Xu, X., Xu, P., Ma, C., Tang, J., and Zhang, X. (2013). Gut microbiota, host health, and polysaccharides. *Biotechnology Advances* **31**, 318-337.

Zechel, D. L., and Withers, S. G. (1999). Glycosidase Mechanisms: Anatomy of a Finely Tuned Catalyst. *In* "Accounts of Chemical Research", Vol. 33, pp. 11-18. American Chemical Society.

Zhang, M., Chekan, J. R., Dodd, D., Hong, P. Y., Radlinski, L., Revindran, V., Nair, S. K., Mackie, R. I., and Cann, I. (2014). Xylan utilization in human gut commensal bacteria is orchestrated by unique modular organization of polysaccharide-degrading enzymes. *Proceedings of the National Academy of Sciences* **111**, E3708-E3717.

Zhou, S., Liu, X., Guo, Y., Wang, Q., Peng, D., and Cao, L. (2010). Comparison of the immunological activities of arabinoxylans from wheat bran with alkali and xylanase-aided extraction. *Carbohydrate Polymers* **81**, 784-789.

CHAPTER 2. PRODUCTION OF STRUCTURALLY DIVERSE WHEAT ARABINOXYLAN HYDROLYZATES USING COMBINATIONS OF XYLANASE AND ARABINOFURANOSIDASE

2.1. Abstract

Arabinoxylan (AX) is the predominant polysaccharide in the cell wall of wheat grain. It consists mainly of a xylan backbone on which arabinose side groups are substituted on some xylose. Xylanase and arabinofuranosidase are the main enzymes involved in hydrolysis of AX. The current research was carried out to generate thirty structurally different wheat arabinoxylan hydrolyzates (AXH) by means of different combinations of xylanases (*Cellvibrio japonicas* xylanase (CJX) and *Aspergillus niger* xylanase (ANX)) and arabinofuranosidases (*Bifidobacterium adolescentis* arabinofuranosidase (BAF) and *Clostridium thermocellum arabinofuranosidase* (CAF)). The AXH were grouped into four groups based on the initial enzymatic treatment (ANX, CJX, CAF and BAF series). The AXH were analyzed using GC-FID, GC-MS, ^{1}H-NMR and SEC-MALS techniques to elucidate composition and structural details. In general, the AXH had high proportion of unsubstituted xylose and lesser amount of di- or mono-substituted xylose. The average molecular weights of the AXH varied between 0.78-5.64 million Da. Between the two xylanases, ANX might be an enzyme of choice for the production of arabinoxylan hydrolyzates with simple structural details while, CJX might be selected for the production of arabinoxylan hydrolyzates with more complex structural features. Addition of BAF followed by CAF is more effective in generating AXH with higher amounts of unsubstituted xylose as well as lesser amounts of disubstituted xylose. The CJX series resulted in lower molecular weights compared to ANX series. CAF series yielded larger polysaccharides

compared to the BAF series. Overall, the BAF series gave the lowest polydispersity index values followed by CAF series while the ANX and CJX series had higher polydispersity index values.

The enzymatic treatments applied in the current research effectively generated thirty different arabinoxylan hydrolyzates. The information derived about the capabilities of the two xylanases and two arabinofuranosidase could provide important information in choices made regarding enzymes used to generate arabinoxylan hydrolyzates with specific structural details. Also, these hydrolyzates could be useful as substrate for future research exploring the effect of fine structural details in arabinoxylan hydrolyzates on their biological and physical properties.

2.2. Introduction

Arabinoxylan (AX) is the predominant polysaccharide in the cell wall of wheat grain (Saulnier et al., 2007). It consists of a backbone of β-(1,4)-linked xylose residues, which are substituted with arabinose residues on the C(O)-2 and/or C(O)-3 position (Dornez et al., 2009). Since AX is mainly composed of xylose and arabinose, it is commonly referred to as pentosans. Phenolic acids such as ferulic acid can be ester linked on the C(O)-5 position of arabinose (Figure 1.2). Due to the complex structure of AX it is evident that the degradation of the molecule requires a diverse array of enzymes with varying substrate specificities. Endo-β-(1,4)-d-xylanases (EC 3.2.1.8, xylanase) are the major enzymes involved in AX degradation. They cleave AX by internally hydrolyzing the 1,4- β-D-xylosidic linkage between xylose residues in the xylan backbone (Collins et al., 2005; Dornez et al., 2009) giving rise to arabinoxylan hydrolyzates (AXH) of different degree of polymerization (DP). The enzyme α-l-arabinofuranosidases (EC 3.2.1.55) remove arabinose substituents from the xylan backbone (Dornez et al., 2009) yielding AX of different degree of arabinose substitution (DS). Thus, treatment of AX polysaccharide with various xylanase and arabinofuranosidase can yield AXH

with variable DP and DS. Most of the glycoside hydrolases that are classified in Glycoside hydrolase family 10 (GH10) are endo-β-1,4-xylanases (e.g. endo-1,4-β-xylanase from *Cellvibrio japonicus*) (Pollet et al., 2010). GH10 xylanases attack both linear substrates as well as substituted heteroxylans. They attack the xylosidic linkage next to a single or double substituted xylose toward the non-reducing end and require two unsubstituted xylose residues between branched residues (Figure 2.2). Thus, it can hydrolyze AX with high degree of substitution (DS) into smaller fragments. GH11 xylanase (e.g. endo-1,4-β-xylanase M4 from *Aspergillus niger*) exclusively consist of true endo-β-1,4-xylanases that cleave internal β-1,4-xylosidic bonds and preferably cleave unsubstiuted regions of the backbone (Pollet et al., 2010). GH11 cannot attack the xylosidic linkage toward the non-reducing end next to a branched xylose and require three unsubstituted consecutive xylose residues for hydrolysis (Figure 1.6). Hence, GH11 xylanases have a low activity on heteroxylans with a high DS. Only C3-linked arabinose residues from double-substituted xylose residues are hydrolyzed by Arabinoxylan arabinofuranohydrolase from *Bifidobacterium adolescentis* (GH 43) (van den Broek et al., 2005) while α-L-arabinofuranosidase from *Clostridium thermocellum* (GH51) catalyses the hydrolysis of "α-1,5-linked arabino-oligosaccharides and the α-1,3 arabinosyl side chain decorations of xylan with equal efficiency" (Taylor et al., 2006). Thus, it is also highly efficient in the removal of the α-1,3-linked arabinoside substitutions from wheat arabinoxylan itself (Taylor et al., 2006).

There is a growing awareness for the production of dietary fibers and prebiotics with health benefits. The production of structurally defined fibers from plant polysaccharides such as wheat AX is highly encouraged. Thus, based on the enzymatic specificities, we wanted to investigate how these enzymes could be utilized to produce hydrolysis products of desired characteristics. Similar approaches to produced enzymatically tailored AX hydrolyzates from

corn AX had been previously reported (Xu, 2012). However there are significant structural differences between wheat AX and corn AX (Rose et al., 2010). Alkaline extractable AX from wheat bran has large proportion of unsubstituted xylose regions compared to corn and rice bran AX (Rose et al., 2010). Thus, the objective of this research was to produce structurally different arabinoxylan hydrolyzates (AXH) derived from wheat AX by means of enzymatic treatments. The insight we get about the capabilities of the enzymes used in the current study might benefit many industries (Beg et al., 2001; Clarke et al., 1997; Falck et al., 2013; Spagna et al., 1998) that employ different xylanases and arabinofuranosidases.

2.3. Materials and Methods

2.3.1. Materials

Wheat samples were of variety Glenn grown in Casselton, ND in 2011. Heat stable α-amylase from *Bacillus licheniformis* (Termamyl ® 120, 1186 units/mg protein; 19.8 mg protein/ mL; A-3403-1MU) and protease from *Bacillus amyloliquefaciens* (P-1236-50 ML) were purchased from Sigma-Aldrich Inc. (Saint Louis, MO). Endo-1,4-β-xylanase (*Cellvibrio japonicus*) (EC 3.2.1.8; CAZY Family: GH10; Cat. No: E-XYNACJ), endo-1,4-β-xylanase M4 (*Aspergillus niger*)(EC 3.2.1.8; CAZY Family: GH11; Cat. No: E-XYAN4), α-L-arabinofuranosidase (*Clostridium thermocellum*) EC 3.2.1.55; CAZy family: GH51; Cat. No: E-ABFCT) and α-L-arabinofuranosidase (novel specificity) (*Bifidobacterium adolescentis*) (EC 3.2.1.55; CAZy Family: GH43; Cat. No: E-AFAM2) were purchased from Megazyme International Ireland, Wicklow, Ireland. All the other chemicals were of analytical grade.

2.3.2. Procedure for arabinoxylan hydrolyzate preparation

2.3.2.1. Preparation of wheat bran for arabinoxylan extraction

Wheat variety Glenn was used to extract arabinoxylans from wheat bran. The whole grain was milled in a Bühler MLU-202 mill (Bühler Industries Inc., Uzwil, Switzerland) and bran fraction was collected. The bran was then sieved on No 35 (500 micrometer mesh) sieve (100 g each for four minutes). This was done to further remove any flour remaining with the bran. The sieved bran was stored at 4 ^{o}C until further treatment. The bran was then ground using a hammer laboratory mill 3100 equipped with a 0.8 mm screen (Perten Instruments North America, Inc.) The ground bran was stored at 4 ^{o}C.

2.3.2.2. Production of partially defatted wheat bran

Ground wheat bran (500 g) was extracted with hexane (2 L) for two hours on a Orbit shaker (Lab-Line instrumnts Inc. Melrose Park, IL, USA). The material was then filtered through Watmann No 1 filter paper using vacuum and dried under the hood for two days until no hexane smell was detected. The resulting material was called partially defatted bran (PDB) and was stored at 4 ^{o}C until further treatment.

2.3.2.3. Production of destarched and deprotinized bran

Preparation of destarched deprotinized bran was carried out according to the method described by Rose et al., (2010) with some modifications. Partially defatted bran (250 g) was mixed with deionized water (2 L) and pH was adjusted to pH 7.0 using 1M NaOH. The solution was then boiled for 20 min. to inactivate the endogenous enzymes. Then 250 µL of heat stable α-amylase from *Bacillus licheniformis* was added. Starch was hydrolyzed at 90-95 ^{o}C for 2 h, and then cooled in an ice bath to 50 ^{o}C. The pH was adjusted to 6.0 using 1 M HCl, and 10 mL of

protease was added and protein was hydrolyzed at 50 ^{o}C for 4 h with shaking (200 strokes/min) in a water bath (Type: 89032, VWR International, PA, USA). Next, the enzymes were inactivated by boiling the mixture for 30 min. and were cooled in an ice bath to room temperature and pH was adjusted to 7.0. The slurry was centrifuged at 3000*g* for 15 min. The residue was termed destarched, deprotenized wheat bran (DSDPB) and stored in freezer (-4 ^{o}C) until further purification.

2.3.2.4. Alkaline-hydrogen peroxide extraction

Alkaline hydrogen peroxide extraction of the DSDPB was carried out as previously described by Rose et al., (2010) with some modifications. Destarched deprotinized bran (half of the slurry: ~100g) was suspended in 1L of 1M sodium hydroxide using a conical flask of 4L, allowing space for foam generation during hydrogen peroxide addition. Under constant mixing at 60 ^{o}C, 42 mL of 30% hydrogen peroxide was slowly added to the mixture and was stirred for 4 h at 60 ^{o}C using magnetic stir bars. The resulting slurry was centrifuged at 3000*g* for 15 min at 20 ^{o}C. The pellet was discarded and three volumes of ethanol (95% v/v) were added to the supernatant. The mixture was held overnight at 4 ^{o}C, and then the aqueous ethanol portion, containing the liberated ferulic acid, was siphoned off as much as possible and discarded. When separation of precipitate and supernatant was difficult the remainder of the mixture was centrifuged at 3000*g* for 15 min at 20 ^{o}C. The precipitated material was collected on to a Buchner funnel and washed with ethanol (80% v/v), anhydrous ethanol and acetone. The resulting material was air-dried until no solvent could be detected by odor. The material was termed alkaline extractable arabinoxylans (AE-AX).

2.3.2.5. Further purification of alkaline extractable arabinoxylans

To further purify the AE-AX, treatments with alpha amylase, protease, ethanol precipitation and washing were repeated. In detail, AE-AX (125g) was dissolved in 1L of deionized water. The pH was adjusted to 7 and boiled for 20 min to bring the internal temperature to 90-95 ^{o}C. Then 125 µL of heat stable α-amylase (Termamyl ® 120, 1186 units/mg protein; 19.8 mg protein/ mL; A-3403-1MU, Sigma-Aldrich Inc. Saint Louis, MO) was added. Starch was hydrolyzed at 90-95 ^{o}C for 2 h, and then mixture was cooled in an ice bath to 50 ^{o}C. The pH was adjusted to 6.0 using 1 M HCl, and 5 mL of protease was added and protein was hydrolyzed at 50 ^{o}C for 4 h with shaking (200 strokes/min) in a water bath. Next, the enzymes were inactivated by boiling the mixture for 30 min. the mixture was cooled in an ice bath to room temperature and pH was adjusted to 7.0. The slurry was centrifuged at 3000*g* for 15 min and the pellet was collected. The pellet was termed destarched deprotinized AE-AX. Then 1.25 L of 1M NaOH was added to the pellet and mixed for 30 min at 60 ^{o}C. The resulting slurry was centrifuged at 3000*g* for 15 min at 20 ^{o}C. The pellet was discarded and three volumes of ethanol (95% v/v) were added to the supernatant. The mixture was held overnight at 4 ^{o}C, and then the aqueous ethanol portion, containing the liberated ferulic acid, was siphoned off as much as possible and discarded. When separation of precipitate and supernatant was difficult the remainder of the mixture was centrifuged at 3000*g* for 15 min at 20 ^{o}C. The precipitated material was collected on to a Buchner funnel and washed with ethanol (80% v/v), anhydrous ethanol and acetone. The resulting material was air-dried until no solvent could be detected by odor. The air-dried material was ground in a small electrical blender (Model 51BL30, Waring Commercial, Torrington, CT, USA) to produce a powder. The resulting powder was the purified wheat arabinoxylan (WAX) and was used in the preparation of different arabinoxylan

hydrolyzates. A schematic representation of the process involved in the production of arabinoxylan hydrolyzates is given in Figure. 2.1.

2.3.2.6. Preparation of arabinoxylan hydrolyzates (AXH)

Wheat arabinoxylan hydrolyzates were prepared by the methods described by Verwimp et al., (2007), Xu, (2012) and Sorensen et al., (2003) with some modifications. Each AXH was prepared using different combinations of xylanase and arabinofuranosidases enzyme. WAX (1 g) was mixed with sodium acetate buffer (50 mL, 25mM, pH 5.5) and homogenized using a homogenizer (Polytron PT10-35 by Kinematica AG, Switzerland) for few minutes. Endo-1,4-β-Xylanase (*Cellvibrio japonicus*) (CJX) (4µL) was added to the mixture and immediately boiled for 15 min. to inactivate the enzymes and centrifuged at 10,000g for 30 min. The residue was discarded. Four volumes of absolute ethanol was added to the supernatant under continuous stirring and allowed to sit for 15 min. for arabinoxylan hydrolyzate to precipitate. The precipitate was collected by centrifuging at 10,000g for 15 min. The pellet was air dried until no ethanol smell was detected and freeze dried to obtain the first arabinoxylan hydrolyzate called CJX-1-P. The procedure was repeated using endo-1,4-β-Xylanase M4 (*Aspergillus niger*) (ANX) (2µL) as the starting enzyme to produce ANX-1-P.

In a similar way WAX (1 g) was mixed with sodium acetate buffer (50 mL, 25mM, pH 5.5) and homogenized using a homogenizer for few minutes. Endo-1,4-β-Xylanase (*Cellvibrio japonicus*) (CJX) (4µL) was added to the mixture and incubated at 50 ^{0}C with continuous shaking at 150 rpm in a water bath for 3 hours. The mixture was boiled for 15 min. to inactivate the enzymes and centrifuged at 10,000g for 30 min. The residue was discarded. Four volumes of absolute ethanol was added to the supernatant under continuous stirring and allowed to sit for 15 min. for arabinoxylan hydrolyzate to precipitate. The precipitate was collected by centrifuging at

10,000g for 15 min. The pellet was air dried until no ethanol smell was detected and freeze dried to obtain arabinoxylan hydrolyzate called CJX-2-P. Similarly, a series of AXH was prepared. In CAF series the first enzyme treatment was with α-L-Arabinofuranosidase (*Clostridium thermocellum*) (CAF) (8 µL) followed by other enzymes while in BAF series the first enzymes treatment was with α-L-Arabinofuranosidase (novel specificity) (*Bifidobacterium adolescentis*) (BAF) (10 µL). A summary of the treatments and the abbreviation given to the resulting AXH is given in Table 2.1.

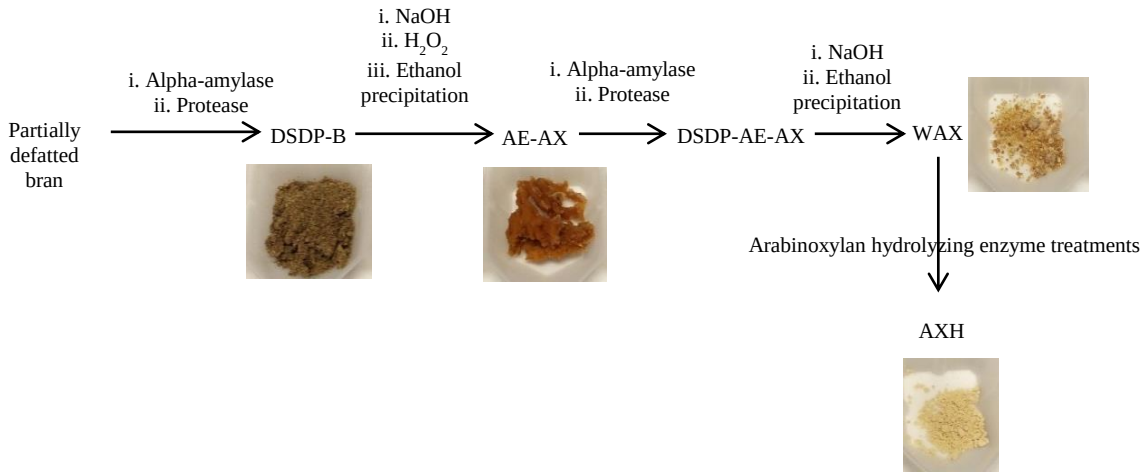

Figure 2.1. Schematic representation of the process involved in the production of arabinoxylan hydrolyzates. DSDP-B, destarched deprteinized bran; AE-AX, alkaline extractable arabinoxylan; DSDP-AE-AX, destarched deproteinized alkaline extractable arabinoxylans; WAX, wheat arabinoxylan; AXH, arabinoxylan hydrolyzates. Each treatment indicated on the arrows was applied consecutively in the order of listing.

2.3.3. Chemical analysis

2.3.3.1. Determination of sugar composition and arabinose to xylose ratio (A/X) of arabinoxylan hydrolyzates using gas chromatography (GC)

Sugar composition and the ratio between arabinose to xylose in arabinoxylans in AXH were determined following acid hydrolysis and preparation of alditol acetates as described by Blakeney et al., (1983).

2.3.3.1.1. *Hydrolysis*

To hydrolyze the polysaccharide to its monomeric constituents (Fox et al., 1989), samples (7 mg) were hydrolyzed with Trifluoroacetic acid (TFA) (2 M, 250 µL) for 1 h at 121 ^{o}C. Myo-Inositol (75 µL of 10 mg/mL solution) was added to the hydrolyzed samples as an internal standard and dried under nitrogen (Gys et al., 2003). The excess acid was neutralized by adding NH_4OH (1 M, 100 µL). The resulting mixture contains the hydrolyzed products.

2.3.3.1.2. *Reduction*

The hydrolyzed samples were reduced by adding sodium borohydride ($NaBH_4$) in a dimethylsulfoxide (DMSO) solution (20 mg/mL, 500 µL) (Blakeney et al., 1983). In this step, the aldose form of the sugars is reduced to an alditol by $NaBH_4$ (Fox et al., 1989). If this reduction is not carried out the acetylation of ring form of aldose complicates the chromatogram (in aqueous solution aldoses exist in equilibrium between ring form and open chain but alditols only occur as open chain). After reduction to alditols, excess $NaBH_4$ was decomposed by the addition of glacial acetic acid (ca. 300 µL).

2.3.3.1.3. *Acetylation*

Alditol acetates were prepared according to the method described by Blakney et al., (1983) for the preparation of alditol acetates for monosaccharide analysis. 1-methylimidazol (100

µL) was added as a catalyst for the acetylation reaction (Blakeney et al., 1983; Fox et al., 1989). Acetic anhydride (500 µL) was added to the reduced monosaccharides and the contents were mixed. The reaction was stopped with the addition of 4 mL of H_2O. The acetylated monosaccharides were extracted twice with methylene chloride (1 mL). The methylene chloride was evaporated under N_2. The residue was dissolved in acetone (1 mL) and transferred to vials for analysis in GC. Arabinose and xylose were used as monosaccharide standards in the analysis. *Myo*-inositol was used as the internal standard. The derivatized alditol acetate samples were analyzed on a Hewlet Packard 5890 series II GC system with a flame ionization detector (FID) (Agilent Technologies, Inc. Santa Clara, CA).

Supelco SP-2380 fused silica capillary column (30 m × 0.25 mm × 2 µm) (Supelco Bellefonte, PA) was used in the GC system. The system parameters were as follows: flow rate of 0.8 mL/min, 82737 Pa flow pressure, oven temperature of 100 ^{o}C, 250 ^{o}C of detector temperature, and 230 ^{o}C of injector temperature. The carrier gas was Helium.

2.3.3.2. Determination of weight average molecular weight of arabinoxylan hydrolyzates using HPLC-MALS-RI system

The weight average molecular weight (M_w) and polydispersity index, defined by the ratio M_w/M_n, where M_w represents the weight average molar mass and M_n the number average molar mass, of arabinoxylan hydrolyzates were determined according to the method of Storsley et al., (2003), with some modifications.

Table 2.1. Summarized information about the sequence of treatments and the abbreviation given to each AXH.

Treatment[1]	Abbreviation of the AXH
ANX-Series	
ANX → 0 h	ANX-1
ANX → 3h	ANX-2
ANX → 6 h	ANX-3
ANX → 12h	ANX-4
ANX → 24 h	ANX-5
ANX → 24 h → BAF → 6 h	ANX-6
ANX → 24 h → BAF → 6 h → CAF → 6 h	ANX-7
ANX → 24 h → CAF → 6 h	ANX-8
ANX → 24 h → CAF → 6 h → BAF → 6 h	ANX-9
CJX- Series	
CJX → 0 h	CJX-1
CJX → 3h	CJX-2
CJX → 6 h	CJX-3
CJX → 12h	CJX-4
CJX → 24 h	CJX-5
CJX → 24 h → BAF → 6 h	CJX-6
CJX → 24 h → BAF → 6 h → CAF → 6 h	CJX-7
CJX → 24 h → CAF → 6 h	CJX-8
CJX → 24 h → CAF → 6 h → BAF → 6 h	CJX-9
BAF-Series	
BAF → 6 h	BAF-1
BAF → 6 h → CJX → 24 h	BAF-2
BAF → 6 h → ANX → 24 h	BAF-3
BAF → 6 h → CAF → 6 h	BAF-4
BAF → 6 h → CAF → 6 h → CJX → 24 h	BAF-5
BAF → 6 h → CAF → 6 h → ANX → 24 h	BAF-6
CAF-Series	
CAF → 6 h	CAF-1
CAF → 6 h → CJX → 24 h	CAF-2
CAF → 6 h → ANX → 24 h	CAF-3
CAF → 6 h → BAF → 6 h	CAF-4
CAF → 6 h → BAF → 6 h → CJX → 24 h	CAF-5
CAF → 6 h → BAF → 6 h → ANX → 24 h	CAF-6

[1]Enzymatic treatments were carried out using the following enzymes: ANX, endo-1,4-β-Xylanase M4 (*Aspergillus niger*); CJX, Endo-1,4-β-Xylanase (*Cellvibrio japonicus*); BAF, α-L-Arabinofuranosidase (novel specificity) (*Bifidobacterium adolescentis*); CAF, α-L-Arabinofuranosidase (*Clostridium thermocellum*).

Arabinoxylan hydrolyzate (4 mg) was dissolved in deionized water (filtered via 0.1 µm filter) by heating at 40 ^{o}C with continuous stirring for few minutes. The sample solution was then filtered via 1.5 µm filter. Analysis was done on an Agilent 1200 high performance liquid chromatograph (HPLC) with refractive index detector (RI) and a Wyatt Dawn Helios-II multi-angle light scattering (MALS) detector. 300 kDa pullulan was used for normalization of the MALS detector. Shodex OHpak guard column and Shodex SB 806-HQ column were used. Water at 0.5ml/ml flow rate was used as the mobile phase. The calculation of M_w and polydispersity index (M_w/M_n) were performed by Astra 6.0.5 software (Wyatt Technology), based on the Debye plot with a second-order polynomial fit. Water at 0.5mL/min flow rate was used as the mobile phase. Values of d*n*/d*c*, defined as the proportional change in refractive index with change in polymer concentration were assumed to be 0.146 for arabinoxylans, as determine by Dervilly et al., (2000).

2.3.3.3. Determination of arabinose substitution pattern using proton nuclear magnetic resonance (^{1}H-NMR) spectroscopy

Arabinoxylan hydrolyzate polysaccharides (5 mg) were dissolved in D_2O (600 µL) by heating at 40 ^{o}C with continuous stirring on a heating/ stirring module (Reacti-therm III #18823, Thermo Scientific, USA). The samples were then freeze-dried. The dissolving and freeze-drying steps were repeated two more times and the final freeze dried sample was dissolved in D_2O (650 µL) and used for NMR analysis. The spectra were recorded on a 400 MHz spectrometer (Bruker AV3 HD 400 MHz NMR with a 5 mm PABBO BB/19F-!H/D Z-GRD Z probe) at 80 ^{o}C. Data were analyzed using the TopSpin 3.2 software (Bruker BioSpin Corporation, Billerica, MA. Partial structural assignment of peaks was made by comparison with previously published data (Hoffmann et al., 1992; Rose et al., 2010).

2.3.3.4. Linkage analysis of arabinoxylan hydrolyzates using GC-MS

Linkage analysis was performed according to the method described by Carpita and Shea (1989) with some modifications: Dried samples (3 mg) were dissolved in anhydrous DMSO (250 µL), and methylated. The methylated samples were hydrolyzed using 2N trifluoroacetic acid (250 µL) at 121 ^{o}C for 1 h. The hydrolyzed samples were dried under N_2 and dissolved in ammonium hydroxide (1M, 100 µL) and 500 µL of DMSO containing 20 mg/mL of sodium borodeuteride was added and incubated at 40 ^{o}C for 90 min. Six to nine drops of glacial acetic acid were added to the mixture to stop the reduction reaction following incubation. 1-methylimidazole (100 µL) and acetic anhydride (500 µL) were added for acetylation. Partially methylated alditol acetates in acetone were quantified by GC-MS (Model no 6890N Network GC System and 5973 Mass Selective detector, Agilent technologies, Inc., Santa Clare, CA) using a Restek™ RTX™-35 MS (Thermo Fisher Scientific Inc. MA, USA) capillary column (injector volume, 2µL; injector temperature, 250 ^{o}C; detector temperature, 250 ^{o}C; carrier gas, Helium; rate,1.0 mL/min; split ratio10:1; temperature program 170 ^{o}C for 2 min., 3 ^{o}C/min. to 250 ^{o}C, 250 ^{o}C for 2 min.; run time 30.67 min.). Data processing was carried out using Enhanced ChemStation software (MSD Chem Station D.01.00, Agilent technologies, Inc., Santa Clare, CA).

2.3.4. Statistical analysis

The data are presented as the means ± SE and were subjected to one way ANOVA using LSD test procedure employing Statistical Analysis System software package version 9.4 (SAS Institute, Cary, NC). A least significant difference (LSD) with a 5 % significance level was used to declare differences. Differences were considered significant when the probability value *p* was

lower than 0.05. Pearson's correlation analysis was conducted to evaluate relationships between AXH composition/structural details.

The 30 AXH samples were grouped into four groups (ANX series, CJX series, CAF series and BAF series) according to the first hydrolysis enzyme applied to generate each series. Canonical discriminant analysis (CDA) was performed on data expressing chemical/fine structural details (e.g. total AX %, A/X ratio, resonance integration results from ^{1}H-NMR, linkage analysis data from GC-MS) in each AXH (independent variables), in order to classify different types of AXH (grouping variable): ANX, CJX, CAF and BAF. The statistical analysis of the data was performed using 'CANDISC' procedure in SAS (V. 9.2, SAS Institute, Cary, NC).

2.4. Results and Discussion

2.4.1. Sugar composition

The sugar composition and the A/X ratio of the WAX and the resulting AXH are given in Table 2.2. A sample chromatogram obtained for the AXH after GC-FID analysis is shown in Appendix A. The samples consisted predominantly of xylose (14.36-38.77%), followed by arabinose (8.26-18.79%). Glucose was found to a lesser amount (2.26-4.85%) and traces of galactose (0.18-0.83%) were also detectable. The wheat AX (WAX) which was the starting substrate for the rest of the AXH had low amount of total AX and A/X ratio compared to the rest of the arabinoxylan hydrolyzate (AXH) samples. The treatment of WAX with the xylanase and arabinofuranosidase enzymes and the subsequent treatments could have yielded a much purer arabinoxylan sample compared to the starting material, WAX because the AXH samples have undergone an extra ethanol precipitation step compared to WAX and this extra step results in

much more pure AX. This could be the reason behind the apparent increase in the total AX % in the AXH compared to the WAX.

In the ANX series, as expected most of the AXH samples that underwent treatment with arabinofuranosidase, the enzymes that hydrolyze the arabinose substitution from xylose backbone (ANX-6, ANX-7 and ANX-8) resulted in lower A/X ratio compared to treatments receiving only xylanase treatment (ANX-5) due to the removal of arabinose by the debranching enzymes. Surprisingly, ANX-9 which was treated with ANX; followed by CAF; followed by BAF resulted in higher A/X ratio compared to the rest of the samples in ANX series. However, upon a closer look, it could be noted that the higher A/X ratio is not due to higher arabinose content but rather due to reduced xylose content.

In the CJX series, treatment with BAF in CJX-6 gave higher A/X ratio compared to CJX-5 (the treatment that didn't undergo hydrolysis by arabinofuranosidase). However, here again a lower xylose content could be responsible for the higher A/X ratio. But rest of the debranched treatments gave similar or lower A/X ratios (CJX-7, CJX-8 and CJX-9) as expected due to the removal of arabinose from the xylose backbone.

Overall in both ANX and CJX series the debranching with CAF gave lower A/X compared to debranching with BAF: ANX-6 vs. ANX-8 and CJX-6 vs. CJX-8. Thus, CAF might be the better enzyme choice to debranch AX that has already undergone depolymerization by xylanase.

When the CAF and BAF series were compared, treatment of WAX with CAF (CAF-1) gave slightly higher A/X ratio (0.53) compared to treatment of WAX with BAF (BAF-1) (0.52). Also, the arabinose content in CAF-1 (14.24%) was higher than that for BAF-1 (11.02%). This indicates that BAF removed more arabinose side groups from WAX compared to CAF. When

the substrate specificity of the two enzymes are considered, BAF releases only C3-linked arabinose residues from double-substituted xylose residues (van den Broek et al., 2005) while CAF catalyzes the hydrolysis of C3-linked arabinosyl side chain of xylan (Taylor et al., 2006). Also, this hydrolysis of C3-linked arabinose by CAF might be on monosubstituted xylose as observed for other similar arabinofuranosidases belonging to same GH family as CAF (Sorensen et al., 2006). Based on fine structural details of wheat bran AX, it is suggested that it possess large proportion of disubstituted xylose regions (Rose et al., 2010). Thus, the BAF might have an advantage over CAF because higher proportion of disubstituted xylose might provide BAF with higher substrate to act upon. Since CAF did seem to have this advantage coming from disubstituted xylose, we suggest that CAF has a higher possibility of being an rabinofuranosidase that only hydrolyze C3 linked arabinose from monosubstituted xylose falling into place with other GH51 arabinofuranosidases. The discrepancies observed with some of the expected outcomes and the results obtained for the A/X ratio might also be due to the heterogeneous distribution of arabinose along the xylan backbone in wheat AX (Beaugrand et al., 2004).

2.4.2. Weight average molecular weight and polydispersity index of AXH

The average molecular weights of the AXH varied from 0.78 to 5.64 million Da for the AXH (Table 2.3). An example of the superimposed chromatograms of refractive index and light scattering detector outputs for AXH is shown in Appendix 1. The starting material WAX had an average molecular weight of 5.61 million Da. In general, as the WAX was subjected to more enzymatic treatments, the molecular weight decreased as expected.

The CJX series resulted in lower molecular weights compared to ANX series which is in agreement with the substrate specificity of the each of the two xylanases. GH10 xylanases such as CJX can even degrade AX with high degree of substitution (DS) into smaller fragments

(Pollet et al., 2010). GH11 xylanases such as ANX on the other hand preferably cleave unsubstituted regions of the xylan backbone (Pollet et al., 2010) and due to such restrictions yield much larger fragments.

BAF series AXH yielded larger polysaccharides compared to the corresponding CAF series AXH. Treatment with CJX following arabinofuranosidase treatment yielded higher molecular weight AXH (BAF-2 and CAF-2) compared to treatment with ANX following arabinofuranosidase treatment (BAF-3 and CAF-3) in both BAF and CAF series. Adding the arabinofuranosidase treatments in sequence of CAF followed by BAF (CAF-5 and CAF-6) was more effective in producing smaller molecular weight polysaccharides compared to adding BAF followed by CAF (BAF-5 and BAF-6).

Generally, the xylanases are known to prefer unsubstituted xylose and the presence of arabinose exert a hindrance to xylanase activity on AX (Remond et al., 2008). Overall, as expected, initial hydrolysis of arabinose from the AX with arabinofuranosidase prior to hydrolysis by xylanase as in BAF and CAF series yielded AXH with much smaller average molecular weights comparted to initial hydrolysis by xylanase followed by arabinofuranosidase.

The polydispersity index of a polysaccharide gives an indication about the molecular weight distribution of the polysaccharide (Agilent Technologies, 2011). Large polydispersity index values thus indicate that the polymer has a broad molecular weight distribution. A monodispersed polymer where all the chain lengths are equal has a polydispersity index of 1. However, biological polymers such as polysaccharides have a wide chain length distribution. The polydispersity index of the WAX used in the current study had a polydispersity index of 1.6. This indicates that most of the molecules in WAX were somewhat similar in weight. Overall, the polydispersity index values ranged from 1.4-2.4 for the AXH.

2.4.3. ^{1}H-NMR of the AXH

A sample ^{1}H-NMR resonance spectrum of arabinoxylan is given in Figure 2.2. The spectrum consists of two distinct groups of resonances. The resonates at δ 5.90 to 5.73 ppm represents the anomeric protons of terminal arabinose units (α -L-arabinofuranosyl (α -Ara*f*)) linked to xylose main chain (Hoffmann et al., 1992) (Rose et al., 2010). The resonates at δ 5.00 to 5.20 ppm can be attributed to the anomeric protons of β -D-xylopyranosyl residues (β -Xyl*p*) (Hoffmann et al., 1992). The anomeric proton of arabinose linked to the monosubstituted xylose at O-3 position corresponds to the resonance at δ 5.90 ppm (Resonance 1).

The resonance at δ 5.81 and 5.80 ppm corresponds to anomeric proton of arabinose residue linked to the disubstituted xylose at O-3 position (Resonance 2) and resonance at δ 5.75 to 5.73 ppm accounts for anomeric proton of arabinose residue linked to the di-substituted xylose at O-2 position (Resonance3). The anomeric proton of di-substituted xylose accounts for the resonances at δ 5.18 to5.17 ppm (Resonance 4). The anomeric proton mono-substituted xylose corresponds to resonances at δ 5.04 to 5.03 ppm (Resonance 5) and anomeric proton of unsubstituted xylose residues corresponds to resonances at δ 5.00 ppm (Resonance 6). The quantitative integration of the resonances for each of the AXH was carried out (Table 2.4). The samples had high proportion of unsubstituted xylose (Resonance 6) and lesser amount of di- or mono-substituted xylose. A distinct difference among the AXH for the resonance integrations for the disubstituted xylose (Resonance 4) was evident. However, it was difficult to relate the observed results with the expected outcomes with respect to enzymatic substrate specificities. Except for resonance 4 integration values, all the other resonance integration values varied between a very narrow range and this also made it difficult to identify significant differences

among samples. During the experimental procedure, AXH seemed to precipitate at the bottom of the NMR tube and this could have influenced the final outcomes.

2.4.4. Glycosidic linkage profiles of the AXH

To further understand the structural details of the AXH, linkage analysis was carried out using GC-MS. The fragment identification was based on the online data base of University of Georgia, complex carbohydrate resource center (2014), Carpita and Shea (1989) and personal communications with Dr. Brad L. Reuhs (Department of Food Science, Purdue University, West Lafayette, IN). The results are depicted in Figure 2.3. The total ion chromatogram (TIC) and the mass spectrum of the corresponding peak in the TIC is shown in Appendix B. As expected, structural heterogeneity was observed with respect to linkage types present in each arabinoxylan hydrolyzate. After extensive enzymatic treatments, most of the AXH consists largely of unsubstituted xylose, indicating that the debranching enzymes were effective in removing the substituted arabinose. In the ANX series, the as the reaction time was increased from 0 h (ANX-1), 3 h (ANX-2), 6 h (ANX-3) and 12 h (ANX-4) the enzymes successively hydrolyzes more xylosidic bonds. The hydrolysis by ANX seems to result in highly unsubstituted AX. Among ANX-1, ANX-2, ANX-3 and ANX-4, as the enzyme reaction time increased, the unsubstituted xylose content increased and the structural complexity such as disubstituted xylose content and substituted arabinose content decreased. However, this trend was reversed with CJX series.

In CJX series as enzymatic reaction time increased from 0 h (CJX-1) to 3 h (CJX-2) to 12 h (CJX-3) the amount of unsubstituted xylose decreased and the disubstituted xylose content and substituted arabinose content increased. This indicate that between the two xylanases, ANX might be an enzyme of choice for the production of arabinoxylan hydrolyzates with simple

structural details while CJX might be selected for the production of arabinoxylan hydrolyzates with more complex structural features.

Hydrolysis of the sample with BAF (ANX-6), BAF and CAF (ANX-7), and CAF (ANX-8) in the ANX series resulted in AXH with apparently similar linkage profiles. Thus, initial depolymerization of WAX with ANX might result in hydrolyzates that are not easily accessible for the arabinofuranosidase. The arabinose substitution on the xylan backbone contributes to the solubility of the AX. The presence of arabinose in AX prevent the aggregation of unsubstituted xylose regions and help maintain the rod-like structure of AX in solution, making it soluble (Andrewartha et al., 1979).

It has been suggested that partial removal of such arabinose residues from the xylan backbone results in intermolecular insoluble aggregates of the molecule (Andrewartha et al., 1979). The initial hydrolysis of WAX by ANX might result in highly unsubstituted arabinoxylan hydrolyzates as seen in ANX-6, ANX-7 and ANX-8. Thus, these hydrolyzates might form aggregates and become partially insoluble. This might render a physical barrier for the arabinofuranosidase to bring about its action. Treatment of WAX with CJX resulted in a decrease in unsubstituted xylose proportion in the AXH as seen in CJX-6, CJX-7, CJX-8 and CJX-9. This was contradictory to what was expected. The expectation was that the subsequent arabinofuranosidase treatment would remove arabinose from the AX and yield a less complex highly unsubstituted AXH. One possible explanation is that once arabinofuranosidase removed the arabinose, CJX was still acting upon that hydrolysis product and cleaved off fractions of much of the easily accessible unsubstituted regions of the molecule off to the solution as oligomers. Thus, after the ethanol precipitation of the hydrolysis products the products with much complex structures are left to precipitate and constitute the AXH.

Table 2.2. Sugar composition of wheat AX (WAX) and its enzymatic products.

AXH[a]	Sugar composition % (w/w)				A/X ratio
	Arabinose	Xylose	Galactose	Glucose	
WAX	8.46	26.58	0.26	2.56	0.32
ANX-1	12.62	31.09	0.50	4.48	0.41
ANX-2	12.74	26.87	0.55	4.36	0.47
ANX-3	13.72	28.37	0.65	4.06	0.48
ANX-4	13.99	24.66	0.57	4.05	0.57
ANX-5	14.47	25.24	0.73	3.73	0.57
ANX-6	16.13	29.20	0.73	4.54	0.55
ANX-7	15.51	28.32	0.83	4.06	0.55
ANX-8	11.12	22.00	0.40	2.82	0.51
ANX-9	11.40	17.11	0.37	2.57	0.67
CJX-1	13.03	28.86	0.68	4.58	0.45
CJX-2	12.50	25.08	0.26	4.98	0.50
CJX-3	14.53	29.38	0.81	3.90	0.49
CJX-4	8.26	14.36	0.21	2.26	0.58
CJX-5	15.95	29.61	0.69	4.61	0.54
CJX-6	11.39	19.88	0.47	3.03	0.57
CJX-7	11.01	20.51	0.52	3.29	0.54
CJX-8	13.01	26.32	0.56	3.37	0.49
CJX-9	13.51	25.60	0.18	4.02	0.53
CAF-1	14.24	26.96	0.51	4.01	0.53
CAF-2	15.80	32.09	0.20	3.56	0.49
CAF-3	18.05	35.43	0.23	3.87	0.51
CAF-4	16.40	27.33	0.65	4.42	0.60
CAF-5	14.69	28.00	0.21	3.61	0.52
CAF-6	18.79	38.77	0.21	4.47	0.48
BAF-1	11.02	21.36	0.46	3.64	0.52
BAF-2	12.29	19.81	0.30	2.62	0.62
BAF-3	15.49	27.68	0.68	3.25	0.56
BAF-4	13.93	24.62	0.31	4.85	0.57
BAF-5	12.76	24.22	0.46	4.10	0.53
BAF-6	15.16	28.60	0.25	3.35	0.53
LSD	0.84	1.4	0.03	0.02	0.01

LSD = least significant difference ($P < 0.05$)

[a]Enzymatic treatments were carried out using the following enzymes: ANX, endo-1,4-β-Xylanase M4 (*Aspergillus niger*); CJX, Endo-1,4-β-Xylanase (*Cellvibrio japonicus*); BAF, α-L-Arabinofuranosidase (novel specificity) (*Bifidobacterium adolescentis*); CAF, α-L-Arabinofuranosidase (*Clostridium thermocellum*); each sample name starting with corresponding enzyme abbreviation received that specific enzyme treatment first.

Table 2.3. Weight average molecular weight and polydispersity index of AXH.

AXH[a]	Weight average molecular weight (million Da)	Polydispersity index (*M*w/*M*n)
WAX	5.61	1.6
ANX-1	5.56	2.2
ANX-2	4.54	1.5
ANX-3	4.03	2.2
ANX-4	3.68	1.5
ANX-5	3.64	1.8
ANX-6	3.58	1.5
ANX-7	3.33	1.4
ANX-8	2.91	1.8
ANX-9	2.06	1.8
CJX-1	5.64	1.8
CJX-2	4.02	1.7
CJX-3	2.25	1.6
CJX-4	1.84	1.7
CJX-5	1.81	1.6
CJX-6	1.53	1.8
CJX-7	1.27	1.6
CJX-8	1.22	1.7
CJX-9	1.11	1.9
CAF-1	3.31	2.3
CAF-2	1.28	1.5
CAF-3	1.11	1.3
CAF-4	1.89	1.6
CAF-5	0.93	1.8
CAF-6	0.78	1.4
BAF-1	3.35	2.0
BAF-2	1.64	1.9
BAF-3	1.33	2.1
BAF-4	2.31	1.6
BAF-5	1.14	1.8
BAF-6	1.28	2.0
LSD	0.04	0.4

LSD = least significant difference ($P < 0.05$)

[a]Enzymatic treatments were carried out using the following enzymes: ANX, endo-1,4-β-Xylanase M4 (*Aspergillus niger*); CJX, Endo-1,4-β-Xylanase (*Cellvibrio japonicus*); BAF, α-L-Arabinofuranosidase (novel specificity) (*Bifidobacterium adolescentis*); CAF, α-L-Arabinofuranosidase (*Clostridium thermocellum*); each sample name starting with corresponding enzyme abbreviation received that specific enzyme treatment first.

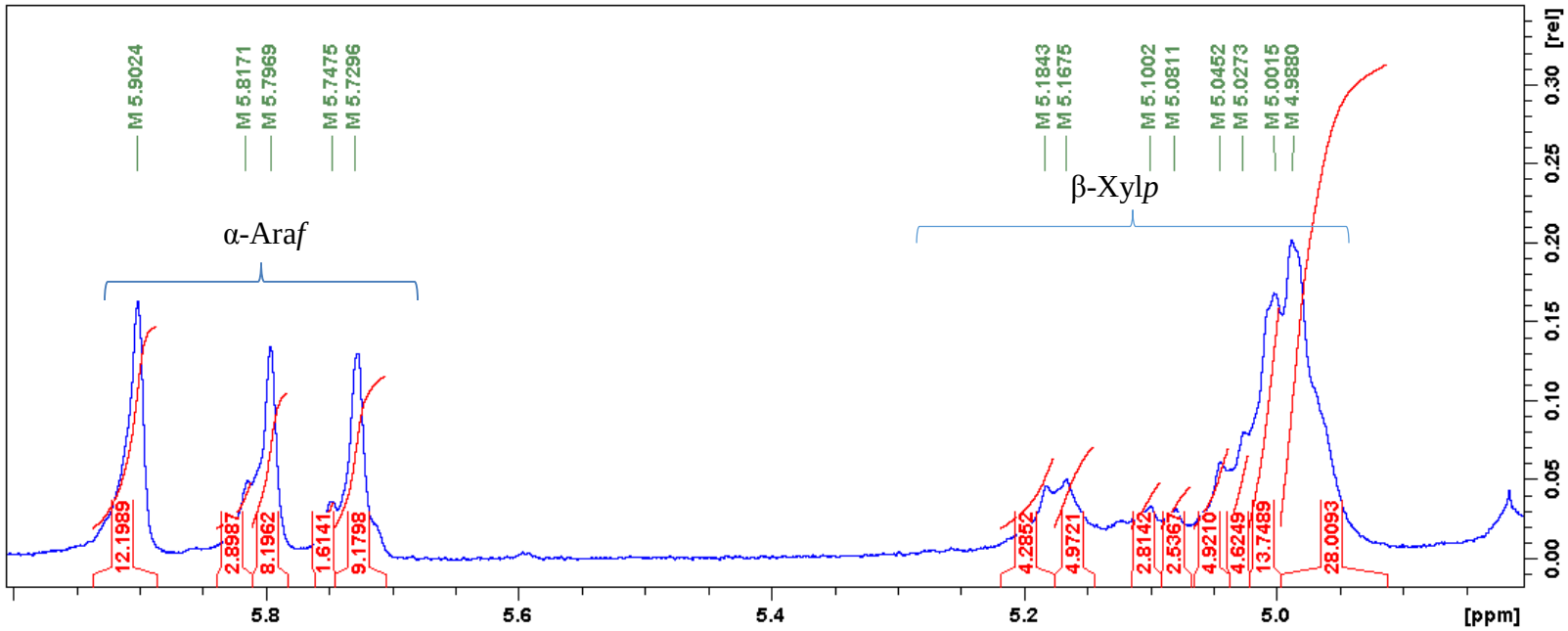

Figure 2.2. Example ^{1}H-NMR resonance spectrum of arabinoxylan.

Table 2.4. ^{1}H-NMR resonance integrations for WAX and AXH.

	Resonance integration as % of total resonance					
AXH	Resonance 1	Resonance 2	Resonance 3	Resonance 4	Resonance 5	Resonance 6
WAX	11	7	11	20	12	39
ANX-1	14	11	10	11	18	35
ANX-2	11	8	10	9	14	48
ANX-3	11	10	10	10	15	44
ANX-4	13	14	9	14	12	38
ANX-5	14	12	10	14	12	37
ANX-6	14	13	10	11	14	38
ANX-7	15	11	10	9	14	40
ANX-8	10	13	11	11	14	42
ANX-9	13	14	11	5	13	43
CJX-1	12	11	10	12	13	42
CJX-2	10	13	10	10	15	42
CJX-3	13	12	12	10	12	41
CJX-4	13	13	11	7	13	43
CJX-5	14	12	10	8	15	42
CJX-6	13	12	11	6	13	45
CJX-7	14	11	11	8	14	43
CJX-8	11	10	9	14	13	43
CJX-9	13	11	11	11	13	42
CAF-1	14	12	11	5	13	44
CAF-2	13	11	9	8	13	46
CAF-3	14	12	10	11	12	42
CAF-4	13	11	11	9	13	43
CAF-5	14	11	10	9	12	44
CAF-6	13	9	9	11	13	44
BAF-1	13	11	9	11	13	43
BAF-2	14	10	10	11	14	40
BAF-3	13	10	9	11	13	44
BAF-4	14	10	9	11	13	44
BAF-5	13	11	9	7	13	47
BAF-6	15	11	10	9	13	43

Each resonance corresponds to the following anomeric protons: Resonance 1, Anomeric proton of O-3 linked arabinose linked to monosubstituted xylose; Resonance 2, Anomeric proton of O-3 linked arabinose linked to disubstituted xylose; Resonance 3, Anomeric proton of O-2 linked arabinose linked to disubstituted xylose; Resonance 4, Anomeric proton of disubstituted xylose; Resonance 5, Anomeric proton of monosubstituted xylose; Resonance 6, Anomeric proton of unsubstituted xylose

[a]Enzymatic treatments were carried out using the following enzymes: ANX, endo-1,4-β-Xylanase M4 (*Aspergillus niger*); CJX, Endo-1,4-β-Xylanase (*Cellvibrio japonicus*); BAF, α-L-Arabinofuranosidase (novel specificity) (*Bifidobacterium adolescentis*); CAF, α-L-Arabinofuranosidase (*Clostridium thermocellum*); each sample name starting with corresponding enzyme abbreviation received that specific enzyme treatment first.

When CAF-1 and BAF-1 was considered, as expected the CAF-1 consisted with lesser linkages corresponding to 3-substituted xylose compared to BAF-1. This is in agreement with the substrate specificity of the CAF enzyme which preferentially hydrolyzes the O-3-substitutes

arabinose from monosubstituted xylose (Taylor et al., 2006). On the other hand, BAF-1 contains slightly lesser proportion of disubstituted xylose compared to CAF-1. This is in agreement with the substrate specificity of BAF enzyme which hydrolyzes the O-3 linked arabinose from disubstituted xylose (Van den Broek et al., 2005). These indicate that the two arabinofuranosidases used in the current research can be effectively used for the specific hydrolysis of desired arabinose side groups to produce hydrolysis products with intended properties. According to the GC-FID results between BAF-1 and CAF-1, BAF enzyme was shown to be better equipped for the removal of arabinose as evident by the low A/X ratio for BAF-1 compared to CAF-1. However, this observation was not supported by the linkage analysis results. Both BAF-1 and CAF-1 had linkage profiles with close resemblance.

Between BAF-1 (hydrolysis with BAF only) and BAF-4 (hydrolysis with BAF followed by CAF), BAF-4 as expected, consists of high proportion of unsubstituted xylose indicating that the two enzymes considerably removed the arabinose side groups from the xylan backbone resulting in a less complex structure. Between CAF-1 (hydrolysis with CAF only) and CAF-4 (hydrolysis with CAF followed by BAF) also a similar increase in unsubstituted xylose proportion was observed. However, this change was more prominent for the BAF series. Between BAF-4 and CAF-4, BAF-4 had higher amount of unsubstituted xylose as well as lesser amount of disubstituted xylose indicating that although both BAF-4 and CAF-4 received similar enzymatic treatments the sequence of each enzyme addition (BAF followed by CAF *vs* CAF followed by BAF) is important.

2.4.5. Canonical discriminant analysis of the AXH

Canonical discriminant analysis (CDA) was performed on the chemical/ structural detail to classify the 30 AXH into four groups according to the first hydrolysis enzyme applied. Total

AX %, A/X ratio, resonance integration results from ^{1}H-NMR (resonance 1-6), linkage analysis data from GC-MS (9 linkage types and product of total AX% × O-3 substituted xylose proportion) were considered in the CAD. Two canonical variables in the form:

$CS = b_1x_1 + b_2x_2 + \cdots + b_nx_n + c$

were created, where *CS* is the canonical score formed by the canonical function; the *b*'s are canonical coefficients that reflect the unique contribution of each chemical/structural detail to the classification of AXH, the *x's are* individual chemical/structural parameters, and *c* is a constant. Two canonical variables accounted for 75.7 % of variance (44.6% for canonical variable 1 and 31.0 % for canonical variable 2). A scatterplot (Figure 2.4) relative to two canonical variables shows a good separation among different types of AXH indicating that there were chemical/ structural similarities in AXH belonging to a specific series.

2.5. Conclusions

The current research was carried out to generate structurally different arabinoxylan hydrolyzates (AXH) by means of using different combinations of xylanase and arabinofuranosidase enzymes. The AXH consisted predominantly of xylose (14.36-38.77%), followed by arabinose (8.26-18.79%). The average molecular weights of the AXH varied between 0.78-5.64 million Da. The starting material WAX had an average molecular weight of 5.61 million Da.The CJX series resulted in lower molecular weights compared to ANX series which is in agreement with the substrate specificity of each of the two xylanases. BAF series AXH yielded larger polysaccharides compared to the corresponding CAF series AXH. Treatment with CJX following arabinofuranosidase treatment yielded higher molecular weight AXH compared to treatment with ANX following arabinofuranosidase treatment in both BAF and CAF series. Adding the arabinofuranosidase treatments in sequence of CAF followed by BAF

was more effective in producing smaller molecular weight polysaccharides compared to adding BAF followed by CAF.

In general, the AXH had high proportion of unsubstituted xylose and lesser amount of di- or mono-substituted xylose as indicated by ^{1}H-NMR and GC-MS data. In the ANX series, as the reaction time was increased from 0-12 h the proportion of unsubstituted xylose increased and structural complexity such as disubstituted xylose content and substituted arabinose content decreased.

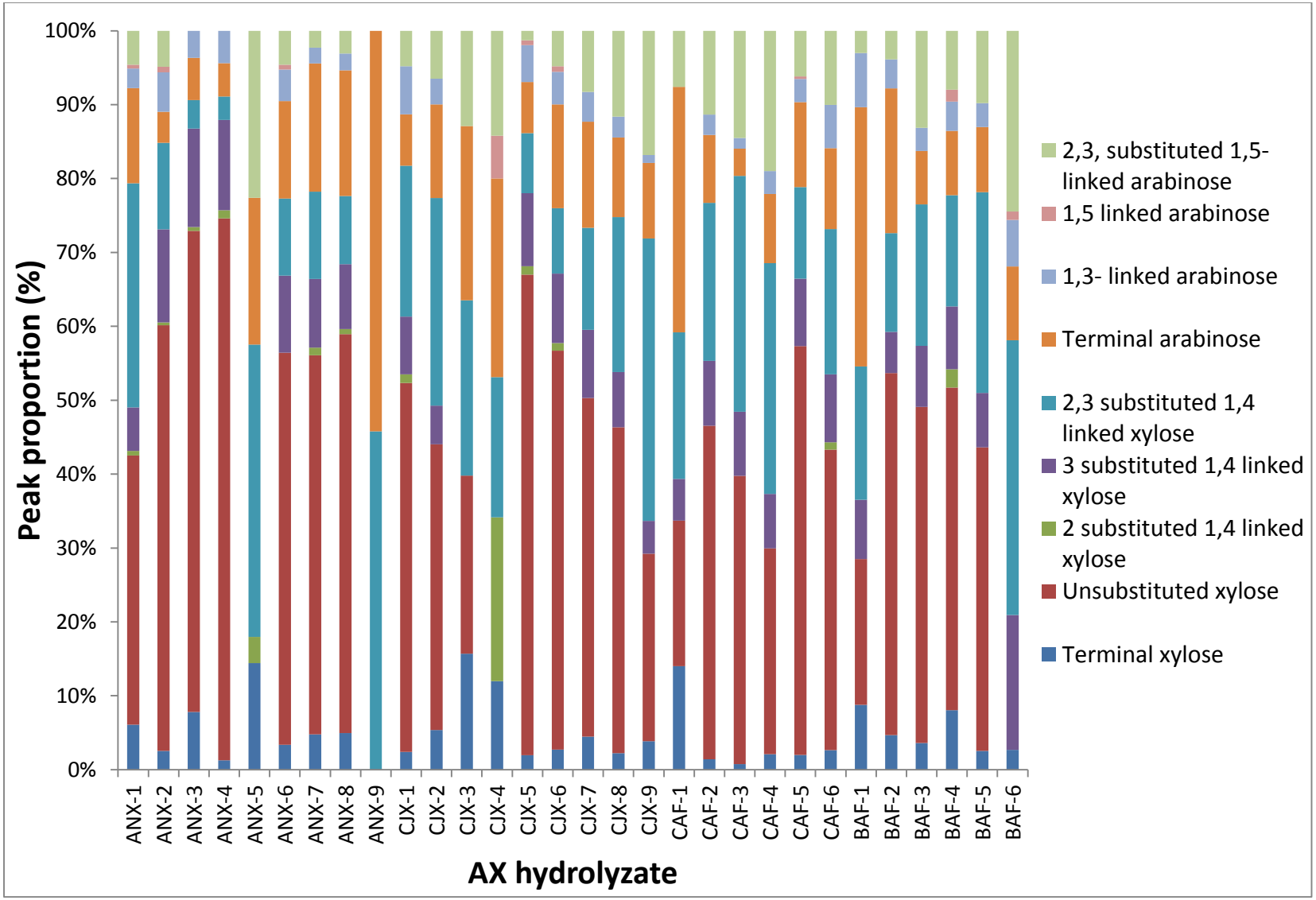

Figure 2.3. Occurrence of each linkage type in each AXH as determined by GC-MS techniques.

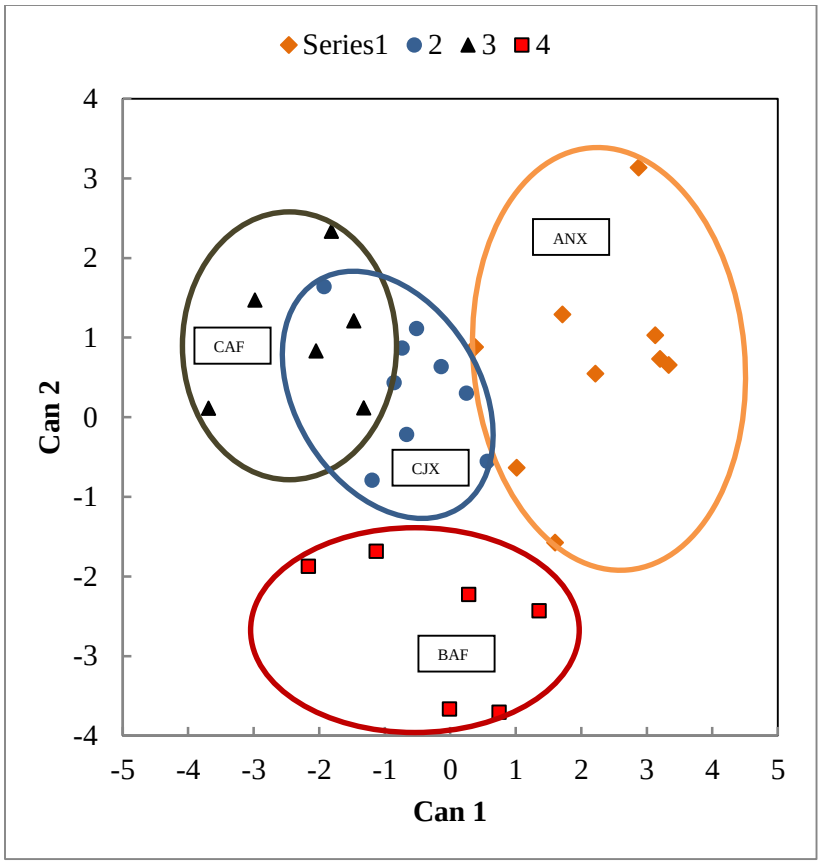

Figure 2.4. 2D scatterplot of canonical scores. Scatterplot relative to two canonical variables (Can 1 and Can 2) showed separation among different types of AXH. The two canonical variables accounted for 75.7 % of variance (44.6% for canonical variable 1 and 31.0 % for canonical variable 2) indicating that there were chemical/ structural similarities in AXH belonging to a specific series. Can 1: canonical variable 1; Can 2: canonical variable 2; Series 1: ANX series; Series 2: CJX series; Series 3: CAF series; Series 4: BAF series.

Thus, ANX seems to result in highly unsubstituted AXH. However, this trend was reversed with CJX series. In CJX series as enzymatic reaction time increased from 0-12 h (CJX-3) the amount of unsubstituted xylose decreased and the disubstituted xylose content and substituted arabinose content increased. This indicate that between the two xylanases, ANX might be an enzyme of choice for the production of arabinoxylan hydrolyzates with simple structural details while CJX might be selected for the production of arabinoxylan hydrolyzates with more complex structural features.

Comparison of BAF-4 and CAF-4 indicating that addition BAF followed by CAF is more effective in generating AXH with higher amount of unsubstituted xylose as well as lesser amount of disubstituted xylose.

Overall, the enzymatic treatments applied in the current research effectively generated thirty different arabinoxylan hydrolyzates. The information derived about the capabilities of the two xylanases and two arabinofuranosidase could be important information in decisions made regarding which enzyme to be applied in a process to generate hydrolysis products of desired structural features. Also, these hydrolyzates could be useful as substrate for future research exploring the effect of each of these fine structural details on different physiological properties. Such research could indicate the importance specific composition/structure details have on the wheat derived arabinoxylan hydrolyzates as biological functional molecules within the human body or as physical functional molecules in wheat based processing industries such as baking.

2.6. References

Agilent Technologies, I. (2011). Polymer molecular weight distribution and definition of MW averages. Vol. 2014.

Andrewartha, K. A., Phillips, D. R., and Stone, B. A. (1979). Solution properties of wheat-flour arabinoxylans and enzymically modified arabinoxylans. *Carbohydrate Research* **77**, 191-204.

Beaugrand, J., Chambat, G., Wong, V. W. K., Goubet, F., Rémond, C., Paës, G., Benamrouche, S., Debeire, P., O'Donohue, M., and Chabbert, B. (2004). Impact and efficiency of GH10 and GH11 thermostable endoxylanases on wheat bran and alkali-extractable arabinoxylans. *Carbohydrate Research* **339**, 2529-2540.

Beg, Q. K., Kapoor, M., Mahajan, L., and Hoondal, G. S. (2001). Microbial xylanases and their industrial applications: a review. *Applied Microbiology and Biotechnology* **56**, 326-338.

Blakeney, A. B., Harris, P. J., Henry, R. J., and Stone, B. A. (1983). A simple and rapid preperation of alditol acetates for monosaccharide analysis. *Carbohydrate Research* **113**, 291-299.

Carpita, N. C., and Shea, E. M. (1989). Linkage Structure of Charbohydrates by Gas Chromatography-Mass Spectrometry (GC-MS) of Partially Methylated Alditol Acetates. *In* "Analysis of Charbohydrates by GLC and MS" (C. J. Biermann and G. D. McGinnins, eds.), pp. 157-216. CRC Press, New York.

Clarke, J. H., Rixon, J. E., Ciruela, A., Gilbert, H. J., and Hazlewood, G. P. (1997). Family-10 and family-11 xylanases differ in their capacity to enhance the bleachability of hardwood and softwood paper pulps. *Appl Microbiol Biotechnol* **48**, 177-83.

Collins, T., Gerday, C., and Feller, G. (2005). Xylanases, xylanase families and extremophilic xylanases. *FEMS Microbiology Reviews* **29**, 3-23.

Dervilly, G., Saulnier, L., Roger, P., and Thibault, J. F. (2000). Isolation of Homogeneous Fractions from Wheat Water-Soluble Arabinoxylans. Influence of the Structure on Their Macromolecular Characteristics. *Journal of Agricultural and Food Chemistry* **48**, 270-278

Dornez, E., Gebruers, K., Delcour, J., and Courtin, C. (2009). Grain-associated xylanases: occurrence, variability, and implications for cereal processing. *Trends in food science & technology* **20**, 495-510.

Falck, P., Precha-Atsawanan, S., Grey, C., Immerzeel, P., Stalbrand, H., Adlercreutz, P., and Karlsson, E. N. (2013). Xylooligosaccharides from hardwood and cereal xylans produced

by a thermostable xylanase as carbon sources for *Lactobacillus brevis* and *Bifidobacterium adolescentis*. *J Agric Food Chem* **61**, 7333-40.

Fox, A., Morgan, S. L., and Gilbart, J. (1989). Preperation of alditol acetates and their analysis by gas chromatography and mass spectroscory. *In* "Analysis of Carbohydrates by GLC and MS" (C. J. Biermann and G. D. McGinnins, eds.), pp. 87-125. CRC Prsaa, Inc., Florida.

Gys, W., Courtin, C. M., and Delcour, J. A. (2003). Refrigerated Dough Syruping in Relation to the Arabinoxylan Population. *Journal of Agricultural and Food Chemistry* **51**, 4119-4125.

Hoffmann, R. A., Kamerling, J. P., and Vliegenthart, J. F. G. (1992). Structural features of a water-soluble arabinoxylan from the endosperm of wheat. *Carbohydrate Research* **226**, 303-311.

Pollet, A., Delcour, J. A., and Courtin, C. M. (2010). Structural determinants of the substrate specificities of xylanases from different glycoside hydrolase families. *Critical reviews in biotechnology* **30**, 176-191.

Remond, C., Boukari, I., Chambat, G., and O'Donohue, M. (2008). Action of a GH 51 alpha-L-arabinofuranosidase on wheat-derived arabinoxylans and arabino-xylooligosaccharides. *Carbohydrate Polymers* **72**, 424-430.

Rose, D. J., Patterson, J. A., and Hamaker, B. R. (2010). Structural differences among alkali-soluble arabinoxylans from maize (Zea mays), rice (Oryza sativa), and wheat (Triticum aestivum) brans influence human fecal fermentation profiles. *Journal of Agricultural and Food Chemistry* **58**, 493-499.

Saulnier, L., Sado, P. E., Branlard, G., Charmet, G., and Guillon, F. (2007). Wheat arabinoxylans: Exploiting variation in amount and composition to develop enhanced varieties. *Journal of Cereal Science* **46**, 261-281.

Sorensen, H. R., Jorgensen, C. T., Hansen, C. H., Jorgensen, C. I., Pedersen, S., and Meyer, A. S. (2006). A novel GH43 alpha-L-arabinofuranosidase from Humicola insolens: mode of action and synergy with GH51 alpha-L-arabinofuranosidases on wheat arabinoxylan. *Appl Microbiol Biotechnol* **73**, 850-61.

Sorensen, H. R., Meyer, A. S., and Pedersen, S. (2003). Enzymatic hydrolysis of water-soluble wheat arabinoxylan. 1. Synergy between alpha-L-arabinofuranosidases, endo-1,4-beta-xylanases, and beta-xylosidase activities *Biotechnology and Bioengineering* **81**, 726-731.

Spagna, G., Andreani, F., Salatelli, E., Romagnoli, D., and Pifferi, P. G. (1998). Immobilization of α-l-arabinofuranosidase on chitin and chitosan. *Process Biochemistry* **33**, 57-62.

Storsley, J. M., Izydorczyk, M. S., You, S., Biliaderis, C. G., and Rossnagel, B. (2003). Structure and physicochemical properties of beta-glucans and arabinoxylans isolated from hull-less barley. *Food Hydrocolloids 6th International Hydrocolloids Conference - Part 2* **17**, 831-844.

Taylor, E., Smith, N., Turkenburg, J., D'souza, S., Gilbert, H., and Davies, G. (2006). Structural insight into the ligand specificity of a thermostable family 51 arabinofuranosidase, Araf51, from Clostridium thermocellum. *Biochem.J* **395**, 31-37.

University of Georgia, complex carbohydrate resource center. (2014). GC-EIMS of partially methylated alditol acetates. http://www.ccrc.uga.edu/specdb/ms/pmaa/pframe.html

Van den Broek, L., Lloyd, R., Beldman, G., Verdoes, J., McCleary, B., and Voragen, A. (2005). Cloning and characterization of arabinoxylan arabinofuranohydrolase-D3 (AXHd3) from

Bifidobacterium adolescentis DSM20083. *Appl Microbiol Biotechnol Applied Microbiology and Biotechnology* **67**, 641-647.

Verwimp, T., Van Craeyveld, V., Courtin, C. M., and Delcour, J. A. (2007). Variability in the Structure of Rye Flour Alkali-Extractable Arabinoxylans. *Journal of Agricultural and Food Chemistry* **55**, 1985-1992.

Xu, H. (2012). Influence of the structural complexicity of cereal arabinoxylans on human fecal fermentation and their degradation mechanism by gut bacteria. Dissertation, Purdue University, Indiana.U.S.A.

CHAPTER 3. ARABINOXYLAN HYDROLYZATES AS IMMUNOMODULATORS IN LIPOPOLYSACCHARIDE-INDUCED RAW 264.7 MACROPHAGES.

3.1. Abstract

Inflammation is an important healthy immune response by the body during lesions and infection. However, uncontrolled excessive inflammation can be damaging to the cells. The specific objective of this research was to evaluate the effect of structural details of enzymatically derived wheat arabinoxylan hydrolyzates (AXH) on their immunomodulatory properties. The LPS induced macrophage cell line is a model widely used to study inflammation. The AXH being tested exhibited both pro- and anti-inflammatory properties. Some of the hydrolyzates increased the production of NO compared to the control while some AXH decreased the NO production. Out of the 30 AXH, six showed anti-inflammatory properties while four exhibited pro-inflammatory properties. ANX-6 displayed the highest anti-inflammatory property while CJX-2 showed the highest pro-inflammatory property. The AXH with pro-inflammatory properties had higher weight average molecular weights while lower molecular weights were seen for AXH with anti-inflammatory properties. Apart from molecular weight, total AX content also played a role in governing the anti/pro-inflammatory properties. Anti-inflammatory compounds had higher total AX content compared to pro-inflammatory compounds. A strong negative correlation was seen between NO production and total AX × amount of 1,4-linked xylose with arabinose substituted at O- 3- position. Thus, AXH with higher AX and substitution at O-3 position are favorable candidates to reduce the LPS induced inflammation. These results indicate that there might be a structure-function relationship for these AXH as immunomodulators.

3.2. Introduction

Arabinoxylan (AX) is the predominant polysaccharide in the cell wall of wheat grain (Saulnier et al., 2007). It consists of a backbone of β-(1,4)-linked xylose residues, which are substituted with arabinose residues on the C(O)-2 and/or C(O)-3 position (Dornez et al., 2009). Since AX is mainly composed of xylose and arabinose, it is commonly referred to as pentosans. Phenolic acids such as ferulic acid can be ester linked on the C(O)-5 position of arabinose (Figure 1.2). Endo-β-(1,4)-d-xylanases (EC 3.2.1.8, xylanase) are the major enzymes involved in AX degradation. They cleave AX by internally hydrolyzing the 1,4- β-D-xylosidic linkage between xylose residues in the xylan backbone in a random manner (Collins et al., 2005; Dornez et al., 2009) giving rise to arabinoxylan hydrolyzates (AXH) of different degree of polymerization (DP). The enzyme α-l-arabinofuranosidases (EC 3.2.1.55) remove arabinose substituents from the xylan backbone (Dornez et al., 2009) yielding AX of different degree of arabinose substitution (DS). Thus, treatment of AX polysaccharide with various xylanases and arabinofuranosidases can yield AXH with variable DP and DS. Most of the glycoside hydrolases that are classified in Glycoside hydrolase family 10 (GH10) are endo-β-1,4-xylanases (e.g. endo-1,4-β-xylanase from *Cellvibrio japonicus*) (Pollet et al., 2010). GH10 xylanases attack both linear substrates as well as substituted heteroxylans. They attack the xylosidic linkage next to a single or double substituted xylose toward the non-reducing end and require two unsubstituted xylose residues between branched residues (Figure 2.2). Thus, they can hydrolyze AX with high degree of substitution (DS) into smaller fragments. GH11 xylanases (e.g. endo-1,4-β-xylanase M4 from *Aspergillus niger*) exclusively consist of true endo-β-1,4-xylanases that cleave internal β-1,4-xylosidic bonds and preferably cleave unsubstiuted regions of the backbone (Pollet et al., 2010). GH11 cannot attack the xylosidic linkage toward the non-reducing end next to a branched

xylose and require three unsubstituted consecutive xylose residues for hydrolysis (Figure 2.2). Hence, GH11 xylanases have a low activity on heteroxylans with a high DS. Only C3-linked arabinose residues from double-substituted xylose residues are hydrolyzed by Arabinoxylan arabinofuranohydrolases from *Bifidobacterium adolescentis* (GH 43) (van den Broek et al., 2005) while α-L-arabinofuranosidase from *Clostridium thermocellum* (GH51) catalyse the hydrolysis of "α-1,5-linked arabino-oligosaccharides and the α-1,3 arabinosyl side chain decorations of xylan with equal efficiency" (Taylor et al., 2006). Thus, it is also highly efficient in the removal of the α-1,3-linked arabinoside substitutions from wheat arabinoxylan itself (Taylor et al., 2006).

Inflammation is an adaptive response that is triggered by noxious stimuli and conditions, such as infection and tissue injury (Medzhitov, 2008). Under healthy physiological conditions inflammation is a defense response that serves a protective function in the body. However, inflammation can be detrimental if deregulated. At a basic level, acute inflammatory responses triggered by infection and tissue injury involve the organized delivery of blood components to the site of injury. This response, when triggered by microbial infections is prompted by receptors of the innate immune system such as Toll-like receptors (TLRs)) and NOD (nucleotide-binding oligomerization-domain protein)-like receptors (NLRs). Recognition of these triggers by macrophages and mast cells lead to the production of inflammatory mediators (chemokines, cytokines, vasoactive amines, eicosanoids and products of proteolytic cascades). One outcome of this initial inflammatory response is the production of large amount of reactive oxygen species (ROS), a process known as respiratory burst (Gwinn and Vallyathan, 2006; Robinson, 2009). Toxic compounds such as ROS, reactive nitrogen species, proteinase 3, cathepsin G and elastase are released by leucocytes with an attempt to mitigate invading agents. However, these highly

reactive compounds do not distinguish between microbial and self-cells leading to unavoidable collateral damage. After a successful elimination of the infection, the recovery phase is initiated. This is mainly mediated by macrophages (Medzhitov, 2008). A shift in lipid mediators from pro-inflammatory prostaglandins to anti-inflammatory lipoxins helps towards recovery. Also, growth factors produced by macrophages plays a role in tissue recovery. An overview of the inflammatory outcomes is given in Figure 3.1. Although the mechanisms of infection-induced inflammation are understood to a higher extent, knowledge about mechanisms governing other forms of inflammation such as systemic chronic inflammation is still at its initial stages.

Macrophages are tissue-based phagocytic cells derived from blood monocytes (Abbas and Lichtman, 2011). They play an important role in innate and adaptive immunity. Upon activation by microbial byproducts such as lipopolysaccharides (LPS) and T-cell cytokines such as interferon-γ, activated macrophages phagocytose and kill microbes, secrete proinflammatory cytokines and present antigens to helper T-cells. Macrophages express inducible isoforms of nitric oxide (NO) synthase (iNOS) upon activation by microbial or cytokine stimuli, which leads to the production of NO from L-arginine. Nitric oxide functions as a microbicidal agent that kills ingested microbes and also acts as a mediator of the immune system (Abbas and Lichtman, 2011; Moncada et al., 1991). Thus, LPS induced RAW 264.7 murine macrophages have been widely used as a model to study inflammatory responses (Fujihara et al., 2003; Liu et al., 2008; MacKenzie et al., 2013; MacKichan and DeFranco, 1999; Xu et al., 2012). Although NO is an essential bioregulatory molecule with diverse functions including neural signal transmission, immune response, and control of blood pressure, elevated levels of NO can lead to pathological inflammatory conditions (Moncada et al., 1991). Thus, mediation of the production of such inflammatory effector molecules is beneficial in the treatment of chronic inflammation derived

diseases such as rheumatoid arthritis, diabetes, atherosclerosis inflammatory bowel disease and cancer (Kim et al., 2012; Moncada et al., 1991).

Immunomodulators are medications used to help regulate or normalize the immune system (American academy of allergy, 2014). The immunomodulatory effects of AX have been demonstrated by several researches in the recent years. AX extracted from wheat bran has been shown to have potent effects on innate and acquired immune response in mice (Cao et al., 2011). AX significantly increases the activation potential of T and B cells and enhances the humoral and cell-mediated immunity in tumor bearing mice. Akhtar et al. (2012) demonstrated that wheat bran derived AX has the potential to stimulate the antibody mediated immune response in chickens. However, there is a scarcity of research on understanding how the fine chemical structure of this complex polysaccharide affects its immunomodulatory properties. More so, no recent research is available on the immunomodulatory properties of enzymatically derived arabinoxylan hydrolyzates from wheat. Thus, we aimed to investigate how the fine chemical structure of enzymatically hydrolyzed AXH affects its immunomodulatory properties.

3.3. Materials and Methods

3.3.1. Materials

Materials used for the production of AXH were previously described in section 2.3.1. Murine macrophage RAW 264.7 cell line (obtained from the American Type Culture Collection, ATCC), was a generous gift from Dr. Estelle Leclerc (Department of Pharmaceutical Sciences, North Dakota State University, ND). Dulbecco's Modified Eagle's Medium (DMEM) (ATCC® 30-2002™) and Fetal Bovine Serum (FBS) (ATCC® 30-2020™) were from ATCC (Manassas, VA). Penicillin-Streptomycin solution (10,000 units/mL Penicillin/ 10,000 µg/mL Streptomycin) was purchased from HyClone Laboratories, Inc. (Logan, UT).

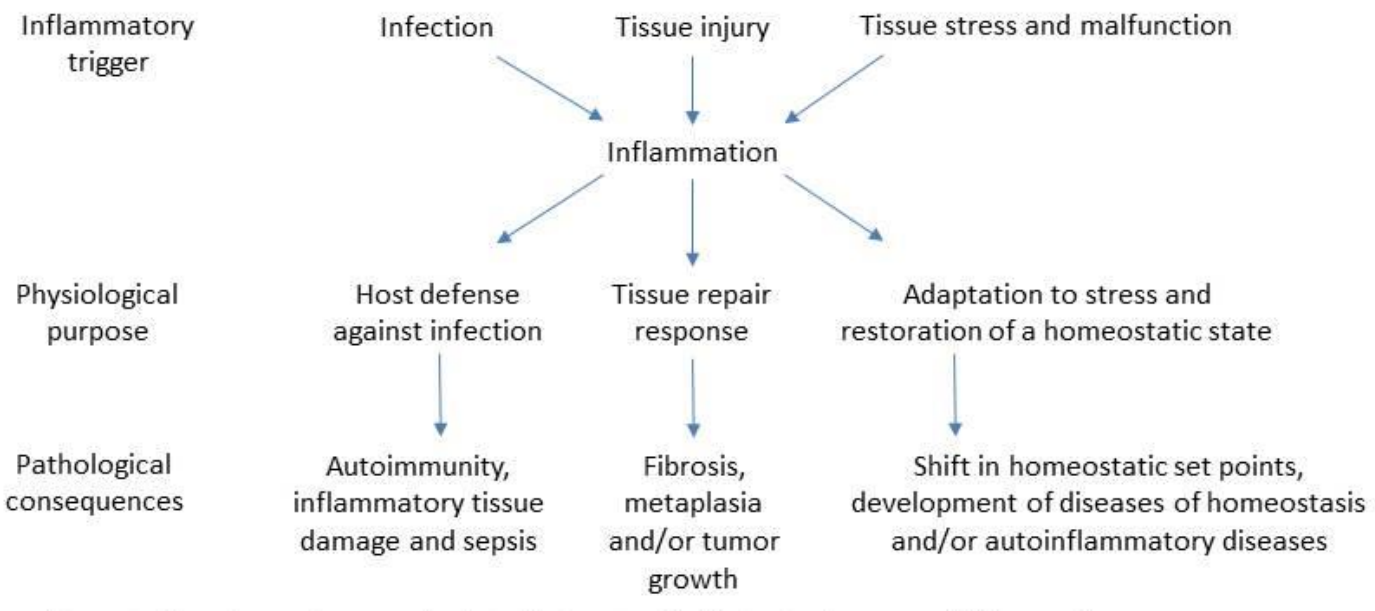

Figure 3.1. Overview of cause, physiological and pathological outcomes of inflammation (adapted from Medzhitov (2008)).

Lipopolysaccharides (LPS) (*Escherichia coli* 0111:B4, L4391-1MG, Lot No: 043M4089V) were purchased from Sigma-Aldrich (St. Louis MO). The Griess Reagent Kit for Nitrite Determination was from Molecular Probes, Inc. (Eugene, OR).

3.3.2. Procedure for arabinoxylan hydrolyzate preparation

AXH preparation was carried out as described in section 2.3.2 in a previous chapter. A summary of the treatments and the abbreviation given to the resulting AXH is given in Table 2.1.

3.3.3. Chemical analysis

The chemical analysis of the AXH was carried out as described in section 2.3.3 using GC-FID, SEC-MALS, ^{1}H-NMR and GC-FID techniques.

3.3.4. Determination of immunomodulatory properties of AXH

Thirty different arabinoxylan hydrolyzates were evaluated for their immunomodulatory properties in LPS induced macrophages. RAW 264.7 macrophages were grown in DMEM media supplemented with 10% FBS and 1% Penicillin-Streptomycin solution at 37 ^{o}C under a humidified atmosphere of 95% air and 5% CO_2.

3.3.4.1. Effect of AXH on NO production in RAW 264.7 cells

RAW 264.7 cells were plated at $1x10^5$ cells/100 µL cell density (100 µL) in 96 well plate wells and incubated overnight. Next day, the AXH (2000 µg/mL) dissolved in serum free-antibiotic free DMEM were added (50 µL) to each well. Wells receiving serum free-antibiotic free DMEM were used as control wells. Indomethacin (50 µL, 80 µg/mL, PHR1247 Fluka, Sigma-Aldrich (St. Louis MO)), a nonsteroidal anti-inflammatory drug (NSAID) which brings about its anti-inflammatory effects through the inhibition of cyclooxygenase (COX) (Edogawa et

al., 2014), in serum free-antibiotic free DMEM was used as the positive control. After 2 h incubation with each pre-treatment, 50 µL of LPS dissolved in serum free-antibiotic free DMEM (4 µg/mL) was added to each well to induce inflammation at a final concentration of 1 µg/mL. Thus, the final concentration of the AXH in a well was 500 µg/mL. The cells were incubated for 24 h. Nitric oxide production was determined based on the amount of nitrite, a stable end product of NO. Nitrite concentration in media supernatants was determined using the Griess reaction. Griess reaction was carried out according to manufacturer's instructions with some modifications: media supernatant (100 µL) was aspired out from each well and transferred to a new 96 well plate where the Griess reagent (1% sulfanilamide in 2.5% phosphoric acid and 0.1% naphthylenediamine dihydrochloride in water, 100 µL) was added. Nitrite standard solutions provided with the kit were used to develop a standard curve for absorbance vs. nitrite concentration. The Griess reaction was allowed to take place in the dark for 30 min. Absorbance of each well was read at 548 nm using a microplate reader (Molecular Devices, Sunnyvale, CA). The amount of nitrite produced in each treatment group was calculated based on the standard curve.

3.3.4.2. Effect of different AXH doses on NO production in RAW 264.7 cells

Six AXH (CJX-1, CJX-2, CJX-3, ANX-6, ANX-7 and ANX-8) were further evaluated for their effect on NO production at different doses. The experimental procedure was carried out as described in section 3.2.4.1. and six different doses (1000, 500, 250, 125, 62.5 and 31.25 µg/mL final concentration in each well) of each of the six AXH were used in the assay. The experiments were conducted in duplicate.

3.3.5. Statistical analysis

All the cell culture experiments were done in duplicate. The data are presented as the means ± SE and were subjected to one way ANOVA using LSD test procedure employing Statistical Analysis System software package version 9.4 (SAS Institute, Cary, NC). A least significant difference (LSD) with a 5 % significance level was used to declare differences. Differences were considered significant when the probability value *p* was lower than 0.05.

Pearson's correlation analysis was conducted to evaluate relationships between immunological outcomes and AXH composition/structural details.

3.4. Results and Discussion

3.4.1. Composition and structural analysis of AXH

Extensive discussions on the fine structural details of the AXH are discussed in a previous chapter (Chapter 2). The sugar composition, total AX % and the A/X ration of the WAX and the resulting AXH are given in Table 2.2. The weight average molecular weights and polydispersity index of each AXH is presented in Table 2.3.The ^{1}H-NMR resonance integrations for WAX and AXH are in Table 2.4. The linkage analysis results of each AXH are depicted in Figure 2.3.

3.4.2. Immunomodulatory properties of thirty AXH

The specific objective of this research was to evaluate the effect of structural details of AXH on their immunomodulatory properties. The LPS induced macrophage cell line is a model widely used to study inflammation. Thus, the effect of each AX hydrolyzates on altering the LPS induced inflammation with respect to NO was evaluated. The cells that were induced with LPS but did not receive any AXH was regarded as the control treatment. Indomethacin was used as the positive control. The results are illustrated in Figure 3.2. Inflammation is an important

healthy immune response by the body during lesions and infection. However, uncontrolled excessive inflammation can be damaging to the cells. Excessive inflammation can lead to several acute and chronic diseases characterized by excessive production of pro-inflammatory cytokines, eicosanoids derived from arachidonic acid, reactive oxygen species and adhesion molecules (Kumar et al., 2002; Vernaza et al., 2012). Thus, food components that regulate inflammatory and oxidative stress responses are of vital need. On the other hand, inflammation is not necessarily a negative response. A healthy amount of inflammation is necessary for the maintenance of health. This fine balance between acute inflammation and chronic inflammation lead to health or disease. The AXH being tested exhibited both pro- and anti-inflammatory properties. Some of the hydrolyzates increased the production of NO compared to the control while some AXH decreased the NO production.

As shown in Figure. 3.2, the effects of AXH varied from each other. Indomethacin was used as a positive control. The treatment of cells with AXH without LPS induction did not result in a significant increase in NO production compared to cells that did not receive an AXH treatment which indicates that AXH themselves are not inducing NO production in macrophages. This ruled out possible LPS contamination in the AXH.

Physiologically, NO induces oxidative stress and causes the release of oxygen and nitrogen reactive species which are important in the elimination of engulfed microbes by macrophages (Vernaza et al., 2012). It also contributes to the killing of tumor cells through activated macrophages and mediates a variety of biological functions as an intracellular messenger molecule (Palmer et al., 1988). However, enhanced NO production, mainly via inducible nitric oxide synthase (iNOS) activity is also associated with colonic inflammation (Rodriüguez-Cabezas et al., 2003). Thus, AXH that reduce the production of NO might be

beneficial for patients with inflammatory bowel disease (IBD) and need further investigation. Rodriüguez-Cabezas et al., (2003) observed that anti-inflammatory effects of dietary fibers were associated with a significant inhibition of colonic nitric oxide synthase (NOS) activity.

Seventeen of the 30 AXH lowered LPS induced NO production in macrophages compared to cells that did not receive an AXH treatment. These results indicate some anti-inflammatory properties among these AXH. Indomethacin was displaying higher NO suppression than the AXH. In a dietary point of view, these polysaccharides are intended to enforce immunological outcomes as a result of frequent consumption of these wheat derived polysaccharides over a period of time. Thus, consumption of food rich in AXH of this nature could be beneficial. Future research on the dose dependent effect of these AXH could provide more information about their potency. The rest of the AXH caused an increase in NO production in the LPS induced cells. This suggests immune-stimulatory properties of these AXH. Although over expression of immune responses are detrimental to the health, immune-enhancing properties can be beneficial in terms of NO mediated cytotoxicity properties in macrophages (Moncada et al., 1991). Such pro-inflammatory compounds could exert benefits to the immune system by stimulating the immune cells. These pro-inflammatory AXH could have potential role as immunostimulator which might be beneficial in immune compromised individuals.

Out of the 30 AXH, ten AXH were identified to contain statistically significant differences compared to the control (Table 3.1). Six AXH (ANX-6, CAF-3, ANX-8, CAF-6, CAF-2 and ANX-7 in the descending order of activity) showed anti-inflammatory properties while four AXH (CJX-2, CAF-1, CJX-1 and CJX-3 in the descending order of activity) exhibited pro-inflammatory properties. ANX-6 displayed the highest anti-inflammatory property while CJX-2 showed the highest pro-inflammatory property.

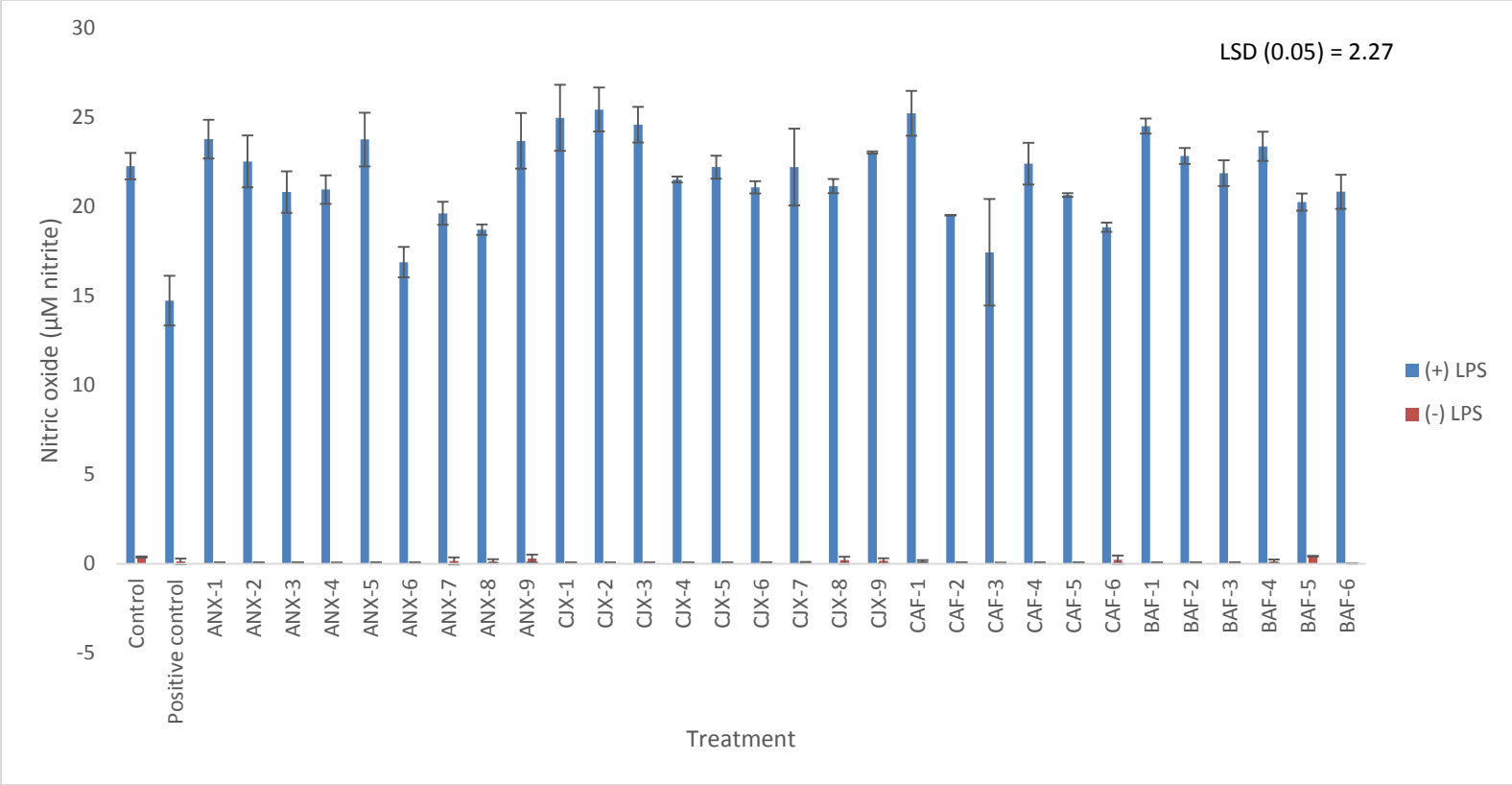

Figure 3.2. Effect of AXH on nitric oxide production in LPS induced NO production in macrophages. Control: cells treated with DMEM; positive control: cells treated with Indomethacin; ANX-1 to BAF-6: cells treated with corresponding AXH. Data are presented as mean ± SD. LSD, least significant difference ($P<0.05$). Values differing more than LSD are significantly different from each other.

The AXH with the highest anti-inflammatory properties and those with the highest pro-inflammatory properties were selected and further evaluated for the contribution of their structure to such properties. We compared the structures of CJX-2 and CAF-1 (highest pro-inflammatory properties) and ANX-6 and CAF-3 (highest anti-inflammatory properties) to identify any structure function relationship. Several important differences were evident among the two groups of AXH. The AXH with pro-inflammatory properties had higher weight average molecular weights (e.g. 5.64 million Da) while lower molecular weights (e.g. 0.78 million Da) were seen for AXH with anti-inflammatory properties. This suggests that the weight of the AXH polymers seems to have an effect in governing their immunomodulatory properties. This contradicts Mikkelsen et al (2014), who evaluated the immunological properties of beta-glucan and concluded that the immune response doesn't depend on molecular mass of the beta-glucan polysaccharides. However, Mikkelsen et al. (2014) also stated that these conclusions could have been caused by the narrow molecular mass range (130-410 kDa) used in that study. In the contrary, the current study employed AXH of a wider range of molecular weights ranging from c.a. 0.78 to 5.64 million Da. Thus, the contribution from molecular weight to immunomodulatory properties was more detectable in the current study. Even though the molecular weight of a polysaccharide does not give an idea about its size in the solution, we could assume that the AXH with larger molecular weights were of larger size compared to the AXH with smaller molecular weight. Using the Dectin-1 receptor, a receptor for beta-glucan, Goodridge et al (2011) showed that unlike some other pattern recognition receptors, such as Toll-like receptors (TLRs) which are activated by soluble ligands, Dectin-1 receptors are only activated by particulate beta-glucans, (and not soluble beta-glucans) "which cluster the receptor in synapse-like structures from which regulatory tyrosine phosphatases CD45 and CD148 are excluded"

which results in its activation. Mikkelsen et al (2014) also hypothesized a similar model to explain his finding regarding soluble and aggregated beta-glucan in solution. In a similar sense, the higher molecular weight AXH might have a clustering effect on its receptors due to its larger sizes that might result in activation of its receptors, and account for the pro-inflammatory properties of AXH with larger molecular weights. In general, to trigger an immune response, the polysaccharide must collide with its receptor on the cell surface. The polysaccharides with larger molecular weights, and thus, with larger sizes, are more effective in making sufficient collisions with their receptors (Leung et al., 2006). Also, polysaccharides with larger molecular weights have larger number of repeating units that increases their chances of making effective bonding with the receptors (Leung et al., 2006).

Table 3.1. AXH[a] with anti-inflammatory and pro-inflammatory properties[b].

Anti-inflammatory properties	Percent decrease in NO production compared to control (%)	Pro-inflammatory properties	Percent increase in NO production compared to control (%)
ANX-6	24.1	CJX-2	14.2
CAF-3	21.7	CAF-1	13.3
ANX-8	16.0	CJX-1	12.2
CAF-6	15.4	CJX-3	10.4
CAF-2	12.4		
ANX-7	11.9		

[a]Enzymatic treatments were carried out using the following enzymes: ANX, endo-1,4-β-Xylanase M4 (*Aspergillus niger*); CJX, Endo-1,4-β-Xylanase (*Cellvibrio japonicus*); CAF, α-L-Arabinofuranosidase (*Clostridium thermocellum*); each sample name starting with corresponding enzyme abbreviation received that specific enzyme treatment first. [b]The AXH are presented in their descending order of potency.

Apart from molecular weight, total AX content in each AXH also played a role in governing the anti/pro-inflammatory properties of these compounds. ANX-6 and CAF-3 which showed the highest anti-inflammatory properties had higher total AX content compared to CJX-2 and CAF-1 which exhibited the highest pro-inflammatory properties. There were significant

differences among the fine structural details of these AXH as well. The three anti-inflammatory AXH, ANX-6 and CAF-3 had lower amount of terminal xylose residues, higher amount of 1-4-linked xylose residues and higher amount of 1-4-linked xylose with substitution at O-3- position compared to the three pro-inflammatory AXH, CJX-2 and CAF-1. The importance of polymer side branching on its immunological properties has also been emphasized by other researches (Adams et al., 2008; Mikkelsen et al., 2014). Zhou et al (2010) suggested that "immune-enhancing function of wheat bran AX is related to the molecular weight, chemical composition and substituted degree or branch of arabinose." Similarly, the fine structural details might play a role in governing the immunological properties of the AXH in the current study.

3.4.3. Effect of different AXH doses on NO production

Six AXH were further investigated for their dose-dependent effect on LPS induced RAW 264.7 cells. The cells were treated with different doses of six AXH and NO levels were investigated. Although there was a slight increase in NO production in cells treated with each AXH at highest concentration (1000 μg/mL) compared to the cells that did not receive any AXH treatment, this increased NO production was relatively low compared to NO production in cells upon induction with LPS (Figure 3.3). Thus, we could assume that the endotoxin levels in AXH used in this study was negligible.

Overall, all the six AXH dose-dependently increased LPS induced NO production. However, CJX-3, ANX-6 and ANX-8 showed prominent dose dependent responses. Previous researches had demonstrated dose-dependent suppression of NO production in LPS induced cells upon treatment with yeast beta-glucans (Xu et al., 2012). However, other researches had reported dose-dependent increase of NO production by mushroom derived beta-glucans (Volman et al., 2010). In the current research, AXH increased NO production with increasing concentration.

This indicates that the AXH being investigated might have pro-inflammatory effects in a dose-dependent manner. These results make AXH an interesting food component that needs to be further investigated as immunomodulators that can be useful to revive depressed states of immunity. Activation of macrophages is an important innate immune response that serves a defense purpose. Wheat bran AX has been shown to enhance phagocytic activity of macrophages in animals (Zhou et al., 2010). Our results also indicate activation of LPS induced macrophages by AXH under study.

3.4.4. Correlation analysis between NO production and chemical properties of thirty AXH

Correlation analysis of the data indicates that there is a strong negative correlation (-0.538) between the amount of 1,4-linked xylose with arabinose substituted at O- 3- position and the NO production. A stronger negative correlation (-0.616) was seen when the amount of total AX was also taken into account (i.e. correlation between NO production and total AX into amount of 1,4-linked xylose with arabinose substituted at O- 3- position). This association is shown in Figure 3.4. This indicates that AXH with higher AX and substitution at O-3 position are favorable candidates to reduce the LPS induced inflammation. Kim et al (2012) investigated the anti-inflammatory activity of hydroxycinnamic acid derivatives isolated from corn bran in LPS-stimulated Raw 264.7 macrophages and observed that phenolic amide and ferulic acid moieties may be responsible for inhibiting NO production.

These results support our finding in which higher amount of arabinose substituted at O-3- position (GP9) might carry higher phenolic moieties along with it and result in higher inhibition of NO production. The exact molecular mechanisms involved in AX uptake by the intestinal epithelial cells or the macrophages are not yet clearly understood. However, in the case

of beta-glucan, a vastly studied polysaccharide, there is extensive literature identifying the specific receptors involved in recognition of beta-glucan by cells.

There are two main receptors involved in beta-glucan recognition (Hong et al., 2004). Dectin-1, a signaling non-TLR pattern recognition receptor is a major receptor involved in beta-glucan recognition in macrophages (Brown, 2006; Brown et al., 2002; Hong et al., 2004). The second receptor, CR3 is less present in macrophages (Hong et al., 2004). While dectin-1 exerts its action via phagocytosis, CR3 achieves this function via granulocytes and relies on the complement system (Hong et al., 2004). Just as macrophages possesses specific receptors that ligate with beta-glucan, it is possible that the macrophages possess other pattern recognition receptors that specifically identify AX and that these receptors are involved in bringing about the specific immunological outcomes as evident by increased NO production. Lee et al (2008) demonstrated that NO production induced by mushroom polysaccharide can be markedly suppressed by function blocking antibodies to dectin-1. Though it is still too early to draw such conclusions about the molecular mechanism as to how the AXH exhibit its anti-inflammatory properties, the possibility of these AXH acting as inhibitory molecules to specific pattern recognition molecules in the cell surface can be a potential research area that needs to be explored.

Nuclear factor-κB (NF-κB) is an important transcription factor involved in various immunological processes including cytokine production, phagocytosis and respiratory burst (Volman et al., 2008). Mitogen-activated protein kinase (MAPK) phosphorylation is a prerequisite for NO and cytokine productions in stimulated macrophages (Dean et al., 1999) and NF-κB activation is dependent on activation of MAPK (Olson et al., 2007).

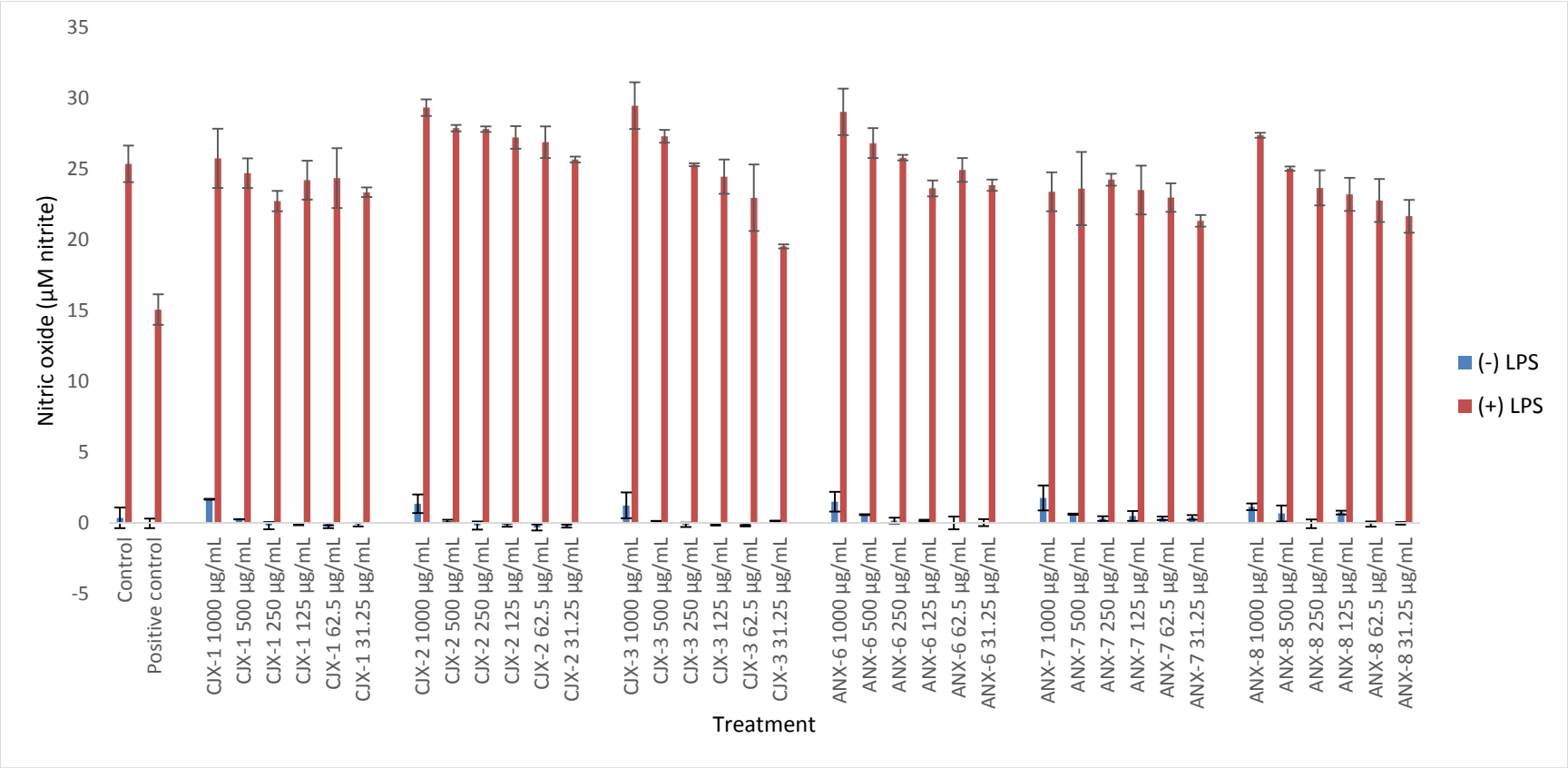

Figure 3.3. Effect of different doses of six AXH on nitric oxide production in LPS induced NO production in macrophages. Control: cells treated with DMEM; positive control: cells treated with Indomethacin; CJX-1 to ANX-8: cells treated with corresponding AXH. Data are presented as mean ± SD. LSD, least significant difference ($P<0.05$). Values differing more than LSD are significantly different from each other.

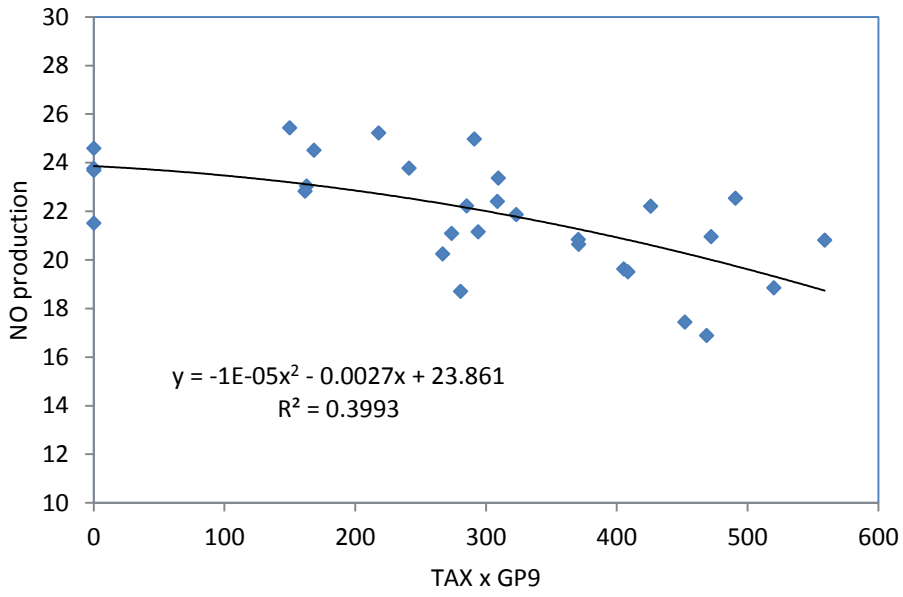

Figure 3.4. Association between NO production and total AX (TAX) into amount of 1,4-linked xylose with arabinose substituted at O- 3- position (GP9).

Several researches have demonstrated the involvement of NF-κB in cellular pathways triggered by botanical polysaccharides (Lee et al., 2013; Schepetkin and Quinn, 2006; Volman et al., 2008). Polysaccharides from fermented soybean were shown to increase NO and TNF-α production by activating the MAPK and NF-κB signaling pathways in macrophages (Lee et al., 2013). Reviews by Schepetkin and Quinn (2006) and Volman et al. (2008) describe the involvement of pattern recognition receptors such as toll-like receptor (TLR), scavenger receptor (SR), complement receptor type 3 (CR3), and mannose receptor (MR) in recognition of botanical polysaccharides by cells. "Plant polysaccharides can also be phagocytosed, leading to activation of unknown intracellular targets" and it is also "likely that several different receptor types cooperate with each other, forming clusters of signaling complexes" (Schepetkin and Quinn, 2006). A schematic model illustrating potential signaling pathways involved in macrophage activation by botanical polysaccharides can be illustrated as follows (Figure 3.5) as reviewed by Schepetkin and Quinn (2006). However, there is scarcity of research investigating the

underlining molecular mechanisms of how AXH modulate the immune function in cells and this area needs to be further investigated. To date, the exact mechanism of processes executed by cells upon encounter of arabinoxylans has not been well defined.

3.5. Conclusions

Use of plant derived polysaccharides as health promoter has gained immense interest in the past few years. The current research aimed to investigate the structure-function relationship of enzymatically tailored AXH as immunomodulators using LPS induced RAW 264.7 macrophage cell line. Our results indicate that under the enzymatic conditions used, structurally different AXH could be produced and that these AXH had varying immunomodulatory properties. Out of the 30 different AXH, 10 AXH that indicated strong immunomodulatory properties were identified. These AXH had either pro-inflammatory properties or anti-inflammatory properties. The pro-inflammatory AXH had higher molecular weights compared to the anti-inflammatory AXH. Fine structural differences were also evident between these two pro- and anti- inflammatory groups of AXH. These results indicate that there might be a structure-function relationship for these AXH as immunomodulators. Further research is needed to evaluate the dose dependence of these AXH on immune system cells and also to identify the cellular mechanisms involved in exerting the observed outcomes for these compounds.

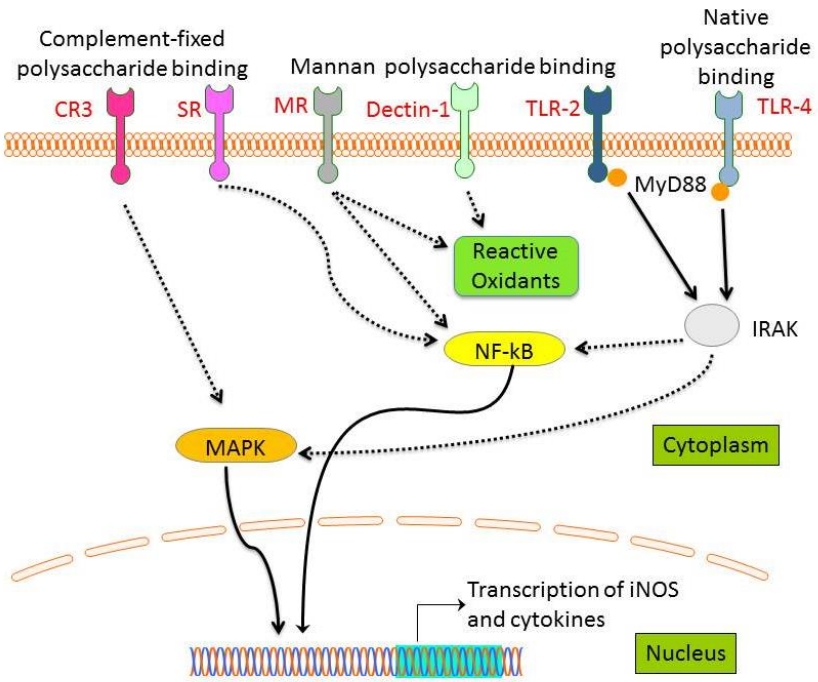

Figure 3.5. Schematic model illustrating potential signaling pathways involved in macrophage activation by botanical polysaccharides. Polysaccharides can activate macrophages via complement receptor 3 (CR3), mannose receptor (MR), scavenger receptor (SR), Dectin-1 and Toll-like receptor 4 (TLR4). SR- and CR3-activated signaling pathways lead to activation of mitogen-activated protein kinase (MAPK) and nuclear factor-κB (NF-κB). Ultimately, these pathways lead to induction of gene transcription. MR activation leads to activation of macrophage phagocytosis, oxidant production, endocytosis and NF-κB. TLR-4 ligation leads to the activation of IL-1R-associated kinase (IRAK) via an adaptor myeloid differentiation protein 88 (MyD88), with subsequent activation of MAPK and NF-κB. Activation of these transcription pathways induces expression of pro-inflammatory cytokines and inducible nitric oxide synthase (iNOS). Adapted from Schepetkin and Quinn (2006).

3.6. References

Abbas, A. K., and Lichtman, A. H., eds. (2011). "Basic immunology: functions and disorders of the immune system." Saunders Elsevier, Philadelphia, PA, USA.

Adams, E. L., Rice, P. J., Graves, B., Ensley, H. E., Yu, H., Brown, G. D., Gordon, S., Monteiro, M. A., Papp-Szabo, E., and Lowman, D. W. (2008). Differential high-affinity interaction of dectin-1 with natural or synthetic glucans is dependent upon primary structure and is

influenced by polymer chain length and side-chain branching. *Journal of Pharmacology and Experimental Therapeutics* **325**, 115-123.

Akhtar, M., Tariq, A. F., Awais, M. M., Iqbal, Z., Muhammad, F., Shahid, M., and Hiszczynska-Sawicka, E. (2012). Studies on wheat bran Arabinoxylan for its immunostimulatory and protective effects against avian coccidiosis. *Carbohydrate Polymers* **90**, 333-339.

American academy of allergy, a. a. i. (2014). Immunomodulators. American Academy of Allergy, Asthma & Immunology. http://www.aaaai.org/conditions-and-treatments/conditions-dictionary/immunomodulators.aspx

Brown, G. D. (2006). Dectin-1: a signalling non-TLR pattern-recognition receptor. *Nat Rev Immunol* **6**, 33-43.

Brown, G. D., Taylor, P. R., Reid, D. M., Willment, J. A., Williams, D. L., Martinez-Pomares, L., Wong, S. Y., and Gordon, S. (2002). Dectin-1 is a major beta-glucan receptor on macrophages. *The Journal of experimental medicine* **196**, 407-412.

Cao, L., Liu, X., Qian, T., Sun, G., Guo, Y., Chang, F., Zhou, S., and Sun, X. (2011). Antitumor and immunomodulatory activity of arabinoxylans: A major constituent of wheat bran. *International Journal of Biological Macromolecules* **48**, 160-164.

Collins, T., Gerday, C., and Feller, G. (2005). Xylanases, xylanase families and extremophilic xylanases. *FEMS Microbiology Reviews* **29**, 3-23.

Dean, J. L. E., Brook, M., Clark, A. R., and Saklatvala, J. (1999). p38 Mitogen-activated Protein Kinase Regulates Cyclooxygenase-2 mRNA Stability and Transcription in Lipopolysaccharide-treated Human Monocytes. *Journal of Biological Chemistry* **274**, 264-269.

Dornez, E., Gebruers, K., Delcour, J., and Courtin, C. (2009). Grain-associated xylanases: occurrence, variability, and implications for cereal processing. *Trends in food science & technology*. **20**, 495-510.

Edogawa, S., Sakai, A., Inoue, T., Harada, S., Takeuchi, T., Umegaki, E., Hayashi, H., and Higuchi, K. (2014). Down-regulation of collagen I biosynthesis in intestinal epithelial cells exposed to indomethacin: A comparative proteome analysis. *Journal of Proteomics* **103**, 35-46.

Fujihara, M., Muroi, M., Tanamoto, K., Suzuki, T., Azuma, H., and Ikeda, H. (2003). Molecular mechanisms of macrophage activation and deactivation by lipopolysaccharide: roles of the receptor complex. *Pharmacol Ther* **100**, 171-94.

Goodridge, H. S., Reyes, C. N., Becker, C., Katsumoto, T. R., Ma, J., Wolf, A. J., Bose, N., Chan, A. S., Magee, A. S., and Danielson, M. E. (2011). Activation of the innate immune receptor Dectin-1 upon formation of a 'phagocytic synapse'. *Nature* **472**, 471-475.

Gwinn, M. R., and Vallyathan, V. (2006). Respiratory burst: role in signal transduction in alveolar macrophages. *Journal of Toxicology and Environmental Health, Part B* **9**, 27-39.

Hong, F., Yan, J., Baran, J. T., Allendorf, D. J., Hansen, R. D., Ostroff, G. R., Xing, P. X., Cheung, N. K., and Ross, G. D. (2004). Mechanism by Which Orally Administered beta-1,3-Glucans Enhance the Tumoricidal Activity of Antitumor Monoclonal Antibodies in Murine Tumor Models. *The Journal of Immunology* **173**, 797-806.

Kim, E. O., Min, K. J., Kwon, T. K., Um, B. H., Moreau, R. A., and Choi, S. W. (2012). Anti-inflammatory activity of hydroxycinnamic acid derivatives isolated from corn bran in lipopolysaccharide-stimulated Raw 264.7 macrophages. *Food and Chemical Toxicology* **50**, 1309-1316.

Kumar, M. V., Shimokawa, T., Nagy, T. R., and Lane, M. D. (2002). Differential effects of a centrally acting fatty acid synthase inhibitor in lean and obese mice. *Proceedings of the National Academy of Sciences* **99**, 1921-1925.

Lee, J. Y., Kim, J. Y., Lee, Y. G., Rhee, M. H., Hong, E. K., and Cho, J. Y. (2008). Molecular mechanism of macrophage activation by Exopolysaccharides from liquid culture of Lentinus edodes. *Journal of microbiology and biotechnology* **18**, 355-364.

Lee, S. J., Rim, H. K., Jung, J. Y., An, H. J., Shin, J. S., Cho, C. W., Rhee, Y. K., Hong, H. D., and Lee, K. T. (2013). Immunostimulatory activity of polysaccharides from Cheonggukjang. *Food and Chemical Toxicology* **59**, 476-484.

Leung, M. Y. K., Liu, C., Koon, J. C. M., and Fung, K. P. (2006). Polysaccharide biological response modifiers. *Immunology Letters* **105**, 101-114.

Liu, F., Liu, Y., Lui, V. C. H., Lamb, J. R., Tam, P. K. H., and Chen, Y. (2008). Hypoxia modulates lipopolysaccharide induced TNF-α expression in murine macrophages. *Experimental Cell Research* **314**, 1327-1336.

MacKenzie, K. F., Van Den Bosch, M. W., Naqvi, S., Elcombe, S. E., McGuire, V. A., Reith, A. D., Blackshear, P. J., Dean, J. L., and Arthur, J. S. (2013). MSK1 and MSK2 inhibit lipopolysaccharide-induced prostaglandin production via an interleukin-10 feedback loop. *Mol Cell Biol* **33**, 1456-67.

MacKichan, M. L., and DeFranco, A. L. (1999). Role of ceramide in lipopolysaccharide (LPS)-induced signaling. LPS increases ceramide rather than acting as a structural homolog. *J Biol Chem* **274**, 1767-75.

Medzhitov, R. (2008). Origin and physiological roles of inflammation. *Nature* **454**, 428-435.

Mikkelsen, M. S., Jespersen, B. M., Mehlsen, A., Engelsen, S. B., and Frokiaer, H. (2014). Cereal bets-glucan immune modulating activity depends on the polymer fine structure. *Food Research International* **62**, 829-836.

Moncada, S., Palmer, R. M., and Higgs, E. A. (1991). Nitric oxide: physiology, pathophysiology, and pharmacology. *Pharmacological Reviews* **43**, 109-142.

Olson, C. M., Hedrick, M. N., Izadi, H., Bates, T. C., Olivera, E. R., and Anguita, J. (2007). p38 Mitogen-Activated Protein Kinase Controls NF-kB Transcriptional Activation and Tumor Necrosis Factor Alpha Production through RelA Phosphorylation Mediated by Mitogen- and Stress-Activated Protein Kinase 1 in Response to Borrelia burgdorferi Antigens. *Infection and Immunity* **75**, 270-277.

Palmer, R. M. J., Ashton, D. S., and Moncada, S. (1988). Vascular endothelial cells synthesize nitric oxide from L-arginine. *Nature* **333**, 664-666.

Pollet, A., Delcour, J. A., and Courtin, C. M. (2010). Structural determinants of the substrate specificities of xylanases from different glycoside hydrolase families. *In* "Critical reviews in biotechnology", Vol. 30, pp. 176-191. Informa Healthcare.

Robinson, J. M. (2009). Phagocytic leukocytes and reactive oxygen species. *Histochemistry and cell biology* **131**, 465-469.

Rodriüguez-Cabezas, M. E., Gaílvez, J., Camuesco, D., Lorente, M. D., Concha, A., Martinez-Augustin, O., Redondo, L., and Zarzuelo, A. (2003). Intestinal anti-inflammatory activity of dietary fiber (*Plantago ovata* seeds) in HLA-B27 transgenic rats. *Clinical Nutrition* **22**, 463-471.

Saulnier, L., Sado, P. E., Branlard, G., Charmet, G., and Guillon, F. (2007). Wheat arabinoxylans: Exploiting variation in amount and composition to develop enhanced varieties. *Journal of Cereal Science* **46**, 261-281.

Schepetkin, I. A., and Quinn, M. T. (2006). Botanical polysaccharides: Macrophage immunomodulation and therapeutic potential. *International Immunopharmacology* **6**, 317-333.

Taylor, E., Smith, N., Turkenburg, J., D'souza, S., Gilbert, H., and Davies, G. (2006). Structural insight into the ligand specificity of a thermostable family 51 arabinofuranosidase, Araf51, from *Clostridium thermocellum*. *Biochem.J* **395**, 31-37.

van den Broek, L., Lloyd, R., Beldman, G., Verdoes, J., McCleary, B., and Voragen, A. (2005). Cloning and characterization of arabinoxylan arabinofuranohydrolase-D3 (AXHd3) from *Bifidobacterium adolescentis* DSM20083. *Applied Microbiology and Biotechnology* **67**, 641-647.

Vernaza, M. G., Dia, V. P., Gonzalez de Mejia, E., and Chang, Y. K. (2012). Antioxidant and antiinflammatory properties of germinated and hydrolysed Brazilian soybean flours. *Food Chemistry* **134**, 2217-2225.

Volman, J. J., Helsper, J. P. F. G., Wei, S., Baars, J. J. P., van Griensven, L. J. L. D., Sonnenberg, A. S. M., Mensink, R. P., & Plat, J. (2010). Effects of mushroom-derived β-glucan-rich polysaccharide extracts on nitric oxide production by bone marrow-derived macrophages and nuclear factor-κB transactivation in Caco-2 reporter cells: Can effects be explained by structure? *Molecular Nutrition & Food Research* 54, 268-276.

Volman, J. J., Ramakers, J. D., and Plat, J. (2008). Dietary modulation of immune function by beta-glucans. *Physiology & behavior* **94**, 276-284.

Xu, X., Yasuda, M., Mizuno, M., and Ashida, H. (2012). Beta-Glucan from Saccharomyces cerevisiae reduces lipopolysaccharide-induced inflammatory responses in RAW264.7 macrophages. *Biochimica et Biophysica Acta (BBA) - General Subjects* **1820**, 1656-1663.

Zhou, S., Liu, X., Guo, Y., Wang, Q., Peng, D., and Cao, L. (2010). Comparison of the immunological activities of arabinoxylans from wheat bran with alkali and xylanase-aided extraction. *Carbohydrate Polymers* **81**, 784-789.

CHAPTER 4. ARABINOXYLAN HYDROLYZATES AS IMMUNOMODULATORS IN CACO-2 AND HT-29 HUMAN INTESTINAL CELL LINES

4.1. Abstract

Use of plant derived polysaccharides as health promoter has gained immense interest in the past few years. Arabinoxylans (AX) are the predominant non-starch polysaccharide in cereals and grasses including wheat. The current research aimed to investigate the structure-function relationship of arabinoxylan hydrolyzates (AXH) obtained by enzymatic hydrolysis of AX using xylanase and arabinofuranosidase as immunomodulators using LPS induced colon cancer cell lines: Caco-2 and HT-29. Fine structural details had a strong correlation with the immunological properties of the wheat AXH. The immunological properties of the AXH might not be dependent on each fine structural detail independently but rather dependent upon a combination of structural details. The 12 different AXH being tested showed different immunological properties with respect to cell type and the cytokine of interest. These results indicate that there might be a structure-function relationship for these AXH as immunomodulators.

4.2. Introduction

Arabinoxylan (AX) is the predominant polysaccharide in the cell wall of wheat grain (Saulnier et al., 2007). It consists of a backbone of β-(1,4)-linked xylose residues, which are substituted with arabinose residues on the C(O)-2 and/or C(O)-3 position (Dornez et al., 2009). Since AX is mainly composed of xylose and arabinose, it is commonly referred to as pentosans. Phenolic acids such as ferulic acid can be ester linked on the C(O)-5 position of arabinose (Figure 1.2).

As the human body lack the enzymes required to hydrolyze the β-glycosidic linkages, AX are not digested by the human digestive enzymes (Carvalho et al., 2013). Thus, they reach the large intestine intact and are considered dietary fibers (under the category of non-starch polysaccharides) (Lafiandra et al., 2014). Owing to these properties they are capable of exerting the health benefits such as weight management, lowering glycemic response, prevention of several non-communicable diseases such as cardiovascular diseases, type II diabetes and cancer (Lafiandra et al., 2014; Mendis and Simsek, 2014). Most of these effects are related to the viscosity effects of dietary fibers which hinder the mixing and diffusion of enzymes to the substrate as well as diffusion of products such as glucose to the enterocytes (Lafiandra et al., 2014). The anti-cancer effects of dietary fibers are mostly related to the effects of short chain fatty acids that are produced by the microbial fermentation of these dietary fibers. However, the immunomodulatory properties of dietary fibers are not to be undermined (Mendis and Simsek, 2014; Tzianabos, 2000; Zhou et al., 2010).

Inflammation is an adaptive response that is triggered by noxious stimuli and conditions, such as infection and tissue injury (Medzhitov, 2008). Under healthy physiological conditions inflammation is a defense response that serves a protective function in the body. However, inflammation can be detrimental if deregulated. At a basic level, acute inflammatory responses triggered by infection and tissue injury involve the organized delivery of blood components to the site of injury. This response, when triggered by microbial infections is activated by receptors of the innate immune system such as Toll-like receptors (TLRs)) and NOD (nucleotide-binding oligomerization-domain protein)-like receptors (NLRs). Recognition of these triggers by cells leads to the production of inflammatory mediators (chemokines, cytokines, vasoactive amines, eicosanoids and products of proteolytic cascades).

The intestinal barrier acts as a first line of defense against many foreign agents that pass through the intestinal tract (Figure 1.10). It comprises of the monolayer of intestinal epithelial cells that display a number of specialized adaptations to maintain its barrier function (Schenk and Mueller, 2008). These include the formation of tight junctions to seal the paracellular spaces, secretion of mucins by globlet cells that form the mucus layer at the apical surface of the intestinal epithelial cells, and secretion of antimicrobial agents such as alpha-defensins, and secretion of lysozyme and cathelicidins by Paneth cells that hinders the penetration of luminal agents and microbes into the intestinal mucosa (Schenk and Mueller, 2008). Thus, intestinal epithelial cells play a vital role in contributing to gut immune system, mediating mucosal defense, barrier repair and identifying and developing tolerance to commensal microbes (Cario et al., 2000).

Thus, intestinal epithelial cells maintain a cross talk between the intestinal lumen and the underling immune cells (Van De Walle et al., 2010). On one hand, they selectively identify and response to luminal content by modulating the barrier permeability and produce inflammatory mediators which facilitate immune response by the underling immune cells. On the other hand, they respond to various inflammatory mediators secreted by immune cells by altering the barrier permeability and cellular secretions and result in amplification or attenuation of the inflammatory process. Thus, intestinal inflammation is a natural and protective function of the gastro-intestinal tract which helps maintain the health of the individual (Martin and Wallace, 2006). However, dysregulation of this inflammatory response can lead to detrimental effects. Inflammatory bowel disease (IBD), the collective name for Crohn's disease and ulcerative colitis, is one such outcome (Neuman, 2007). The disease is characterized by "unpredictable attacks of inflammation of the intestine". It affects as many as 1.4 million persons in the United

States and about 2.2 million persons in Europe (Loftus Jr, 2004). The clinical symptoms include weight loss, diarrhea accompanied by blood, and abdominal pain (Podolsky, 2002). Although the etiology of the disease is not fully understood, a combination of environmental, genetic and immunologic factors seem to initiate an uncontrolled immune response in genetically predisposed individuals leading to the disease (Karlinger et al., 2000). A defective epithelial cell barrier function and elevated immune response leads to a self-amplifying loop, where increased epithelial permeability leads to increased introduction of luminal agents to the underlying immune cells, resulting in increased inflammatory response (Van De Walle et al., 2010). Cytokines are signaling proteins involved in inter-cell communication (Volman et al., 2008). The broadly pro-inflammatory cytokines, specifically tumor necrosis factor (TNF) and interleukin (IL)-1 and 6, which enhance the inflammatory processes, have been linked to the manifestation of the disease (Podolsky, 2002). In vitro, cytokines such as IL-1β, TNF-α, interferon (IFN)-ɣ and lipopolysaccharides (LPS) are capable of activating intracellular cascades in intestinal epithelial cells, increasing the transcription and secretion of IL-6 (Parikh et al., 1997), prostaglandin (PG)-E2 (Grishin et al., 2004) (Wright et al., 2004) and nitric oxide (Forsythe et al., 2002).

The human intestinal cell line, Caco-2 has been extensively used over the last years as a model of the intestinal barrier (Cosentino et al., 2010; Guo et al., 2014; Jung et al., 1995; Liboni et al., 2004; Morita et al., 2002; Sambuy et al., 2005; Van De Walle et al., 2010; Wang et al., 2013). The parental cell line, originally obtained from a human colon adenocarcinoma, undergoes a process of spontaneous differentiation in culture leading to the formation of a monolayer of cells with several morphological and functional characteristics of mature enterocytes (Pinto M, 1983; Sambuy et al., 2005). They grow into monolayer of cells with a cylindrical polarized morphology exhibiting microvilli on the apical side, tight junctions between

adjacent cells. The human colorectal adenocarcinoma cell line, HT-29 established in 1964 (Rousset, 1986) is another widely used model cell line for the study of intestinal features (Gong et al., 2014; Guri et al., 2012; Hajiaghaalipour et al., 2015; Huet et al., 1995; Kim et al., 2012; Rieder et al., 2011; Rousset, 1986). Under standard culture conditions HT-29 cells are undifferentiated and grow as a multilayer of unpolarized cells (Rousset, 1986). However, although mainly undifferentiated they contain a small proportion of mucus-secreting cells and columnar absorptive cells (Gagnon et al., 2013). These two model cell lines were employed in the current research to evaluate the immunomodulatory properties of the different AXH with respect to their structure.

Immunomodulators or biologic response modifiers are compounds that interact with the host immune system and bring about upregulation or downregulation of specific immune responses (Tzianabos, 2000). The immunomodulatory properties of arabinoxylans and their enzymatic products such as xylo-oligosaccharides have been explored in the recent years. Immunostimulating activity of wheat bran derived AX was found to be higher than that for AX derived from corn husk or rice bran (Monobe et al., 2008). Arabinoxylans from wheat bran exert potent effects on innate and acquired immune system (Zhou et al., 2010). Cao et al. (2011) investigated the anti-tumor activity of AX using mice and found that AX from wheat bran were significantly effective in inhibiting the growth of transplanted tumors. They classified AX as anti-tumor agents with immunomodulatory activity. Also, AX were shown to have a possible effect on stimulating the antibody mediated immune response in chicken (Akhtar et al., 2012). As evident as it is, the exact cellular mechanism of how these immunomodulatory effects are brought about by the AX are still not well understood. More so, there is a scarcity of research on understanding how the fine chemical structure of this complex polysaccharide affects its

immunomodulatory properties. No recent research is available on the immunomodulatory properties of enzymatically derived arabinoxylan hydrolyzates from wheat. Thus, we aimed to investigate how the fine chemical structure of enzymatically hydrolyzed AXH affects its immunomodulatory properties.

4.3. Materials and Methods

4.3.1. Materials

Materials used for the production of AXH were previously described in section 2.3.1. Human colorectal adenocarcinoma cell line HT-29 with epithelial morphology was a generous gift from Dr. Bin Guo (Department of Pharmaceutical Sciences, North Dakota State University, ND). The human colorectal adenocarcinoma cell line, Caco-2 was purchased from American Type Culture Collection (ATCC) (Manassas, VA). Eagle's Minimum Essential Medium (EMEM) (ATCC® 30-2003™), Dulbecco's Modified Eagle's Medium (DMEM) (ATCC® 30-2002™) and Fetal Bovine Serum (FBS) (ATCC® 30-2020™) were from ATCC (Manassas, VA). Penicillin-Streptomycin solution (10,000 units/mL Penicillin/ 10,000 µg/mL Streptomycin) was purchased from HyClone Laboratories, Inc. (Logan, UT). Trypsin (1x, 0.25% Trypsin in HBSS without Calcium and Magnesium) was from Mediatech Inc. (Manassas, VA). Lipopolysaccharides (LPS) (*Escherichia coli* 0111:B4, L4391-1MG, Lot No: 043M4089V) and Indomethacin (PHR1247 Fluka) were from Sigma-Aldrich (St. Louis MO). PARIS™ Kit: protein and RNA isolation system (AM1921) was purchased from Ambion® by Life Technologies (Carlsbad, CA). The Reverse Transcription System (A3500) used for the production of cDNA was from Promega Corporation (Madison, WI). The Brilliant II SYBR® Green QRT-PCR Master Mix with Low ROX kit (600835) was purchased from Agilent Technologies, USA.

4.3.2. Procedure for arabinoxylan hydrolyzate preparation

AXH preparation was carried out as described in section 2.3.2 in a previous chapter. A summary of the treatments and the abbreviation given to the resulting AXH is given in Table 4.1.

4.3.3. Chemical analysis

The chemical analysis of the AXH was carried out as described in section 2.3.3 using GC-FID, SEC-MALS, ^{1}H-NMR and GC-FID techniques.

4.3.4. Determination of immunomodulatory properties of AXH

Enzymatically derived arabinoxylan hydrolyzates were evaluated for their immunomodulatory properties using LPS induced intestinal epithelial cell lines Caco-2 and HT-29. Caco-2 cells were grown in EMEM media supplemented with 20% FBS and 1% Penicillin-Streptomycin solution. HT-29 cells were grown in DMEM media supplemented with 10% FBS and 1% Penicillin-Streptomycin solution. The cells were grown at 37 ^{o}C under a humidified atmosphere of 95% air and 5% CO_2.

4.3.4.1. Treatment of cells with AXH

Caco-2 cells were plated at 2×10^{6} cells/mL cell density (400 µL) in 24 well plate wells and incubated overnight. Next day, AXH (2000 µg/mL) dissolved in serum free-antibiotic free EMEM was added (200 µL) to each well. The negative control wells and control wells both received serum free-antibiotic free EMEM (200 µL). Indomethacin (200 µL, 80 µg/mL, PHR1247 Fluka, Sigma-Aldrich (St. Louis MO)), a nonsteroidal antiinflammatory drug (NSAID) which brings about its anti-inflammatory effects through the inhibition of cyclooxygenase (COX) (Edogawa et al., 2014), in serum free-antibiotic free DMEM was added to the positive control wells.

After 2 h incubation with each treatment, 200 µL of LPS dissolved in serum free-antibiotic free EMEM (4 µg/mL) was added to each well to induce inflammation. However, no LPS stimulation was done on the negative control wells, and 200 µL of serum free-antibiotic free EMEM was added to them instead of LPS solution. Thus, the final concentration of each compound in a well was: AXH (500 µg/mL), or Indomethacin (20 µg/mL) and LPS (1 µg/mL). The cells were incubated for 24 h. The same procedure was carried out using HT-29 cells. The cells were plated at 1×10^6 cells/mL cell density and the media used was DMEM. The EMEM media used for dissolving the compounds was replaced with DMEM. A simplified presentation of the AXH treatment procedure carried out on each cell line is given in Figure 4.1.

Table 4.1. Summarized information about the treatments and the abbreviation given to each AXH.

Treatment[1]	Abbreviation of the AXH
ANX → 6 h	ANX-3
ANX → 12h	ANX-4
ANX → BAF	ANX-6
ANX → BAF → CAF	ANX-7
ANX → CAF	ANX-8
CJX → BAF	CJX-6
CAF → CJX	CAF-2
CAF→ ANX	CAF-3
CAF → BAF → CJX	CAF-5
CAF → BAF → ANX	CAF-6
BAF → CAF → CJX	BAF-5
BAF → CAF → ANX	BAF-6

[1]Enzymatic treatments were carried out using the following enzymes: ANX, endo-1,4-β-Xylanase M4 (*Aspergillus niger*); CJX, Endo-1,4-β-Xylanase (*Cellvibrio japonicus*); BAF, α-L-Arabinofuranosidase (novel specificity) (*Bifidobacterium adolescentis*); CAF, α-L-Arabinofuranosidase (*Clostridium thermocellum*)

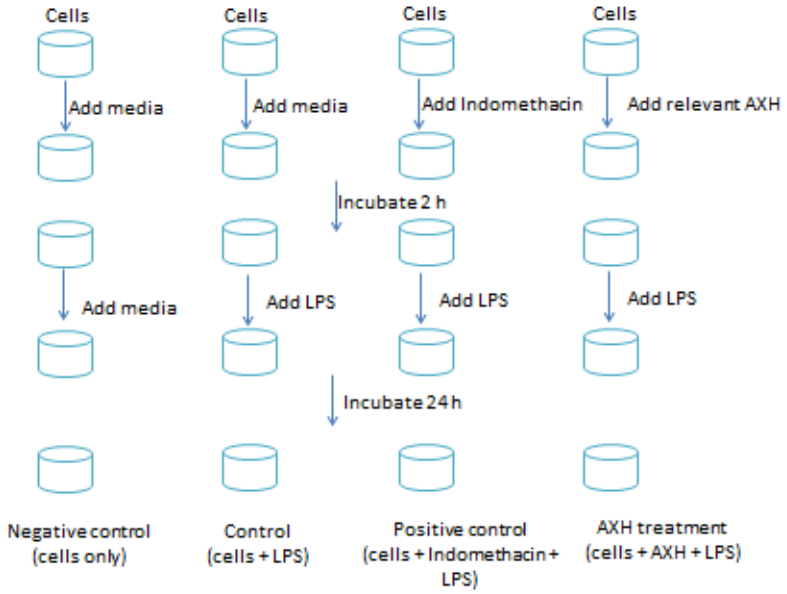

Figure 4.1. Schematic presentations of treatments carried out on cells. Each cylinder represents a well in the 24 well plate. AXH, arabinoxylan hydrolyzate; LPS, lipopolysaccharide.

4.3.4.2. Determination of PG-E2, IL-1β, IL-6, IL-8 and TNF-α using ELISA techniques

The extracellular media were collected and centrifuged at 13,000 rpm for 3 min to precipitate the cell debris. The supernatants were aliquoted out and stored at -20 ^{o}C until further analysis. Human Prostaglandin E2 ELISA kit (KHL 1701) and human IL-8 ELISA Kit (KHC0081) were purchased from Invitrogen Corporation (Camarillo, CA). Human IL-1β Quantikine ELISA kit (DLB50), human IL-6 Quantikine ELISA kit (D6050) and human TNF-α Quantikine ELISA kit (DTA00C) were purchased from R&D Systems, Inc. (Minneapolis, MN). The amount of PG-E2 and each cytokine in the media were determined using the appropriate ELISA kit following the manufacturer's instructions. The results were quantified using the corresponding standard provided with each kit.

4.3.4.3. Quantification of human COX-2, TLR-4, TNF-α and IL-8 mRNAs using quantitative reverse transcriptase real-time polymerase chain reaction (qRT-PCR) techniques

In qRT-PCR the initial amount of mRNA of the gene of interest is assessed by indirectly using its complementary DNA. Throughout the quantitative PCR reaction the amplified transcripts of the gene is responsible for the emission of fluorescence signal and the intensity of this signal is indicative of the number of copies of the amplicon produced after each cycle (Skrzypski, 2008). The greater the number of amplicons, the greater the fluorescence signal. Once a sufficient amount of amplicons are produced after a number of PCR cycles, the fluorescence signal reaches a detectable level (threshold cycle, Ct) and result in exponential increase in fluorescence. If the initial amount of studied transcript is high in a sample the required number of amplicons to produce a detectable fluorescence signal will be produced in fewer PCR cycles (Skrzypski, 2008). Thus, lower Ct values are indicative of higher amount of gene of interest (and in turn higher amount of mRNA of the gene) and vice versa.

The cells were detached using a cell scraper and washed with PBS according to the manufacturer's instructions for the total RNA isolation using the PARIS™ Kit: protein and RNA isolation system (Ambion® by Life Technologies, Carlsbad, CA).The Reverse Transcription System (A3500) (Promega Corporation, Madison, WI) was used for the production of cDNA. The cDNA samples were stored at -20 ^{o}C until use. The qRT-PCR mixture system was set up as follows according to the manufacturer's instructions with some modifications: 10 µL of 2× Brilliant II SYBR® Green QRT-PCR Master Mix with Low ROX (Agilent Technologies, USA), 2 µL of primer mix (5 µM of forward primer and 5 µM of reverse primer), 1 µL of cDNA (5 ng/µL) and 7 µL of nuclease free PCR grade water. The primers purchased from The Midland Certified Reagent Company, Incorporated (Midland, TX) were as follows: Actin (forward)

CATGTACGTTGCTATCCAGGC (reverse) CTCCTTAATGTCACGCACGAT; COX-2 (forward) CAGCAAATCCTTGCTGTTCC (reverse) GTGCACTGTGTTTGGAGTGG; TLR-4 (forward) ATATTGACAGGAAACCCCATCCA (reverse) TAGAACCCGCAAGTCTGTGC; TNF-α (forward) ATGAGCACTGAAAGCATGATCC (reverse) GAGGGCTGATTAGAGAGAGGTC; IL-8 (forward) TTTTGCCAAGGAGTGCTAAAGA (reverse) AACCCTCTGCACCCAGTTTTC. The reaction protocol was as follows: 95 ºC for 10 min; 40 cycles at 95 ºC for 30 s, 60 ºC for 1 min, 72 ºC for 1 min; 95 ºC for 1min; 55 ºC for 30 s; 95 ºC for 30 s. Actin was used as the housekeeping gene and ΔCt values were calculated taking LPS induced cells without any AXH treatment as control.

4.3.5. Statistical analysis

All the cell culture experiments were done in duplicate. All statistical analyses were performed using the Statistical Analysis System software package version 9.4 (SAS Institute, Cary, NC)

The data are presented as the means ± SE and were subjected to one way ANOVA using LSD test procedure. A least significant difference (LSD) with a 5 % significance level was used to declare differences. Differences were considered significant when the probability value *p* was lower than 0.05.

Pearson's correlation analysis was conducted to evaluate relationships between immunological outcomes and AXH composition/structural details.

Stepwise multiple linear regression (SMR) was used to identify and quantify the relationships of immunological outcomes and AXH composition/structural details. The stepping criteria employed for entry and removal were based on the significance level of the F-value and set at 0.05. SMR can provide an equation linking immunological outcomes to the structural

details of the AXH. Stepwise SMR constructs a multivariate model for the dependent variable, Y, based on a few deliberately selected explanatory variables. The best equation is selected on the basis of the highest coefficient of determination (R^2) of a model. The equation takes the following form:

$Y=b_0+b_1X_1+b_2X_2+\cdots+b_nX_n$

where Y is the dependent variable (i.e. the immunological outcome (e.g. cytokine production); $X_1, X_2, \ldots, X_n$ are the independent variables (descriptive variables, i.e. the composition/structural details of AXH such as total AX, unsubstituted xylose %, etc.); b_0 is the constant, where the regression line intercepts the Y axis, representing the amount the dependent Y will be when all the explanatory variables are 0; b_i $(1 \leq i \leq n)$ is the regression coefficient, representing the amount the response variable Y changes when the explanatory variable changes 1 unit. The equation represents a model of the system under study, which can be used to investigate which variables influence its response and at what extent, and/or to predict the value of one variable when the others are known.

4.4. Results and Discussion

4.4.1. Chemical characteristics of the AXH

The sugar composition, A/X ration of the WAX and the resulting AXH are given in Table 4.2. The xylose was the predominant sugar in all the AXH samples followed by arabinose. Glucose was present to a lesser extent and trace amounts of galactose was also present. The total AX ranged between 57.56% in CAF-6 to 31.27% in CJX-6. The arabinose to xylose (A/X) ratio ranged from 0.57 in CJX-6 to 0.48 in ANX-3 and CAF-6. Thus enzymatic treatment on WAX to produce AXH resulted in products with higher A/X ratio. The enzymatic treatment on WAX resulted in AXH products with drastically reduced molecular weights (Table 4.3). The weight

average molecular weight of the AXH ranged from from 0.78- 4.03 million Da. ANX-3 had the highest molecular weight (4.03 million Da) followed by ANX-4 (3.68 million Da) and ANX-6 (3.58 million Da). The lowest molecular weight of 0.78 million Da was observed for CAF-6.

The ^{1}H-NMR results of the different hydrolyzates are summarized in Table 4.4. Each AXH has its own pattern of resonances corresponding to different anomeric protons in the arabinoxylan molecule. Resonances 1-3 correspond to anomeric protons of arabinose, while resonances 4-6 corresponds to anomeric proton in xylose. These fine structural details of the AXH were used in correlating the structural details with biological properties later in the chapter.

Table 4.2. Sugar composition of wheat AX (WAX) and its enzymatic products.

AXH	Sugar composition % (w/w)				A/X ratio
	Arabinose	Xylose	Galactose	Glucose	
WAX	8.46	26.58	0.26	2.56	0.32
ANX-3	13.72	28.37	0.65	4.06	0.48
ANX-4	13.99	24.66	0.57	4.05	0.57
ANX-6	16.13	29.20	0.73	4.54	0.55
ANX-7	15.51	28.32	0.83	4.06	0.55
ANX-8	11.12	22.00	0.40	2.82	0.51
CJX-6	11.39	19.88	0.47	3.03	0.57
CAF-2	15.80	32.09	0.20	3.56	0.49
CAF-3	18.05	35.43	0.23	3.87	0.51
CAF-5	14.69	28.00	0.21	3.61	0.52
CAF-6	18.79	38.77	0.21	4.47	0.48
BAF-5	12.76	24.22	0.46	4.10	0.53
BAF-6	15.16	28.60	0.25	3.35	0.53
LSD	0.84	1.4	0.03	0.02	0.01

LSD = least significant difference ($P < 0.05$)

[a]Enzymatic treatments were carried out using the following enzymes: ANX, endo-1,4-β-Xylanase M4 (*Aspergillus niger*); CJX, Endo-1,4-β-Xylanase (*Cellvibrio japonicus*); BAF, α-L-Arabinofuranosidase (novel specificity) (*Bifidobacterium adolescentis*); CAF, α-L-Arabinofuranosidase (*Clostridium thermocellum*); each sample name starting with corresponding enzyme abbreviation received that specific enzyme treatment first.

To further understand the structural details of the AXH, linkage analysis was carried out using GC-MS techniques. The results are depicted in Figure 4.2. As expected, structural heterogeneity was observed with respect to linkage types present in each arabinoxylan hydrolyzate. As a general trend, the amount of linkages corresponding to unsubstituted xylose is lower in CAF- and BAF- series compared to ANX- and CJX- series. However, this trend is reversed with respect to linkages corresponding to 2,3-disubstituted-1,4,-linked xylose. Thus, the structural complexity is lower in ANX- and CJX- compared to CAF- and BAF- series.

Table 4.3. Weight average molecular weight and polydispersity index of AX hydrolyzates (AXH).

AXH[a]	Molecular weight (Million Da)	Polydispersity index
ANX-3	4.03	2.2
ANX-4	3.68	1.5
ANX-6	3.58	1.5
ANX-7	3.33	1.4
ANX-8	2.91	1.8
CJX-6	1.53	1.8
CAF-2	1.28	1.5
CAF-3	1.11	1.3
CAF-5	0.93	1.8
CAF-6	0.78	1.4
BAF-5	1.14	1.8
BAF-6	1.28	2.0
LSD	0.04	0.4

LSD = least significant difference ($P < 0.05$)

[a]Enzymatic treatments were carried out using the following enzymes: ANX, endo-1,4-β-Xylanase M4 (*Aspergillus niger*); CJX, Endo-1,4-β-Xylanase (*Cellvibrio japonicus*); BAF, α-L-Arabinofuranosidase (novel specificity) (*Bifidobacterium adolescentis*); CAF, α-L-Arabinofuranosidase (*Clostridium thermocellum*); each sample name starting with corresponding enzyme abbreviation received that specific enzyme treatment first.

4.4.2. Immunological activity of AXH

The specific objective of this research was to evaluate the effect of structural details on the immunomodulatory properties of these AXH. The LPS induced colon cancer cell lines Caco-2 and HT-29 were used in this study. Thus, the effect of each AX hydrolyzate on altering the LPS induced inflammation was evaluated.

Table 4.4. ^{1}H-NMR resonance integrations for wheat AX (WAX) and AX hydrolyzates (AXH).

	Resonance integration as % of total resonance					
AXH[a]	Resonance 1	Resonance 2	Resonance 3	Resonance 4	Resonance 5	Resonance 6
WAX	11	7	11	20	12	39
ANX-3	11	10	10	10	15	44
ANX-4	13	14	9	14	12	38
ANX-6	14	13	10	11	14	38
ANX-7	15	11	10	9	14	40
ANX-8	10	13	11	11	14	42
CJX-6	13	12	11	6	13	45
CAF-2	13	11	9	8	13	46
CAF-3	14	12	10	11	12	42
CAF-5	14	11	10	9	12	44
CAF-6	13	9	9	11	13	44
BAF-5	13	11	9	7	13	47
BAF-6	15	11	10	9	13	43

Each resonance corresponds to the following anomeric protons:
Resonance 1, Anomeric proton of O-3 linked arabinose linked to monosubstituted xylose; Resonance 2, Anomeric proton of O-3 linked arabinose linked to disubstituted xylose; Resonance 3, Anomeric proton of O-2 linked arabinose linked to disubstituted xylose; Resonance 4, Anomeric proton of disubstituted xylose; Resonance 5, Anomeric proton of monosubstituted xylose;
Resonance 6, Anomeric proton of unsubstituted xylose
[a]Enzymatic treatments were carried out using the following enzymes: ANX, endo-1,4-β-Xylanase M4 (*Aspergillus niger*); CJX, Endo-1,4-β-Xylanase (*Cellvibrio japonicus*); BAF, α-L-Arabinofuranosidase (novel specificity) (*Bifidobacterium adolescentis*); CAF, α-L-Arabinofuranosidase (*Clostridium thermocellum*); each sample name starting with corresponding enzyme abbreviation received that specific enzyme treatment first.

The cells that were induced with LPS but did not receive any AXH were regarded as the control treatment. Indomethacin (20 µg/mL) is a nonsteroidal anti-inflammatory drug (NSAID) which brings about its anti-inflammatory effects through the inhibition of cyclooxygenase (COX) (Edogawa et al., 2014). Both COX-1 and COX-2 are inhibited by indomethacin with selectivity for COX-1 (Sigma-Aldrich, 2014) which results in the inhibition of prostaglandin production at inflamed sites. The cells that did not receive any LPS and AXH/Indomethacin were also included in the assays to compare with the effect of LPS on the cells.

4.4.2.1. Effect of AXH on PG-E2 and COX-2 production

The effect of AXH on LPS induced prostaglandin (PG)-E2 production in Caco-2 and HT-29 cells were evaluated. PG-E2 is a bioactive lipid that elicits a wide range of biological outcomes related to inflammation and cancer (Nakanishi and Rosenberg, 2013). PG-E2 exerts diverse effects on cell proliferation, apoptosis, inflammation and immune surveillance. Epithelial cells play a key role in maintaining the homeostasis within the gut and inducible formation of PG-E2 plays a vital role in achieving this function, specially maintaining epithelial barrier function (Montrose et al., 2010). It is involved in epithelial regeneration and reconstitution following tissue injury (Iizuka and Konno, 2011) and inducing epithelial cell proliferation (Castellone et al., 2005). The effect of AXH on LPS induced PG-E2 production was evaluated (Figure 4.3). Contrary to what was expected, induction of cells with LPS (control treatment) displayed a reduced PG-E2 production compared to the cells that were not induced by LPS (negative control treatment). This trend was observed for both Caco-2 and HT-29 cell lines. In Caco-2 cells, Indomethacin (positive control) caused an increase in PG-E2 production compared to the control. In the biosynthesis of prostaglandins, phospholipids are converted to arachidonic acid by the action of phospholipase A2 (MacKenzie et al., 2013; Nakanishi and Rosenberg,

2013). Arachidonic acid is next converted into prostaglandin H2 (PGH2) via the action of cyclooxygenases (COX) which is the rate limiting step of PG synthesis. PGH2 is next quickly converted into thromboxane, prostacyclin, or prostaglandin D, E, or F via the action of specific prostaglandin synthases. In mammalian cells two main isoforms of cyclooxygenase exists, cyclooxygenase 1 (COX-1) and COX-2. COX-1 is constitutively expressed in most tissues. COX-2 is highly inducible in many cells by pro-inflammatory stimuli. Thus, production of PG-E2 under no inflammatory stimuli should mainly be due to COX-1 (Surh et al., 2001) and should be responsible for the PG-E2 production in negative control treatment. On the other hand, the PG-E2 produced in the rest of the treatments should be mediated via COX-1 as well as COX-2 (Romier-Crouzet et al., 2009). Mitogen and stress activated protein kinase (MAPK) have been suggested to exert control on the induction of COX-2 mRNA by Toll-like receptor (TLR) agonists (e.g. LPS) (MacKenzie et al., 2013). It was found that MAPK regulated LPS induced prostaglandin and COX-2 protein levels in a time dependent manner. While MAPK promoted COX-2 mRNA transcription initially, following longer LPS stimulation MAPK inhibit LPS-induced prostaglandin production via a negative feedback loop involving IL-10 (Figure 4.5). A similar cellular mechanism might be responsible for the reduced PG-E2 production observed upon LPS stimulation of Caco-2 and HT-29 cells in the control compared to the negative control. However, AXH treatments exerted variable effects on the LPS-induced PG-E2 production in Caco-2 and HT-29 cells. Some AXH exhibited pro-inflammatory properties while others displayed anti-inflammatory properties. However, due to the complex nature of the cellular mechanisms involved in PG-E2 regulation by the cells, the current study alone is not sufficient to draw solid conclusions about the mechanisms involved in up-regulation or down-regulation of

PG-E2 by AXH. A side by side comparison of effect of each of these AXH on cells with and without LPS induction would be a potential approach to be explored in the future.

To further understand the cellular responses involved in immunomodulatory properties of AXH in LPS induced intestinal cells, expression of COX-2 at the mRNA level was investigated using real time quantitative reverse transcriptase polymerase chain reaction (qRT- PCR). Lower Ct values are indicative of higher amount of gene of interest (and in turn higher amount of mRNA of the gene) and vice versa.

Two isoforms of enzyme COX: COX-1 and COX-2 are responsible for prostaglandin synthesis (Martinez-Cutillas et al., In press). While high levels of COX-1 is expressed during physiological conditions, level of COX-2 remains at low levels (Dey et al., 2006). On the contrary, COX- 2 is considered an inducible form of COX and elevated levels are observed during inflammation (Porcher et al., 2004). Up-regulation of COX-2 induces production of PG-E2 which is associated with pathological conditions such as inflammatory bowel disease (Dey et al., 2006) and slow transit constipation (Cong et al., 2007). In the presence of endotoxins such as LPS, mitogen-activated protein kinase (MAPK) (specifically p38 MAPK) is involved in regulation of COX-2 mRNA transcription (Grishin et al., 2004) (Grishin et al., 2006). Also, the anti-inflammatory properties of many phytochemicals have been predicted to be achieved by the down regulation of COX-2 (via suppression of NF-κB activation) (Surh et al., 2001). The effect of different AXH on LPS induced COX-2 gene expression was evaluated by assessing the COX-2 mRNA levels in Caco-2 and HT-29 cells (Figure 4.4). In Caco-2 the COX-2 mRNA expression in LPS induced cells (control) was significantly higher than the none-LPS induced cells (negative control).

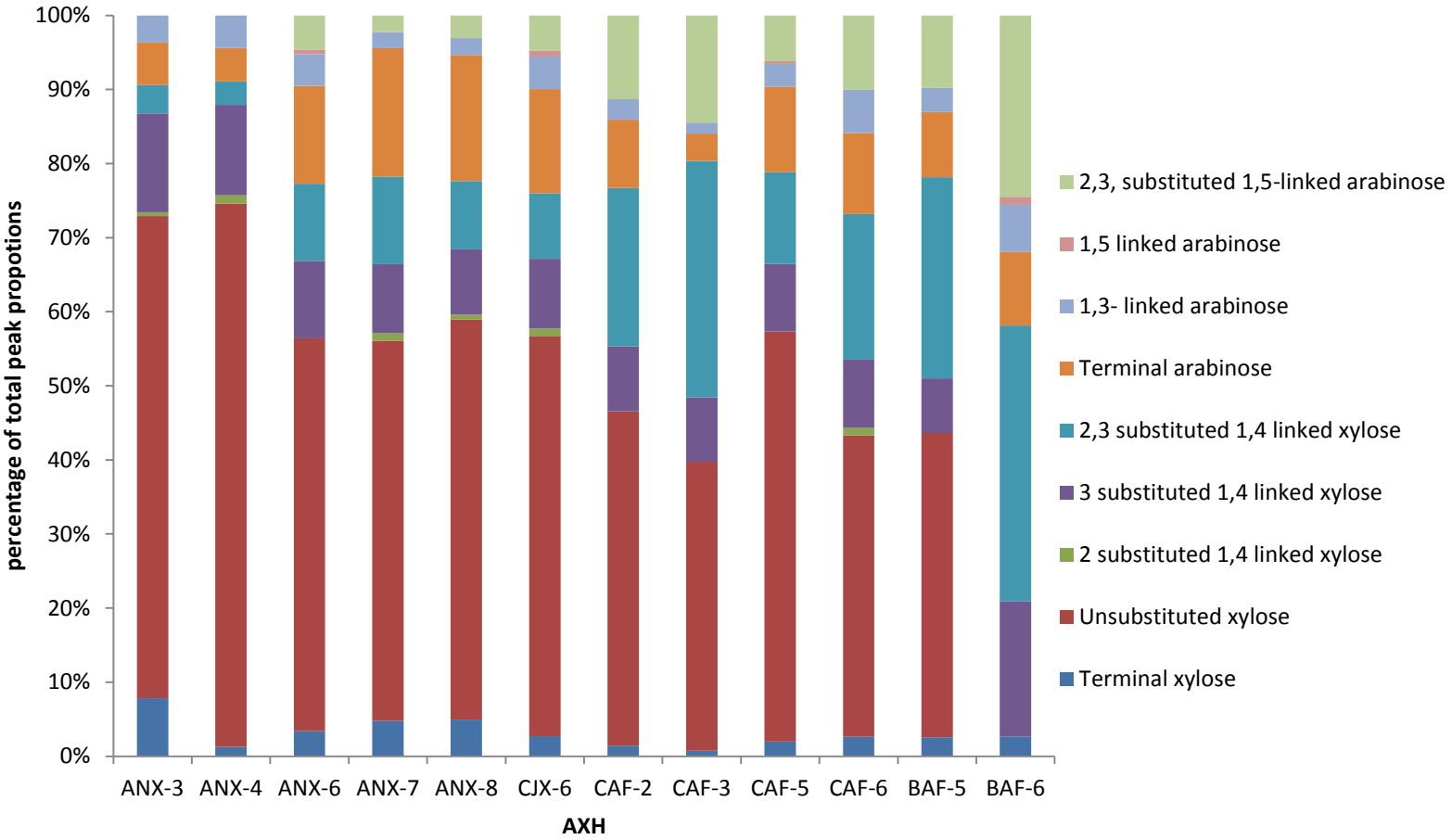

Figure 4.2. Occurrence of each linkage type in each AXH as determined by GC-MS techniques.

As expected, the LPS induced cells had lower Ct values compared to the none-induced cells, translating to higher COX-2 mRNA in the LPS induced cells. All the treatments except CAF-2, ANX-8 and BAF-6 displayed significant differences from the control. Nine of the AXH being tested resulted in higher Ct values compared to the control indicating that the treatment with these AXH decreased the LPS induced COX-2 mRNA production in Caco-2 cells with ANX-6 having the highest inhibitory effect. However, no significant differences were observed between the control and negative control with respect to COX-2 mRNA production in HT-29 cells. Ct values for ANX-4 and BAF-5 were significantly lower than the control indicating increased COX-2 mRNA production in LPS induced HT-29 cells upon treatment with these AXH.

Surprisingly, higher COX-2 mRNA expression in the cells did not result in higher PG-E2 production in the cells for some of the treatments. However, in the biosynthesis of PG-E2, COX-1 and COX-2 are responsible for the conversion of arachidonic acid to PG-G2 and conversion of PG-G2 to PG-H2 (Nakanishi and Rosenberg, 2013). PG-H2 is the precursor for three different PG: PG-D2, PG-I2 and PG-E2. Therefore, one explanation for the reduced production of PG-E2 even under increased COX-2 mRNA might be that once PG-H2 was produced via COX-2, the PG-H2 was involved in the production of other PG (PG-D2, PG-I2) and PG-E2 was not a predominant product. Also, the production of PG-E2 is catalyzed by different set of enzymes whose expression might not have been induced by the treatments under the current study. Moreover, the catabolism of the PG-E2 during the incubation period might also play a role in eliminating the produced PG-E2 from the system (Nakanishi and Rosenberg, 2013). Also, with respect to COX-2 mRNA levels in the cell, with longer stimulation with LPS,

the COX-2 mRNA degradation is accelerated via IL-10 mediated pathways leading to lesser amounts of COX-2 mRNA available for detection (MacKenzie et al., 2013).

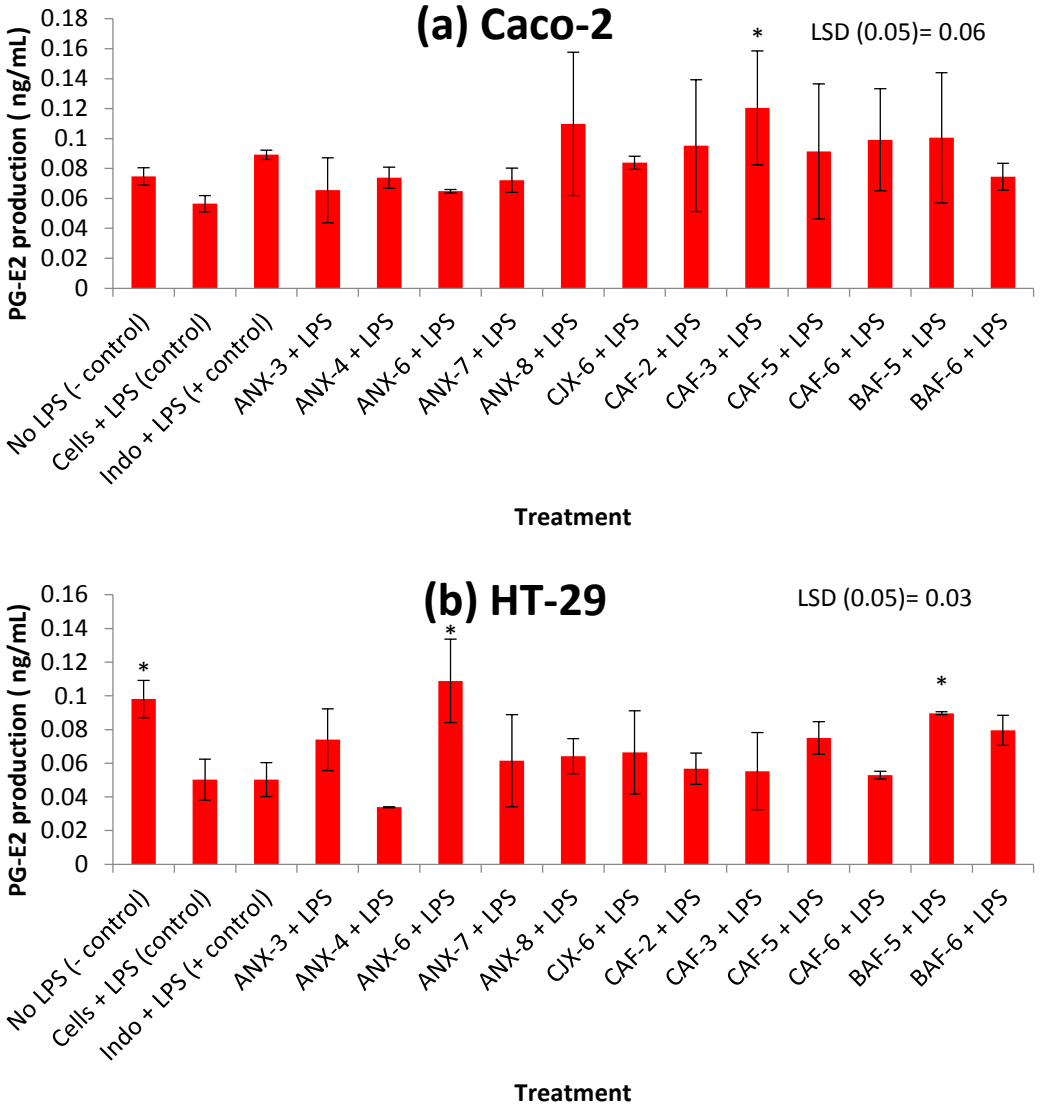

Figure 4.3. Immunomodulatory effect of AXH on LPS induced PG-E2 production in (a) Caco-2 cells and (b) HT-29 cells. Cells only, cells not induced with LPS (negative control); Cells with LPS, cells induced with LPS (control); cells treated with indomethacin (Indo) and induced with LPS (positive control); ANX-3 to BAF-6, cells treated with corresponding AXH and induced with LPS. Data are presented as mean ± SD. LSD, least significant difference (P<0.05). Values differing more than LSD between each other are significantly different (P<0.05) from each other. Bars with an asterisk are significantly different from the control (P<0.05).

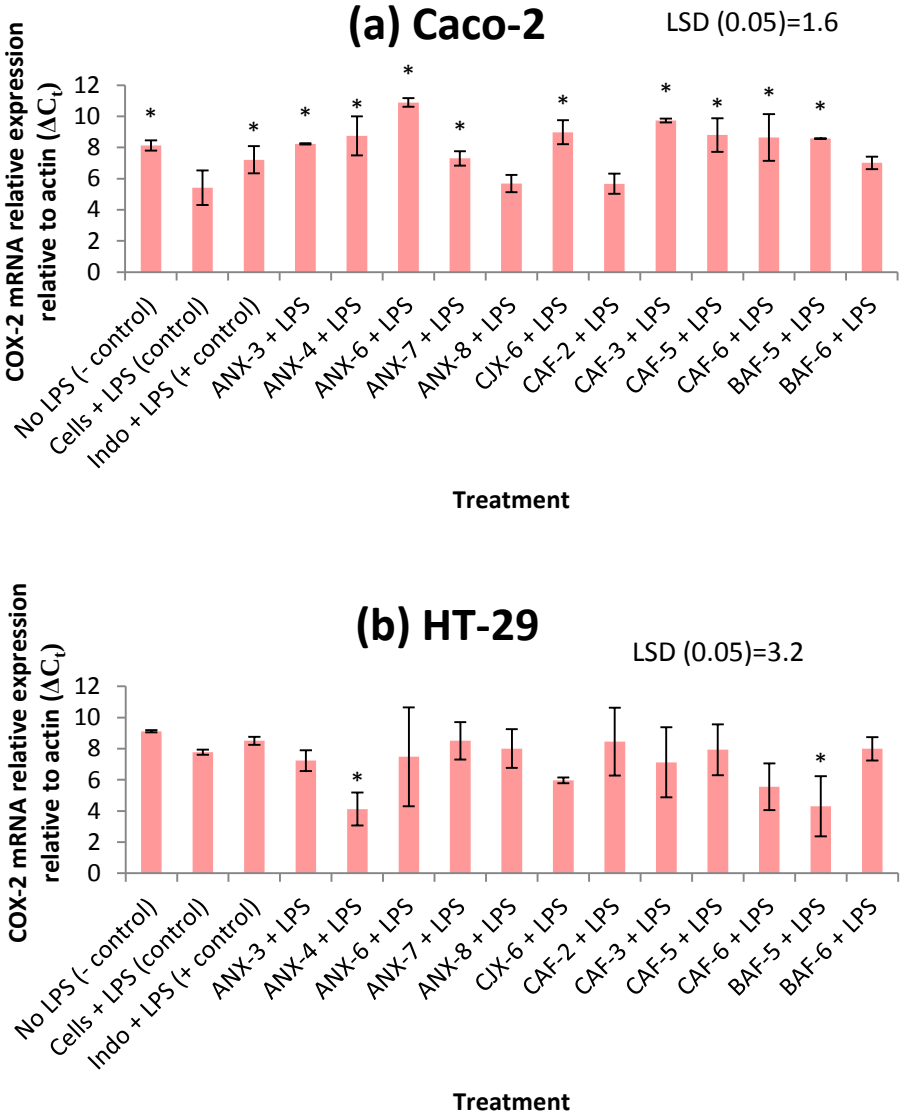

Figure 4.4. Immunomodulatory effect of AXH on LPS induced COX-2 mRNA production in (a) Caco-2 cells and (b) HT-29 cells. $\Delta Ct = Ct_{(gene)} - Ct_{(actin)}$. Cells only, cells not induced with LPS (negative control); Cells with LPS, cells induced with LPS (control); cells treated with indomethacin (Indo) and induced with LPS (positive control); ANX-3 to BAF-6, cells treated with corresponding AXH and induced with LPS. Data are presented as mean ± SD. LSD, least significant difference ($P<0.05$). Values differing more than LSD between each other are significantly different ($P<0.05$) from each other. Bars with an asterisk are significantly different from the control ($P<0.05$).

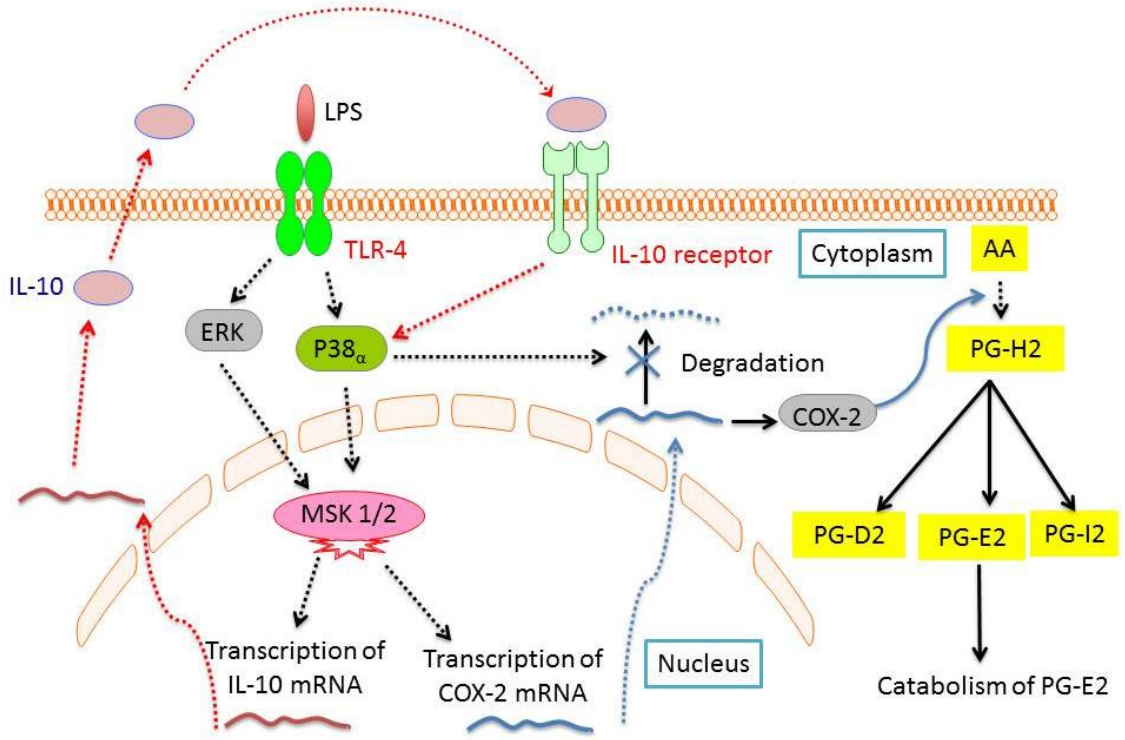

Figure 4.5. Regulation of COX-2 mRNA and PG-E2 production via an IL-10 feedback mechanism. Initially upon activation of TLR-4 by LPS, MSK 1/ 2 is activated resulting in transcription of COX-2 and IL-10 mRNA. Moreover, activation of P38α leads to the inhibition of COX-2 mRNA degradation by mRNA degrading proteins. Thus, more COX-2 mRNA is available for translation to produce COX-2. COX-2 catalyzes the conversion of AA (arachidonic acid) to PG-H2. PG-H2 subsequently gets converted to PG-D2 or PG-E2 or PG-I2. PG-E2 is eventually degraded and eliminated. However, with time, more and more IL-10 is produced and secreted from the cells. The IL-10 generated a feedback loop (indicated by red dashed arrows). The activation of IL-10 receptor by IL-10 lead to downstream pathways that inhibit P38α. Thus, the inhibition it had upon COX-2 mRNA degrading proteins gets eliminated and results in increased degradation of COX-2 mRNA. Based on (MacKenzie et al., 2013; Nakanishi and Rosenberg, 2013).

Thus, ultimately the higher expression of COX-2 mRNA might not necessarily be reflected with higher PG-E2 levels.

4.4.2.2. Effect of AXH on IL-8 production

IL-8 is an important cytokine involved initiation and amplification of inflammatory responses resulting in tissue damage and injury (Al-Sadi and Ma, 2007). Thus, IL-8 is a primary

target for treatment of intestinal inflammation (Sartor, 1994). The increased production of pro-inflammatory cytokine IL-8 by Caco-2 and HT-29 cells in response to bacterial invasion has been previously shown (Jung et al., 1995). LPS, a bacterial polysaccharide, can activate sphingomyelinases SMases which causes an increase in cellular ceramide (MacKichan and DeFranco, 1999; Medvedev et al., 1999). Ceramide triggers mitogen-activated protein kinase (MAPK), which lead to the expression of several inflammation related genes (Spiegel et al., 1996). LPS efficiently increases the release of IL-8 from HT-29 intestinal epithelial cells by activating SMases and NF-κB in the cells (Sakata et al., 2007). Control of excess cytokine production induced by LPS is important because uncontrolled inflammation can be cytotoxic to enterocytes and cause systemic inflammatory response syndrome, leading to sepsis, septic shock, multiple organ failure, necrotizing enterocolitis and other organ damages (Houdijk et al., 1998; Nanthakumar et al., 2000; Wischmeyer et al., 2001). Also, elevated mucosal IL-8 levels were observed in patients with acute ulcerative colitis (Murata et al., 1995).

We investigated the effect of each AXH on LPS induced IL-8 production on Caco-2 and HT-29 cells. In both cell lines, LPS induced IL-8 production compared to the cells that were not stimulated by LPS (Figure 4.6). Previous studies have shown that IL-8 secretion by LPS induced Caco-2 cells occurred 10-24 h after LPS stimulation (Liboni et al., 2004). We also observed increased IL-8 secretion in Caco-2 cells following stimulation with LPS for 24 h. At the present seeding density, Caco-2 cells produced small amount of IL-8 compared to the HT-29 cells. Similar observations regarding the differences in IL-8 production between these two cell lines have also been reported previously (Rieder et al., 2011; Samuelsen et al., 2011). Eight of the 12 AXH used caused a significant decrease in LPS induced IL-8 production in Caco-2 cells. CJX-6 lowered LPS induced IL-8 significantly compared to the cells induced with LPS (control). Eight

of the AXH been tested lowered IL-8 in Caco-2 cells. However, in the case of HT-29, none of the AXH significantly lowered the LPS induced IL-8 production. In the contrary, three of the AXH significantly increased LPS induced IL-8 production in HT-29 cells. ANX-8 caused the highest increase in IL-8 followed by CAF-3 and ANX-3.

There was a significant difference observed between the control and the negative control in the IL-8 mRNA expression in Caco-2 cells (Figure 4.7). Five of the AXH resulted in significantly increased Ct values (indicating significantly reduced IL-8 mRNA expression) compared to the control in LPS induced Caco-2 cells. ANX-7 displayed the highest inhibitory effect followed by ANX-6, CAF-6, CJX-6 and ANX-4 consecutively. However, there were no statistically significant differences in Ct values observed among the treatments for the HT-29 cell line. There were large error bars observed for the IL-8 mRNA expression calculated for HT-29 cells and this might mask the actual differences between the treatments which might be preserved as not being significantly different from each other statistically.

4.4.2.3. Effect of AXH on TNF-α production

TNF-α is a pro-inflammatory cytokine produced during acute inflammation leading to a wide range of intracellular signaling events (Wang et al., 2013). It is involved in inducing anti-microbial effects in response to bacterial infection in cells (Andrade et al., 2005; Liu et al., 2008; Zakharova and Ziegler, 2005). It also leads to the production of other related chemokines and cytokines that directs progression of disease (Liu et al., 2008). In Caco-2, 1µg/mL LPS was unable to induce TNF-α production significantly compared to the control (Figure 4.8). However, Indomethacin was effective in reducing the TNF-α production significantly. Also, CAF-5, BAF-4 and ANX-8 were able to reduce TNF-α production significantly compared to the control in Caco-2 cells.

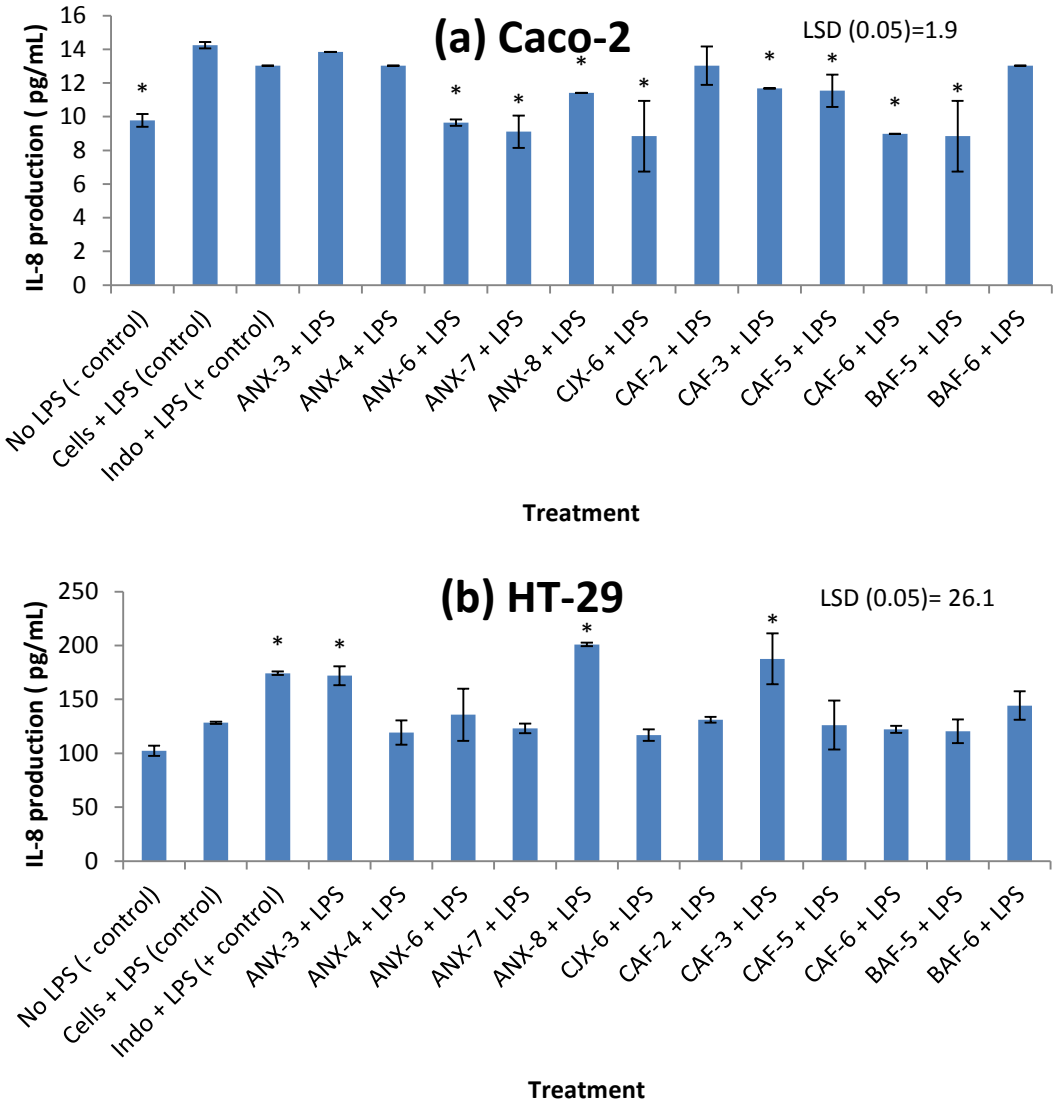

Figure 4.6. Immunomodulatory effect of AXH on LPS induced IL-8 production in (a) Caco-2 cells and (b) HT-29 cells. Cells only, cells not induced with LPS (negative control); cells with LPS, cells induced with LPS (control); cells treated with indomethacin (Indo) and induced with LPS (positive control); ANX-3 to BAF-6, cells treated with corresponding AXH and induced with LPS. Data are presented as mean ± SD. LSD, least significant difference (P<0.05). Values differing more than LSD between each other are significantly different (P<0.05) from each other. Bars with an asterisk are significantly different from the control (P<0.05).

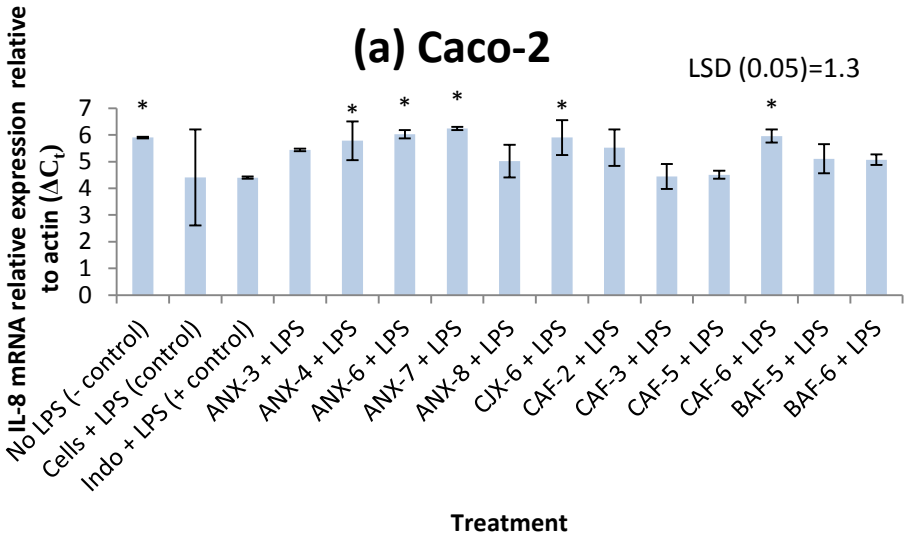

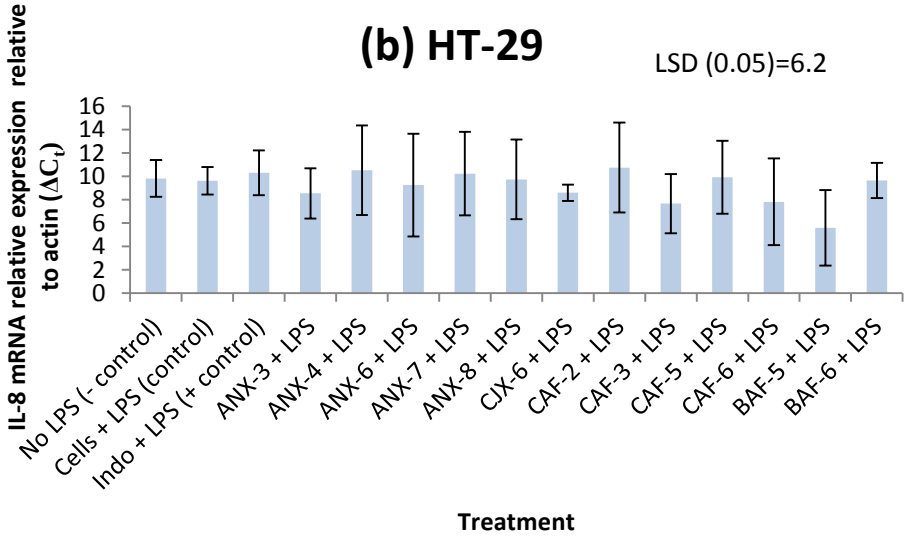

Figure 4.7. Immunomodulatory effect of AXH on LPS induced IL-8 mRNA production in (a) Caco-2 cells and (b) HT-29 cells. $\Delta Ct = Ct_{(gene)} - Ct_{(actin)}$. Cells only, cells not induced with LPS (negative control); Cells with LPS, cells induced with LPS (control); cells treated with indomethacin (Indo) and induced with LPS (positive control); ANX-3 to BAF-6, cells treated with corresponding AXH and induced with LPS. Data are presented as mean ± SD. LSD, least significant difference ($P<0.05$). Values differing more than LSD between each other are significantly different ($P<0.05$) from each other. Bars with an asterisk are significantly different from the control ($P<0.05$).

The rest of the AXH did not exert a significant effect on the TNF-α production in Caco-2. In the case of HT-29, a similar scenario was observed where the TNF-α production in LPS induced cells did not show a significant difference from the non-induced cells. Also, there was no significant difference among Indomethacin treated LPS induced cells with the non-induced cells or only LPS induced cells. However, there was a significant increase in TNF-α production in cells treated with CJX-6, ANX-4 and CAF-3 prior to stimulation with LPS compared to the control (cells treated with LPS only). The TNF-α mRNA expression was not significantly different between the LPS induced and none-LPS induced Caco-2 cells (Figure 4.9). However, CAF-2, ANX-6, CAF-6 and CAF-5 treated LPS induced Caco-2 cells displayed a reduction in TNF-α mRNA expression in LPS induced cells compared to the control. Similarly, TNF-α mRNA expression was not significantly different between the LPS induced and none-LPS induced HT-29 cells while BAF-5 treated LPS induced HT-29 cells displayed a significant increase in TNF-α mRNA expression compared to the control.

The effect of AXH on IL-1β and IL-6 production in LPS induced Caco-2 and HT-29 cells were also investigated. However, no detectable level of these cytokines was produced by either of the cell lines under any of the conditions exerted during the current study that was detectable by the ELISA techniques being used.

4.4.2.4. Effect of AXH on TLR-4 production

TLR-4 is a pattern recognition receptor that is involved in the recognition of bacterial membrane components such as LPS (Liu et al., 2008). TLR-4 along with its intracellular co-receptor MD88, leads to the activation of NF-κB (Fujihara et al., 2003; Liu et al., 2008). NF-κB is an important transcription factor involved in various immunological processes including cytokine production, phagocytosis and respiratory burst (Volman et al., 2008).

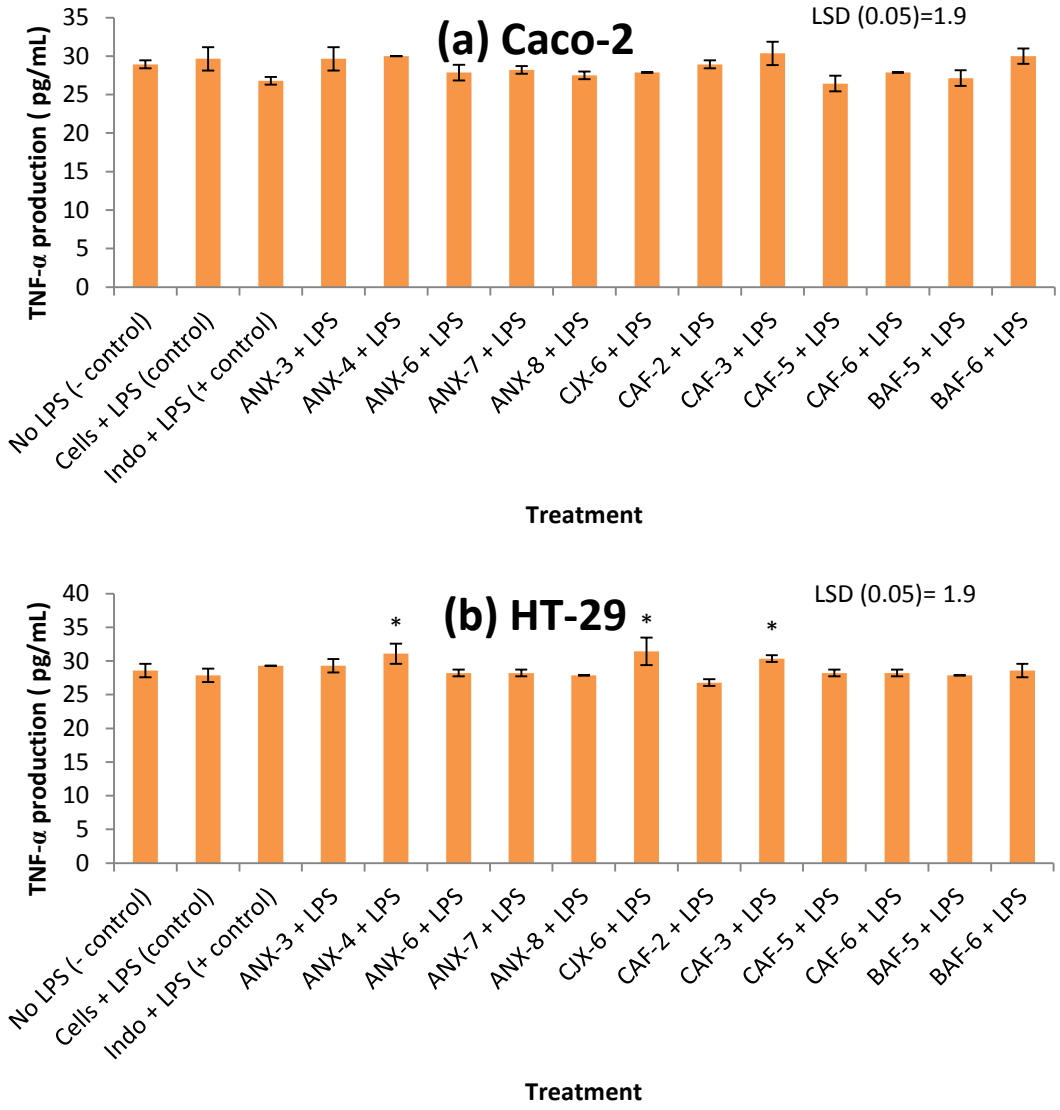

Figure 4.8. Immunomodulatory effect of AXH on LPS induced TNF-α production in (a) Caco-2 cells and (b) HT-29 cells. Cells only, cells not induced with LPS (negative control); Cells with LPS, cells induced with LPS (control); cells treated with indomethacin (Indo) and induced with LPS (positive control); ANX-3 to BAF-6, cells treated with corresponding AXH and induced with LPS. Data are presented as mean ± SD. LSD, least significant difference (P<0.05). Values differing more than LSD between each other are significantly different (P<0.05) from each other. Bars with an asterisk are significantly different from the control (P<0.05).

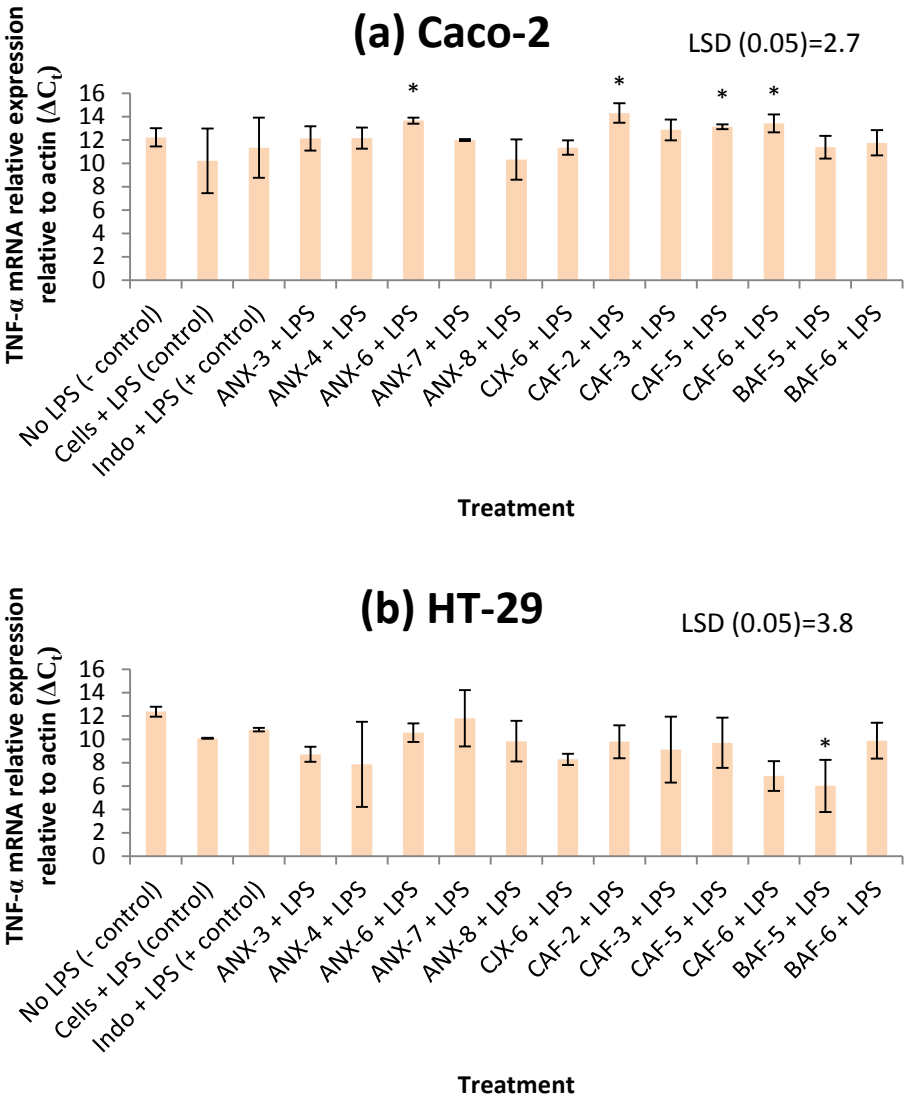

Figure 4.9. Immunomodulatory effect of AXH on LPS induced TNF-α mRNA production in (a) Caco-2 cells and (b) HT-29 cells. $\Delta Ct = Ct_{(gene)} - Ct_{(actin)}$. Cells only, cells not induced with LPS (negative control); Cells with LPS, cells induced with LPS (control); cells treated with indomethacin (Indo) and induced with LPS (positive control); ANX-3 to BAF-6, cells treated with corresponding AXH and induced with LPS. Data are presented as mean ± SD. LSD, least significant difference ($P<0.05$). Values differing more than LSD between each other are significantly different ($P<0.05$) from each other. Bars with an asterisk are significantly different from the control ($P<0.05$).

Eventually NF-κB triggers the MAPK pathways (Akira and Takeda, 2004) and MAPK pathways, specifically p38 MAPK pathway is involved in the biosynthesis of LPS induced TNF-α (Brook et al., 2000), a cytokine that promotes the production of other inflammatory cytokines (Liu et al., 2008). Several researches have demonstrated the involvement of NF-κB in cellular pathways triggered by botanical polysaccharides (Lee et al., 2013; Schepetkin and Quinn, 2006; Volman et al., 2008). In Caco-2 cells, TLR-4 mRNA expression was reduced by ten of the AXH being tested compared to the control (LPS induced cells without AXH treatment) with ANX-6 having the most significant inhibitory effect (Figure 4.10). In HT-29 cells there was no significant difference between the control and negative control in TLR-4 mRNA expression. However, ANX-4 and BAF-5 displayed an increased TLR-4 mRNA expression in LPS induced HT-29 cells compared to the rest of the treatments.

According to the correlation analysis of the data strong correlations were observed among some mRNA expression levels in certain genes. There was a strong positive correlation (0.968) between the TLR-4 mRNA expression and COX-2 mRNA expression in Caco-2 cells. A similar trend was observed for HT-29 cells with a strong positive correlation of 0.991 between the TLR-4 mRNA expression and COX-2 mRNA expression. Also, in HT-29, the TNF-α mRNA expression was strongly positively correlated with COX-2 mRNA expression (0.871) and TLR-4 mRNA expression (0.840). To understand the structure function relationship among the AXH structure and its immunological properties, correlation was tested among the composition/structure properties of AXH with their immunological properties determined by ELISA techniques (Table 4.5). Strong negative correlations were observed between PG-E2 production in Caco-2 and product of A/X ratio and 3 substituted 1,4 linked xylose (-0.725) and product of NMR resonance 1 data and 3 substituted 1,4 linked xylose (-0.727).

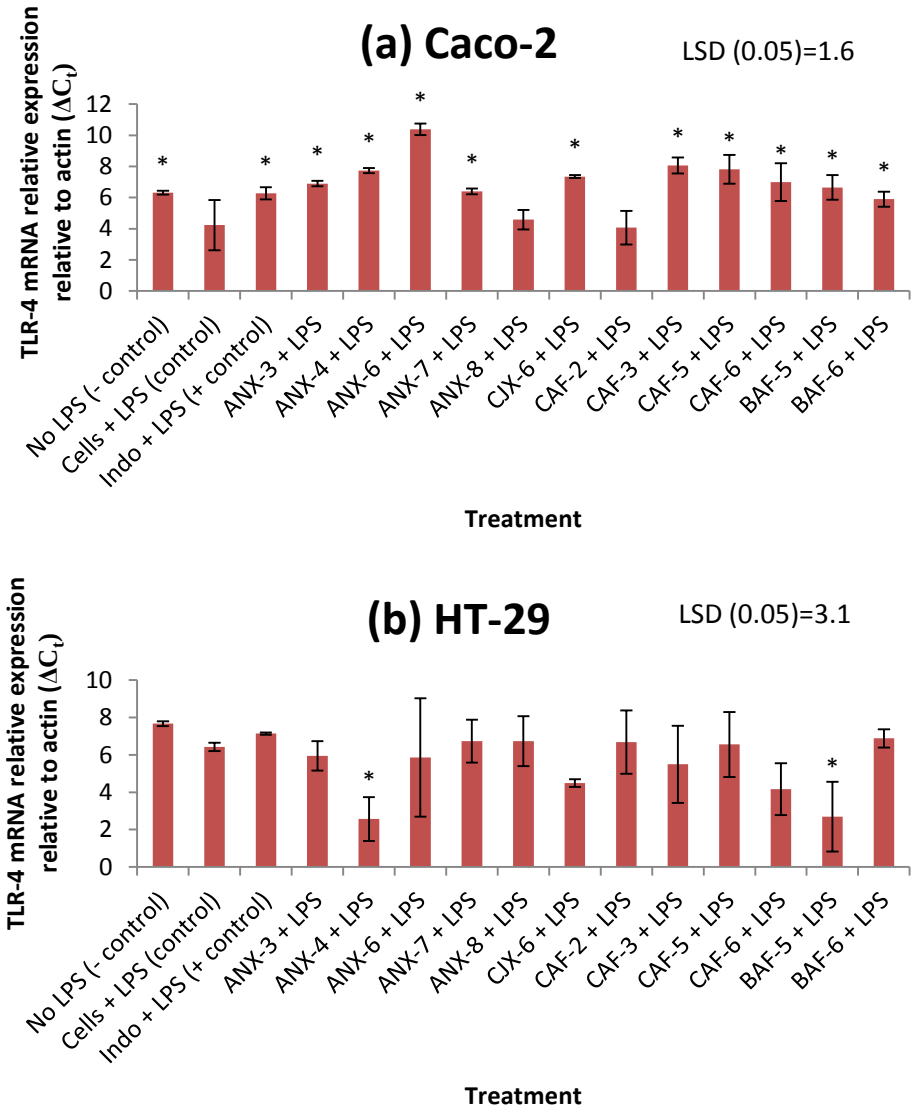

Figure 4.10. Immunomodulatory effect of AXH on LPS induced TLR-4 mRNA production in (a) Caco-2 cells and (b) HT-29 cells. $\Delta Ct = Ct_{(gene)} - Ct_{(actin)}$. Cells only, cells not induced with LPS (negative control); Cells with LPS, cells induced with LPS (control); cells treated with indomethacin (Indo) and induced with LPS (positive control); ANX-3 to BAF-6, cells treated with corresponding AXH and induced with LPS. Data are presented as mean ± SD. LSD, least significant difference ($P<0.05$). Values differing more than LSD between each other are significantly different ($P<0.05$) from each other. Bars with an asterisk are significantly different from the control ($P<0.05$).

Also, strong positive correlations were observed between product of NMR resonance 4 and 2,3 substituted 1,4 linked xylose (AX24 × AX39) (+0.715) and product of 1,4- linked xylose and 2,3, substituted 1,5-linked arabinose (AX35 × AX38) (+0.73) with PG-E2 production in Caco-2 cells. IL-8 production in Caco-2 was negatively correlated with product of terminal arabinose and 1,3- linked arabinose (AX31 × AX36) (-0.72) and TNF-α production was negatively correlated with the product of NMR resonance 6 and terminal arabinose (AX26 × AX31) (-0.763) in Caco-2 cells.

Correlation was tested among the composition/structure properties of AXH with their immunological properties determined by qRT-PCR techniques (Table 4.6). Strong positive correlations were observed between the ΔCt values for TNF-α in Caco-2 and product of total AX and A/X ratio (AX11 × AX12) (0.735) and product of total AX and NMR resonance 1 (AX11 × AX21) (0.735).

It is suggested that recognition of plant polysaccharides by cells involves pattern recognition receptors such as toll-like receptor (TLR) (Schepetkin and Quinn, 2006). TLR receptors are expressed in many cell types including epithelial cells (Iwasaki and Medzhitov, 2004). Out of the ten TLR receptors identified in humans, TLR-2 and TLR-4 are involved in recognition of polysaccharides (Brown et al., 2003; Leung et al., 2006; Li et al., 2004). The likelihood of several different receptors cooperating with each other to form "clusters of signaling complexes" have also been proposed (Schepetkin and Quinn, 2006). Interestingly, although lesser significant correlations were observed among the immunological parameters being tested with single structural features being tested, stronger correlations were observed when the effect of two structural features were considered in combination for correlation analysis. Combining two or more structural features might give a better understanding about the

overall structure/ pattern of the AXH being tested because at the cellular level it is the overall structure of the molecule that is at play. At the cellular level the recognition of these AXH by the cells might be via pattern recognition receptors on the cell surfaces. Thus, overall structural features that are better depicted by combined structural properties might display better correlations with immunological properties compared to considering these structural features individually. Also, there might be a synergistic effect from two different structural properties that determine the ultimate immunological property of the AXH.

Based on the data gathered for the structural properties of each of the AXH, we further constructed the prediction equations for each of the parameters being tested using stepwise regression analysis (Table 4.7). These equations can be used to identify the different structural properties of AXH that had most significant contribution to production of PG-E2, cytokines and mRNA expression of specific genes.

4.5. Conclusions

Use of plant derived polysaccharides as health promoter has gained immense interest in the past few years. The current research aimed to investigate the structure-function relationship of enzymatically tailored AXH as immunomodulators using LPS induced colon cancer cell lines: Caco-2 and HT-29. Twelve structurally different AXH were prepared from wheat AX, using different enzymatic conditions. The importance of polymer side branching on the immunological properties of AXH has also been emphasized by others (Adams et al., 2008; Mikkelsen et al., 2014). Zhou et al (2010) also suggested that the immunological effects of wheat bran AX depend on the molecular weight, chemical composition and substituted degree or branch of arabinose. Similarly, we demonstrated that the fine structural details had a strong correlation with the immunological properties of the wheat AXH.

Table 4.5. Correlation coefficients among parameters tested on chemical characteristics (using GC-FID, ^{1}H-NMR and GC-MS) and immunomodulatory properties (using ELISA).

	Caco-2 PG-E2		Caco-2 IL-8		Caco-2 TNF-α		HT-29 PG-E2		HT-29 IL-8		HT-29 TNF-α
NMR resonance 1 3 substituted 1,4 linked xylose	-0.581	*							-0.700	*	
AX11 × AX31			-0.632	*	-0.647	*					
AX11 × AX33							-0.590	*			
AX11 × AX34							0.619	*			
AX11 × AX38	0.610	*									
AX11 × AX39	0.671	*									
AX12 × AX21									-0.588	*	
AX12 × AX25	-0.665	*									
AX12 × AX31			-0.650	*	-0.700	*					
AX12 × AX33							-0.604	*			
AX12 × AX36									-0.596	*	
AX12 × AX37	-0.725	**									
AX12 × AX38	0.586	*									
AX12 × AX39	0.662	*									
AX21 × AX31			-0.671	*	-0.669	*					
AX21 × AX33							-0.596	*			
AX21 × AX36									-0.660	*	
AX21 × AX37	-0.727	**									
AX21 × AX39	0.629	*									
AX22 × AX31					-0.648	*					
AX22 × AX33							-0.623	*			
AX22 × AX38	0.611	*									
AX22 × AX39	0.690	*									
AX23 × AX31					-0.684	*					
AX23 × AX37	-0.645	*									
AX23 × AX38	0.597	*									
AX23 × AX39	0.695	*									
AX24 × AX31					-0.614	*					
AX24 × AX33							-0.678	*			
AX24 × AX34							0.656	*			
AX24 × AX38	0.639	*									
AX24 × AX39	0.715	**									
AX25 × AX31			-0.619	*	-0.672	*					
AX25 × AX37	-0.697	*									
AX25 × AX39	0.645	*									
AX26 × AX31			-0.635	*	-0.763	**					
AX26 × AX38	0.614	*									

Table 4.5. Correlation coefficients among parameters tested on chemical characteristics (using GC-FID, ^{1}H-NMR and GC-MS) and immunomodulatory properties (using ELISA) (continued).

	Caco-2 PG-E2		Caco-2 IL-8		Caco-2 TNF-α		HT-29 PG-E2		HT-29 IL-8	HT-29 TNF-α	
AX26 × AX39	0.687	*									
AX31 × AX31					-0.605	*					
AX31 × AX35					-0.655	*					
AX31 × AX36			-0.720	**	-0.653	*					
AX31 × AX37					-0.613	*					
AX31 × AX39			-0.690	*	-0.606	*				-0.651	*
AX32 × AX34							0.586	*			
AX32 × AX38			-0.640	*							
AX32 × AX39			-0.639	*						-0.595	*
AX33 × AX33							-0.634	*			
AX33 × AX34										0.577	*
AX33 × AX35							-0.640	*			
AX33 × AX36							-0.609	*			
AX33 × AX37							-0.634	*			
AX34 × AX37							0.581	*			
AX35 × AX38	0.730	**									
AX35 × AX39	0.706	*									
AX37 × AX37	-0.631	*									
AX37 × AX39	0.652	*									
AX38 × AX38	0.601	*									
AX38 × AX39	0.680	*									

*** *P*-value <0.0001; ** *P*-value <0.001; * *P*-value <0.05

[a] The abbreviations used for each parameter is as follows:
Composition data obtained by GC-FID: AX11, Total AX; AX12, A/X ratio.
Structural data obtained by ^{1}H-NMR: AX21, NMR resonance 1; AX22,NMR resonance 2; AX23NMR resonance 3; AX24, NMR resonance 4; AX25, NMR resonance 5; AX26, NMR resonance 6.
Structural data obtained by GC-MS: AX31, Terminal Arabinose; AX32,Terminal Xylose; AX33, 2 substituted 1,4 linked xylose; AX34, 1,5 linked arabinose; AX35, 1,4- linked xylose; AX36, 1,3- linked arabinose; AX37, 3 substituted 1,4 linked xylose; AX38, 2,3, substituted 1,5-linked arabinose; AX39, 2,3 substituted 1,4 linked xylose.
AX11 × AX11, product of AX11 by AX11; AX11 × AX12, product of AX11 by AX12; and so on.

Table 4.6.Correlation coefficients among parameters tested[a] on chemical characteristics (using GC-FID, ^{1}H-NMR and GC-MS) and immunomodulatory properties (using qRT-PCR).

	Caco-2 TLR-4 ΔCt		Caco-2 TNF-α ΔCt		Caco-2 IL-8 ΔCt		HT-29 COX-2 ΔCt		HT-29 TLR-4 ΔCt		HT-29 TNF-α ΔCt		HT-29 IL-8 ΔCt	
A/X ratio													0.622	*
NMR resonance 1			0.678	*										
NMR resonance 2													0.704	*
NMR resonance 3									0.615	*				
2 substituted 1,4 linked xylose			-0.607	*										
1,3- linked arabinose							-0.645	*	-0.640	*				
AX11 × AX11			0.715	**										
AX11 × AX12			0.753	**										
AX11 × AX21			0.735	**										
AX11 × AX22			0.657	*										
AX11 × AX23			0.596	*										
AX11 × AX25			0.624	*										
AX11 × AX26			0.698	*										
AX11 × AX33					0.642	*								
AX11 × AX37			0.585	*										
AX12 × AX23			-0.578	*										
AX12 × AX25					0.648	*								
AX12 × AX33					0.631	*								
AX12 × AX36					0.602	*	-0.597	*						
AX21 × AX33					0.667	*								
AX21 × AX36					0.580	*								
AX22 × AX33					0.591	*								
AX22 × AX36					0.604	*	-0.578	*						
AX23 × AX23			-0.654	*										
AX23 × AX25			-0.594	*										
AX23 × AX26			-0.583	*										
AX23 × AX33					0.611	*								
AX25 × AX33					0.636	*								
AX25 × AX36					0.607	*								
AX25 × AX39													-0.578	*
AX26 × AX33					0.630	*								
AX26 × AX36											-0.596	*		
AX31 × AX33					0.579	*								
AX31 × AX36					0.625	*								
AX32 × AX34	0.589	*												
AX33 × AX33					0.650	*								
AX33 × AX36					0.581	*								

Table 4.6.Correlation coefficients among parameters tested[a] on chemical characteristics (using GC-FID, ^{1}H-NMR and GC-MS) and immunomodulatory properties (using qRT-PCR) (continued).

	Caco-2 TLR-4 ΔCt		Caco-2 TNF-α ΔCt		Caco-2 IL-8 ΔCt		HT-29 COX-2 ΔCt	HT-29 TLR-4 ΔCt	HT-29 TNF-α ΔCt	HT-29 IL-8 ΔCt
AX33 × AX37					0.601	*				
AX34 × AX35	0.592	*								

*** *P*-value <0.0001; ** *P*-value <0.001; * *P*-value <0.05

[a] The abbreviations used for each parameter is as follows:
Composition data obtained by GC-FID: AX11, Total AX; AX12, A/X ratio.
Structural data obtained by ^{1}H-NMR: AX21, NMR resonance 1; AX22,NMR resonance 2; AX23NMR resonance 3; AX24, NMR resonance 4; AX25, NMR resonance 5; AX26, NMR resonance 6.
Structural data obtained by GC-MS: AX31, Terminal Arabinose; AX32,Terminal Xylose; AX33, 2 substituted 1,4 linked xylose; AX34, 1,5 linked arabinose; AX35, 1,4- linked xylose; AX36, 1,3- linked arabinose; AX37, 3 substituted 1,4 linked xylose; AX38, 2,3, substituted 1,5-linked arabinose; AX39, 2,3 substituted 1,4 linked xylose.
AX11 × AX11, product of AX11 by AX11; AX11 × AX12, product of AX11 by AX12; and so on.

More so, we indicated that there might be a synergistic effect of combination of different fine structural details that exert a significant impact on the polysaccharide's immunological properties rather than one single structural detail of the AXH. This might be further explained by the cellular mechanisms involved in recognition of these polysaccharides by the cells. The pattern recognition receptors that identify specific polysaccharides might identify them based on the collective structural features of the polysaccharide *vs* one specific structural detail. The 12 different AXH being tested showed different immunological properties with respect to cell type, the cytokine of interest, etc. The current research indicates that there is a structure driven immunological properties for wheat bran derived AX polysaccharides. However, the exact cellular mechanisms involved in recognition of these polysaccharides need to be further elucidated. Also, the inflammatory mediator pathways that are triggered upon encounter of each of these AXH which might be structure dependent need to be further explored.

Table 4.7. Prediction equation for the dependent variables related to immunomodulatory properties.

Dependent variable	Prediction equation	Model R^2
Caco-2 PG-E2	Caco-2 PG-E2 = 0.19 - 6.32×10^{-3} (AX21)- 3.1×10^{-4} (AX25×AX37) + 6.32×10^{-5} (AX35×AX38)	0.8604
Caco-2 IL-8	Caco-2 IL-8 = 16.3 + 6.84×10^{-3} (AX11×AX38) – 0.55 (AX12×AX39) – 9.63×10^{-2} (AX31×AX36)	0.9104
Caco-2 TNF-α	Caco-2 TNF-α = 32.5 + 8.96×10^{-7} MWT – 5.73×10^{-2} (AX11) – 5.31×10^{-3} (AX26×AX31)	0.8683
HT-29 PG-E2	HT-29 PG-E2 = -7.8×10^{-2} + 2.1×10^{-2} (AX12×AX25) – 3.74×10^{-3} (AX24×AX33) – 5.37×10^{-4} (AX24×AX36)	0.9155
HT-29 IL-8	HT-29 IL-8 = 307.1 – 17.7 (AX21) +.203 (AX11×AX22) - .87 (AX22×AX36)	0.9548
HT-29 TNF-α	HT-29 TNF-α = 52.39 - .11 (AX11) – 1.7 (AX23) – 1×10^{-2} (AX31×AX39)	0.9303
Caco-2 COX (ΔCt)	Caco-2 COX (ΔCt) = 20.1 – 1.7 (AX23) + 3.5×10^{-2} (AX24×AX25) + 0.43 (AX24×AX34)	0.8884
Caco-2 TLR-4 (ΔCt)	Caco-2 TLR-4 (ΔCt) = 7.4 – 0.69 (AX22) + 5.2×10^{-2} (AX21×AX24) + 9.9×10^{-2} (AX34×AX35)	0.8091
Caco-2 TNF-α (ΔCt)	Caco-2 TNF-α (ΔCt) = 6.4 – 0.17 (AX31) + 0.29 (AX11×AX12) + 8.8×10^{-3} (AX22×AX31)	0.8605
Caco-2 IL-8 (ΔCt)	Caco-2 IL-8 (ΔCt) = 4.03 + 1.6 (AX34) + 6.9×10^{-2} (AX21×AX33) +1.16×10^{-3} (AX25×AX35)	0.8309
HT-29 COX-2 (ΔCt)	HT-29 COX-2 (ΔCt) = 2.01 + 0.809 (AX23) – 0.76 (AX36) – 0.37 (AX33×AX36)	0.8733
HT-29 TLR-4 (ΔCt)	HT-29 TLR-4 (ΔCt) = -1.02 + 0.96 (AX23) – 0.74 (AX36) – 0.36 (AX33×AX36)	0.9054
HT-29 TNF-α (ΔCt)	HT-29 TNF-α (ΔCt) = 9.7 + 2.4 (AX34) – 2.1×10^{-2} (AX26×AX36) + 2.1×10^{-2} (AX31×AX37)	0.7784
HT-29 IL-8 (ΔCt)	HT-29 IL-8 (ΔCt) = -4.8 + 22.8 (AX12) + 0.33 (AX22) – 0.58 (AX36)	0.7344

*** *P*-value <0.0001; ** *P*-value <0.001; * *P*-value <0.05

[a] The abbreviations used for each parameter is as follows:

MWT, weight average molecular weight; composition data obtained by GC-FID: AX11, Total AX; AX12, A/X ratio; structural data obtained by ^{1}H-NMR: AX21, NMR resonance 1; AX22,NMR resonance 2; AX23NMR resonance 3; AX24, NMR resonance 4; AX25, NMR resonance 5; AX26, NMR resonance 6; structural data obtained by GC-MS: AX31, Terminal Arabinose; AX32,Terminal Xylose; AX33, 2 substituted 1,4 linked xylose; AX34, 1,5 linked arabinose; AX35, 1,4- linked xylose; AX36, 1,3-linked arabinose; AX37, 3 substituted 1,4 linked xylose; AX38, 2,3, substituted 1,5-linked arabinose; AX39, 2,3 substituted 1,4 linked xylose.

AX11 × AX11, product of AX11 by AX11; AX11 × AX12, product of AX11 by AX12; and so on.

To date, the exact mechanism of processes executed by cells upon encounter of arabinoxylans has not been well defined.

These results indicate that there might be a structure-function relationship for these AXH as immunomodulators. Further research is needed to evaluate the dose dependence of these AXH on immune system cells and also to identify the cellular mechanisms involved in exerting the observed outcomes for these compounds.

4.6. Future Research

In the current study the induction of inflammation in the cells were achieved via stimulation with LPS, a commonly used pro-inflammatory agent. However, with respect to some cytokine production, the LPS induced cells did not produce significantly higher amounts of cytokine compared to the none-LPS induced cells. Many researches have reported using pro-inflammatory cytokines instead of LPS to induce immunological outcomes in intestinal cell lines (Andoh et al., 1995; Kim et al., 2004; Kim et al., 2005; Mukherjee and Biswas, 2014; Rieder et al., 2011; Son et al., 2005; Van De Walle et al., 2010). Thus, evaluating the immunomodulatory effects of AXH on inflammation induced by some of these cytokines in cells would help mitigate the above drawback and also help understand the cellular mechanisms involved in immunomodulation by cereal fibers such as arabinoxylan.

Although changes in production of inflammatory mediators such as PG-E2 and cytokines were observed under the current study in response to different AXH these inflammatory mediators are regulated by feedback mechanisms in vivo. Thus, further research employing animal models would be able to shed better light on the role of AX in animals.

4.7. References

Adams, E. L., Rice, P. J., Graves, B., Ensley, H. E., Yu, H., Brown, G. D., Gordon, S., Monteiro, M. A., Papp-Szabo, E., and Lowman, D. W. (2008). Differential high-affinity interaction of dectin-1 with natural or synthetic glucans is dependent upon primary structure and is influenced by polymer chain length and side-chain branching. *Journal of Pharmacology and Experimental Therapeutics* **325**, 115-123.

Akhtar, M., Tariq, A. F., Awais, M. M., Iqbal, Z., Muhammad, F., Shahid, M., and Hiszczynska-Sawicka, E. (2012). Studies on wheat bran Arabinoxylan for its immunostimulatory and protective effects against avian coccidiosis. *Carbohydrate Polymers* **90**, 333-339.

Akira, S., and Takeda, K. (2004). Toll-like receptor signalling. *Nat Rev Immunol* **4**, 499-511.

Al-Sadi, R. M., and Ma, T. Y. (2007). IL-1beta causes an increase in intestinal epithelial tight junction permeability. *J Immunol* **178**, 4641-9.

Andoh, A., Fujiyama, Y., Sumiyoshi, K., Hodohara, K., Hidetoshi, O., Ochi, Y., Bamba, T., and Brown, W. R. (1995). Modulation of complement C3, C4, and factor B production in human intestinal epithelial cells: differential effects of TNF-α, IFN-γ, and IL-4. *Pathophysiology* **2**, 251-259.

Andrade, R. M., Wessendarp, M., Portillo, J. A., Yang, J. Q., Gomez, F. J., Durbin, J. E., Bishop, G. A., and Subauste, C. S. (2005). TNF receptor-associated factor 6-dependent CD40 signaling primes macrophages to acquire antimicrobial activity in response to TNF-alpha. *J Immunol* **175**, 6014-21.

Brook, M., Sully, G., Clark, A. R., and Saklatvala, J. (2000). Regulation of tumour necrosis factor α mRNA stability by the mitogen-activated protein kinase p38 signalling cascade. *FEBS Letters* **483**, 57-61.

Brown, G. D., Herre, J., Williams, D. L., Willment, J. A., Marshall, A. S., and Gordon, S. (2003). Dectin-1 mediates the biological effects of beta-glucans. *J Exp Med* **197**, 1119-24.

Cao, L., Liu, X., Qian, T., Sun, G., Guo, Y., Chang, F., Zhou, S., and Sun, X. (2011). Antitumor and immunomodulatory activity of arabinoxylans: A major constituent of wheat bran. *International Journal of Biological Macromolecules* **48**, 160-164.

Cario, E., Rosenberg, I. M., Brandwein, S. L., Beck, P. L., Reinecker, H.-C., and Podolsky, D. K. (2000). Lipopolysaccharide Activates Distinct Signaling Pathways in Intestinal Epithelial Cell Lines Expressing Toll-Like Receptors. *The Journal of Immunology* **164**, 966-972.

Carvalho, A. F. í. A., Neto, P. d. O., Da Silva, D. F., and Pastore, G. í. M. (2013). Xylo-oligosaccharides from lignocellulosic materials: Chemical structure, health benefits and production by chemical and enzymatic hydrolysis. *Food Research International* **51**, 75-85.

Castellone, M. D., Teramoto, H., Williams, B. O., Druey, K. M., and Gutkind, J. S. (2005). Prostaglandin E2 promotes colon cancer cell growth through a Gs-axin-beta-catenin signaling axis. *Science* **310**, 1504-10.

Cong, P., Pricolo, V., Biancani, P., and Behar, J. (2007). Abnormalities of Prostaglandins and Cyclooxygenase Enzymes in Female Patients With Slow-Transit Constipation. *Gastroenterology* **133**, 445-453.

Cosentino, S., Gravaghi, C., Donetti, E., Donida, B. M., Lombardi, G., Bedoni, M., Fiorilli, A., Tettamanti, G., and Ferraretto, A. (2010). Caseinphosphopeptide-induced calcium uptake in human intestinal cell lines HT-29 and Caco2 is correlated to cellular differentiation. *The Journal of Nutritional Biochemistry* **21**, 247-254.

Dey, I., Lejeune, M., and Chadee, K. (2006). Prostaglandin E2 receptor distribution and function in the gastrointestinal tract. *Br J Pharmacol* **149**, 611-23.

Dornez, E., Gebruers, K., Delcour, J., and Courtin, C. (2009). Grain-associated xylanases: occurrence, variability, and implications for cereal processing. *Trends in food science & technology*. **20**, 495-510.

Edogawa, S., Sakai, A., Inoue, T., Harada, S., Takeuchi, T., Umegaki, E., Hayashi, H., and Higuchi, K. (2014). Down-regulation of collagen I biosynthesis in intestinal epithelial cells exposed to indomethacin: A comparative proteome analysis. *Journal of Proteomics* **103**, 35-46.

Forsythe, R. M., Xu, D. Z., Lu, Q., and Deitch, E. A. (2002). Lipopolysaccharide-induced enterocyte-derived nitric oxide induces intestinal monolayer permeability in an autocrine fashion. *Shock* **17**, 180-4.

Fujihara, M., Muroi, M., Tanamoto, K., Suzuki, T., Azuma, H., and Ikeda, H. (2003). Molecular mechanisms of macrophage activation and deactivation by lipopolysaccharide: roles of the receptor complex. *Pharmacol Ther* **100**, 171-94.

Gagnon, M., Zihler Berner, A., Chervet, N., Chassard, C., and Lacroix, C. (2013). Comparison of the Caco-2, HT-29 and the mucus-secreting HT29-MTX intestinal cell models to investigate Salmonella adhesion and invasion. *Journal of Microbiological Methods* **94**, 274-279.

Gong, J., Chen, Q., Yan, Y., and Pang, G. (2014). Effect of casein glycomacropeptide on subunit p65 of nuclear transcription factor-κB in lipopolysaccharide-stimulated human colorectal tumor HT-29 cells. *Food Science and Human Wellness* **3**, 51-55.

Grishin, A., Wang, J., Hackam, D., Qureshi, F., Upperman, J., Zamora, R., and Ford, H. R. (2004). p38 MAP kinase mediates endotoxin-induced expression of cyclooxygenase-2 in enterocytes. *Surgery* **136**, 329-35.

Grishin, A. V., Wang, J., Potoka, D. A., Hackam, D. J., Upperman, J. S., Boyle, P., Zamora, R., and Ford, H. R. (2006). Lipopolysaccharide induces cyclooxygenase-2 in intestinal epithelium via a noncanonical p38 MAPK pathway. *J Immunol* **176**, 580-8.

Guo, Y., Zhang, T., Jiang, B., Miao, M., and Mu, W. (2014). The effects of an antioxidative pentapeptide derived from chickpea protein hydrolysates on oxidative stress in Caco-2 and HT-29 cell lines. *Journal of Functional Foods* **7**, 719-726.

Guri, A., Griffiths, M., Khursigara, C. M., and Corredig, M. (2012). The effect of milk fat globules on adherence and internalization of Salmonella Enteritidis to HT-29 cells. *Journal of Dairy Science* **95**, 6937-6945.

Hajiaghaalipour, F., Kanthimathi, M. S., Sanusi, J., and Rajarajeswaran, J. (2015). White tea (Camellia sinensis) inhibits proliferation of the colon cancer cell line, HT-29, activates caspases and protects DNA of normal cells against oxidative damage. *Food Chemistry* **169**, 401-410.

Houdijk, A. P., Rijnsburger, E. R., Jansen, J., Wesdorp, R. I., Weiss, J. K., McCamish, M. A., Teerlink, T., Meuwissen, S. G., Haarman, H. J., Thijs, L. G., and van Leeuwen, P. A. (1998). Randomised trial of glutamine-enriched enteral nutrition on infectious morbidity in patients with multiple trauma. *Lancet* **352**, 772-6.

Huet, G., Kim, I., de Bolos, C., Lo-Guidice, J. M., Moreau, O., Hemon, B., Richet, C., Delannoy, P., Real, F. X., and Degand, P. (1995). Characterization of mucins and proteoglycans

synthesized by a mucin-secreting HT-29 cell subpopulation. *J Cell Sci* **108 (Pt 3)**, 1275-85.

Iizuka, M., and Konno, S. (2011). Wound healing of intestinal epithelial cells. *World J Gastroenterol* **17**, 2161-71.

Iwasaki, A., and Medzhitov, R. (2004). Toll-like receptor control of the adaptive immune responses. *Nat Immunol* **5**, 987-95.

Jung, H. C., Eckmann, L., Yang, S. K., Panja, A., Fierer, J., Morzycka-Wroblewska, E., and Kagnoff, M. F. (1995). A distinct array of proinflammatory cytokines is expressed in human colon epithelial cells in response to bacterial invasion. *J Clin Invest* **95**, 55-65.

Karlinger, K., Györke, T., Makö, E., Mester, Á., and Tarján, Z. (2000). The epidemiology and the pathogenesis of inflammatory bowel disease. *European journal of radiology* **35**, 154-167.

Kim, G.-N., Song, J.-H., Kim, E.-S., Choi, H.-T., and Jang, H.-D. (2012). Isoflavone content and apoptotic effect in HT-29 cancer cells of a soy germ extract. *Food Chemistry* **130**, 404-407.

Kim, J.-A., Kim, D.-K., Jin, T., Kang, O.-H., Choi, Y.-A., Choi, S.-C., Kim, T.-H., Nah, Y.-H., Choi, S.-J., Kim, Y.-H., Bae, K.-H., and Lee, Y.-M. (2004). Acanthoic acid inhibits IL-8 production via MAPKs and NF-κB in a TNF-α-stimulated human intestinal epithelial cell line. *Clinica Chimica Acta* **342**, 193-202.

Kim, J.-A., Kim, D.-K., Kang, O.-H., Choi, Y.-A., Park, H.-J., Choi, S.-C., Kim, T.-H., Yun, K.-J., Nah, Y.-H., and Lee, Y.-M. (2005). Inhibitory effect of luteolin on TNF-α-induced IL-8 production in human colon epithelial cells. *International Immunopharmacology* **5**, 209-217.

Lafiandra, D., Riccardi, G., and Shewry, P. R. (2014). Improving cereal grain carbohydrates for diet and health. *Journal of Cereal Science* **59**, 312-326.

Lee, S. J., Rim, H. K., Jung, J. Y., An, H. J., Shin, J. S., Cho, C. W., Rhee, Y. K., Hong, H. D., and Lee, K. T. (2013). Immunostimulatory activity of polysaccharides from Cheonggukjang. *Food and Chemical Toxicology* **59**, 476-484.

Leung, M. Y. K., Liu, C., Koon, J. C. M., and Fung, K. P. (2006). Polysaccharide biological response modifiers. *Immunology Letters* **105**, 101-114.

Li, W., Yajima, T., Saito, K., Nishimura, H., Fushimi, T., Ohshima, Y., Tsukamoto, Y., and Yoshikai, Y. (2004). Immunostimulating properties of intragastrically administered Acetobacter-derived soluble branched (1,4)-beta-D-glucans decrease murine susceptibility to Listeria monocytogenes. *Infect Immun* **72**, 7005-11.

Liboni, K., Li, N., and Neu, J. (2004). Mechanism of glutamine-mediated amelioration of lipopolysaccharide-induced IL-8 production in Caco-2 cells. *Cytokine* **26**, 57-65.

Liu, F., Liu, Y., Lui, V. C. H., Lamb, J. R., Tam, P. K. H., and Chen, Y. (2008). Hypoxia modulates lipopolysaccharide induced TNF-α expression in murine macrophages. *Experimental Cell Research* **314**, 1327-1336.

Loftus Jr, E. V. (2004). Clinical epidemiology of inflammatory bowel disease: incidence, prevalence, and environmental influences. *Gastroenterology* **126**, 1504-1517.

MacKenzie, K. F., Van Den Bosch, M. W., Naqvi, S., Elcombe, S. E., McGuire, V. A., Reith, A. D., Blackshear, P. J., Dean, J. L., and Arthur, J. S. (2013). MSK1 and MSK2 inhibit lipopolysaccharide-induced prostaglandin production via an interleukin-10 feedback loop. *Mol Cell Biol* **33**, 1456-67.

MacKichan, M. L., and DeFranco, A. L. (1999). Role of ceramide in lipopolysaccharide (LPS)-induced signaling. LPS increases ceramide rather than acting as a structural homolog. *J Biol Chem* **274**, 1767-75.

Martin, G. R., and Wallace, J. L. (2006). Gastrointestinal inflammation: a central component of mucosal defense and repair. *Exp Biol Med (Maywood)* **231**, 130-7.

Martinez-Cutillas, M., Mañé, N., Gallego, D., Jimenez, M., and Martin, M. T. (In press). EP2 and EP4 receptors mediate PGE2 induced relaxation in murine colonic circular muscle: Pharmacological characterization. *Pharmacological Research*.

Medvedev, A. E., Blanco, J. C., Qureshi, N., and Vogel, S. N. (1999). Limited role of ceramide in lipopolysaccharide-mediated mitogen-activated protein kinase activation, transcription factor induction, and cytokine release. *J Biol Chem* **274**, 9342-50.

Medzhitov, R. (2008). Origin and physiological roles of inflammation. *Nature* **454**, 428-435.

Mendis, M., and Simsek, S. (2014). Arabinoxylans and human health. *Food Hydrocolloids* Special Issue: International Conference on Halal Gums 2012. **42**, 239-243.

Mikkelsen, M. S., Jespersen, B. M., Mehlsen, A., Engelsen, S. B., and Frokiaer, H. (2014). Cereal bets-glucan immune modulating activity depends on the polymer fine structure. *Food Research International* **62**, 829-836.

Monobe, M., Maeda-Yamamoto, M., Matsuoka, Y., Kaneko, A., and Hiramoto, S. (2008). Immunostimulating activity and molecular weight dependence of an arabinoxylan derived from wheat bran. *Journal of the Japanese Society for Food Science and Technology-Nippon Shokuhin Kagaku Kogaku Kaishi* **55**, 245-249.

Montrose, D. C., Kadaveru, K., Ilsley, J. N., Root, S. H., Rajan, T. V., Ramesh, M., Nichols, F. C., Liang, B. T., Sonin, D., Hand, A. R., Zarini, S., Murphy, R. C., Belinsky, G. S.,

Nakanishi, M., and Rosenberg, D. W. (2010). cPLA2 is protective against COX inhibitor-induced intestinal damage. *Toxicol Sci* **117**, 122-32.

Morita, H., He, F., Fuse, T., Ouwehand, A. C., Hashimoto, H., Hosoda, M., Mizumachi, K., and Kurisaki, J. i. (2002). Adhesion of Lactic Acid Bacteria to Caco-2 Cells and Their Effect on Cytokine Secretion. *Microbiology and Immunology* **46**, 293-297.

Mukherjee, S., and Biswas, T. (2014). Activation of TOLLIP by porin prevents TLR2-associated IFN-γ and TNF-α-induced apoptosis of intestinal epithelial cells. *Cellular Signalling* **26**, 2674-2682.

Murata, Y., Ishiguro, Y., Itoh, J., Munakata, A., and Yoshida, Y. (1995). The role of proinflammatory and immunoregulatory cytokines in the pathogenesis of ulcerative colitis. *J Gastroenterol* **30 Suppl 8**, 56-60.

Nakanishi, M., and Rosenberg, D. W. (2013). Multifaceted roles of PGE2 in inflammation and cancer. *Semin Immunopathol* **35**, 123-37.

Nanthakumar, N. N., Fusunyan, R. D., Sanderson, I., and Walker, W. A. (2000). Inflammation in the developing human intestine: A possible pathophysiologic contribution to necrotizing enterocolitis. *Proc Natl Acad Sci U S A* **97**, 6043-8.

Neuman, M. G. (2007). Immune dysfunction in inflammatory bowel disease. *Translational Research* **149**, 173-186.

Parikh, A. A., Salzman, A. L., Fischer, J. E., Szabo, C., and Hasselgren, P. O. (1997). Interleukin-1 beta and interferon-gamma regulate interleukin-6 production in cultured human intestinal epithelial cells. *Shock* **8**, 249-55.

Pinto M, R.-L. S., Appay M-D, et al. (1983). Enterocyte-like differentiation and polarization of the human colon carcinoma cell line Caco-2 in culture. *Biology of the Cell* **47**.

Podolsky, D. K. (2002). The current future understanding of inflammatory bowel disease. *Best Practice & Research Clinical Gastroenterology* **16**, 933-943.

Porcher, C., Horowitz, B., Ward, S. M., and Sanders, K. M. (2004). Constitutive and functional expression of cyclooxygenase 2 in the murine proximal colon. *Neurogastroenterol Motil* **16**, 785-99.

Rieder, A., Grimmer, S., Kolset, S. O., Michaelsen, T. E., and Knutsen, S. H. (2011). Cereal β-glucan preparations of different weight average molecular weights induce variable cytokine secretion in human intestinal epithelial cell lines. *Food Chemistry* **128**, 1037-1043.

Romier-Crouzet, B., Van De Walle, J., During, A., Joly, A., Rousseau, C., Henry, O., Larondelle, Y., and Schneider, Y.-J. (2009). Inhibition of inflammatory mediators by polyphenolic plant extracts in human intestinal Caco-2 cells. *Food and Chemical Toxicology* **47**, 1221-1230.

Rousset, M. (1986). The human colon carcinoma cell lines HT-29 and Caco-2: Two in vitro models for the study of intestinal differentiation. *Biochimie* **68**, 1035-1040.

Sakata, A., Yasuda, K., Ochiai, T., Shimeno, H., Hikishima, S., Yokomatsu, T., Shibuya, S., and Soeda, S. (2007). Inhibition of lipopolysaccharide-induced release of interleukin-8 from intestinal epithelial cells by SMA, a novel inhibitor of sphingomyelinase and its therapeutic effect on dextran sulphate sodium-induced colitis in mice. *Cellular Immunology* **245**, 24-31.

Sambuy, Y., De Angelis, I., Ranaldi, G., Scarino, M. L., Stammati, A., and Zucco, F. (2005). The Caco-2 cell line as a model of the intestinal barrier: influence of cell and culture-

related factors on Caco-2 cell functional characteristics. *Cell Biology and Toxicology* **21**, 1-26.

Samuelsen, A. B., Rieder, A., Grimmer, S., Michaelsen, T. E., and Knutsen, S. H. (2011). Immunomodulatory activity of dietary fiber: arabinoxylan and mixed-linked beta-glucan isolated from barley show modest activities in vitro. *International journal of molecular sciences* **12**, 570-587.

Sartor, R. B. (1994). Cytokines in intestinal inflammation: pathophysiological and clinical considerations. *Gastroenterology* **106**, 533-9.

Saulnier, L., Sado, P. E., Branlard, G., Charmet, G., and Guillon, F. (2007). Wheat arabinoxylans: Exploiting variation in amount and composition to develop enhanced varieties. *Journal of Cereal Science*l. **46**, 261-281.

Schenk, M., and Mueller, C. (2008). The mucosal immune system at the gastrointestinal barrier. *Best Practice & Research Clinical Gastroenterology* **22**, 391-409.

Schepetkin, I. A., and Quinn, M. T. (2006). Botanical polysaccharides: Macrophage immunomodulation and therapeutic potential. *International Immunopharmacology* **6**, 317-333.

Sigma-Aldrich (2014). Indomethacin. http://www.sigmaaldrich.com/catalog/product/sigma/i7378?lang=en&region=US.

Skrzypski, M. (2008). Quantitative reverse transcriptase real-time polymerase chain reaction (qRT-PCR) in translational oncology: Lung cancer perspective. *Lung Cancer* **59**, 147-154.

Son, D. O., Satsu, H., and Shimizu, M. (2005). Histidine inhibits oxidative stress- and TNF-α-induced interleukin-8 secretion in intestinal epithelial cells. *FEBS Letters* **579**, 4671-4677.

Spiegel, S., Foster, D., and Kolesnick, R. (1996). Signal transduction through lipid second messengers. *Curr Opin Cell Biol* **8**, 159-67.

Surh, Y. J., Chun, K. S., Cha, H. H., Han, S. S., Keum, Y. S., Park, K. K., and Lee, S. S. (2001). Molecular mechanisms underlying chemopreventive activities of anti-inflammatory phytochemicals: down-regulation of COX-2 and iNOS through suppression of NF-kappa B activation. *Mutat Res* **480-481**, 243-68.

Tzianabos, A. O. (2000). Polysaccharide immunomodulators as therapeutic agents: structural aspects and biologic function. *Clin Microbiol Rev* **13**, 523-33.

Van De Walle, J., Hendrickx, A., Romier, B., Larondelle, Y., and Schneider, Y.-J. (2010). Inflammatory parameters in Caco-2 cells: Effect of stimuli nature, concentration, combination and cell differentiation. *Toxicology in Vitro* **24**, 1441-1449.

Volman, J. J., Ramakers, J. D., and Plat, J. (2008). Dietary modulation of immune function by beta-glucans. *Physiology & behavior* **94**, 276-284.

Wang, X., Wang, S., Li, Y., Wang, F., Yang, X., and Yao, J. (2013). Sulfated Astragalus polysaccharide can regulate the inflammatory reaction induced by LPS in Caco2 cells. *Int J Biol Macromol* **60**, 248-52.

Wischmeyer, P. E., Kahana, M., Wolfson, R., Ren, H., Musch, M. M., and Chang, E. B. (2001). Glutamine reduces cytokine release, organ damage, and mortality in a rat model of endotoxemia. *Shock* **16**, 398-402.

Wright, K. L., Weaver, S. A., Patel, K., Coopman, K., Feeney, M., Kolios, G., Robertson, D. A., and Ward, S. G. (2004). Differential regulation of prostaglandin E biosynthesis by interferon-gamma in colonic epithelial cells. *Br J Pharmacol* **141**, 1091-7.

Zakharova, M., and Ziegler, H. K. (2005). Paradoxical anti-inflammatory actions of TNF-alpha: inhibition of IL-12 and IL-23 via TNF receptor 1 in macrophages and dendritic cells. *J Immunol* **175**, 5024-33.

Zhou, S., Liu, X., Guo, Y., Wang, Q., Peng, D., and Cao, L. (2010). Comparison of the immunological activities of arabinoxylans from wheat bran with alkali and xylanase-aided extraction. *Carbohydrate Polymers* **81**, 784-789.

CHAPTER 5. ARABINOXYLAN HYDROLYZATES AS SUBSTRATE FOR THE BACTEROIDES SPECIES

5.1. Abstract

Although the human diet is rich with plant and animal derived polysaccharides, there is a large array of polysaccharides that are resistant to digestion by human enzymes and rely on microbial enzymes for their digestion. The fermentation of these by microbes yield energy for the microbial growth and the end products such as short chain fatty acids has profound effects on the host health. The fine structural details of these polysaccharides might have an influence on their fermentability by the gut bacteria. The current research was carried out to evaluate how the structural differences among arabinoxylan hydrolyzates from wheat influence the growth of human gut microbiota using an idealized experimental model employing Bacteroides strains. In general, *B. cellulosilyticus* DSM 14830 had the highest growth while *B. eggerthii* DSM 20697 had the lowest growth on arabinoxylan hydrolyzates. Interestingly, *B. cellulosilyticus* DSM 14830, *B. ovatus* 3_1_23, *B. ovatus* ATCC 8483 and *B. xylanisolvens* XB1A displayed clearly distinguishable phase shifts along the growth curves. This indicates their ability to tune in their gene expressions to overcome the hindrances to growth exerted by structural details on the substrate polysaccharide. Another explanation for this could be that during growth, the bacteria encounter specific structures that reduce growth rate and these cause the shifts. Overall, this research confirms the ability of Bacteroides to utilize structurally divers array of polysaccharides. The co-existence of these bacteria within the human intestinal tract could lead to maximum utilization of plant polysaccharides and in turn contribute to the many health benefits associated with plant polysaccharides.

5.2. Introduction

The intestine is an important organ that consists of a huge surface area and permits vital interactions with the external world, including the gut microbiota (Cani et al., 2013). The microbiota refers to "*the microbial life forms within a given habitat or host"* (Walter and Ley, 2011). The gut microbiota exerts a significant impact on host physiology, impacting the control of energy homeostasis, the immune system, digestion and vitamin synthesis (Cani et al., 2013) and inhibition of pathogen colonization (Wardwell et al., 2011).

It is then in the large intestine that the saccharolytic bacteria extract additional energy from the dietary substances that are resistant to digestion by the human enzymes (Walter and Ley, 2011). Although the human diet is rich with plant and animal derived glycans, there is a large array of glycans that are resistant to digestion by human enzymes and rely on microbial enzymes for their digestion. The fermentation of these glycans by microbes yield energy for the microbial growth and the end products such as short chain fatty acids (SCFA), mainly acetate, propionate and butyrate has profound effects on the host health (Tremaroli and Backhed, 2012). The functional association among the intestinal microbiota, intestinal epithelial cells and the host immune system help maintain the balance between tolerance and immunity to a particular pathogenic or nonpathogenic microbe or food ingredient.

Studies of healthy adult gut microbiota have shown that it is composed primarily of members of two bacterial phyla, the Bacteroidetes and Firmicutes (McNulty et al., 2013). However, the most expanded glycolytic gene repertoires that target xylan degradation is found in genus *Bacteroides* (Zhang et al., 2014). The Bacteroidetes encode more carbohydrate-active enzyme (CAZyme) families enzymes and processes more CAZyme-encoding genes than other phyla such as Firmicutes, indicating their enhanced capacity to utilize wide range of

polysaccharide substrates (Kaoutari et al., 2013). The members of the genus *Bacteroides* are adept at utilizing plant and host derived polysaccharides (Koropatkin et al., 2012). These *Bacteroides* are rich in genes involved in the acquisition and metabolism of various glycosides including glycoside hydrolases and polysaccharide lyases which are organized into polysaccharide utilization loci (PULs) that are distributed throughout the genome (Koropatkin et al., 2012). In the phylum Bacteroidetes, the metabolism of starch from the external environment is achieved via the starch utilization system (Sus) (Koropatkin et al., 2012). There have been similar systems unique to the phylum Bacteroidetes identified in the Bacteroidetes genome that function by a similar mechanism as Sus but harbor enzymes that target glycans other than starch, thus these systems are termed Sus-like systems (Koropatkin et al., 2012). These Sus-like systems are involved in metabolism of many other glylans by the Bacteroidetes. The molecular mechanisms used to utilize xylan "is analogous to the Sus-like paradigm" (Dodd et al., 2011; Martens et al., 2009). A gene cluster that was highly induced during growth of Bacteroidetes on wheat AX was identified and termed the xylan utilization system (Xus) (Dodd et al., 2011). A schematic model predicting the utilization of xylan by Xus is given in Figure 1.8. The system consists of a set of polysaccharide binding proteins, glycolytic enzymes that hydrolyze large polysaccharides into smaller oligosaccharides and TonB-dependent transporters that transport these oligosaccharides into the periplasm (Zhang et al., 2014). These oligosaccharides are then converted to smaller monosaccharides by an array of glycolytic enzymes before being transported to the cytosol (Martens et al., 2009).

With regard to metabolic syndromes, a statistically significant 50% reduction in Bacteroidetes was observed in cecal microbiota of obese mice compared to lean mice (Ley et al., 2005). A similar observation was made on humans, showing that the relative proportion of

Bacteroidetes is reduced in obese individuals compared to lean individuals (Ley et al., 2006). The beneficial effects of the commensal microbes on human health have been demonstrated by numerous studies. Mazmanian et al. (2008) demonstrated that the "human symbiont *Bacteroides fragilis* protects animals from experimental colitis induced by *Helicobacter hepaticus*". The observed protective action was attributed to the microbial polysaccharide, polysaccharide A (PSA), produced by *Bacteroides fragilis* (Mazmanian et al., 2008). Also, administration of PSA to mice protected the animals from weight loss and caused decreased levels of proinflammatory cytokines such as TNF, IL-17 and IL-23 (Mazmanian et al., 2008). These PSA molecules are suggested to be taken up by dendritic cells in the intestine and presented on MHC II to $CD4^+$ T cells resulting in activation of these T cells (Round and Mazmanian, 2009). In assessing the contribution from intestinal bacteria to development of asthma, Bjorksten (1999) concluded that allergic children had lower levels of colonization by *Bacteroides* spp. compared to non-allergic children. Inflammatory bowel disease (IBD) is a chronic remittent or progressive inflammatory condition in the gastrointestinal tract (Kaser et al., 2010). It affects nearly 1 million persons in North America alone and several million persons worldwide (Bamias et al., 2005). In IBD patients a reduced proportion of Bacteroides and Firmicutes and an increase in *Escherichia coli* and *Shigella flexneri* were observed indicating a possible relationship between these bacteria and IBD (Li et al., 2012).

Previous work has demonstrated the influence of structural differences of cereal polysaccharides such as arabinoxylans on their fermentation profiles. Rose et al. (2010) indicated differences among the fermentation profiles for AX from different cereals (maize, rice and wheat), which consists of different structural features. Xu (2012) concluded that specific molecular regions of dietary fibers differentiate gut bacteria. With such background, the current

research was carried out to evaluate how the structural differences among enzymatically tailored wheat arabinoxylan hydrolyzates influence the growth of human gut microbiota using an idealized experimental model employing Bacteroides strains.

5.3. Materials and Methods

5.3.1. Materials

Materials used for the production of AXH were previously described in section 2.3.1. The bacterial fermentation experiments were carried out using six publicly available Bacteroides strains belonging to 5 different species kindly provided by Dr Eric Martens (Department of Microbiology & Immunology, University of Michigan, Ann Arbor, MI). The strains were: *Bacteroides cellulosilyticus* DSM 14838, *Bacteroides ovatus* ATCC 8483, *Bacteroides ovatus* 3-1-23, *Bacteroides eggerthii* DSM 20697, *Bacteroides intestinalis* DSM 17393, *Bacteroides xylanisolvens* XB1A. All strains were originally isolated from human colon or fecal samples, representative of the most commonly encountered xylanolytic organisms in the gut.

5.3.2. Procedure for arabinoxylan hydrolyzate preparation

AXH preparation was carried out as described in section 2.3.2 in a previous chapter. A summary of the treatments and the abbreviation given to the resulting AXH is given in Table 2.1.

5.3.3. Chemical analysis

The chemical analysis of the AXH was carried out as described in section 2.3.3 using GC-FID, SEC-MALS, ^{1}H-NMR and GC-FID techniques.

5.3.4. Pure bacterial strain growth experiments

The bacterial growth experiments were carried out according to the methods described by Martens et al. (2011). Each freeze dried arabinoxylan hydrolyzates from all the thirty preparations were weighed out (45mg) and dissolved in millipore water (4.5 mL) to prepare 10 mg/mL stock solutions of each hydrolyzate. Xylose (10 mg/mL) stocks were also prepared as standard and for comparisons. Each substrate was autoclaved at 121 ºC for 20 min. Substrate solution was pipetted into one of the designated wells on a 24 × 16 plate assigning three wells for each substrate per bacterial strain. Each bacterial strain inoculum was added to each well, diluting the final substrate concentration to 5 mg/mL.

The bacterial inocula were prepared as follows: each bacterium was inoculated into custom chopped meat media using sterile wood sticks from glycerol stocks from freezer. These cultures for assay inoculations were grown for 24 h at 37 ^{0}C under an anaerobic atmosphere of 10% H_2, 5% CO_2, and 85% N_2 using an anaerobic chamber (Coy manufacturing, Grass Lake, MI). This culture (1 mL) was drawn into 1.5 mL centrifuge tube and was centrifuged at 10 × 1000g for 1 min. The supernatant was discarded and Bacteroides minimal medium (1 mL) was added and the bacterial pellet was re-suspended in it. This was again centrifuged (10 × 1000g for 1 min) to wash the bacteria. This step was repeated another time. After discarding the second washing, the bacterial pellet was re-suspended in 1 mL of Bacteroides minimal medium. This was the washed culture. Washed culture was pipetted into Bacteroides minimal medium to prepare the "diluted bacterial culture" (1:50 ratio). Diluted bacterial culture was inoculated into the previously prepared microplates containing substrate solution in each well inside the anaerobic chamber.

After inoculation the plates were allowed to equilibrate with the anaerobic conditions for about 30 min. Assay plates were sealed under the atmosphere noted above with an optically clear gas-permeable polyurethane membrane (Diversified Biotech, Boston, MA). The plates were then loaded into a Biostack automated plate handling device coupled to a Powerwave HT absorbance reader (both devices from Biotek Instruments, Winooski, VT). Absorbance at 600 nm (A600) was measured for each well at 10–15 min intervals. Data were processed using Gen5 software (Biotek) and Microsoft Excel.

Several glycans yielded complicated polyphasic growth profiles rather than a single exponential growth phase. Thus, we quantified growth in each assay by first identifying a minimum time point (Amin) at which A600 had increased by 10% over a baseline reading taken during the first 500 min of incubation. Next, we identified the time point at which A600 reached its maximum (Amax) immediately after exponential growth. Total growth parameter was generated for each well (Amax - Amin). Cultures that failed to increase density by at least 0.1 (A600) were scored as no growth.

5.3.5. Statistical analysis

All the experiments were done in duplicate. All statistical analyses were performed using Statistical Analysis System software package version 9.4 (SAS Institute, Cary, NC)

The data are presented as the means ± SE and were subjected to one way ANOVA using LSD test procedure. A least significant difference (LSD) with a 5 % significance level was used to declare differences. Differences were considered significant when the probability value p was lower than 0.05.

Pearson's correlation analysis was conducted to evaluate relationships between bacterial growth and AXH composition/structural details.

5.4. Results and Discussion

5.4.1. Chemical characterization of the AXH

Extensive discussions on the fine structural details of the AXH are discussed in a previous chapter (Chapter 2). The sugar composition, A/X ratio of the WAX and the resulting AXH are given in Table 2.2. The weight average molecular weights and polydispersity index of each AXH is presented in Table 2.3.The ^{1}H-NMR resonance integrations for WAX and AXH are in Table 2.4. The linkage analysis results of each AXH are depicted in Figure 2.3.

5.4.2. Bacterial growth experiments

Each Bacteroides species growing on the same AXH (CJX-1) had different growth curves (Figure 5.1). *B. cellulosilyticus* DSM 14830 had the highest growth while *B. eggerthii* DSM 20697 had the lowest growth on CJX-1. Interestingly, *B. cellulosilyticus* DSM 14830, *B. ovatus* 3_1_23 and *B. ovatus* ATCC 8483 displayed clearly distinguishable phase shifts along the growth curve for growing on CJX-1. *B. xylanisolvens* displayed a less prominent phase shift. *B. intestinalis* DSM 17393 also displayed phase shifts but this occurred much later in the growth. Rose et al. (2010) observed that while the fermentation of maize bran by fecal microbes happened in a linear pattern with high production of short chain fatty acids during the 24 hour fermentation, the fermentation of the wheat bran followed a two phase mechanism. They suggested that the bacteria might utilize the unsubstituted less complex regions initially and upon depletion of unsubstituted regions might proceed to subsequently metabolize the substituted xylose regions. The phase shifts observed for *B. cellulosilyticus* DSM 14830, *B. ovatus* 3_1_23 and *B. ovatus* ATCC 8483 might be due to such two phasic fermentation of complex

arabinoxylan structures. These phase shifts indicate that the above *Bacteroides* species have evolved in such a way to degrade even complex polysaccharides.

None of the *Bacteroides* species under investigation displayed a correlation with the total AX in the substrate, AXH. This suggests that it is not merely the content of AX that influences the growth but the fine structural complexity that is at play. A strong positive correlation (0.751) was seen between the total growth results of *B. cellulosilyticus* DSM 14830 and *B. ovatus* 3_1_23. This correlation between the two strains suggests that these two strains might have similar enzymatic abilities to utilize AXH. Also a strong positive correlation (0.641) was observed for the total growth results between *B. cellulosilyticus* DSM 14830 and *B. ovatus* ATCC 8483. However, although of the same species, no significant correlation was evident for the growth results between *B. ovatus* 3_1_23 and *B. ovatus* ATCC 8483. These indicate the diversity of AX fermentation capacity within the *B. ovatus* species.

A strong positive correlation (0.707) was also observed between the total growth results of *B. eggerthii* DSM 20697 and *B. xylanisolvens* XB1A indicating that both species preferred similar substrates, thus might have similar enzymes at their disposal. Interestingly, no correlation was observed for *B. intestinalis* DSM 17393 with any other five *Bacteroides* species employed in the current study.

Overall, *B. cellulosilyticus* DSM 14830 had the highest growth while *B. eggerthii* DSM 20697 had the lowest growth. Except *B. eggerthii* DSM 20697, all the other strains showed significantly lower growth compared to the control, xylose.

As the name indicates, *B. cellulosilyticus* DSM 14830 is equipped with enzymes to degrade cellulose (Robert et al., 2007). However, the ability of *B. cellulosilyticus* DSM 14830 to ferment other plant cell wall polysaccharides have also been reported (Xu, 2012). The growth

curves of *B. cellulosilyticus* DSM 14830 on different AXH and xylose is given in Figure 5.2. Most of the growth curves followed a similar path with distinguishable phase shifts occurring along the growth. *B. cellulosilyticus* DSM 14830 efficiently fermented most of the AXH being tested (Figure 5.8). However, highest growth was observed for the control substrate, xylose. Out of all the six *Bacteroides* species used in the current study, *B. cellulosilyticus* DSM 14830 had the highest overall growth on AXH substrates. The overall growth on AXH varied from 0.43 to 0.59 (ΔOD_{600}) with lowest growth on CJX-4 and highest growth on CJX-1. A negative correlation (-0.512) was observed between the arabinose to xylose ratio and *B. cellulosilyticus* DSM 14830 growth. This suggests that the bacteria prefer the unsubstituted xylose regions along the AX molecule compared to those having high proportions of arabinose substitution. However, in general, *B. cellulosilyticus* DSM 14830 grew well on all the AXH despite their fine structural differences. The human gut Bacteroide, *B. cellulosilyticus* WH2, a different strain of the same species as *B. cellulosilyticus* DSM 14830, has been shown to contain a genome encoding more carbohydrate active enzymes than any other Bacteroidetes species analyzed to date (McNulty et al., 2013). *B. cellulosilyticus* WH2 is exceptionally capable of adapting to different diets rich in different polysaccharides (McNulty et al., 2013). Depending on the available dietary source, *B. cellulosilyticus* WH2 is capable of tailoring its carbohydrate utilization strategies to adapt to that substrate, with a preference for cereal grain xylans. A similar adaptability might be responsible for the ability of *B. cellulosilyticus* DSM 14830 to grow similarly well on all the AXH under investigation despite their structural differences.

B. ovatus 3_1_23 had similar growth curves upon growth on the 30 different AXH substrates except for xylose (Figure 5.3). Similar to *B. cellulosilyticus* DSM 14830, *B. ovatus* 3_1_23 also indicated phase shifts along its growth curve for the AXH substrates. The total

growth on the AXH substrates ranged between 0.28-0.42 (ΔOD_{600}) with lowest growth on ANX-5 and highest growth on CJX-1 (Figure 5.9). The control, xylose had a growth of 1.54 (ΔOD_{600}). When the structural complexity of the AXH were considered, there was a tendency towards AXH with high proportion of unsubstituted xylose to result in higher growth compared to AXH with lower proportion of unsubstituted xylose. In a similar way, the less complex the structure was, that is, less amount of arabinose substitution was observed in the AXH, the bacteria seemed to prefer that substrate.

The growth curves of *B. ovatus* ATCC 8483 growing on different AXH are given in Figure 5.4. It followed a similar growth to *B. ovatus* 3_1_23 and also displayed a phase shift along the growth curve, although less prominent than *B. ovatus* 3_1_23. The total growth of *B. ovatus* ATCC 8483 on different AXH showed a considerable variation among most of the AXH (Figure 5.10). The lowest growth was observed for BAF-2 (0.27) while highest growth showing AXH was ANX-1 (0.48). Xylose indicated a growth of 0.87. An apparent negative correlation (-0.439) was observed between the growth of *B. ovatus* ATCC 8483 with the arabinose to xylose ratio of the AXH. A similar indication that the bacterial growth is negatively correlated (-0.425) with the amount of terminal arabinose substitution was supportive of the above statement. Thus, *B. ovatus* ATCC 8483 seemed to display a preference for the less substituted, less structurally complex AX.

B. eggerthii DSM 20697 grew well on xylose (ΔOD_{600} of 0.61) following the typical growth curve in xylan medium (Figure 5.5) (Salyers et al., 1981). No apparent phase shift was observed for any of the AXH. Among the AXH substrates, the lowest growth was observed for CJX-3 (0.15) (ΔOD_{600}) while the highest growth was on CJX-1 (0.27) (ΔOD_{600}) (Figure 5.11). Thus, compared to all rest of the strains used in the current research, the weakest growth on

AXH being tested was displayed by *B. eggerthii* DSM 20697. Xu (2012) also investigated the growth of same strains used in the current research and observed that *B. eggerthii* DSM 20697 grew the weakest on wheat arabinoxylan.

The growth curves of *B. intestinalis* DSM 17393 is given in Figure 5.6. There were phase shifts observed for some of the AXH which occurred much later in the log phase compared to other species in the current study. The overall growth of *B. intestinalis* DSM 17393 on AXH was in the range of 0.26-0.0.39 (ΔOD_{600}) with lowest growth on CJX-3 and highest growth on CJX-7 (Figure 5.12). Interestingly, it did not show a drastic growth improvement on xylose (0.39 (ΔOD_{600})). Within the current study, we observed that *B. intestinalis* DSM 17393 had lowest growth on the control, xylose while the other two species, *B. ovatus* ATCC 8483, *B. xylanisolvens* XB1A grew comparably well on xylose. The reduced growth of *B. intestinalis* DSM 17393 on xylose has also been previously reported (Xu, 2012). They observed an apparent preference for arabinose branches of the AX by *B. intestinalis* DSM 17393. According to the model predicted by Dodd et al., (2011) for the transport of xylans across the bacterial outer membrane, the binding of xylan, cleavage and transport of xylan fragments across the outer membrane is achieved via the Xus cluster. XusB/D, XusE, and Xyn10C protein components of the Xus cluster bind to extracellular xylan polymers to facilitate its degradation and subsequent transport in to the cell. Thus, *B. intestinalis* DSM 17393 might be better designed to recognize and bind substituted arabinoxylans or xylan polymers over the monosaccharide, xylose. Among the species *B. intestinalis* DSM 17393, *B. ovatus* ATCC 8483, *B. xylanisolvens* XB1A, *B. intestinalis* DSM 17393 has the highest number of different glycoside hydrolases (GHs) and polysaccharide lyases (PLs) families (Kaoutari et al., 2013). This further indicates that *B. intestinalis* DSM 17393 might prefer polysaccharides over monosaccharides as fermentation of

polysaccharides would require more enzymes than for monosaccharides. Furthermore, utilization of monosaccharide xylose shouldn't require any GH enzymes, but it does require expression of the proper transporter, so these data may indicate that the xylose transporter is controlled by xylan/xylooligosaccharide signals and is therefore not properly expressed in just xylose.

B. xylanisolvens XB1A growth curves are given in Figure 5.7. For most of the AXH, a phase shift was observed towards the beginning of the log phase of the growth curve. Thus, the bacteria seem to adjust its enzyme expression based on the available substrate and once the enzymes are ready, the bacteria seemed to grow exponentially. The total growth on AXH ranged from 0.26 to 0.44 (ΔOD_{600}) with lowest growth on CAF-2 and highest growth on ANX-2 (Figure 5.13). Structural analysis of AXH indicated that there is a negative correlation (-0.471) between the substituted arabinose substitution (2,3-substituted 1,5-linked arabinose) and the bacterial growth.

5.5. Conclusion

When the diversity of glycan cleaving enzymes among the human gut microbiota was considered, the phylum Bacteroidetes had the highest number of genes encoding glycoside hydrolases (GHs) and polysaccharide lyases (PLs) and highest number of carbohydrate-active enzyme (CAZyme) families represented in these genomes compared to the other phyla under review (Kaoutari et al., 2013). This indicates that Bacteroidetes are capable of utilizing a large range of carbohydrate substrates compared to other phyla such as Firmicutes (Kaoutari et al., 2013). The ability of different *Bacteroides* to ferment different polysaccharide substrates has also been indicated by others (Salyers et al., 1977). As the human diet consists of large repertoire of dietary polysaccharides, presence of these diverse array of CAZymes are of vital importance to take maximum benefit from these structurally diverse polysaccharides.

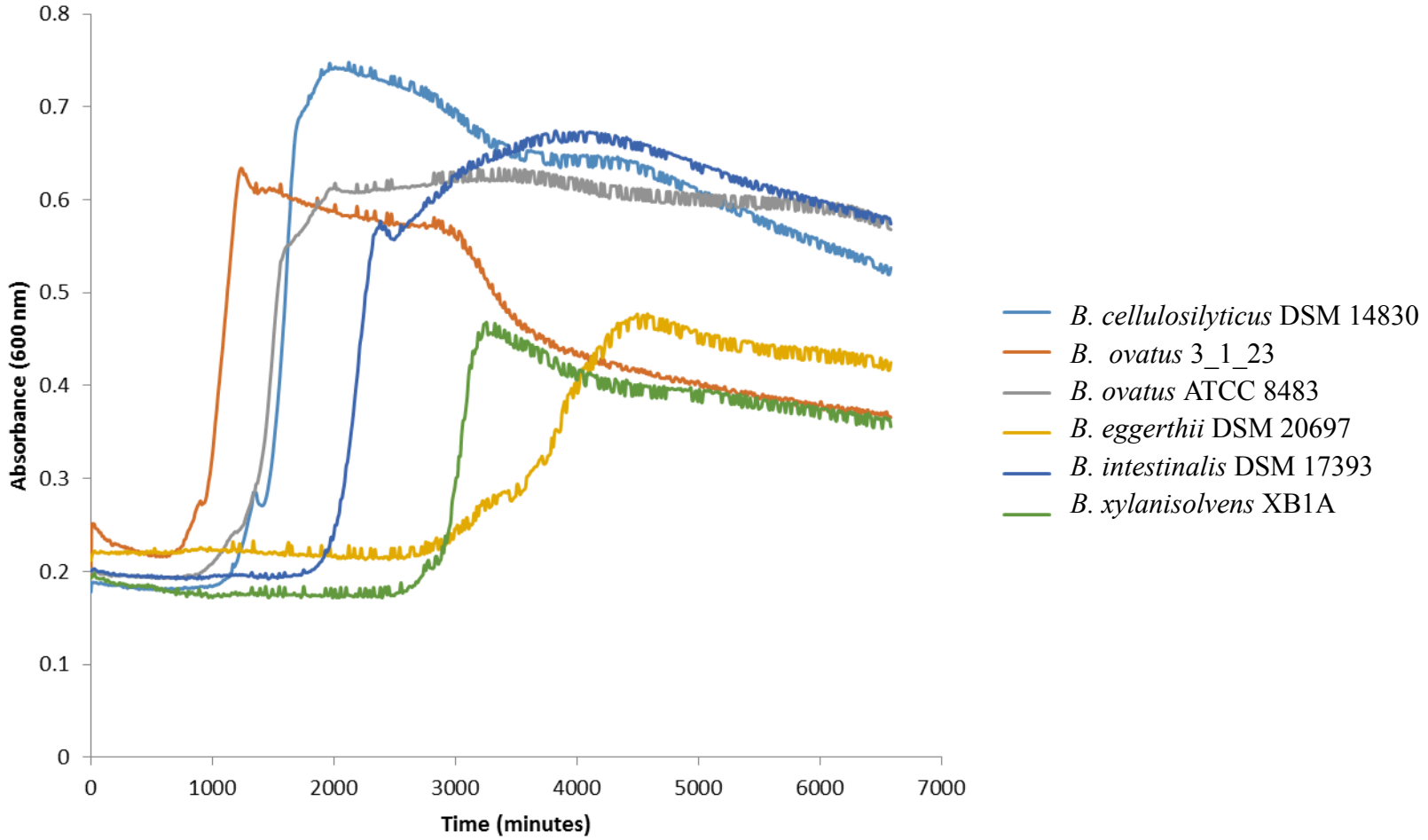

Figure 5.1. Bacterial growth curves of six Bacteroides species on same AXH (CJX-1). The absorbance was measured at 600 nm over a continuous time frame.

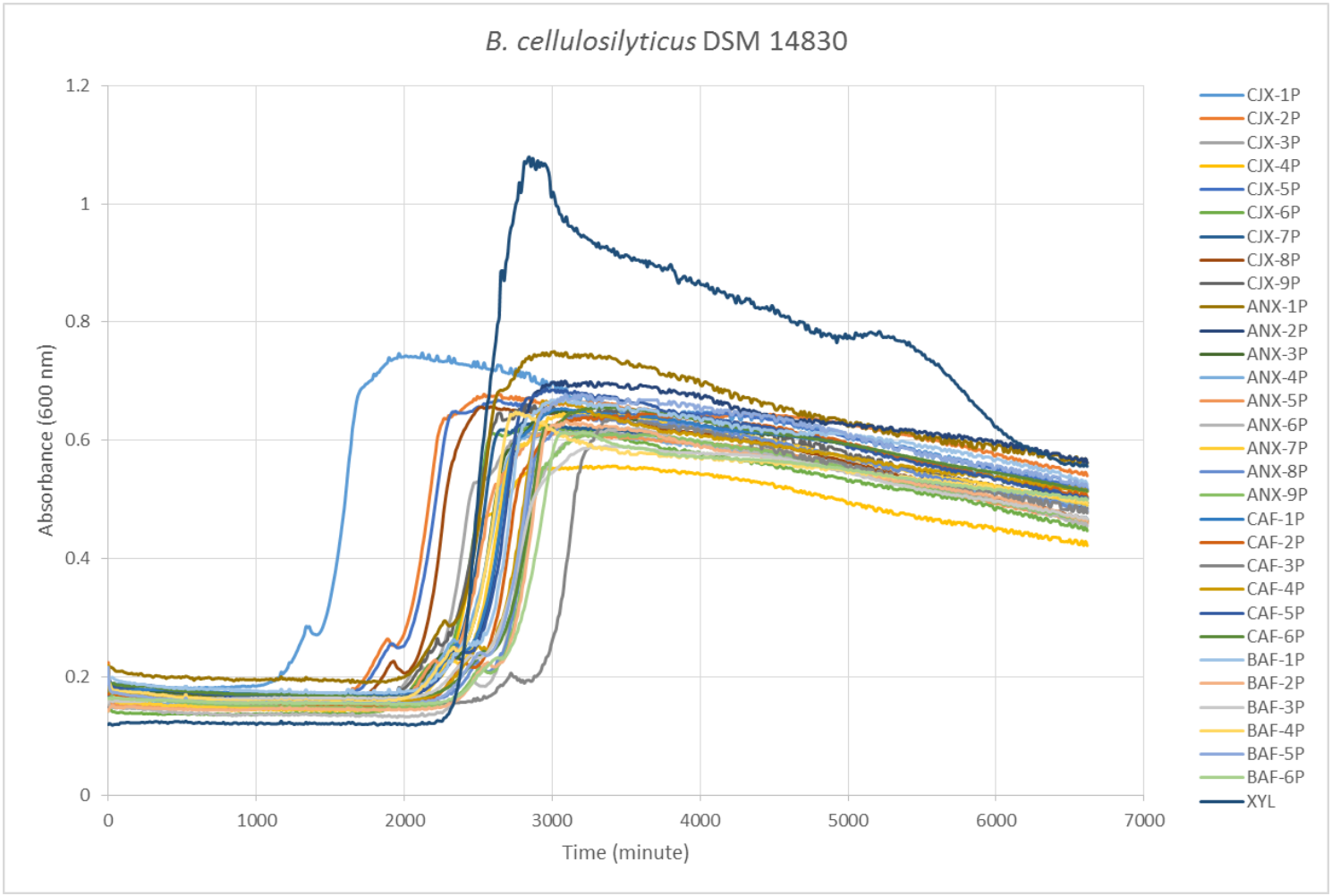

Figure 5.2. Growth curves of *B. cellulosilyticus* DSM 14830 on different arabinoxylan hydrolyzates and xylose. CJX-1P to BAF-6P: different AXH; XYL: xylose.

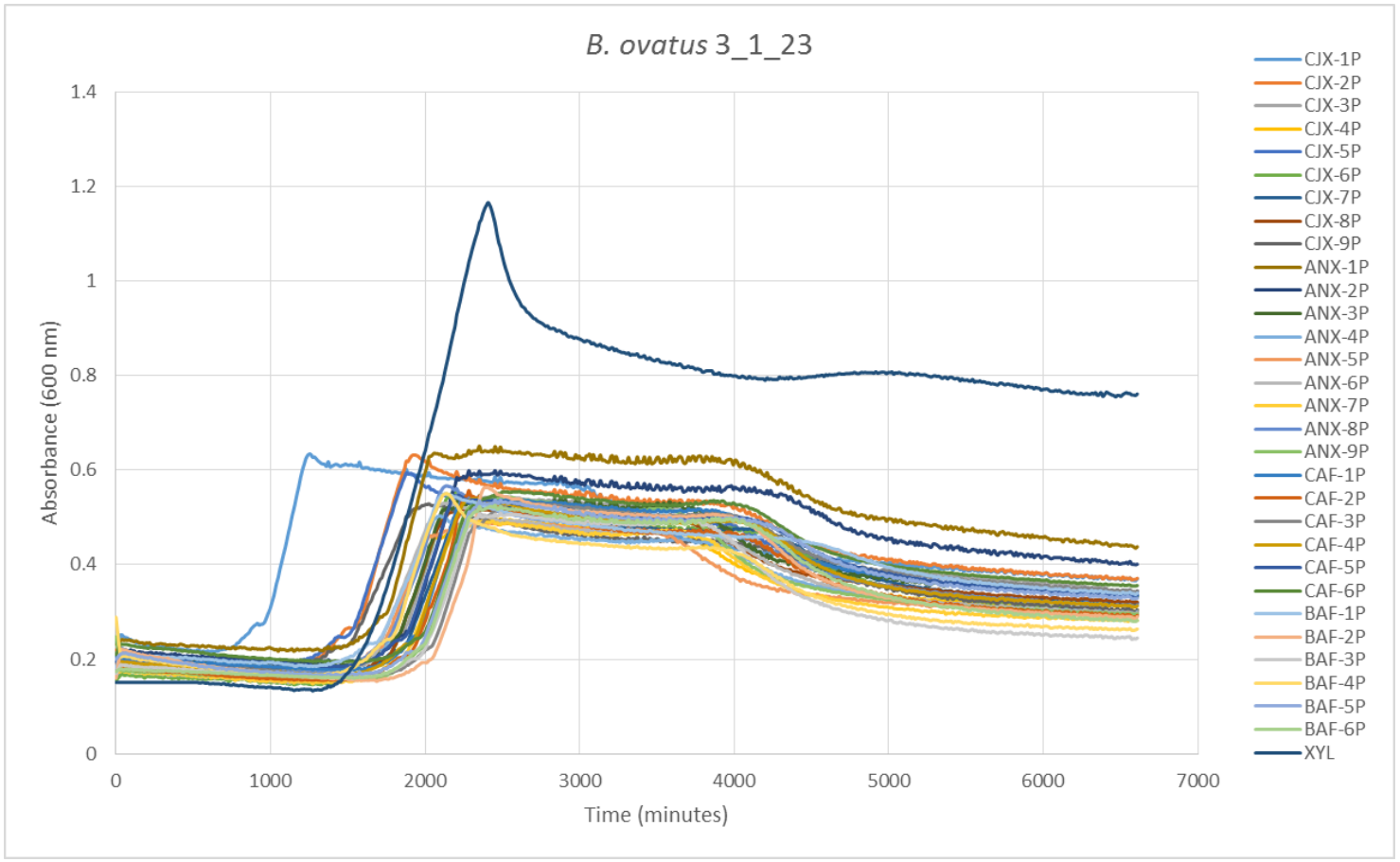

Figure 5.3. Growth curves of *B. ovatus* 3_1_23 on different arabinoxylan hydrolyzates and xylose. CJX-1P to BAF-6P: different AXH; XYL: xylose.

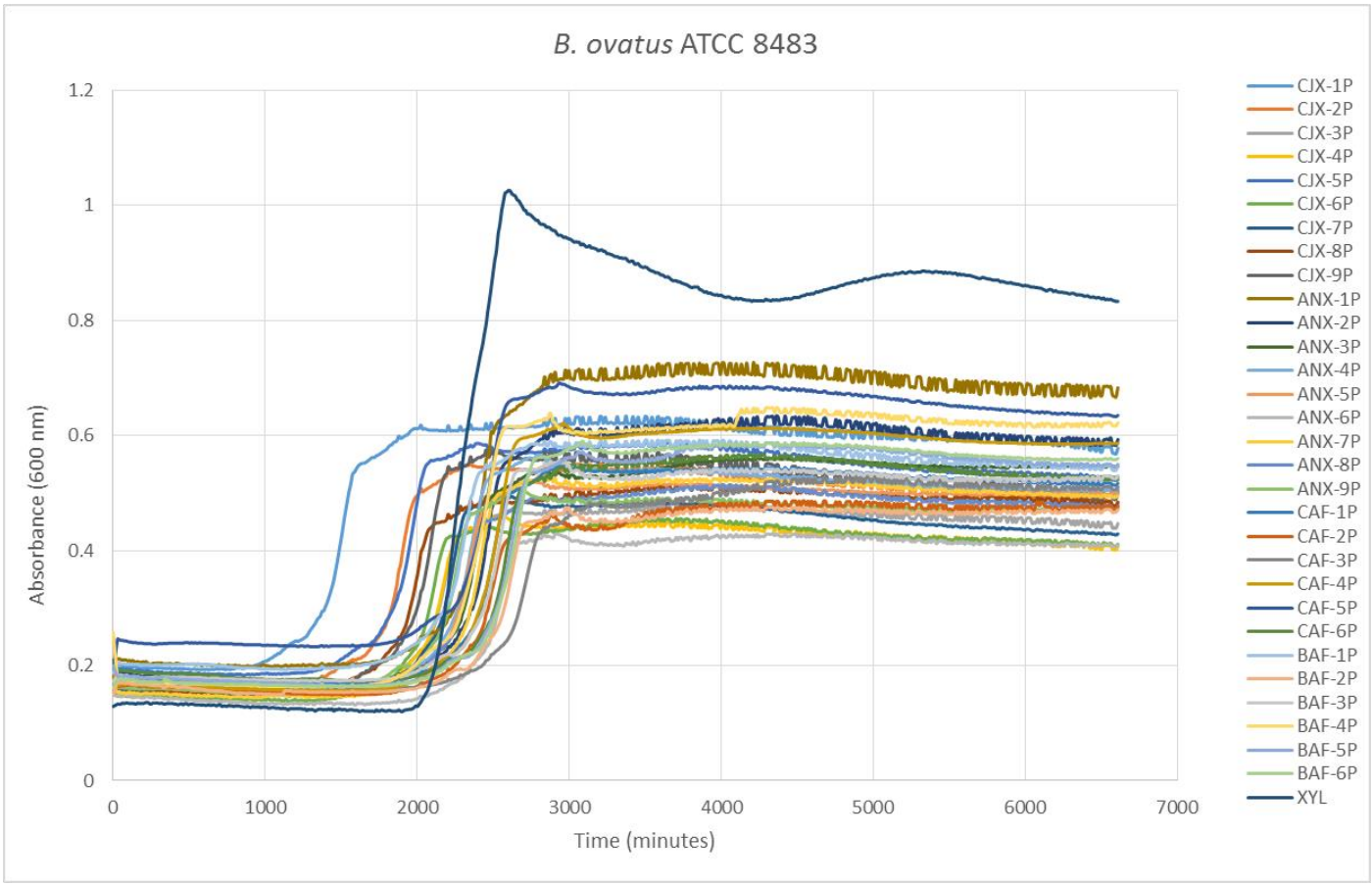

Figure 5.4. Growth curves of *B. ovatus ATCC 8483* on different arabinoxylan hydrolyzates and xylose. CJX-1P to BAF-6P: different AXH; XYL: xylose.

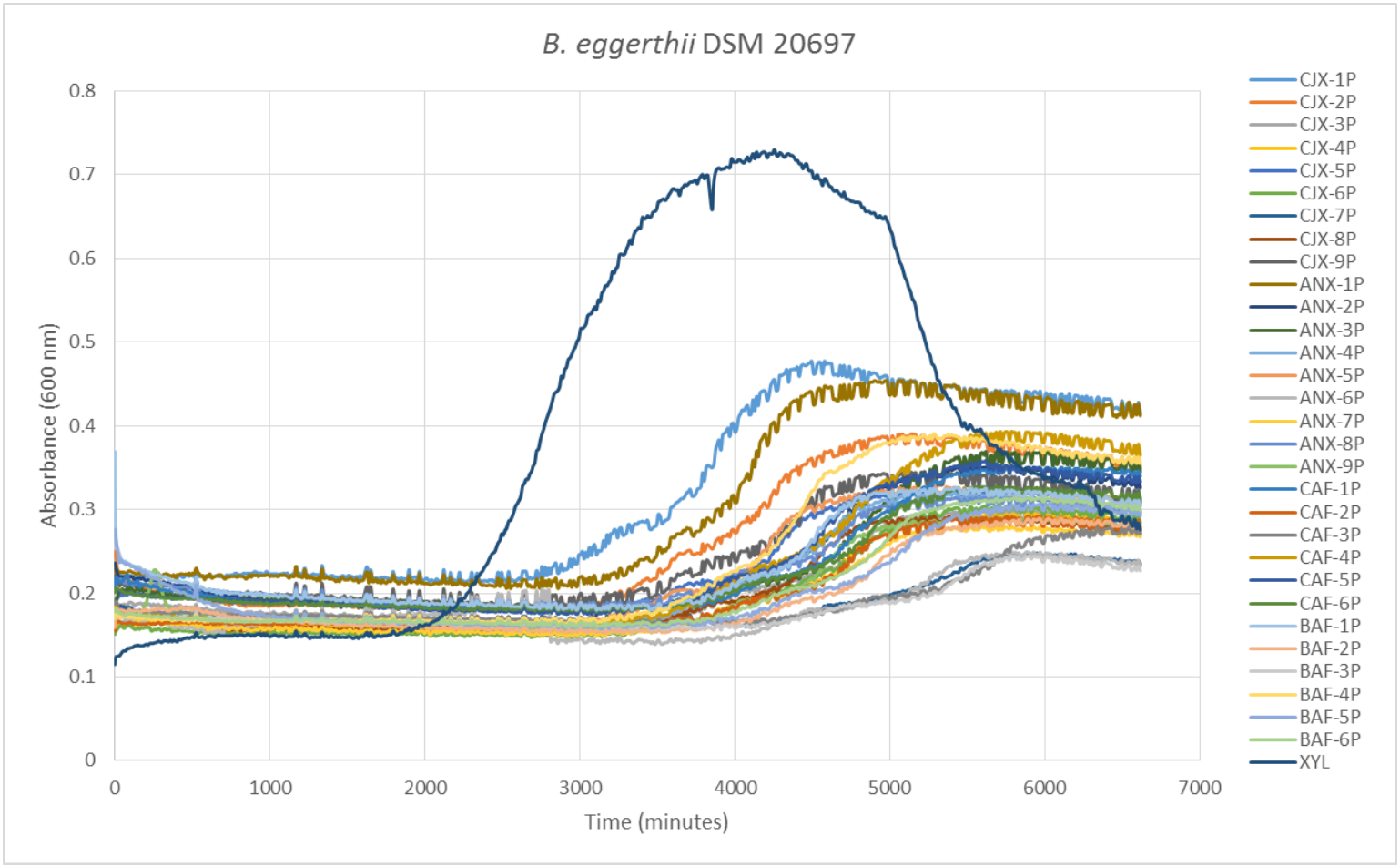

Figure 5.5. Growth curves of *B. eggerthii DSM 20697* on different arabinoxylan hydrolyzates and xylose. CJX-1P to BAF-6P: different AXH; XYL: xylose.

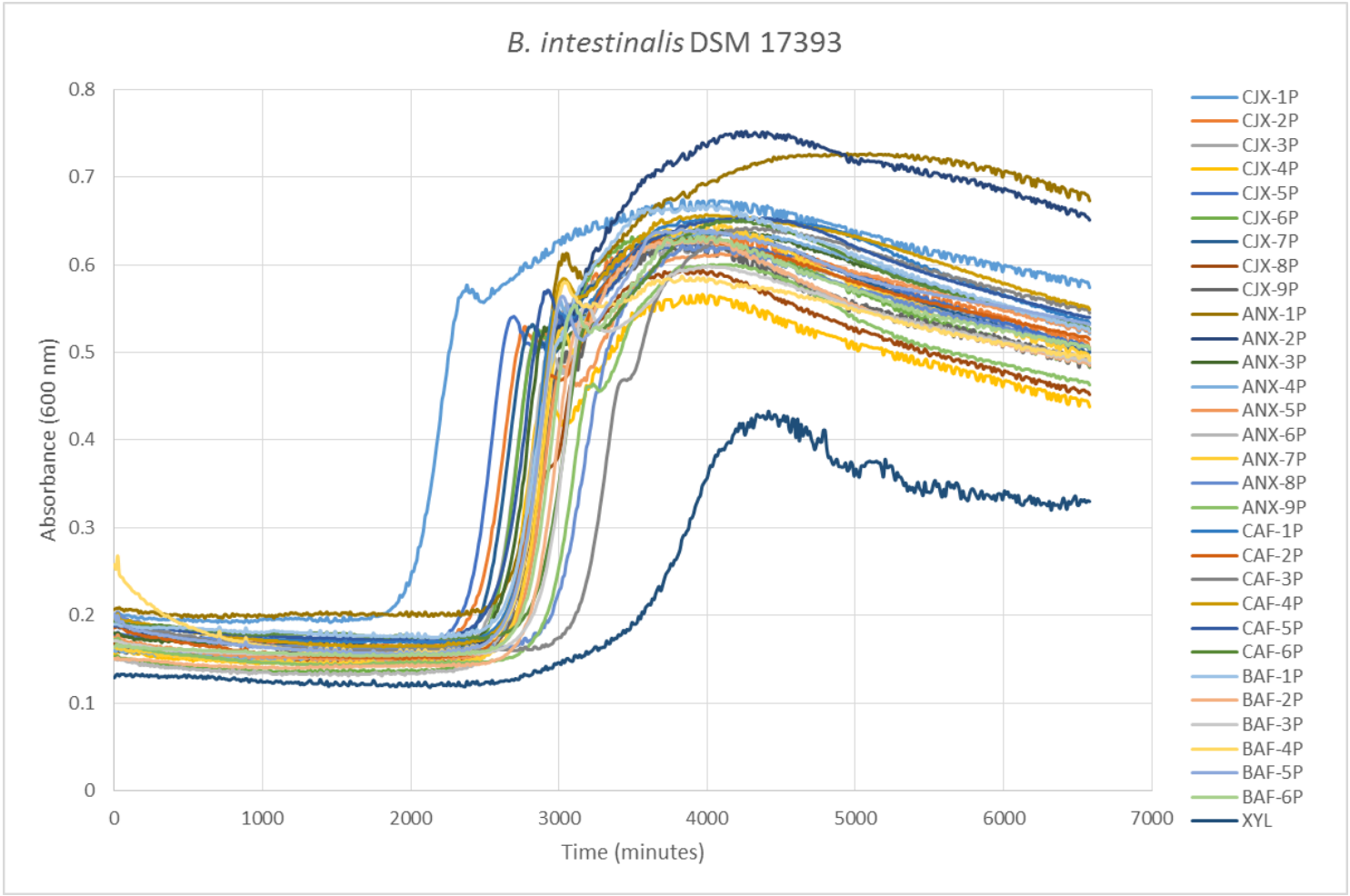

Figure 5.6. Growth curves of *B. intestinalis DSM 17393* on different arabinoxylan hydrolyzates and xylose. CJX-1P to BAF-6P: different AXH; XYL: xylose.

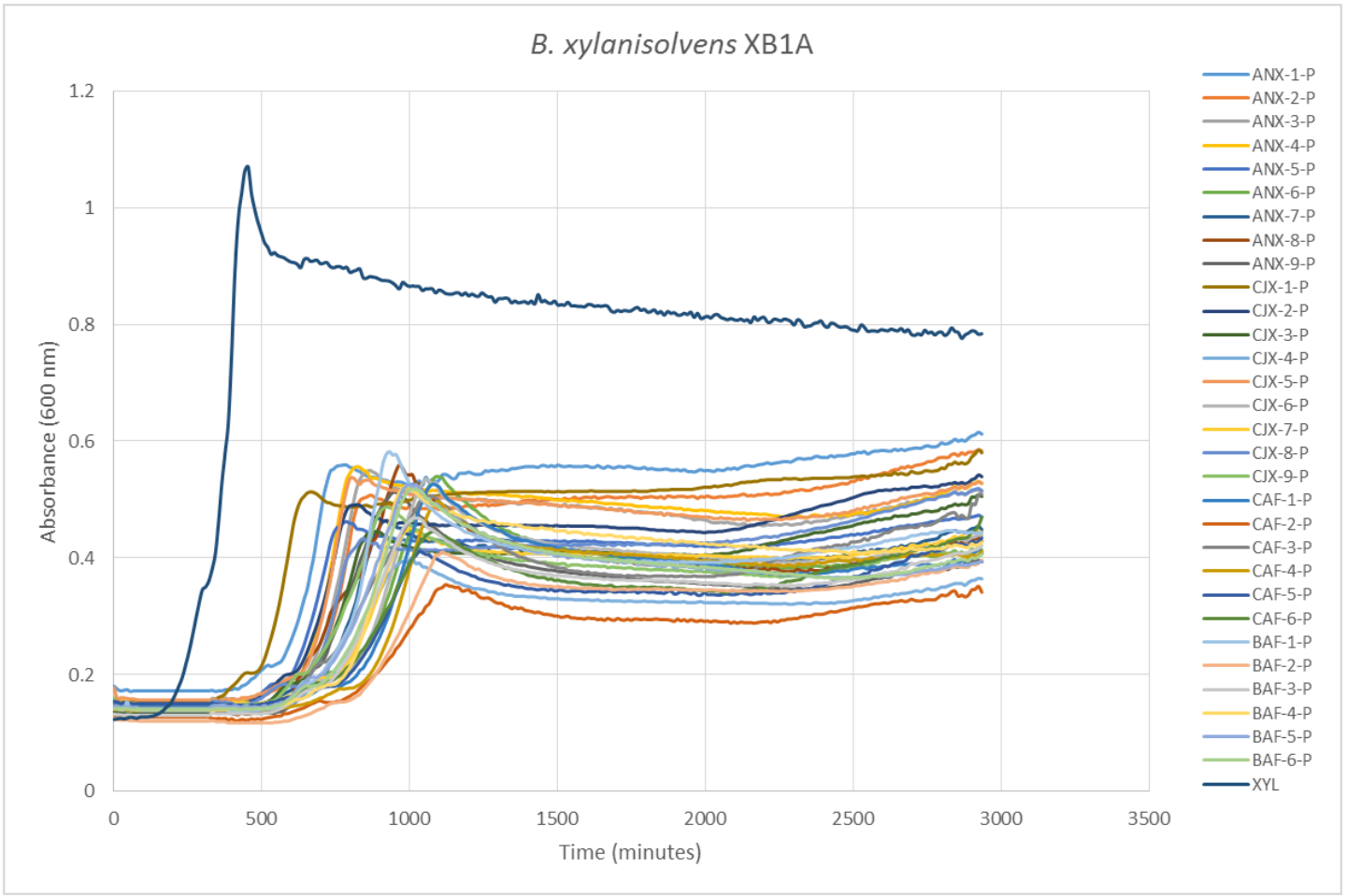

Figure 5.7. Growth curves of *B. xylanisolvens XB1A* on different arabinoxylan hydrolyzates and xylose. CJX-1P to BAF-6P: different AXH; XYL: xylose.

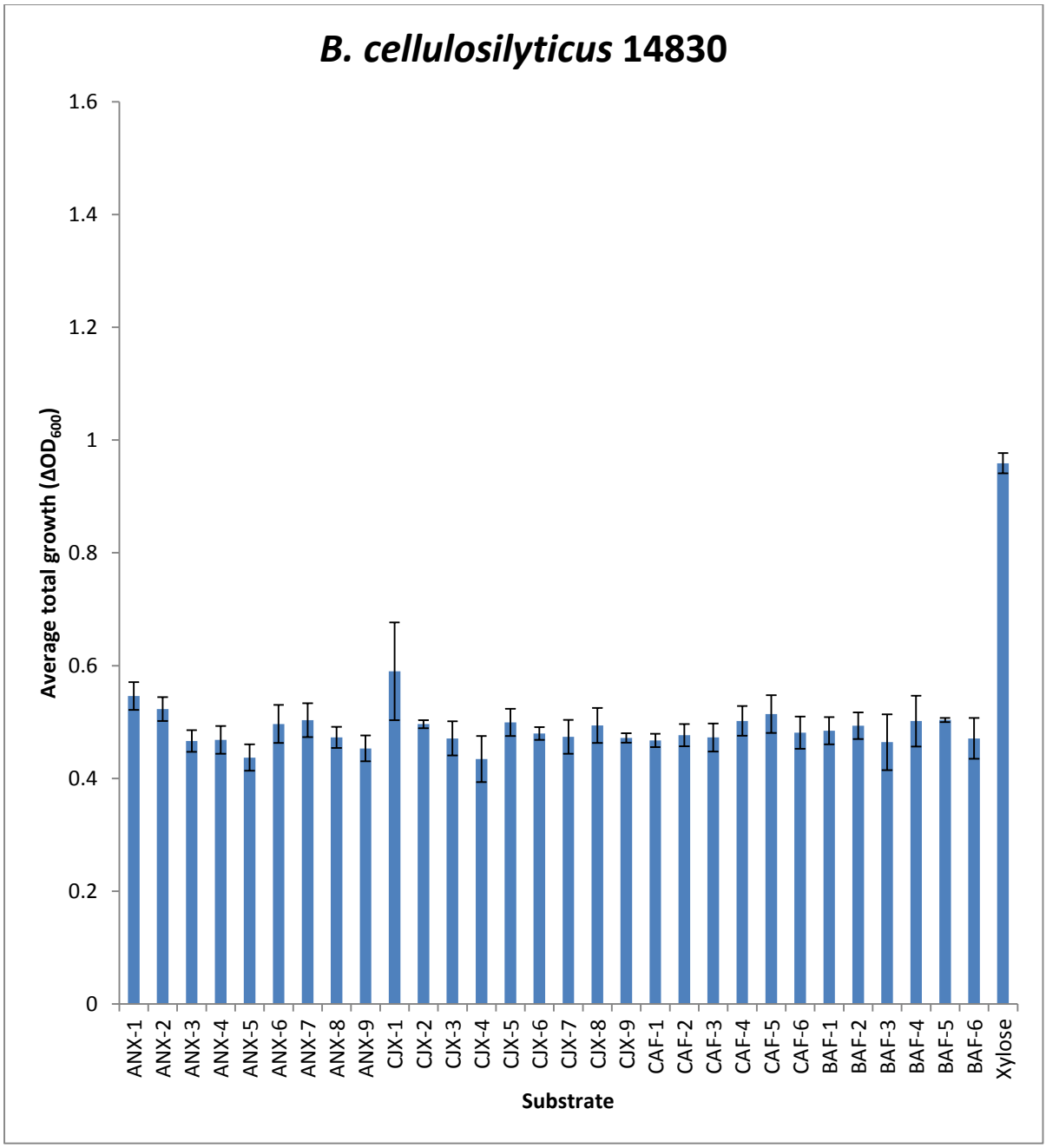

Figure 5.8. Average total growth of *B. cellulosilyticus* DSM 14830 on different arabinoxylan hydrolyzates (ANX-1 to BAF-6) and xylose.

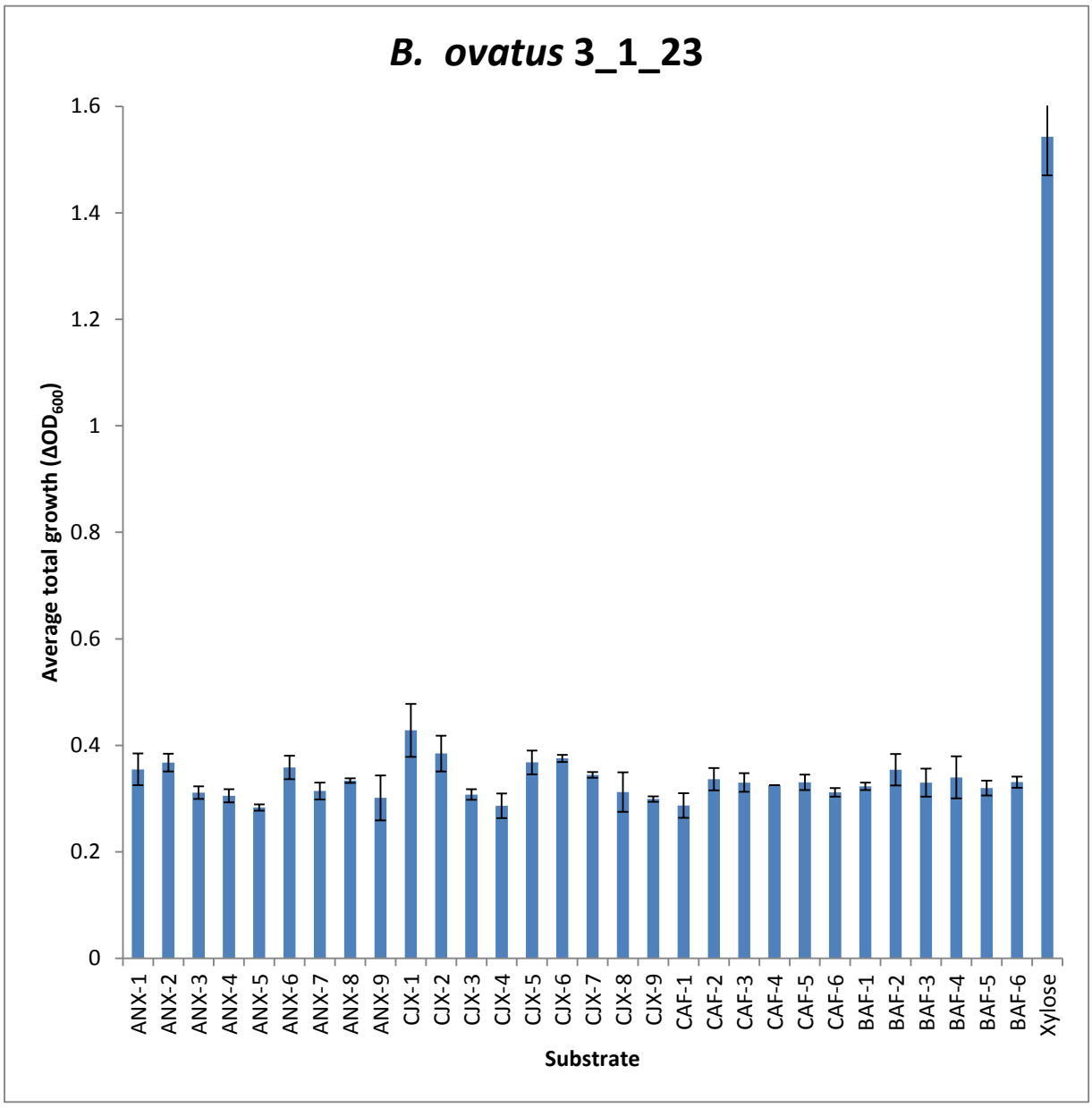

Figure 5.9. Average total growth of *B. ovatus* 3_1_23 on different arabinoxylan hydrolyzates (ANX-1 to BAF-6) and xylose.

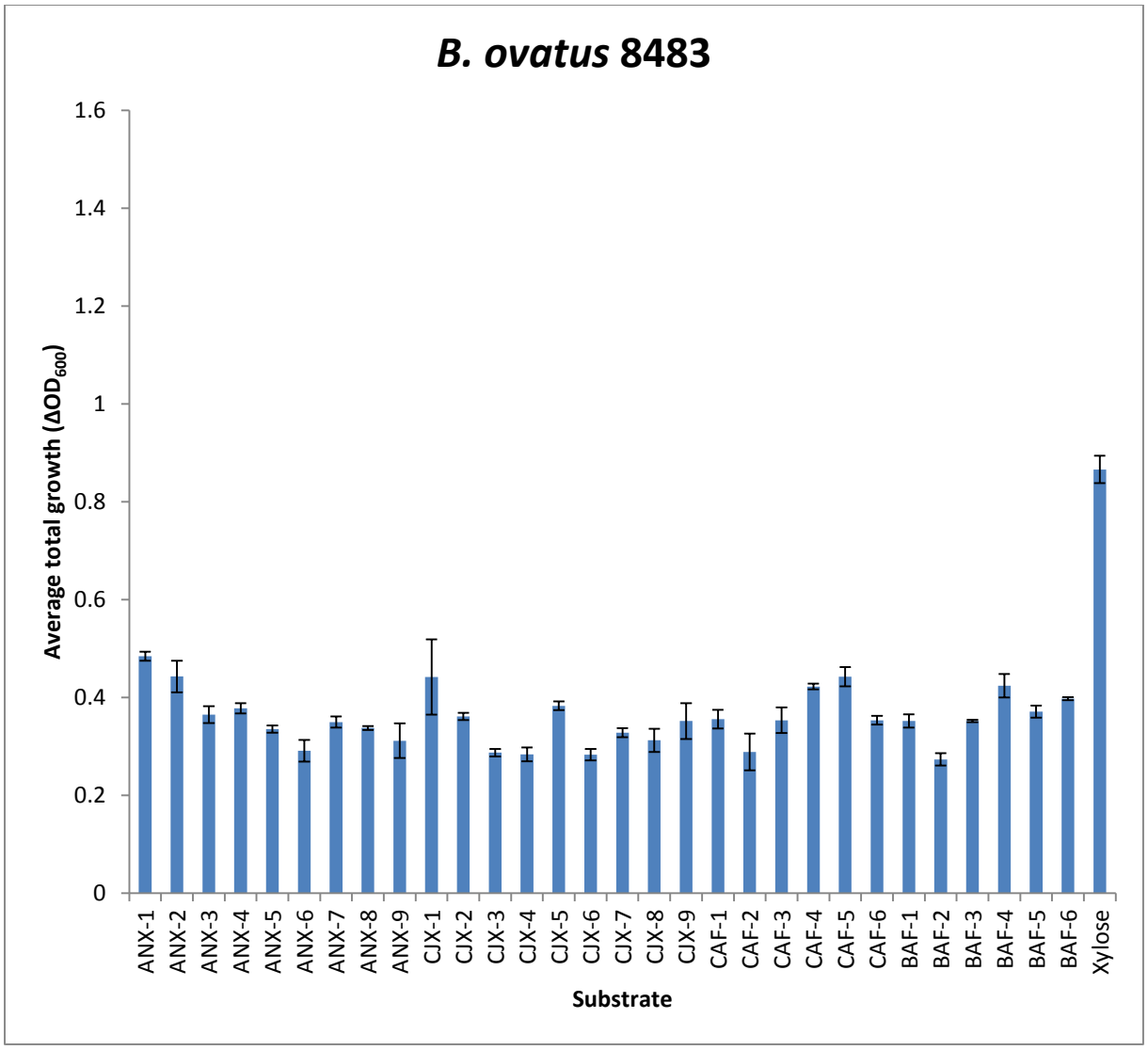

Figure 5.10. Average total growth of *B. ovatus* ATCC 8483 on different arabinoxylan hydrolyzates (ANX-1 to BAF-6) and xylose.

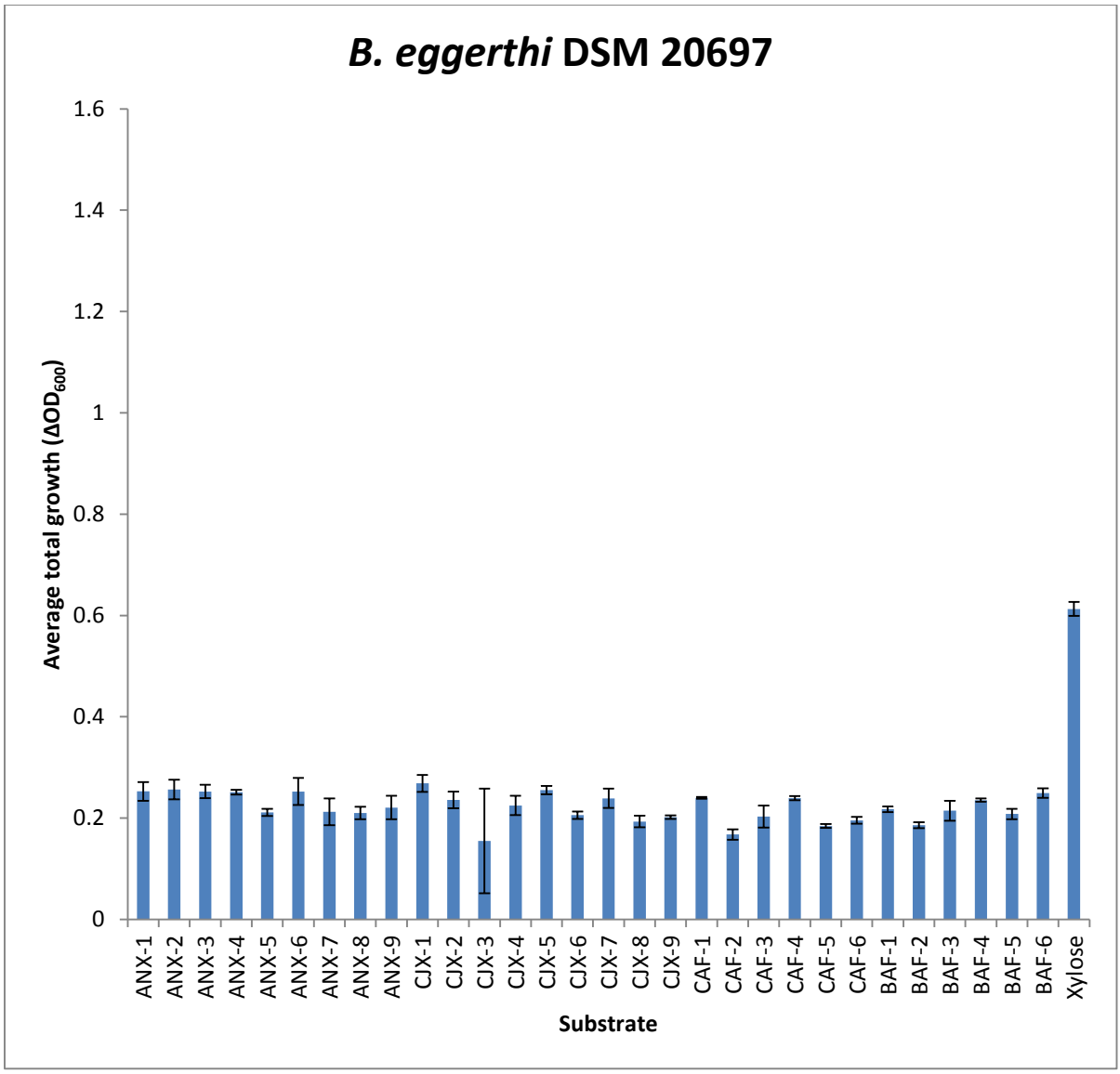

Figure 5.11. Average total growth of *B. eggerthii* DSM 20697 on different arabinoxylan hydrolyzates (ANX-1 to BAF-6) and xylose.

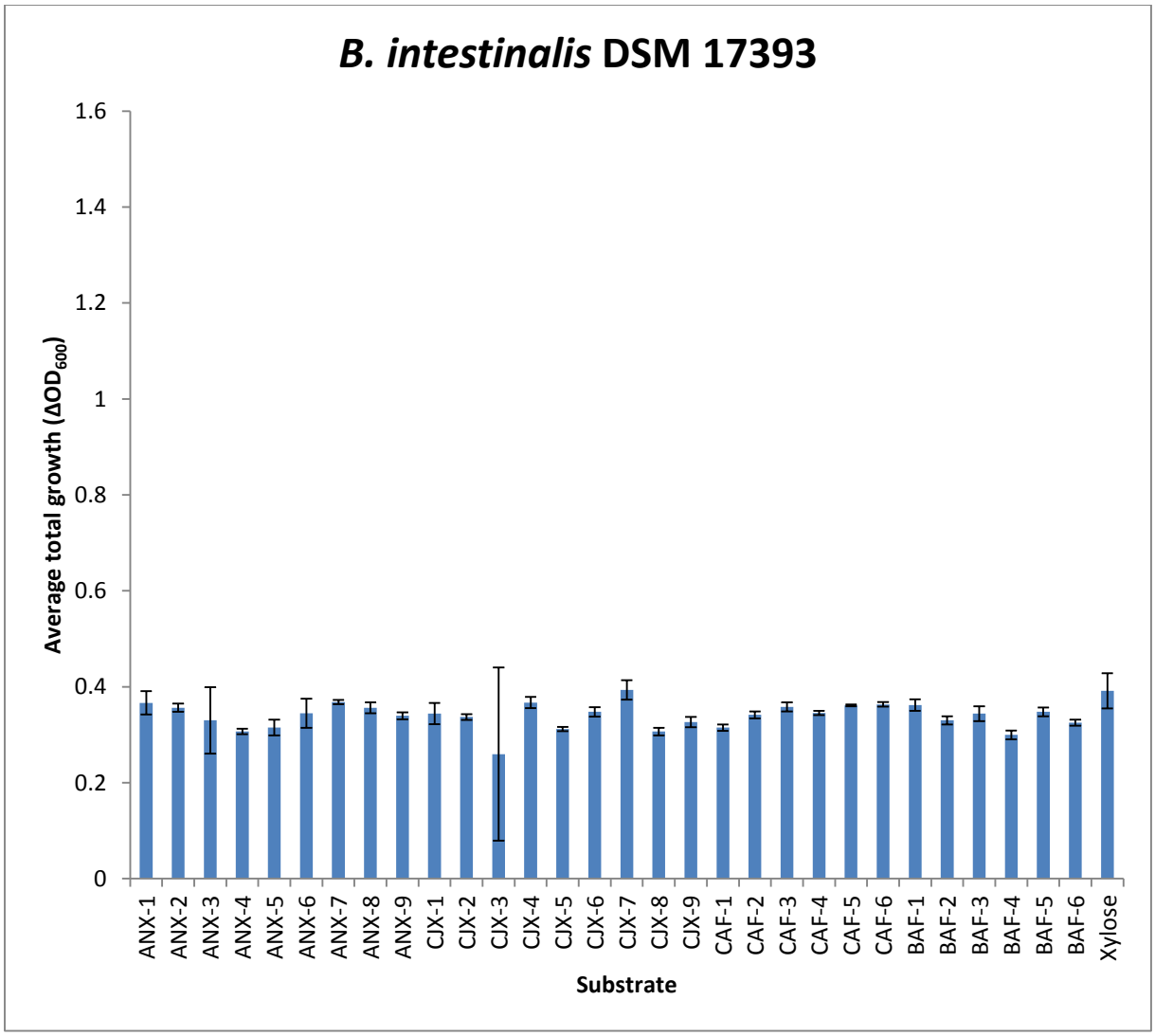

Figure 5.12. Average total growth of *B.intestinalis* DSM 17393 on different arabinoxylan hydrolyzates (ANX-1 to BAF-6) and xylose.

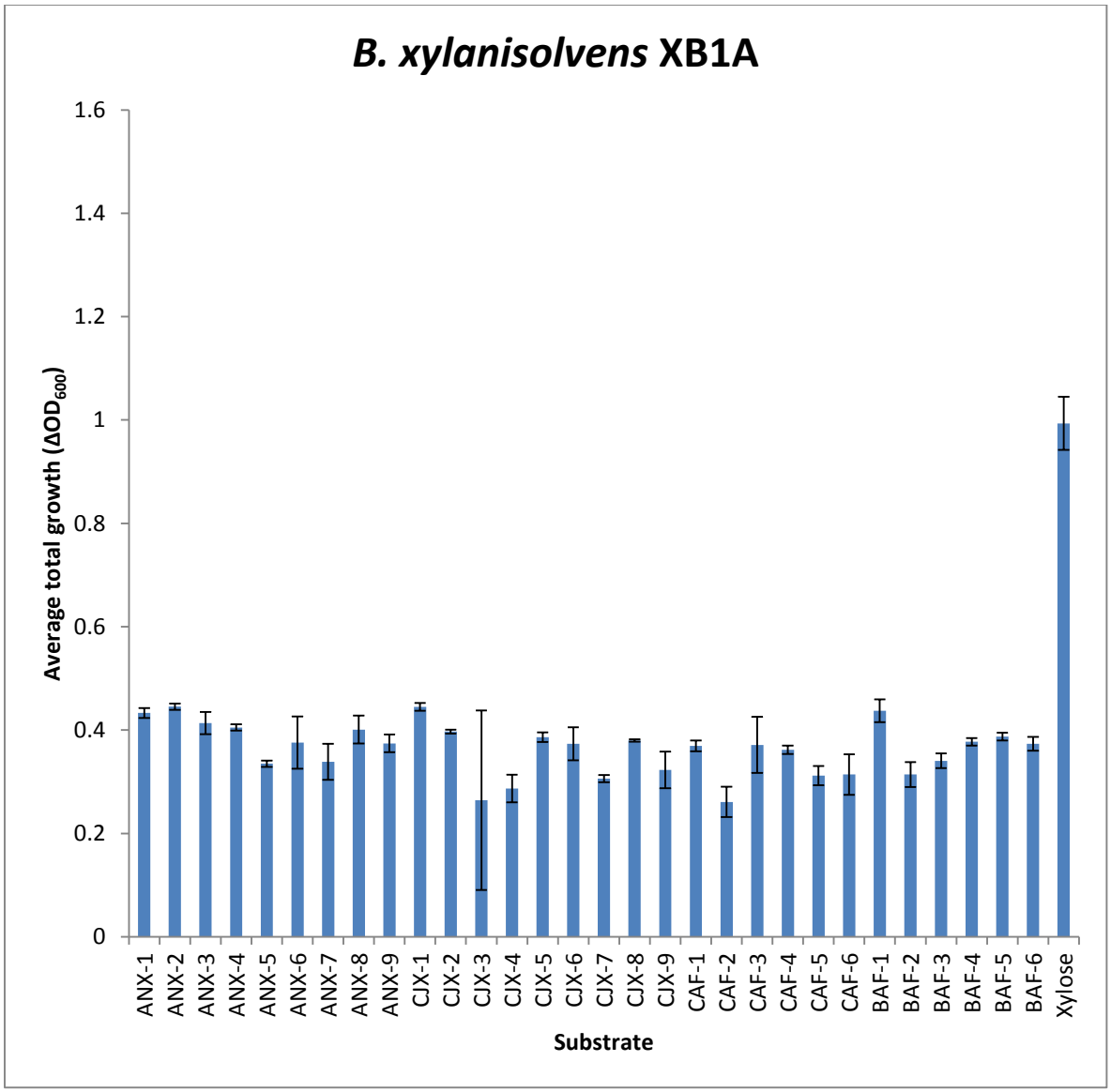

Figure 5.13. Average total growth of *B.xylanisolvens* XB1A on different arabinoxylan hydrolyzates (ANX-1 to BAF-6) and xylose.

The current study indicated that the Bacteroides species employed here were capable of fermenting a diverse array of structurally different wheat derived enzymatically tailored arabinoxylan hydrolyzates (AXH). *B. cellulosilyticus* DSM 14838 displayed the highest preference for wheat AXH while *B. eggerthii* DSM 20697 indicated the least preference for the wheat AXH. All the five strains except *B. eggerthii* DSM 20697 went through phase shifts during their growth on AXH. This suggests that these Bacteroides are capable of altering their

enzyme expression depending on the available substrate, grow at different rates on various regions of these complex molecules, or need to re-configure their cell envelope xylan foraging proteins to deal with variations in structures that are encountered during growth. Overall, the Bacteroides grew on all the AXH despite their structural differences. However, a general tendency to prefer less complex structures was observed for *B. cellulosilyticus* DSM 14838, *B. ovatus* ATCC 8483, *B. ovatus* 3-1-23 and *B. xylanisolvens* XB1A while *B. xylanisolvens* XB1A had a slight preference towards somewhat more complex AXH. The AXH, CJX-1 was a preferred substrate among most of the Bacteroides in this study. The work confirms the ability of Bacteroides to utilize structurally divers array of polysaccharides. The co-existence of these bacteria within the human intestinal tract could lead to maximum utilization of plant polysaccharides and in turn contribute to the many health benefits associated with plant polysaccharides.

5.6. Future Research

Although with some strains a strong structure function relationship was not obvious, it should not be considered as such right away. One reason for this could have been the narrow distribution range of some of the fine structural details among the AXH under investigation. Repeating the bacterial growth experiments employing AXH with much more obvious structural difference might give better insight into the structure function relationship between growth of Bacteroidetes on wheat AX.

The current research was carried out using wheat derived AX polysaccharides. However, an interesting directionality would be to investigate how the wheat derived oligosaccharides would affect the growth of Bacteroidetes.

Bifidobacteria and Lactobacillus are commonly studied probiotic microbes. The effect of AXH on these beneficial bacterial strains need to be evaluated in the future. Due to the readily available resources investigating the effect of different fibers on the growth of these bacteria, it would be beneficial to evaluate the effect of wheat derived AXH on their growth, which might indicate how effective wheat derived AXH are as prebiotics compared to the commonly used prebiotics.

Under normal physiological conditions, the colonic bacteria is under a dynamic system of diverse array of many different bacteria with many different hydrolysis capabilities. The degradation product of one species might be the preferred substrate for another bacteria. Thus, apart from the pure bacterial culture experiments, investigating the growth of combination of bacteria, may be using fecal cultures, or better yet, animal models would give better indication about the health benefits of structurally different AXH.

The health benefits of polysaccharide fibers are not mealy due to their ability to act as food sources for the beneficial microbiota in the gut. The fermentation products of these microbiota, the microbiota it self and the polysaccharides are individually and collectively exerting effects on the intestinal epithelium acting as food sources to the enterocytes or inducing immunological outcomes. Future research exploring the collective effect of fiber and bacteria on the immune function of the gut is much encouraged.

5.7. References

Bamias, G., Nyce, M. R., De La Rue, S. A., and Cominelli, F. (2005). New concepts in the pathophysiology of inflammatory bowel disease. *Ann Intern Med* **143**, 895-904.

Bjorksten, B. (1999). The environmental influence on childhood asthma. *Allergy* **54 Suppl 49**, 17-23.

Cani, P. D., Everard, A., and Duparc, T. (2013). Gut microbiota, enteroendocrine functions and metabolism. *Current Opinion in Pharmacology* **13**, 935-940.

Dodd, D., Mackie, R. I., and Cann, I. K. (2011). Xylan degradation, a metabolic property shared by rumen and human colonic Bacteroidetes. *Molecular microbiology* **79**, 292-304.

Kaoutari, A. E., Armougom, F., Gordon, J. I., Raoult, D., and Henrissat, B. (2013). The abundance and variety of carbohydrate-active enzymes in the human gut microbiota. *Nat Rev Micro* **11**, 497-504.

Kaser, A., Zeissig, S., and Blumberg, R. S. (2010). Inflammatory Bowel Disease. *Annual Review of Immunology* **28**, 573-621.

Koropatkin, N. M., Cameron, E. A., and Martens, E. C. (2012). How glycan metabolism shapes the human gut microbiota. *Nature Reviews Microbiology* **10**, 323-335.

Ley, R. E., Bäckhed, F., Turnbaugh, P., Lozupone, C. A., Knight, R. D., and Gordon, J. I. (2005). Obesity alters gut microbial ecology. *Proceedings of the National Academy of Sciences of the United States of America* **102**, 11070-11075.

Ley, R. E., Turnbaugh, P. J., Klein, S., and Gordon, J. I. (2006). Microbial ecology: Human gut microbes associated with obesity. *Nature* **444**, 1022-1023.

Li, Q., Wang, C., Tang, C., Li, N., and Li, J. (2012). Molecular-phylogenetic characterization of the microbiota in ulcerated and non-ulcerated regions in the patients with Crohn's disease. *PloS one* **7**, e34939.

Martens, E. C., Koropatkin, N. M., Smith, T. J., and Gordon, J. I. (2009). Complex Glycan Catabolism by the Human Gut Microbiota: The Bacteroidetes Sus-like Paradigm. *Journal of Biological Chemistry* **284**, 24673-24677.

Martens, E. C., Lowe, E. C., Chiang, H., Pudlo, N. A., Wu, M., McNulty, N. P., Abbott, D. W., Henrissat, B., Gilbert, H. J., Bolam, D. N., and Gordon, J. I. (2011). Recognition and Degradation of Plant Cell Wall Polysaccharides by Two Human Gut Symbionts. *PLoS Biol* **9**, e1001221.

Mazmanian, S. K., Round, J. L., and Kasper, D. L. (2008). A microbial symbiosis factor prevents intestinal inflammatory disease. *Nature* **453**, 620-625.

McNulty, N. P., Wu, M., Erickson, A. R., Pan, C., Erickson, B. K., Martens, E. C., Pudlo, N. A., Muegge, B. D., Henrissat, B., and Hettich, R. L. (2013). Effects of diet on resource utilization by a model human gut microbiota containing Bacteroides cellulosilyticus WH2, a symbiont with an extensive glycobiome. *PLoS biology* **11**, e1001637.

Robert, C., Chassard, C., Lawson, P. A., and Bernalier-Donadille, A. (2007). Bacteroides cellulosilyticus sp. nov., a cellulolytic bacterium from the human gut microbial community. *Int J Syst Evol Microbiol* **57**, 1516-20.

Rose, D. J., Patterson, J. A., and Hamaker, B. R. (2010). Structural differences among alkali-soluble arabinoxylans from maize (Zea mays), rice (Oryza sativa), and wheat (Triticum aestivum) brans influence human fecal fermentation profiles. *Journal of Agricultural and Food Chemistry* **58**, 493-499.

Round, J. L., and Mazmanian, S. K. (2009). The gut microbiota shapes intestinal immune responses during health and disease. *Nat Rev Immunol* **9**, 313-323.

Salyers, A. A., Gherardini, F., and O'Brien, M. (1981). Utilization of xylan by two species of human colonic Bacteroides. *Appl Environ Microbiol* **41**, 1065-8.

Salyers, A. A., Vercellotti, J. R., West, S. E., and Wilkins, T. D. (1977). Fermentation of mucin and plant polysaccharides by strains of Bacteroides from the human colon. *Appl Environ Microbiol* **33**, 319-22.

Tremaroli, V., and Backhed, F. (2012). Functional interactions between the gut microbiota and host metabolism. *Nature* **489**, 242-249.

Walter, J., and Ley, R. (2011). The Human Gut Microbiome: Ecology and Recent Evolutionary Changes. *In* "Annual Review of Microbiology", Vol. 65, pp. 411-429. Annual Reviews.

Wardwell, L. H., Huttenhower, C., and Garrett, W. S. (2011). Current concepts of the intestinal microbiota and the pathogenesis of infection. *Current infectious disease reports* **13**, 28-34.

Xu, H. (2012). Influence of the structural complexicity of cereal arabinoxylans on human fecal fermentation and their degradation mechanism by gut bacteria. Dissertation, Purdue University, Indiana.

Zhang, M., Chekan, J. R., Dodd, D., Hong, P. Y., Radlinski, L., Revindran, V., Nair, S. K., Mackie, R. I., and Cann, I. (2014). Xylan utilization in human gut commensal bacteria is orchestrated by unique modular organization of polysaccharide-degrading enzymes. *Proceedings of the National Academy of Sciences* **111**, E3708-E3717.

APPENDIX A. SUPERIMPOSED CHROMATOGRAMS OF REFRACTIVE INDEX (RI) AND LIGHT SCATTERING DETECTOR OUTPUTS FOR AXH: (A) ANX-2, (B) CJX-2, (C) CAF-2 AND (D) BAF-2

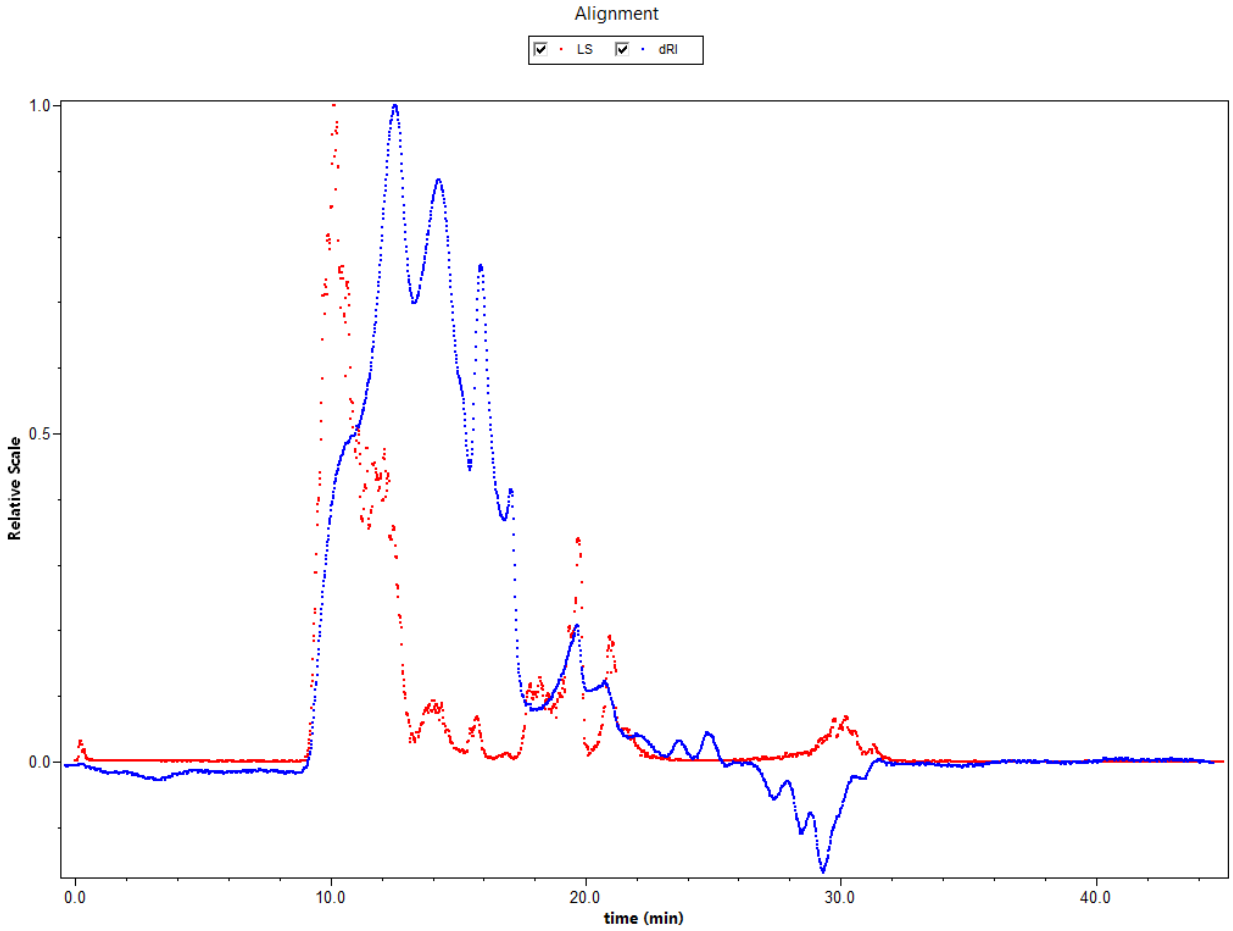

(a)

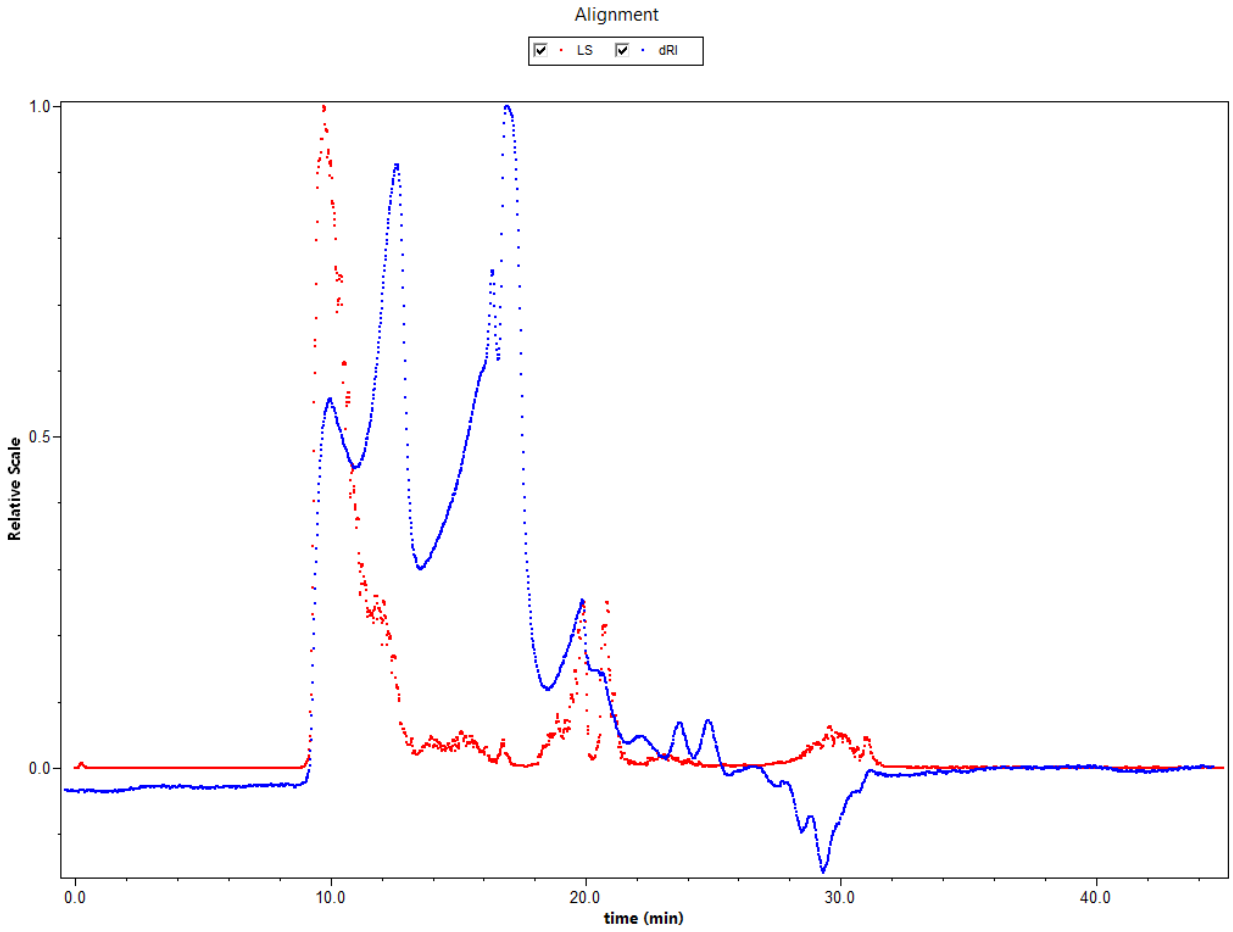
Alignment
LS
dRI
1.0
0.5
0.0
Relative Scale
0.0
10.0
20.0
30.0
40.0
time (min)

(b)

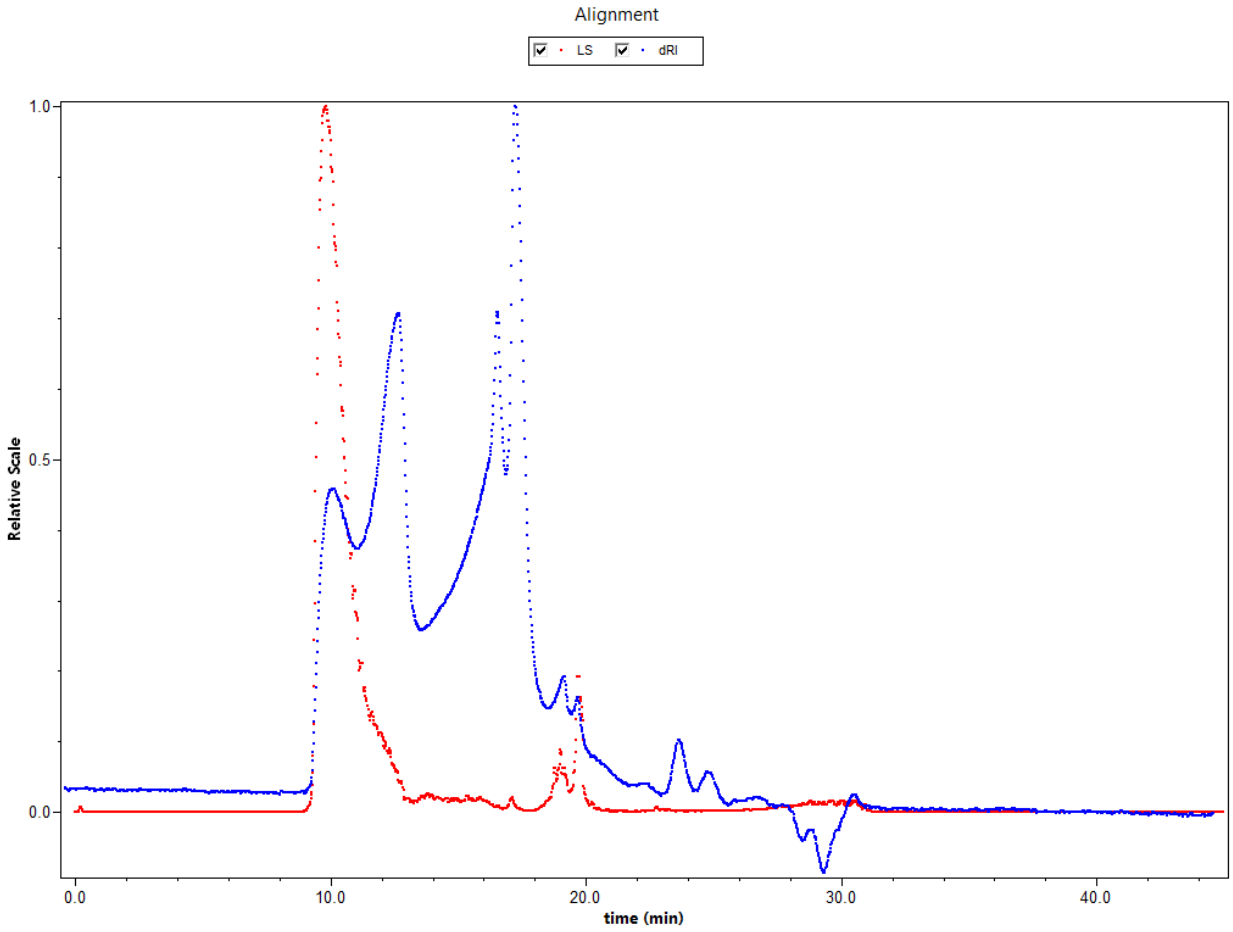
Alignment
LS
dRI
1.0
0.5
0.0
Relative Scale
0.0
10.0
20.0
30.0
40.0
time (min)

(c)

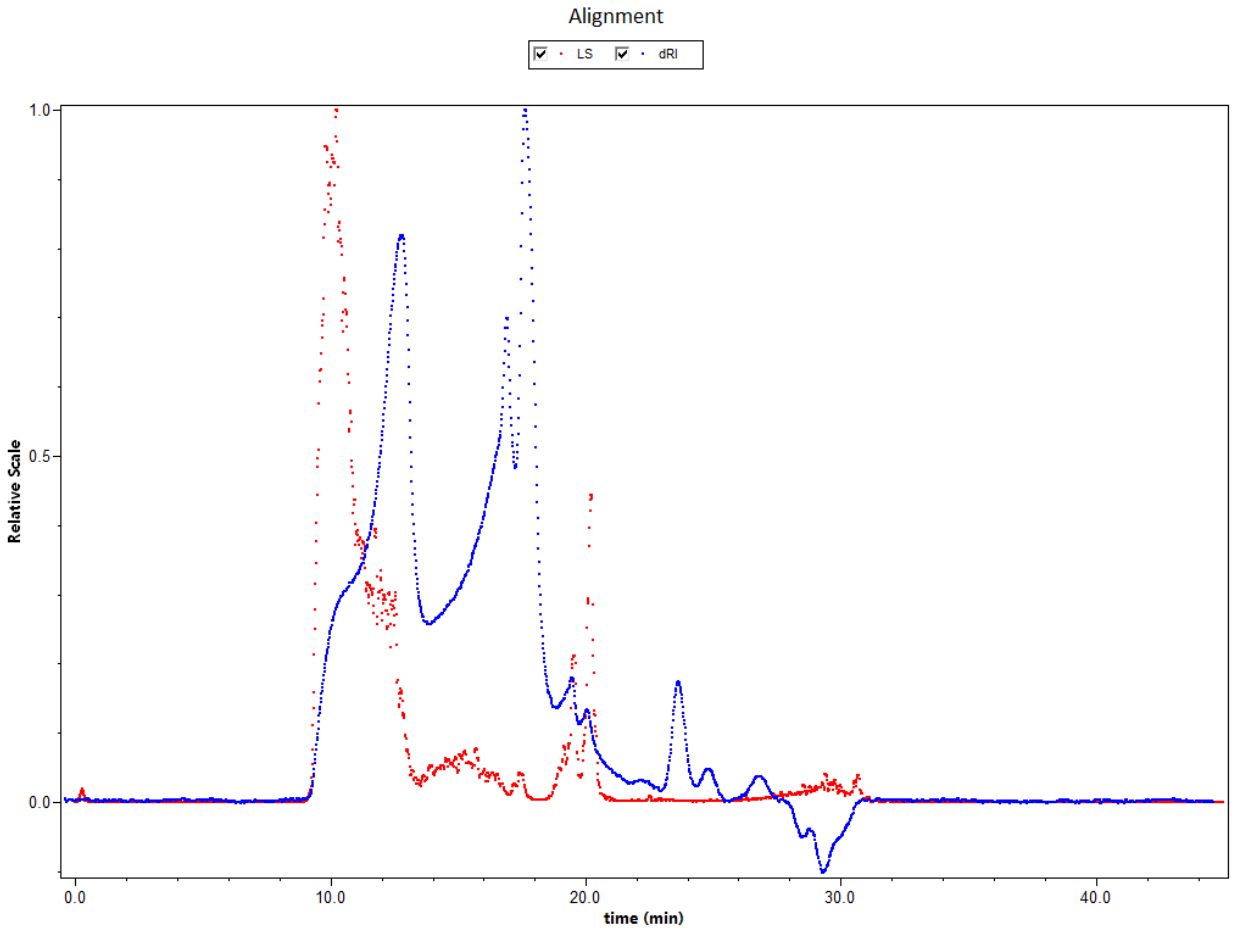
Alignment
LS
dRI
1.0
0.5
0.0
Relative Scale
0.0
10.0
20.0
30.0
40.0
time (min)

(d)

APPENDIX B. THE TOTAL ION CHROMATOGRAM (TIC) AND THE MASS SPECTRUM OF THE CORRESPONDING PEAK IN THE TIC FOR ARABINOXYLAN

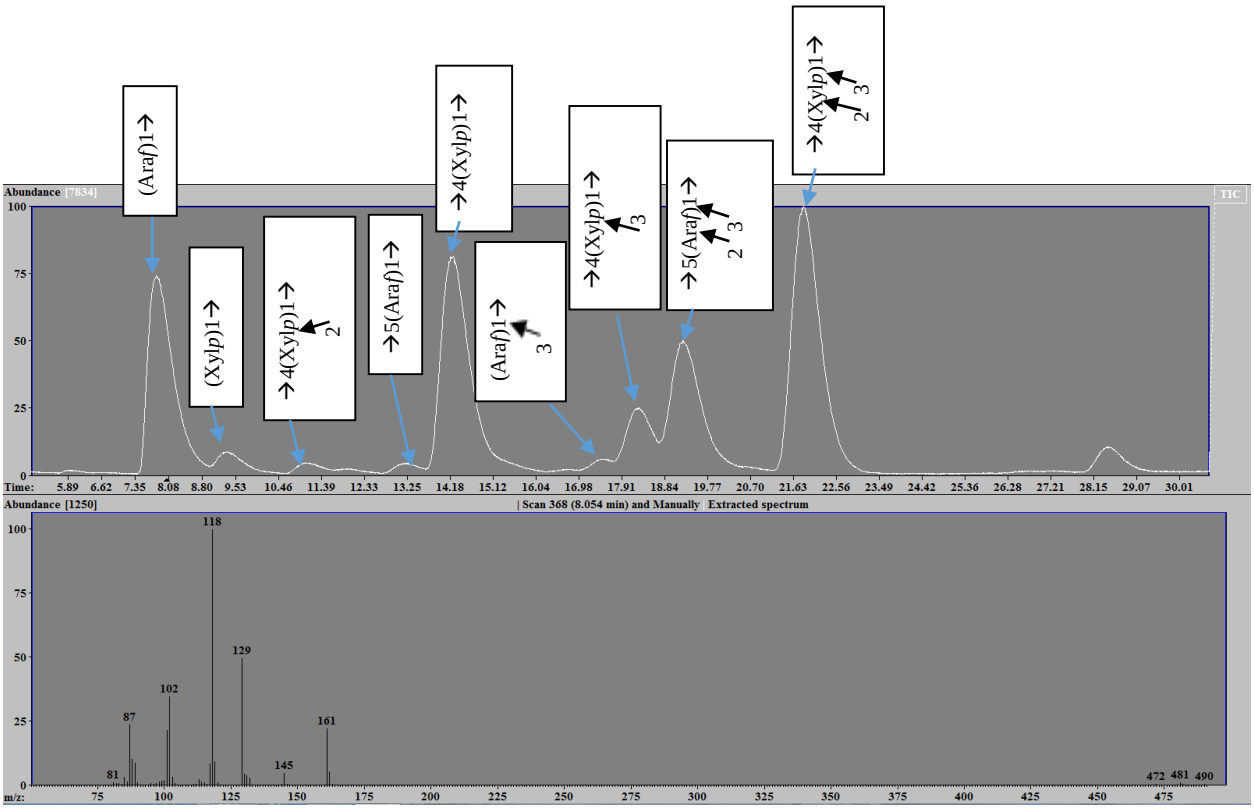

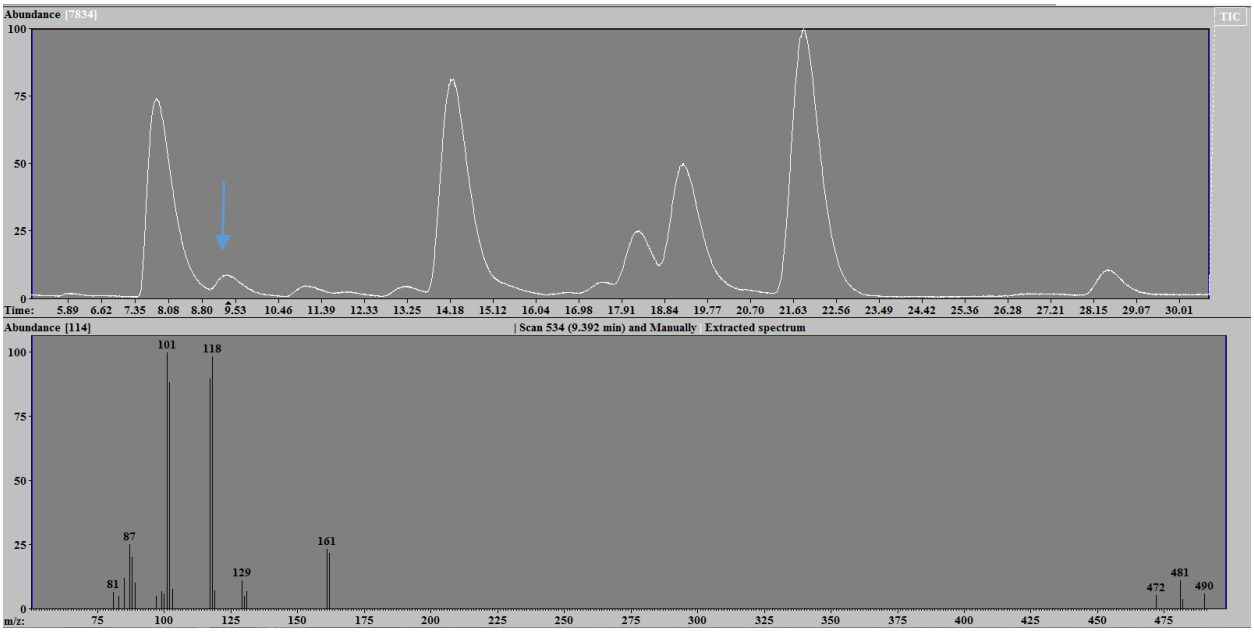
Abundance [7834]
TIC
Time: 5.89 6.62 7.35 8.08 8.80 9.53 10.46 11.39 12.33 13.25 14.18 15.12 16.04 16.98 17.91 18.84 19.77 20.70 21.63 22.56 23.49 24.42 25.36 26.28 27.21 28.15 29.07 30.01
Abundance [114]
| Scan 534 (9.392 min) and Manually Extracted spectrum
101
118
87
161
129
81
481
472
490
m/z: 75 100 125 150 175 200 225 250 275 300 325 350 375 400 425 450 475

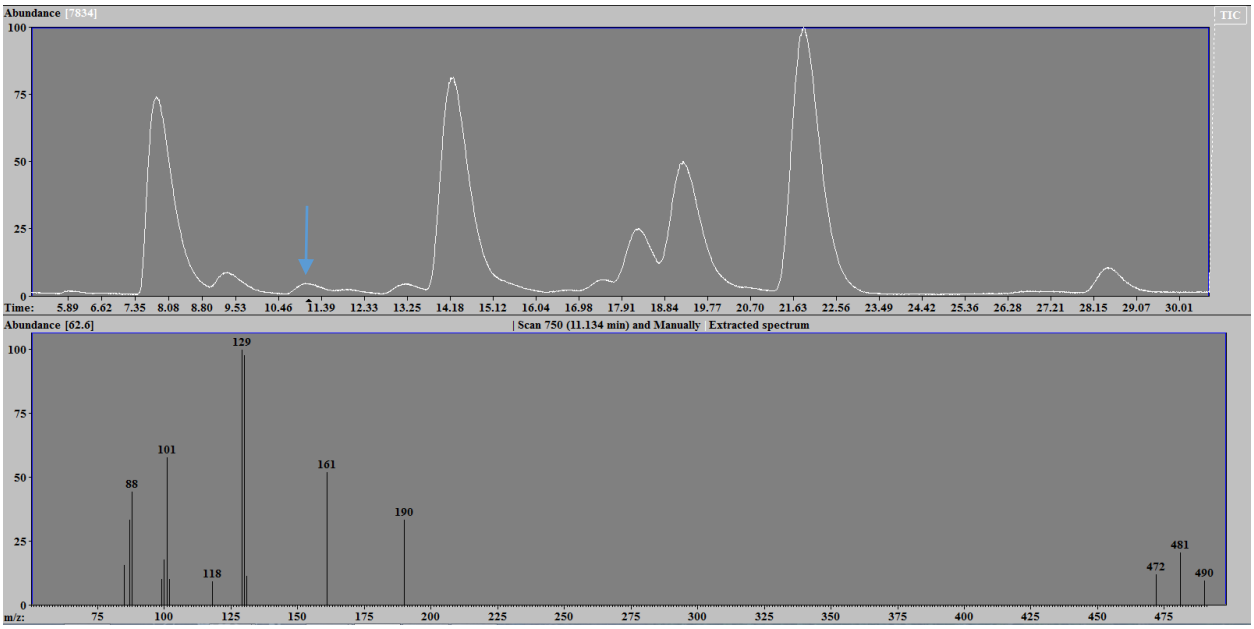
Abundance [7834]
TIC
Time: 5.89 6.62 7.35 8.08 8.80 9.53 10.46 11.39 12.33 13.25 14.18 15.12 16.04 16.98 17.91 18.84 19.77 20.70 21.63 22.56 23.49 24.42 25.36 26.28 27.21 28.15 29.07 30.01
Abundance [62.6]
| Scan 750 (11.134 min) and Manually Extracted spectrum
129
101
161
88
190
118
481
472
490
m/z: 75 100 125 150 175 200 225 250 275 300 325 350 375 400 425 450 475

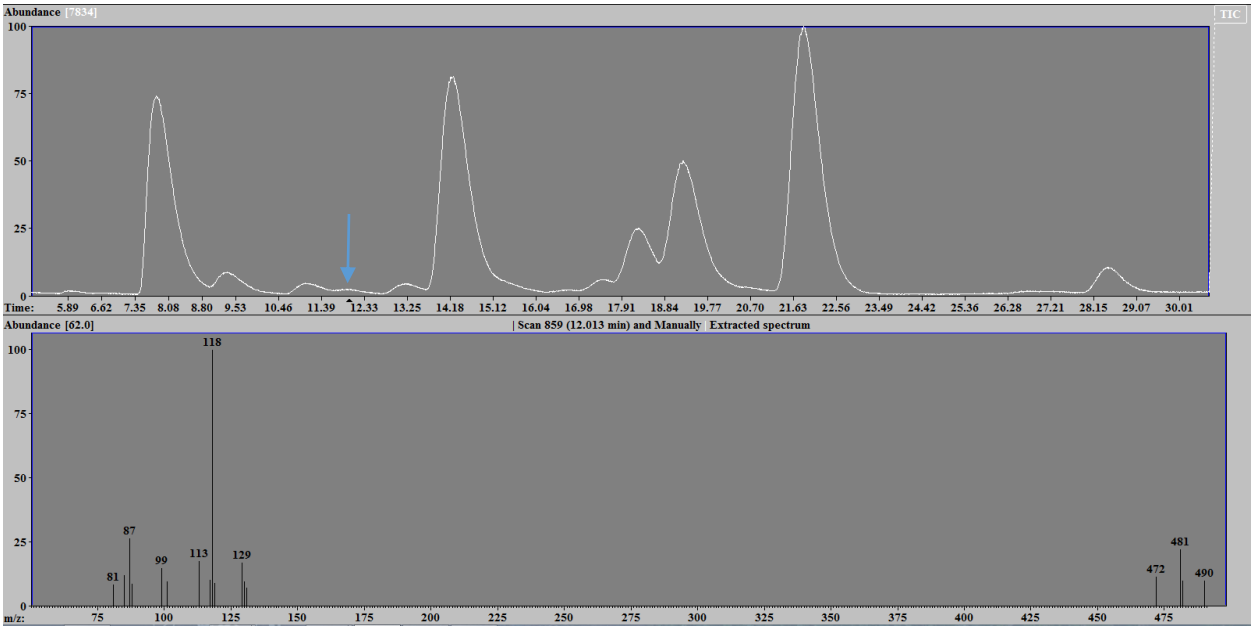
Abundance [7834]
TIC
Time: 5.89 6.62 7.35 8.08 8.80 9.53 10.46 11.39 12.33 13.25 14.18 15.12 16.04 16.98 17.91 18.84 19.77 20.70 21.63 22.56 23.49 24.42 25.36 26.28 27.21 28.15 29.07 30.01
Abundance [62.0]
| Scan 859 (12.013 min) and Manually Extracted spectrum
118
87
99
113
129
81
481
472
490
m/z: 75 100 125 150 175 200 225 250 275 300 325 350 375 400 425 450 475

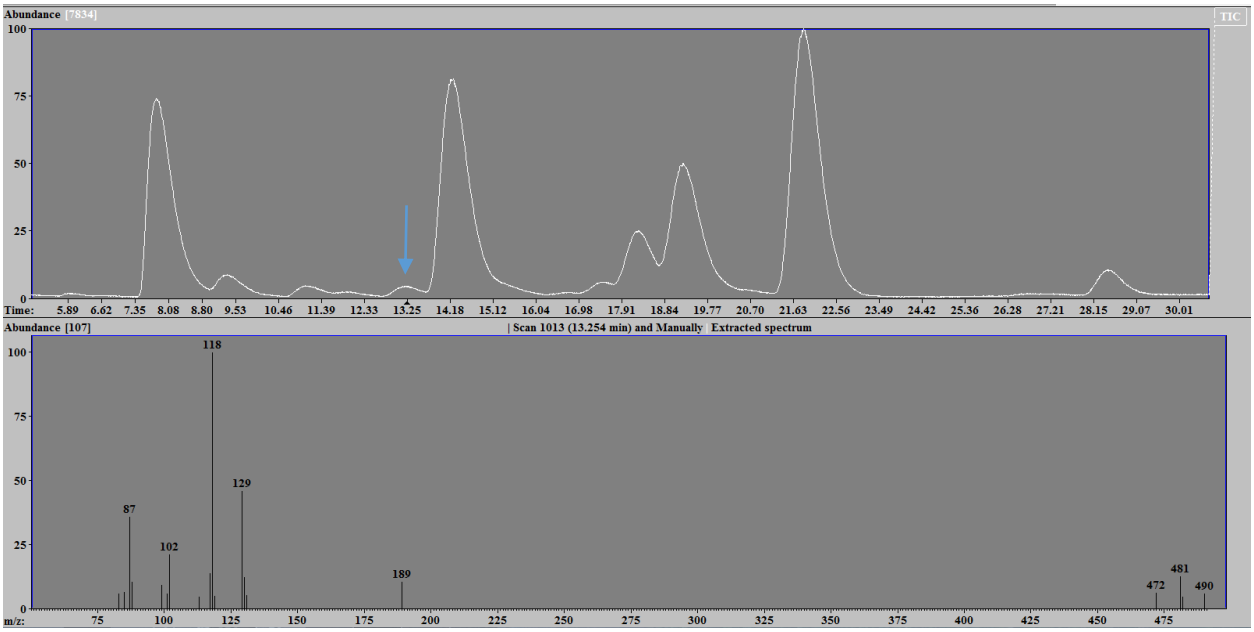
Abundance [7834]
TIC
Time: 5.89 6.62 7.35 8.08 8.80 9.53 10.46 11.39 12.33 13.25 14.18 15.12 16.04 16.98 17.91 18.84 19.77 20.70 21.63 22.56 23.49 24.42 25.36 26.28 27.21 28.15 29.07 30.01
Abundance [107]
| Scan 1013 (13.254 min) and Manually Extracted spectrum
118
129
87
102
189
481
472
490
m/z: 75 100 125 150 175 200 225 250 275 300 325 350 375 400 425 450 475

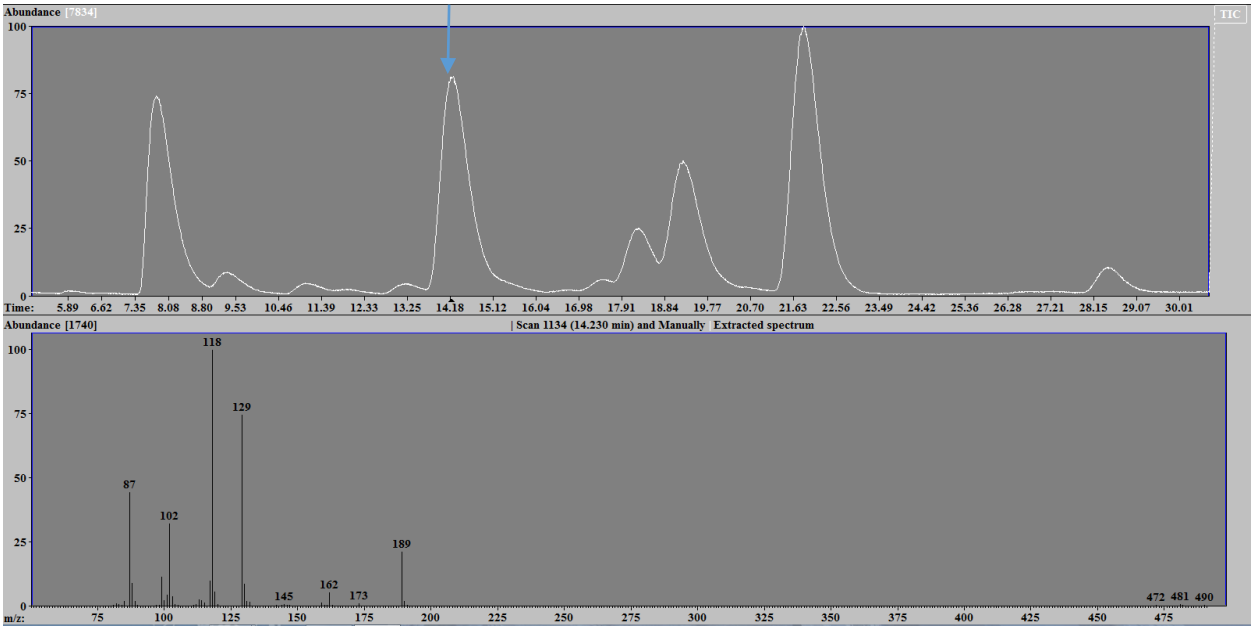
Abundance [7834]
TIC
Time: 5.89 6.62 7.35 8.08 8.80 9.53 10.46 11.39 12.33 13.25 14.18 15.12 16.04 16.98 17.91 18.84 19.77 20.70 21.63 22.56 23.49 24.42 25.36 26.28 27.21 28.15 29.07 30.01
Abundance [1740]
| Scan 1134 (14.230 min) and Manually Extracted spectrum
118
129
87
102
189
145
162
173
472 481 490
m/z: 75 100 125 150 175 200 225 250 275 300 325 350 375 400 425 450 475

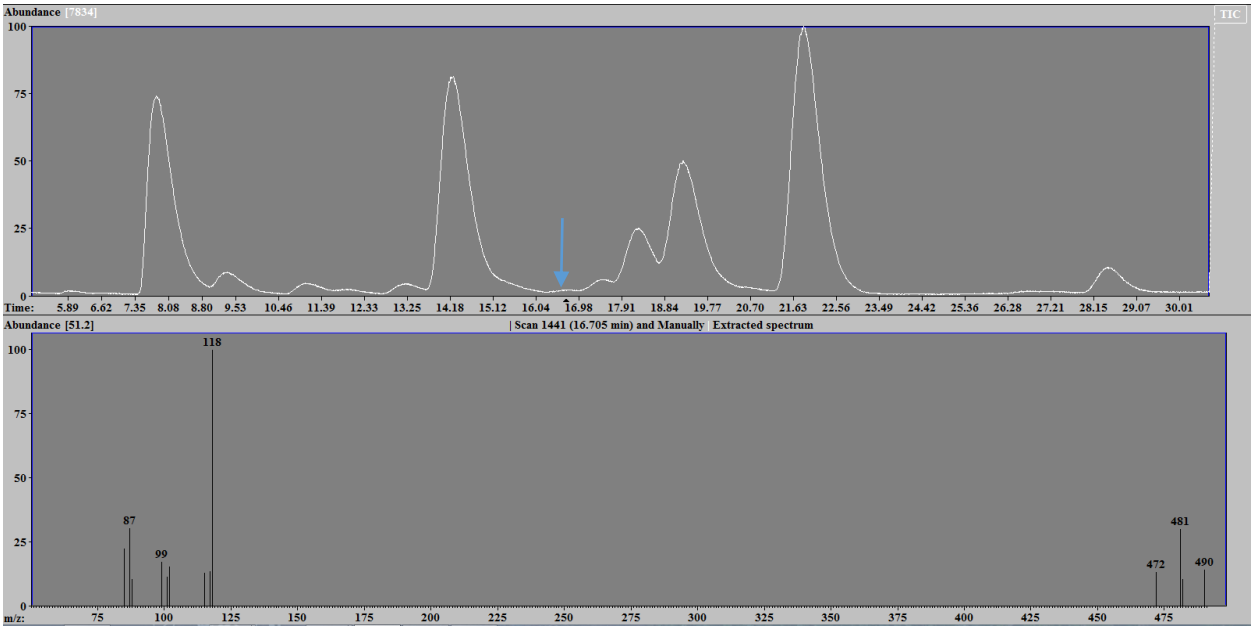
Abundance [7834]
TIC
Time: 5.89 6.62 7.35 8.08 8.80 9.53 10.46 11.39 12.33 13.25 14.18 15.12 16.04 16.98 17.91 18.84 19.77 20.70 21.63 22.56 23.49 24.42 25.36 26.28 27.21 28.15 29.07 30.01
Abundance [51.2]
| Scan 1441 (16.705 min) and Manually Extracted spectrum
118
87
99
481
472
490
m/z: 75 100 125 150 175 200 225 250 275 300 325 350 375 400 425 450 475

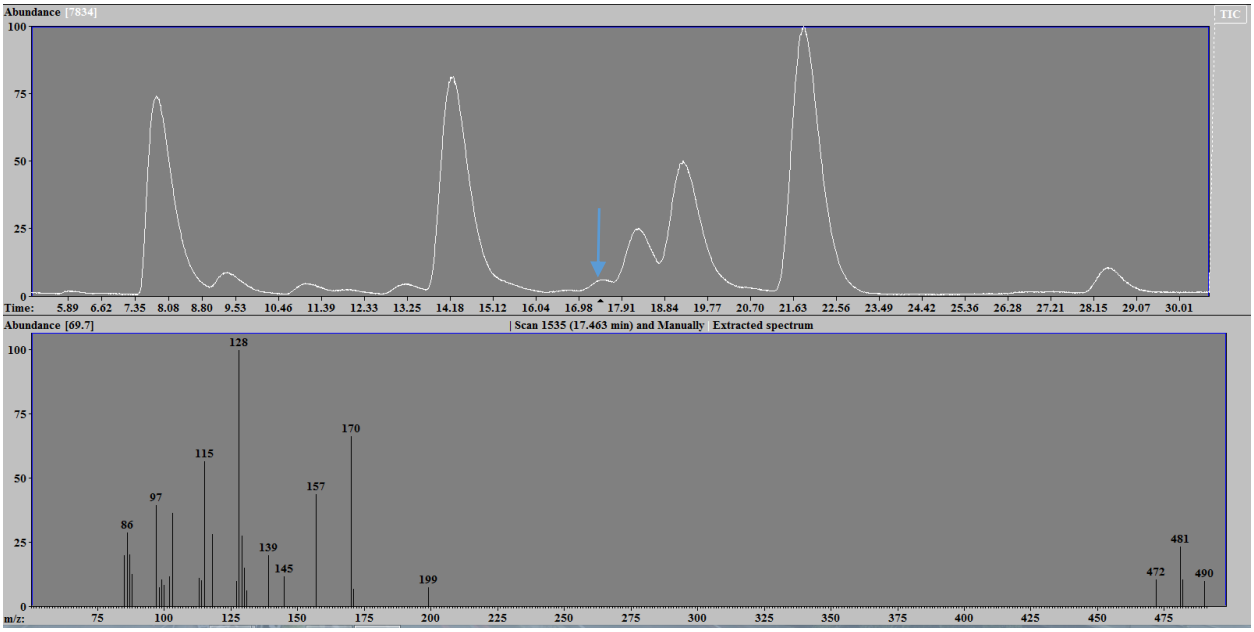
Abundance [7834]
TIC
Time: 5.89 6.62 7.35 8.08 8.80 9.53 10.46 11.39 12.33 13.25 14.18 15.12 16.04 16.98 17.91 18.84 19.77 20.70 21.63 22.56 23.49 24.42 25.36 26.28 27.21 28.15 29.07 30.01
Abundance [69.7]
| Scan 1535 (17.463 min) and Manually Extracted spectrum
128
115
170
97
157
86
139
145
199
481
472
490
m/z: 75 100 125 150 175 200 225 250 275 300 325 350 375 400 425 450 475

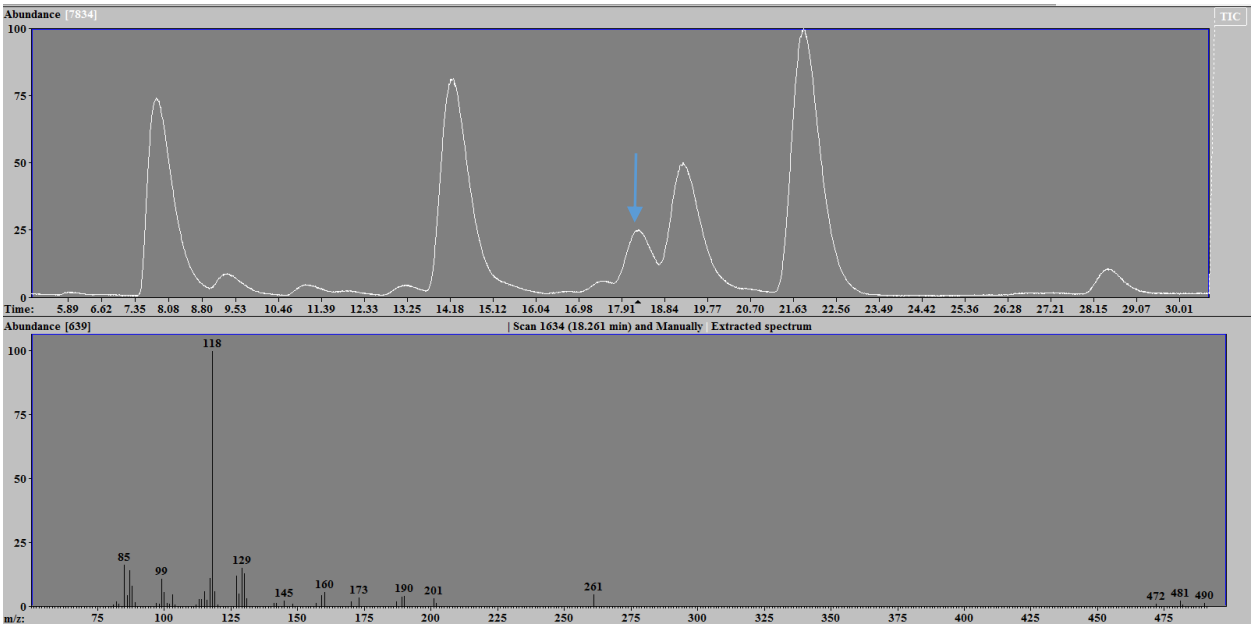
Abundance [7834]
TIC
Time: 5.89 6.62 7.35 8.08 8.80 9.53 10.46 11.39 12.33 13.25 14.18 15.12 16.04 16.98 17.91 18.84 19.77 20.70 21.63 22.56 23.49 24.42 25.36 26.28 27.21 28.15 29.07 30.01
Abundance [639]
| Scan 1634 (18.261 min) and Manually Extracted spectrum
118
85
99
129
145
160
173
190
201
261
472
481
490
m/z: 75 100 125 150 175 200 225 250 275 300 325 350 375 400 425 450 475

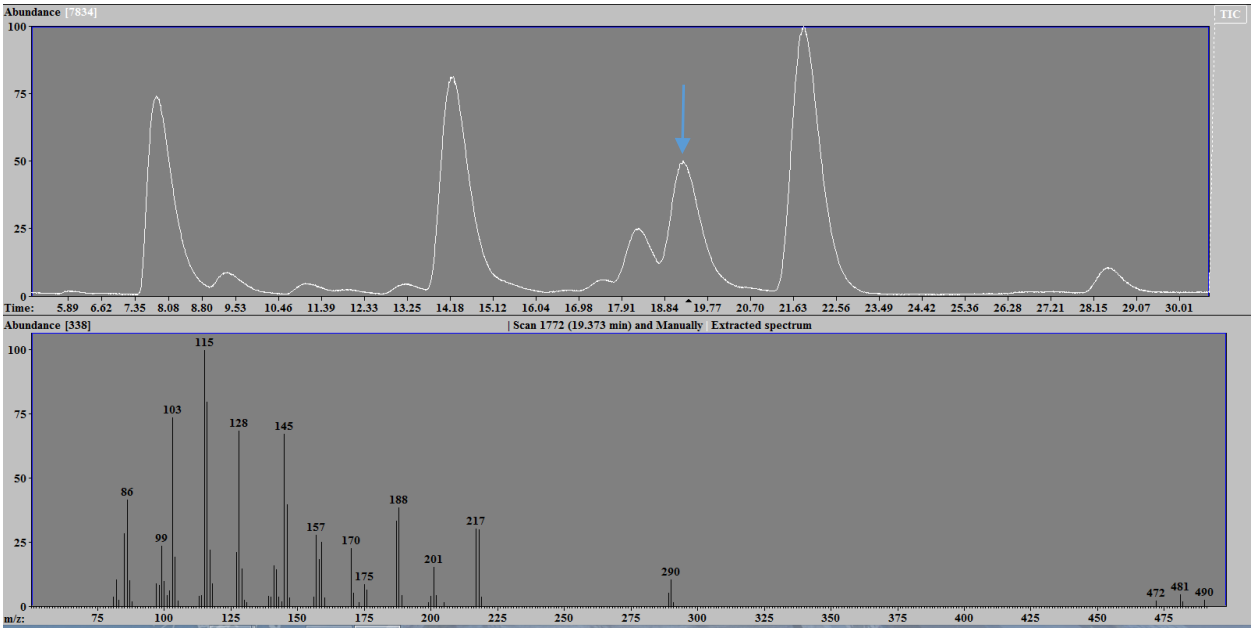
Abundance [7834]
TIC
Time: 5.89 6.62 7.35 8.08 8.80 9.53 10.46 11.39 12.33 13.25 14.18 15.12 16.04 16.98 17.91 18.84 19.77 20.70 21.63 22.56 23.49 24.42 25.36 26.28 27.21 28.15 29.07 30.01
Abundance [338]
| Scan 1772 (19.373 min) and Manually Extracted spectrum
115 103 128 145 86 99 188 157 170 217 175 201 290 472 481 490
m/z: 75 100 125 150 175 200 225 250 275 300 325 350 375 400 425 450 475

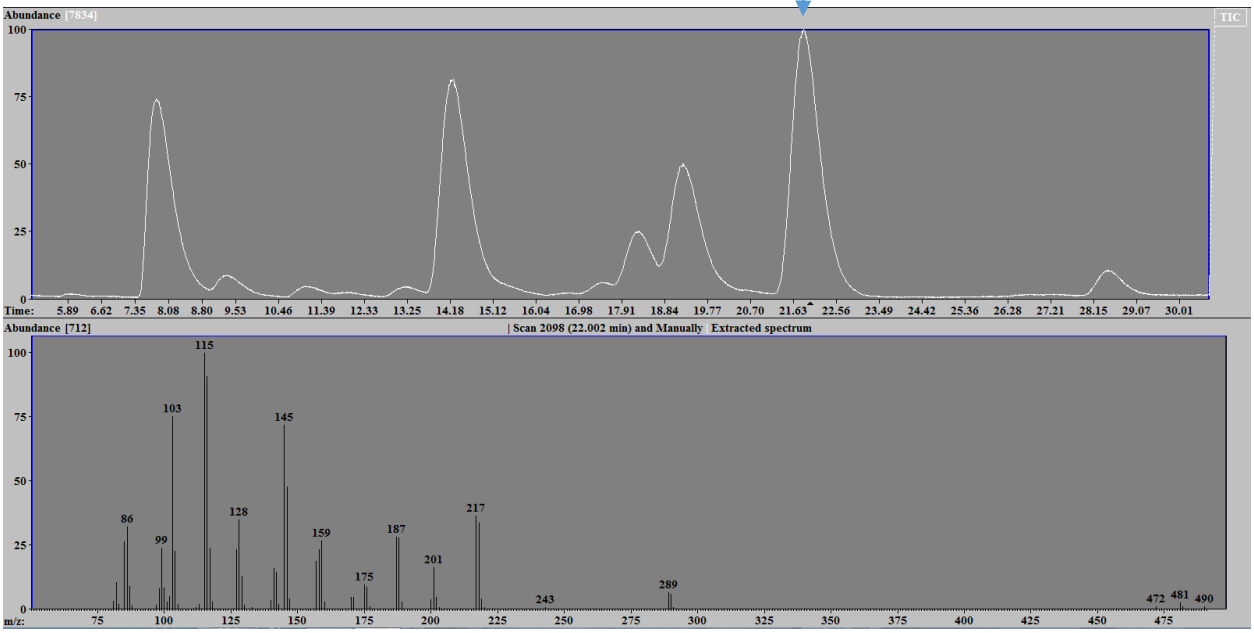
Abundance [7834]
TIC
Time: 5.89 6.62 7.35 8.08 8.80 9.53 10.46 11.39 12.33 13.25 14.18 15.12 16.04 16.98 17.91 18.84 19.77 20.70 21.63 22.56 23.49 24.42 25.36 26.28 27.21 28.15 29.07 30.01
Abundance [712]
| Scan 2098 (22.002 min) and Manually Extracted spectrum
115 103 145 86 99 128 159 187 217 201 175 243 289 472 481 490
m/z: 75 100 125 150 175 200 225 250 275 300 325 350 375 400 425 450 475